

PEOPLE'S DEMOCRATIC REPUBLIC OF ALGERIA MINISTRY OF HIGHER
EDUCATION AND SCIENTIFIC RESEARCH



**IBN KHALDOUN UNIVERSITY OF
TIARET FACULTY OF APPLIED
SCIENCES
ELECTRICAL ENGINEERING DEPARTMENT**



THESIS

Presented by:

Samira HEROUAL

Thesis submitted in fulfillment of the requirements for:

Degree of DOCTORATE (L.M.D) in Electrical Control

**The Impact of Hybrid Storage on Enhancing the
Autonomy of Electric Vehicles and on Their
Energy Management**

Presented on

under board of examiners composed of

President	BELFDHAL Cheikh	Pr	U. Tiaret
Supervisor	BELABBAS Belkacem	MCA	U. Tiaret
Co-Supervisor	ALLAOUI Tayeb	Pr	U. Tiaret
Examiner	SEBAA Morsli	Pr	U. Tiaret
Examiner	BERKANI Abderrahmane	MCA	U. Tiaret
Examiner	TALEB Rachid	Pr	U. Chelef
Examiner	GUENTRI Hocine	MCA	CU. El Bayadh.

2024/2025

Acknowledgements

“I am grateful to the Almighty Allah for His blessings, which have provided me with strength during all these years of study.”

I would like to express my deep gratitude to everyone who contributed directly or indirectly to the completion of this doctoral thesis.

First, I would like to thank my supervisor, **Dr. Belkacem BELABBAS**, from Tiaret University, for his support, constant availability, wise advice, and rigorous supervision throughout this work. His expertise and trust were an essential source of motivation and inspiration.

I also extend my sincere thanks to **Pr. Tayeb ALLAOUI**, from Tiaret University, co-supervisor of this thesis and director of the Energy and Computer Engineering Laboratory (L2GEGI) at Tiaret University, for his invaluable supervision, scientific support, and encouragement throughout this process.

I would like to warmly thank **Pr. Cheikh BELFEDHAL**, chair of the jury, from Tiaret University, for agreeing to chair this thesis defense and for his interest in this work. My thanks also go to **Pr. Rachid TALEB** of the University of Chlef and **Dr. Hocine GUENTRI** of the El Bayadh University Center for agreeing to review this thesis as guest examiners. I am grateful to them for the time they devoted to evaluating this work and for the quality of their comments and suggestions.

I also extend my sincere thanks to **Pro. Morsli SBAA** and **Dr. Abdelrahmane BERKANI**, both of the University of Tiaret, for agreeing to review this work as examiners. Their constructive comments greatly contributed to the enrichment of this thesis.

Finally, I extend a special thanks to **Dr. Yasser DIAB** of the University of Nantes -France, for his invaluable scientific collaboration and support throughout this project. His contribution was instrumental at several stages of this work.

To all of you, I express my most sincere gratitude.

[Samira HEROUAL]

Dedication

This Thesis is dedicated to:

*My parents
My brother and my sisters*

*To my friends and colleagues, who have
offered support, constructive discussions,
and encouragement throughout this journey,
I am sincerely grateful.*

Abstract

Abstract: The seamless integration of energy storage systems into electrical grids necessitates the deployment of a highly efficient energy management system (EMS) to enhance the stability, reliability, and resilience of interconnected electric vehicle networks. This research investigates the optimization of a photovoltaic (PV) system interfaced with a hybrid energy storage system (HESS) combining lithium-ion batteries and supercapacitors. The development of an effective EMS must overcome several challenges, including peak current limitations in supercapacitors, the inherently slow dynamic response of batteries, and their vulnerability to environmental stressors such as solar irradiation fluctuations and load variations. Metaheuristic optimization techniques have demonstrated significant potential in addressing complex multi-objective optimization problems. In this context, this thesis proposes the modeling and optimization of an EMS for HESS using three advanced metaheuristic algorithms: Genetic Algorithm (GA), Ant Colony Optimization (ACO), and Grey Wolf Optimization (GWO). Furthermore, the study presents the design, modeling, and simulation-based validation of a battery electric vehicle (BEV), wherein speed variation is utilized as the reference input to achieve optimal acceleration and deceleration performance. Control is achieved through both conventional PI regulation and PI tuning via the ACO algorithm to enhance dynamic behavior. Finally, a comprehensive comparative analysis is performed to assess the strengths and limitations of each proposed strategy, substantiating the superior performance and robustness of the ACO-based approach, particularly under varying road gradient conditions.

Key words: Hybrid Storage System, Electric Vehicle, Energy Management System, Metaheuristic Optimization, Lithium-ion Batteries, Supercapacitors.

ملخص: يتطلب الدمج الفعال لأنظمة تخزين الطاقة ضمن شبكة الكهرباء نظام إدارة عالي الأداء، قادرًا على تعزيز الاستقرار والموثوقية والمرونة ضمن منظومة المركبات الكهربائية المترابطة. يركز هذا العمل على تحسين نظام كهروضوئي مقترن بجهاز تخزين هجين يدمج بين بطاريات الليثيوم أيون والمكثفات الفائقة. تواجه عملية تصميم نظام إدارة طاقة فعال عدة تحديات، من بينها الحد من تيار الذروة عند مستوى المكثفات الفائقة، الاستجابة الديناميكية البطيئة نسبيًا، وحساسية البطاريات للضغوطات الناتجة عن الظروف المناخية، مثل الإشعاع الشمسي وتغير الحمولات. وقد أثبتت طرق التحسين الميتاهيرستية فعاليتها العالية في معالجة المشكلات المعقدة متعددة الأهداف. يقترح هذا العمل نموذجًا وتحسين نظام إدارة الطاقة لجهاز تخزين هجين، معتمدًا على ثلاث مقاربات: الخوارزمية الجينية، خوارزمية مستعمرات النمل، وخوارزمية الذئب الرمادي. في مرحلة ثانية، يعرض تصميم ونمذجة والتحقق من صحة محاكاة لمركبة كهربائية تعتمد على البطاريات، مع استخدام تغيير السرعة كإشارة مرجعية لضمان أداء مثالي من حيث التسارع والتباطؤ. يتم التحكم في النظام باستخدام كل من الطريقة التقليدية وخوارزمية مستعمرات النمل، من أجل ضبط معلمات المنظم التناسلي-التكاملي (PI) بكفاءة. وأخيرًا، يتم إجراء دراسة مقارنة لتقييم مزايا وعيوب كل استراتيجيات مقترحة، مما يؤكد فعالية ومثانة المنهج المعتمد على خوارزمية مستعمرات النمل، خصوصًا تحت ظروف طرق ذات انحدارات متغيرة.

الكلمات المفتاحية: نظام تخزين هجين، مركبة كهربائية، نظام إدارة الطاقة، تحسين ميتاهيرستية، بطاريات ليثيوم-أيون، مكثفات فائقة.

Résumé : L'intégration harmonieuse des systèmes de stockage d'énergie dans les réseaux électriques requiert la mise en œuvre d'un système de gestion de l'énergie (EMS) hautement performant, afin d'améliorer la stabilité, la fiabilité et la résilience des réseaux de véhicules électriques interconnectés. Ce travail de recherche porte sur l'optimisation d'un système photovoltaïque (PV) couplé à un système de stockage hybride (HESS) combinant des batteries lithium-ion et des supercondensateurs. Le développement d'un EMS efficace doit relever plusieurs défis, notamment les limitations du courant de crête au niveau des supercondensateurs, la réponse dynamique intrinsèquement lente des batteries, ainsi que leur sensibilité aux contraintes environnementales telles que les fluctuations de l'irradiation solaire et les variations de charge. Les techniques d'optimisation métaheuristiques se sont révélées particulièrement efficaces pour résoudre des problèmes complexes d'optimisation multicritères.

Dans ce contexte, cette thèse propose la modélisation et l'optimisation d'un EMS destiné à un HESS, en s'appuyant sur trois algorithmes métaheuristiques avancés : l'Algorithme Génétique (GA), l'Optimisation par Colonies de Fourmis (ACO) et l'Optimisation par Loups Gris (GWO). Par ailleurs, ce travail présente la conception, la modélisation et la validation par simulation d'un véhicule électrique à batterie (BEV), où la variation de vitesse est utilisée comme signal de référence afin d'assurer des performances optimales en matière d'accélération et de décélération. La régulation est assurée à l'aide d'une commande proportionnelle-intégrale (PI) classique ainsi qu'à travers l'ajustement optimisé des paramètres du régulateur via l'algorithme ACO pour améliorer le comportement dynamique. Enfin, une analyse comparative approfondie est menée pour évaluer les avantages et les limites de chaque stratégie proposée, démontrant la supériorité en termes de performance et de robustesse de l'approche basée sur l'ACO, notamment sous des conditions de routes à pentes variables.

Mots clés : Système de stockage hybride, Véhicule électrique, système de gestion de l'énergie, Optimisation métaheuristique, Batteries lithium-ion, Supercondensateurs.

Table of contents

Acknowledgements.....	I
Dedication	II
Abstract:.....	III
Table of contents	IV
List of Figures	IX
List of Tables.....	XII
List of Symbols.....	XII
List of Abbreviations	XVI
General Introduction.....	1
Chapter I:State of the art of electric vehicle.....	12
I.2.Historical Background	13
I.3.Electric vehicle.....	19
I.5.Worldwide electric vehicle sales	21
I.6.Various parameters that can be considered for consumer trends of EVs	22
I.7.Electric Vehicles Taxonomy	23
I.7.1. Battery Electric Vehicles (BEVs).....	23
I.7.2. Hydrogen Fuel Cell Electric Vehicles (FCEVs).....	24
I.7.3. Mild-Hybrid Electric Vehicles (MHEVs).....	24
I.7.4. Extended-Range Electric Vehicles (EREVs).....	25
I.7.5. Plug-in Hybrid Vehicles (PHEVs).....	25
I.7.6. Hybrid Electric Vehicles (HEVs).....	26
I.8. Electric car technical elements.....	27
I.8.1. Driving Cycle.....	27
I.8.2. Electric machine	27
1.8.2.1. AC Motors in EVs	27
1.8.2.2. Types of DC Motors in EVs.....	28
1.8.2.3. Comparison between DC and AC motors	30
I.8.3. Gearbox	30
I.8.4. Energy Sources	31
I.8.5. Power Electronics Converters in EV.....	31
1.8.5.1. DC-DC Converters	31
1.8.5.2. DC-AC Converters	32
I.8.6. Energy management and Regenerative braking.....	33
I.9.Charging of Electric Vehicles	34

Table I.3. Charging classification of the GB/T-20234 [154].....	34
I.10. Positive impact of EV	35
I.11. Negative impact of EV	35
I.12. Conclusion	35
Chapter II: Photovoltaic Energy Conversion: Principles, Modeling and Simulation	36
II.1. Introduction	37
II.2. Photovoltaic Solar Energy	37
II.3. Photovoltaic Solar Effect	38
II.3.1. The procedure working of PV Cells	38
II.4. Different installations of solar photovoltaic	38
II.4. Generations of Photovoltaic Cells	39
II.6. Cells, Modules, Panels and Arrays	40
II.7. Different configurations of photovoltaic array	41
II.7.1. Series Configuration	41
II.7.2. Parallel Configuration	41
II.7.3. Series-Parallel Configuration	42
II.7. The major factors impacting PV electricity generation	42
II.8. Serval Types of PV systems	43
II.8.1. Off-Grid PV system (standalone)	44
II.8.2. Grid-connected PV system	44
II.8.3. Hybrid PV system	45
II.9. Parameters of solar photovoltaic	45
II.10. Modeling of Photovoltaic (PV)	46
II.10.1. Electrical Equivalent Circuit for One-Diode Photovoltaic Cell Model	46
II.10.2. Electrical Equivalent Circuit for Two-Diode Photovoltaic Cell Model	47
II.11. Proposed Modeling of the system (PV connected to DC-DC converter with DC load)	48
II.11.1. DC-DC converter model	48
II.11.1.1. Boost converter model	48
II.11.2. The Control of DC-DC converter	50
II.11.2.1. Perturb and Observe (P&O) methods	51
II.11.3. Performance Effect of Photovoltaic Panels	52
II.12. Simulation results	53
II.13. Conclusion	56
Chapter III: Overview of energy system storage	57
III.1. Introduction	57
III.2. Overview of Energy Storage	58
III.3. Technologies of energy storage	59
III.3.2. Mechanical energy storage	60

III.3.3. Chemical energy storage (CES)	60
III.3.4. Electrical energy storage (EES)	61
III.3.5. Electrochemical energy storage (ECES).....	61
III.4. Battery energy storage.....	62
III.4.1. Lead-Acid (LA).....	62
III.4.2. Nickel-Cadmium	63
II.4.3. Nickel-metal hydride	65
III.4.4. Sodium-Sulfur	66
III.4.5. Vanadium-Redox Flow.....	67
III.4.6. Lithium-ion	68
III.5. Supercapacitor Energy Storage.....	69
III.5.1. Pseudo-capacitors	70
III.5.2. Electric Double Layer Capacitors	70
III.5.2. Hybrid Capacitors.....	71
III.6. Performance of different types of Supercapacitors Energy Storage.....	71
III.7. Comparison between battery and supercapacitor energy storage via diagram Ragone	72
III.7.Hybrid energy storage	73
III.8. Classification of Hybrid energy storage	73
III.7.1. Different configurations used for batteries/supercapacitors Hybrid energy storage.....	74
III.7.2. Basic passive parallel hybrid configuration	74
III.7.3. Basic semi-active parallel hybrid configuration employing batteries	75
III.7.4. Basic semi-active parallel hybrid configuration employing SC.....	75
III.7.5. HESS using multiple converters hybrid configuration	76
III.8. Conclusion	77
Chapter IV:Modeling, Analysis, and management of hybrid energy storage.....	78
IV.1.Introduction	79
IV.2. System Description	79
IV.2.1. Electrical Model of Battery.....	80
IV.2.2. Electrical Model of Supercapacitors	80
IV.3. DC-DC Bidirectional Converter	81
IV.4.Control Strategy of HESS	83
IV.5. Energy Management System of HESS.....	84
IV.6. Generality of optimization.....	85
IV.7. Classification of Optimization Problems	85
IV.8. Different Optimization methods.....	86
IV.8.1. Heuristic algorithm	86
IV.8.2. Meta-heuristic algorithm.....	86

IV.9. Optimized PI Controller Tuning	87
IV.9.1. Optimization criteria for a PI controller	87
IV.9.2. Classic PI Controller Pole Placement Optimization Application to PI Controller Tuning	87
IV.9.3. Optimization of PI parameters using GA heuristic algorithms	88
IV. 9.3.1. Overview of genetic algorithm	88
IV.9.3.2. Details of Different Steps in the GA Process	89
IV.9.4. Background of ACO	94
IV.9.4. Optimization of PI parameters using ACO heuristic algorithms	95
IV.9.5. Optimization of PI parameters using GWO heuristic algorithms	97
IV.9.5.1. Basic of GWO	98
IV.10. Implementation of different algorithms (GA, ACO, and GWO) in Simulink	102
IV.11.RESULTS AND DISCUSSION	104
IV. 11.1. Test 1: Variable solar irradiation and constant load	104
IV.12. The Performance evaluation of the controllers	114
IV.13. Conclusion	115
Chapter V: Application of metaheuristic Algorithms on Battery electric vehicles	117
V.1. Introduction.....	117
V.2.Description of the traction system of BEV with DC motor.....	117
V.3. Modeling of EV	118
V.3.1. Dynamic Modeling of the Electric Vehicle.....	118
V.3.1.1. Rolling resistance force.....	119
V.3.1.2. Aerodynamic drag forces	119
V.3.1.3. Acceleration forces	120
V.3.1.4. Gradient forces	120
V.3.1.5. Inertia forces.....	120
V.3.2. Electric Engines Modeling.....	121
V.3.2.1. PMDC motor	121
V.3.3. Driveline model.....	122
V.3.4. Brake system	122
V.3.5. Driver model	122
V.3.6. Batteries	122
V.4. Optimization of PI parameters using conventional method and meta-heuristic PSO and ACO algorithms.....	123
V.4.1. PI using conventional method.....	123
V.4.2. PI using Particle swarm optimization	124
V.4.2.1. Core Components of PSO	125
V.4.3. PI using Ant colony optimization.....	129
V.4.5. Statistical analysis and robustness between PSO and ACO.....	131

V.4.5. Computational Cost	132
V.5. Results and Discussion	133
V.6. Conclusion	138
General Conclusion	139
Appendix A	142
Appendix B	143
Bibliography	144

Chapter I

Figure I.1. Jedlik’s electric car in 1828	13
Figure I.2. Sibrandus Stratingh ‘s electric horseless carriage	14
Figure I.3. Thomas Davenport and the First Electric Car	14
Figure I.4. Robert Davidson Galvani Electric locomotive	15
Figure I.5. La jamais contente	15
Figure I.6. GM XP 512E EV prototype	16
Figure I.7. Toyota Prius	17
Figure I.8. Tesla Roadster	17
Figure I.9. Electric car Venturi Jamais Contente	18
Figure I.10. Electric car Volt E-REV.....	18
Figure I.11. Electric Vehicle	19
Figure I.12. Electric vehicle battery technology and sustainability articles by publication year.....	20
Figure I.13. Top 20 journals by EV article count	21
Figure I.14. EV Publication trends by journal	21
Figure I. 15. Worldwide electric vehicle sales	22
Figure I.16. Charging Station and Electricity Demand for cars increment over the years	23
Figure I.17. Battery Electric Vehicles	23
Figure I.18. Hydrogen Fuel Cell Electric Vehicles	24
Figure I.19. Mild-Hybrid Electric Vehicles	24
Figure I.20. Extended-Range Electric Vehicles	25
Figure I.21. Plug-in Hybrid Electric Vehicles	26
Figure I.22. Hybrid Electric Vehicles	26
Figure I.23. Standard driving cycles	27
Figure I.24. Asynchronous motor	28
Figure I.25. Synchronous motor	28
Figure I.26. Brushed DC Motors	29
Figure I.27. Brushless DC Motors.....	29
Figure I.28. Gear box in Electric Vehicles	31
Figure I.29. DC-DC Converter in EV and HEV	32
Figure I.30. Regenerative braking work in EV	33

Chapter II

Figure II.1. Solar photovoltaic panels	37
Figure II.2. Solar photovoltaic effect	38
Figure II.3. Different installations of solar photovoltaic	39
Figure II.4. Generations of Photovoltaic Cells	40
Figure II.5. Design of Cells, Modules, Panels, and Arrays	41
Figure II.6. Series Configuration	41
Figure II.7. Parallel Configuration	41
Figure II.8. Series-Parallel Configuration	42
Figure II.9. The factors impacting PV electricity generation.....	43
Figure II.10. The Types of PV system.....	43
Figure II.11. Off-grid PV system.....	44
Figure II.12. Grid-connected PV system.....	44
Figure II.13. Configuration Hybrid PV system.....	45
Figure II.14. Configuration Hybrid PV system [165].....	45
Figure II.15 :Electrical Equivalent Circuit of a One-Diode Photovoltaic Cell Model.....	47
Figure II.16. Electrical Equivalent Circuit: Two-Diode Photovoltaic Cell Model [167].....	48
Figure II.17. Scheme DC load connected with PV panels.....	48
Figure II.18. Boost converter.....	49
Figure II.19. Boost converter in First Phase (when S is open).....	49

Figure II.20. Boost converter in First Phase (when S is close).	50
Figure II.21. Functional characteristics of the P&O Curve [169].	52
Figure II.22. Variation of I – V and P – V curve with solar irradiation.	52
Figure II.23. Variation of I – V and P – V curve with solar temperature.	53
Figure II.24. Abrupt irradiation changes input.	53
Figure II.25. Solar Output Current.	54
Figure II.26. Solar Output Voltage.	54
Figure II.27. Solar Photovoltaic Power.	54
Figure II.28. Gradual ramp evolution of irradiation.	55
Figure II.29. PV Voltage.	55
Figure II.30. PV Current.	55
Figure II.31. PV Power.	56

Chapter III

Figure III.1. Application of Energy storage system	59
Figure III.2. Technologies of electrical energy storage	59
Figure III.3. Thermal energy storage	60
Figure III.4. Mechanical energy storage	60
Figure III.5. Chemical energy storage	61
Figure III.6. Electrical energy storage	61
Figure III.7. Electrochemical energy storage	62
Figure III.8. Lead-Acid Battery	63
Figure III.9. Nickel-Cadmium Battery	64
Figure III.10. Nickel-metal hydride Battery	65
Figure III.11. Sodium-Sulfur Battery	66
Figure III.12. Vanadium-Redox Flow Battery	67
Figure III.13. Lithium-ion Battery	68
Figure III.14. Supercapacitors types.	69
Figure III.15. Pseudo-capacitors	70
Figure III.16. Electric Double Layer Capacitors.	70
Figure III.17. Hybrid capacitors.	71
Figure III.18. Ragone Diagram	72
Figure III.19. structure of HESS	73
Figure III.20. Classification of HESS.	74
Figure III.21. Different configurations of HESS.	74
Figure III.22. Basic passive parallel hybrid configuration.	75
Figure III.23. Basic semi-active parallel hybrid configuration employing batteries.	75
Figure III.24. Basic semi-active parallel hybrid configuration employing SC.	76
Figure III.25. Basic, several converters, parallel hybrid configuration.	77

Chapter IV

Figure IV.1. PV system with HESS.	79
Figure IV.2. Battery cell model.	80
Figure IV.3. SC cell model.	81
Figure IV.4. Circuit for the Buck-Boost in two transfer directions (a) From Vbat to Vdc (forward mode), (b) From Vdc to Vbat (reverse mode) converter of the battery	82
Figure IV.5. Circuit for the Buck-Boost converter in two transfer directions (c) From Vsc to Vdc (forward mode), (d) From Vdc to Vsc (reverse mode) converter of the supercapacitor.	82
Figure IV.6. Control scheme of HESS.	83
Figure IV.7. Flowchart of the EMS.	84
Figure IV.8. Optimization methods	86
Figure IV.9. Binary coding scheme.	89
Figure IV.10. Real coding scheme.	89

Figure IV.11. single-point crossover.	90
Figure IV.12. Two-point crossover.....	91
Figure IV.13. Uniform crossover.....	91
Figure IV.14. bit inversion.	92
Figure IV.15. mutation by the exchange.	92
Figure IV.16. Mutation by reversion.	92
Figure IV.17. The PI-GA flowchart.....	94
Figure IV.18. Ants' foraging activity for food [235].....	95
Figure IV.19. PI-ACO flowchart.	97
Figure IV.20. Social hierarchy of grey wolves [241].....	98
Figure IV.21: The hunting behavior of the grey wolves A chasing, approaching, and tracking the prey B-D pursuing, harassing, and encircling the prey E attacking when the prey stops moving[242].	98
Figure IV. 22. Updates on Wolf's location[244].....	99
Figure IV.23. PI-GWO flowchart.....	102
Figure IV.24. Implementation of several algorithms (GA, ACO, and GWO) in Simulink side battery.	103
Figure IV.25. Implementation of serval algorithms (GA, ACO, and GWO) in Simulink side SC.....	103
Figure IV.26. Power of load.	105
Figure IV.27. Variable irradiation	105
Figure IV.28. The DC voltage with the reference voltage.	105
Figure IV.29. The voltage of Battery.	106
Figure IV.30. Current of battery	106
Figure IV.31. Sate of Charge of the battery.	107
Figure IV.32. Voltage of Supercapacitor.	107
Figure IV.33. current of supercapacitor.	107
Figure IV.34. Power of battery.....	108
Figure IV.35. Power of PV.....	108
Figure IV.36. Power of supercapacitor.	108
Figure IV.37. Battery Current with different optimization methods of the PI controller (scenario1)	109
Figure IV.38. Battery Power with different optimization methods of the PI controller (scenario1) ...	109
Figure IV.39. SC current with different optimization methods of the PI controller (scenario1)	110
Figure IV.40. SC power with different optimization methods of the PI controller (scenario 1)	110
Figure IV.41. Power of variable load.....	110
Figure IV.42. Power of PV.....	111
Figure IV.43. State of charge of the battery (scenario2)	111
Figure IV.44. Power of battery.....	112
Figure IV.45. Power of supercapacitor.	112
Figure IV.46. Current of battery under different optimization methods of the PI controller under variable load.	113
Figure IV.47. Power of battery under different optimization methods of the PI controller under variable load.	113
Figure IV.48. SC current under different optimization methods of the PI controller under variable load.	113
Figure IV.49. SC power under different optimization methods of the PI controller under variable load.	114

Chapter V

Figure V.1. BEV components.....	118
Figure V.2. Basic forces applied on an electric vehicle.	119
Figure V.3. Block diagram of the PMDC motor.	121
Figure V.4. Equivalent circuit of batterie component.	123
Figure V.5. Block diagram of conventional PI.....	124
Figure V.6. Particle Swarm Optimization.	125
Figure V.7. Block diagram of PI tuned by PSO algorithm.....	127

Figure V.8. PI-PSO flowchart.	128
Figure V.9. Convergence of the objective function of PSO.	129
Figure V.10. Block diagram of PI tuned by ACO algorithm.	130
Figure V.11: Convergence of the objective function of ACO algorithm.	130
Figure V.12. Driving cycle profile type US06.....	133
Figure V.13. Vehicle speed tuned with conventional PI, PSO, and ACO algorithms.	134
Figure V.14. Current of the battery.	135
Figure V.15. Power of motor and battery.....	135
Figure V.16. Motor Torque.	136
Figure V. 17. Vehicle speed tuned with conventional PI, PSO, and ACO at 5 degrees' road angle. ...	137
Figure V.18. Vehicle speed tuned with conventional PI, PSO, and ACO 15 degrees' road angle	137
Figure V.19. Vehicle speed tuned with conventional PI, PSO, and ACO at 28 degrees' road angle.	137
Figure V.20. Vehicle speed tuned with conventional PI, PSO, and ACO at 40 degrees' road angle.	138

Chapter I

Table I.1: Charge ratings of the SAE-J1772 .	34
Table I.2: Charge ratings of the IEC-62196 .	34
Table I.3: Charging classification of the GB/T-20234 .	34

Chapter II

Table II.1: Several basic classifications of MPPT methods .	51
--	----

Chapter III

Table III.1: Features of Lead-Acid.....	63
Table III.2 : Features of Nickel-Cadmium (Ni-Cd)	64
Table III.3: Features of Nickel-metal hydride (Ni-MH).....	65
Table III.4: Features of Sodium-Sulfur (Na-S).....	66
Table III.5: Features of Nickel-metal hydride (Ni-MH).....	67
Table III.6: Features of lithium-ion battery	68
Table III.7: Performance of several supercapacitors	71

Chapter IV

Table IV. 1: Parameters of HESS tuned by conventional PI.....	88
Table IV.2: Parameters of HESS tuned by GA.	93
Table IV.3: Parameters of HESS tuned by the Ant colony algorithm.	97
Table IV.4: Parameters of HESS tuned by the Ant colony algorithm.....	101
Table IV.5: Performance of the SC with the various optimization algorithms of the PI controller.....	114
Parameters of HESS tuned by the GWO.	
TableIV.6: Performance of the batteries with the various optimization algorithms of the PI controller.	114

Chapter V

Table V.1: Parameters of EV tuned by PI conventional.....	124
Table V.2: Parameters of EV tuned by PSO.....	128
Table V.3: Parameters of EV tuned by ACO.	130
Table V. 4: Sensitivity analysis result – maximum number of iterations for PSO and ACO algorithms	131
Table V.5: Statistical analysis result for Population size (N) for PSO and ACO algorithm	131
Table V. 6: Statistical analysis result – inertia weight (W) for PSO algorithm and evaporate rate for ACO algorithm.....	132
Table V.7: The Computational cost for PSO algorithm and ACO algorithm.....	133

V_{pv}	Solar cell voltage (V)
I_{PV}	PV current (A)
D_{PV}	The duty ratio of the PV
I_{sc}	Supercapacitor current (A)
D_{sc}	The duty ratio of the SC
I_{bat}	Battery current (A)
D_{bat}	The duty ratio of the battery
V_{dc}	DC link voltage (V)
I_{dc}	DC link current (A)
R_s	Series resistance (Ω)
R_p	Parallel resistance (Ω)
I_{ph}	Photocurrent (A)
I_d	Diode current (A)
I	Solar cell current (A)
I_s	Solar cell saturation of dark current (A)
N_s	Series modules
N_p	Parallels modules
A	Ideality Factor
q	Electron charge (C)
K	Boltzman's constant (J/K)
T_c	Solar cell working temperature
V_{OC}	Open-circuit voltage (V)
C_1	The Helmholtz capacitance (F)
R_1, R_2	Ohmic resistance (Ω)
V_{sc}	Voltage of the SCs (V).
R_1, R_2	Ohmic resistance side SC (F)
C_{BN}	Nominal Capacity of Battery (F)
C_{bu}	Usable Capacity of Battery (F)
SOC_{init}	Initial of State of Charge (%)
SOC_{min}	Minimum value of the state of Charge (%)
SOC_{max}	Maximum value of the state of Charge (%)
R_f	The loss by self-discharging current (Ω)
C_1	Constant capacitance (F)
C_2	The diffuse capacitance (F)
V_{sc}	Voltage of the SC (V)
R_1, R_2	Ohmic resistance side SC (Ω)
V_1	Voltage across the main cell's capacitor C_1 (V)
V_2	Voltage across the main cell's capacitor C_2 (V)
V_{dc_ref}	Reference voltage of DC bus (V)
I_{bat_ref}	Reference current of battery (A)
I_{sc_ref}	Reference current of SC (A)
L_{sc}	Supercapacitors inductance (A)
S_1, S_2, S_3, S_4	Converter switches.
I_L	Load current (A)
C	Capacitor of the DC link (F)
P_{bat}	Battery power (W)
V_{sc}	Supercapacitor Voltage (V).
V_{bat}	Battery voltage (V).
P_L	Load power (W)
P_{pv}	PV power (W)
P_{sc}	Supercapacitor power (W)
K_p, K_i	Proportional and integral gains of the PI regulator
f_{best}	The best objective function

f_{worst}	The worst objective function
$X_\alpha, X_\beta, X_\delta$	Grey Wolf population
f_i	Objective function
F_{rol}	Rolling resistance force.
F_{aero}	Aerodynamic drag forces.
F_{acc}	Inertia resistance force.
F_{grad}	Gradient forces.
m	Vehicle Weight (Kg).
r_w	Tire radius
g	Gravitational acceleration (m/s^2).
C_r	Rolling resistance coefficient of tires.
ρ	Air density.
θ	Road angle.
C_d	Aerodynamic coefficient of friction of penetration in the air.
A_f	Frontal surface of the vehicle (m^2).
v_{meas}	Vehicle speed (m/s).
v_{ref}	Reference speed (m/s).
I_{bat}	Battery current(A).
SOC_{init}	Initial of State of Charge (%).
C_{bu}	Usable Capacity of Battery (F).
R	Internal resistance (Ω).
V_{oc}	Battery open circuit voltage (V).
T_m	Torque of electric motor (N. m).
P_m	Power of electric motor (KW)

ESS	Energy Storage System
RES	Renewable energy source
MPPT	maximum power point tracking
PI	Proportional Integral
PV	Photovoltaic system
PP	Pole Placement
PWM	Pulse Width Modulation
PM	Power management
SOC	State of Charge
P&O	Perturb and Observe
ANN	Artificial Neural Network
ML	Machine Learning
AI	Artificial Intelligence
SMC	Sliding Mode Control
EV	Electric Vehicle
HESS	Hybrid Energy Storage System
BEV	Battery electric Vehicle
FCEV	Hydrogen Fuel Cell Electric Vehicles
MHEV	Mild Hybrid Electric Vehicles
PHEV	Plug Hybrid Electric Vehicles
EREV	Extended-Range Electric Vehicles
BLDC	Brushless DC Motors
UC	Ultracapacitors
SC	Supercapacitors
FCs	Fuel Cell System
IGBT	Insulated-Gate Bipolar Transistors
MOSFET	metal-oxide-semiconductor field-effect transistor
VSI	Voltage Source Inverters
CSI	Current Source Inverters
ZSI	Impedance Source Inverters
VSI	Voltage Source Inverters
EMF	Electro-motive Force
Kwh	Kilowatt hours
TES	Thermal energy storage
MES	Mechanical energy storage
CES	Chemical energy storage
EES	Electrical energy storage
ECES	Electrochemical energy storage
SMES	superconducting magnetic energy storage
SOC	State of Charge
SOC	Bidirectional Converter
GA	Genetic Algorithm
GWO	Grey Wolf Optimization
PSO	Particle Swarm Optimization
ACO	Ant Colony Optimization

General Introduction

The increasing demand for sustainable and efficient energy systems has led to significant advancements in power management and electric vehicle (EV) technology, however, Electric Vehicles (EVs) have gained popularity as a viable solution to fossil fuel prices and regulations requiring a decrease in CO₂ emissions and a transition to sustainable energy sources [1]. Automotive and IT companies like Tesla, Volkswagen, and Toyota are among the most promising sectors for company development. EVs can move air pollution away from heavily populated metropolitan areas and towards remote stationary power facilities, minimizing public health risks and reducing transportation's overall carbon footprint. They can provide distributed storage on the electric grid through coordinated charging efforts, balancing intermittent wind and solar energy penetrations. With the global shift towards renewable and clean energy resources in recent decades, the approach to electricity generation and consumption has changed drastically and the energy landscape is experiencing a major transformation [2-4]. International energy directives advocate for a transition towards sustainable and clean energy sources, emphasizing reducing reliance on fossil fuels to meet global energy demands [5]. As a result, the decreasing costs of solar PV modules, inverters, and related components have made RES increasingly attractive, particularly given the rising electricity generation costs [6]. Notably, the large-scale deployment of RES has reached unprecedented levels in recent years, setting new records annually [7-9].

PV systems are widely used for electricity generation across various applications, including satellites, water pumping, and lighting [10]. These systems can operate independently (stand-alone) or be connected to the grid. Stand-alone systems, ranging from milliwatts to watts, supply power to loads without relying on grid connections [11]. Conversely, grid-connected PV systems in addition to supplying power to the loads, allow the surplus of electricity generated to be fed into the grid, provided it complies with operational regulations [12- [13].

PV systems exhibit non-linear characteristics based on factors such as irradiance and temperature, varying throughout days and across seasons. Consequently, this leads to fluctuations in energy generation resulting in unpredictable energy supply patterns [14-15]. EES play a significant role in enhancing the stability and reliability of the electricity with PV systems. In the design and sizing of ESS, factors such as lifetime, energy density, power density, cycle effectiveness, cost, and storage performance must be considered [16].

Traditionally, batteries have been the primary energy storage devices used with PV systems. However, issues related to charging and discharging efficiency, as well as relatively short lifespans, remain the major challenges. While batteries offer high energy density, making them suitable for constant low-frequency power exchange, they suffer from low power density [17]. This limitation means that batteries with low charge/discharge rates will exhibit interruptions in their cycles, leading to reduced lifespans [18]. In contrast, SC have the advantage of constant charge/discharge cycles without degradation and can operate at high power ratings. However, they have lower energy density [19]. HESS

combines multiple energy storage devices, hence, they can achieve more sustainable and reliable overall performance. HESS provides more efficient energy storage solutions by minimizing the drawbacks of individual components and maximizing their unique strengths [20-21]. Combining batteries and SC presents a viable approach to improve the performance of standalone power systems integrating RES [22]. They can control the power fluctuations of the PV energy under variable meteorological and load variations [23-24]. This combination has also proven beneficial in several applications, including pure battery-powered vehicles such as electric and Hybrid Electric Vehicles (HEVs) [25-26]. These HESS devices are interfaced to the electricity via Bidirectional Converter (BDC) of buck-boost type to control the charging and discharging. In recent years, there has been increasing research interest focusing on the development of power management of RES such as PV and wind with hybrid energy storage technologies and several methods have been reported in the literature:

C. Argyrou and C. Marouchos [27] studied the stability and EMS of grid-connected residential PV systems with batteries and SC energy storage coupled to distinct voltage levels. The current controllers of the bidirectional converters for the HESS were designed based on a rigorous small-signal stability analysis. In [28], the authors proposed a new control scheme based on Fuzzy Logic Control (FLC) to improve the stability and efficiency of a power system combining a PV generator with a HESS consisting of SC and Lithium-Ion batteries. The authors in [29] studied a domestic stand-alone PV system with a HESS consisting of batteries and SC and proposed an EMS to enhance the battery lifespan and reduce maintenance costs, making it an effective alternative for rural applications. S. Aggarwal, and M. Alam [30] presented a control scheme based on FLC for a HESS connected with a DC microgrid. This control method was able to manage dynamic fluctuations in load demand and keep the voltage of the DC connection constant at its nominal level. A. Rahman and I. Ahmad [31] presented a comparison of hydrogen fuel usage with existing Fuel Hydrogen Electric Vehicle (FHEV) and showed that the suggested method successfully decreased hydrogen fuel consumption by 29%. The authors also proposed a variable structure sliding mode control strategy based on FLC for a fuel cell-SC-battery system for hybrid electric vehicles.

A novel design of EMS was proposed by S. Patel. and A. Ghosh [32] to improve power sharing among the battery and SC energy storage devices. The EMS was based on a Hybrid Adaptive Fuzzy Integrated Fractional Order controller and led to an improved control of the DC bus voltage while reducing battery stress.

The authors in [33] presented a hybrid energy storage device including SC in electric vehicles. They proposed a novel control scheme combining a PI and backstepping theory by employing Lyapunov theory to establish the overall system's asymptotic stability in addition to regulating the DC-bus voltage under uncertainties and load variations.

S. Pattnaik and R. Kumar [34] introduced different controllers for DC bus voltage stabilization and State-of-Charge (SOC) management using optimal tuning of controllers for a SC-based PV HESS. N. Nguyen, and C. Yoon [35] presented a Model Predictive Control (MPC) based EMS to enhance the

performance of the HESS in electric vehicles

In [36], the authors used a Neural Network (NN)-based controller for a HESS consisting of a battery and a SC to improve the EMS and decrease stress on batteries, hence increasing their longevity. M. Haasan and A. Chowdhury [37] proposed an improved adaptive hybrid controller based on FLC and ANFIS (Adaptive Neuro-Fuzzy Inference System) model to overcome the limitations of the conventional PI controller for battery to enhance the frequency stability of a low inertia grid. Firstly, a simple controller based on FLC and a conventional PI controller have been implemented to provide inertial support to a low inertia distribution grid, taking frequency error and ROCOF (Rate of Change of Frequency) of the system as inputs. Additionally, the paper presented a comparison between FLC-PI and FLC-ANFIS controllers in terms of transient response characteristics such as settling time. A. Mohammed and S. At Naw [38] discussed several energy management approaches and how they relate to energy source sizing for fuel cell/battery /SC for HEVs. The paper also examined the advantages of implementing an EMS and the control of hybrid energy sources with Artificial Neural Network (ANN), Reinforcement Learning (RL), and MPC. A. Aghmadi and O. Ali [39] discussed the mitigation of dynamic pulsed loads in PV-Battery-SC systems by using a hybrid control strategy combining a conventional PI controller with a NN controller which separates the reference current into low and high-frequency components for battery and SC management. To improve the efficiency of the system under non-linear and dynamic load conditions. The authors in [40] presented a SOC-based adaptive control strategy for pulsed power elimination in hybrid energy storage consisting of battery and SC that can enhance the absorption of pulsed power by HESS to optimize its overall performance and verify its effectiveness and feasibility. D. Karanam and M. Rajib [41] presented the modeling of fuel cell, battery, and SC storage connected with a microgrid. In addition, the proposed method overcomes the hit-and-trial approach for determining the distribution of FIS membership functions via PSO while providing a consistent power supply to the load and control the charge and discharge of the SC and keeping the battery storage system within safe limits.

H. Maghfiroh, and O. Wahyunggoro [42] investigated several uses of FLC as an EMS in HEVs and HESS-EVs, however, giving a comparison with other EMS approaches and exploring the advantages and problems associated with each approach. A. Zermane, and T. Bordjiba [43] discussed the use of HESS such as batteries and SC in off-grid solar systems, emphasizing the relevance of energy autonomy, operational flexibility, and long-term economic savings. In addition, the authors presented the design and simulation of a self-sufficient solar system employing SC and batteries, using the Particle Swarm Optimization (PSO) approach. J. Zhang., and B.Xiao [44] proposed a joint estimation method for the SOC and State-of-Power (SOP) using a fractional-order model and unscented Kalman filter algorithm. It should be noted that the existing approaches in SOP are largely based on integer-order equivalent circuit models, with little emphasis on fractional-order models. An SOP estimate approach based on multiple constraint conditions and integer-order theory is provided, which incorporates voltage constraints, current constraints, power constraints, and SOC boundary restrictions to ensure output

security in all dimensions.

In their work, M. Hilmi, and V. Lystianingrum [45] investigated how power sharing in a HESS may be controlled using the Finite State Machine (FSM) technique. To prevent overcharging and over-discharging, the system is coupled to solar panels and a DC bus voltage. It manages PV and load. R. Kanti, and A. Maung [46] introduced a PID-HOSMC (High Order Sliding Mode Controller), based on a double power reaching law, to improve large-signal stability in DC microgrids. The controller uses efficient DC-DC converters to maintain a constant voltage level, and an ANN to generate the optimal reference voltage for the solar PV system. In addition, Lyapunov stability theory is used to prove the system's closed-loop stability and demonstrate the convergence of tracking errors to zero within a finite time frame.

J. Rocabert, R. Capó-Misut [47] focuses on the integration of electrochemical batteries with supercapacitors for grid-supporting applications. The wide range of SC working voltage requires a power conversion step to integrate the ESS into a common DC bus which is why it was suggested a power control loop distributing power flow for optimized performance and grid-frequency support, typically involving a battery bank however, the power control indicates a slow dynamic response consequently decrease lifespan of the overall system.

V. Jaarsveld, G. Rupert [48] presents an intelligent control system for the HESS such as a battery-supercapacitor using the Fuzzy Logic Controller (FLC) approach. However, this approach is sensitive to changes in the model and data parameters and requires a precise system model.

S. Augustine, M.K. Mishra, and N. Lakshminarasamma [49] combined an adaptive droop-based load sharing, maximum power point tracking, and energy management method for photovoltaic (PV)-based DC microgrid systems. It proposes a proportional droop index technique and generates adaptive virtual resistance R_{droop} , allowing PV converters to function in either MPP or load-sharing mode. The unified control scheme addresses challenges in stabilizing the DC grid voltage, although it acknowledges the complexity of the design process.

M. Khalid [50] discusses the major benefits of integrating batteries with SC and highlights their possible uses in microgrid systems. Also, this work is extensive and will serve as a foundation for future research in energy storage technologies and microgrid applications.

S. Xie Liu, L. Yang [51] presents the new topology of the converter to ensure the exchange of power between hybrid electric vehicle energy storage connected to the grid system. The proposed control strategies focus on extending the life of the electrochemical battery by directing power fluctuations to the SC, accompanied by related current control strategies.

B. Ravada, N. Tummuru. [52] describes a nonlinear control mechanism for a photovoltaic (PV), battery, and supercapacitor-based DC microgrid. Conventional linear control schemes have been based on a single operating point and supercapacitor voltage regulation. The suggested structure employs an Interconnection Damping Assessment-Passivity Based Controller (IDA-PBC) as an outside loop controller and a Finite Control Set-Model Predictive Control (FCS-MPC) as an internal current

controller. The control structure is digitally friendly and overcomes the constraints of linear PI control systems.

In [53] focuses on the EM and control of a PV system with HESS, which combines battery and SC. The control tactics may incorporate methods based on conventional and meta-heuristic methods, recognizing their shortcomings in terms of performance measures like overshoot and rising time.

The Gases Brownian motion optimization (GBMO) technique was used by the authors Z.Abbasali, S.Masoud [54] to optimize a fractional order PI controller based on filtering. A search strategy with a high accuracy and pace of convergence was introduced by GBMO. The controller is made to regulate an operational HESS in a remote region power supply system that is mostly powered by wind. Nevertheless, the control technique is computationally difficult and time-consuming, making it unsuitable for real-time application.

A Model Predictive Control (MPC) and a basic PI control are employed by [55-57] to regulate the HESS. However, MPC uses a discrete-time model of the system to anticipate the best solution in the next instant, with the present system state serving as the beginning value. The suggested control technique extends battery life by directing power surges to the SC and managing charge-discharge current. Although MPC can increase system performance by anticipating future behavior, it is computationally complex and time-consuming.

This research presented by S.Imran H.Farooq [58] describes an artificial neural network (ANN)--based technique for estimating hybrid wind-solar resources and power generation by comparing wind speed and sun radiation with real-time data. Temperature, humidity, air pressure, solar radiation, ideal angle, and goal values are all factors considered by the model. To decrease error, it employs a normalization function as well as an iterative strategy that includes the Levenberg-Marquardt, However, the ANN model does not provide optimal and efficient system performance.

Z. Mohamed, A. Guesmi [59] suggested a sliding-mode control strategy based on artificial neural networks (ANN) for a hybrid PV-battery-SC system. To improve the performance and lifespan of the storage system and prevent the complete disconnection of the load during abrupt fluctuations, Additionally, the DC bus voltage was rapidly regulated, which increased the battery's lifespan and ensured the PV system's continuous flow.

N. Namala, K. NAIDU [60] designing EM control algorithms that combine ANN with Aquila Optimizer Algorithm (AOA). There are four main hunting methods that AOA is known to use, and each offers several unique benefits over the others. Many Aquila are adept in switching between several hunting strategies quickly and effectively, depending on the situation. In conclusion, this hawk is perhaps the second-most intelligent and proficient predator behind humans. This circumstance served as the main impetus for the proposed AOA. A simulation environment was used to replicate similar tasks. Because it also reduces high-speed dynamic battery charging and discharging currents, the hybrid ANN–AOA technique maximizes benefits while restricting battery discharge current.

K.Mohamed, Y.Zyodulla.[61] suggested a PV-battery-fuel cell system control strategy. The

approach uses the phasor feasible alternative from advanced power systems to provide design assessment. The control strategy uses a Genetic Algorithm (GA) and an Adaptive Neuro-Fuzzy Inference System (ANFIS) in this approach. While GA was created to address stability and power quality problems inside the Microgrid, ANFIS gathers system data in electrical power and gives dynamic frequency response. These controls' primary disadvantages, however, are their high computational costs, challenging parameter setting, and essential solution representation.

F. Fareesa, S. Reddy [62] provided an optimal sizing and control that depends on PSO-GA to reduce oscillations in wind power energy and to discover the ideal power and energy capacity of the HESS. PSO outperforms GA in terms of convergence rate, overfitting, and local optimum. Furthermore, the PSO outperformed the GA since it runs both global and local searches at the same time, whereas the GA concentrates just on global searches. The study places insufficient attention on the control side of the entire system.

B. Badis, G. Hatem, D. Habiba [63] focuses on simulating a stand-alone hybrid system made up of PV, wind turbines, a storage system, and a diesel generator. This research employs optimization algorithms to address practical issues linked to the integration of renewable energy sources into the distribution system. The goal is to establish the appropriate size to minimize power costs and assure the availability of electricity at cheaper and more dependable prices in far rural locations.

R. Santosh, S. Raghuvanshi [64] present flamingo swarm intelligence algorithms are used to simulate and optimize hybrid renewable energy systems with storage. The ideal energy system is built utilizing a revolutionary flamingo swarm intelligence algorithm (FSIA) that takes into account the least amount of technical factors, such as the risk of load loss, economic factors (cost of electricity [COE] with net present cost [NPC]), and environmental factors (CO₂ aspects). To improve energy independence in green buildings, an optimum economic analysis of a hybrid solar system with ESS is conducted using PSO.

M. Vijayan [65] Using a shunt active power filter powered by solar energy and energy storage systems to address power quality issues caused by power electronic devices and nonlinear loads. The system makes use of a five-level reduced-switch voltage source converter and a neural network-based reference signal generation approach. The system's purpose is to stabilize the voltage across the DC bus capacitor, reduce overall harmonic distortion, improve power factor, and maintain power management under changing irradiation and load conditions. The system's effectiveness is evaluated using three test scenarios.

A. Annamalaichamy, P. David, P. Balachandran, and I. Colak [66] offers a Shunt active power filter (SAPF) with a multilayer cascaded H-bridge inverter that uses P-Q theory to reduce harmonics in current power systems. The system's voltage controllers are a PI and an FLC. The proposed aggregated PWM signal-switching circuit balances individual capacitor voltages while minimizing overall harmonic distortion. Simulation and prototype findings demonstrate that the aggregated PWM system outperforms the PI controller.

R. Arun, R. Muniraj, N. Karuppiah, B. Kumar, K. Murugaperumal [67] suggests a relay-based automated tuning solution for the Predictive PI control system. The procedure entails finding process models using typical relay feedback testing and calculating the eventual benefit. The First Order Plus Dead-Time model is used to build and improve the controller's dynamic component. The ultimate loop gain is established by relay feedback experiments. The controller gain is adjusted to meet the user-specified gain margin criteria. The method's auto-tuning capability makes it suited for industrial process control applications.

The primary contribution of this thesis is to the design and optimisation of PI controllers using metaheuristic optimization methods such as GA, ACO, and GWO algorithms for EMS of HESS combining batteries and SC an innovative heuristic approach for fine-tuning the parameters of a PI regulator to control the power flow and performance of the charge and discharge of SC storage.

The GWO was compared regularly with conventional PI and GA. Due to its ease of development, the PI is the most popular controller for many control applications. Having been widely employed in many real-world industrial applications, their tuning remains a difficult issue, especially in processes that display nonlinearity. However, it has limited performance, side batteries, and SC and high-order, complicated dynamics with time delay. For this reason, using metaheuristic algorithms such as GA and ant colony algorithms, unfortunately, suffers from issues comprehending intricate gene connections, and low accuracy under different load and irradiation conditions also lacks performance which leads to decreased life of SC and batteries as instead of the algorithm the suggested GWO method helps prevent the load from being completely disconnected and has the benefits of being simple to apply, using little computing power, improving SC storage system performance in term rise time and overshoot time, provide rate peak power with a faster response of SC, and long-term enhancement. Emphasized further are the benefits of the suggested control technique, which include less current stress on the lithium-ion batteries and quicker voltage adjustment.

In the second part of the thesis, Optimizing Battery vehicle performance, health, and safety requires understanding how the EVs operate in various driving and environmental scenarios [68]. To estimate vehicle performance and ensure vehicle dependability, many factors that may impact performance, including temperature, variable speed, road conditions, road slope, conservative driving styles, etc., must be verified [69].

In the literature, many researchers propose the modeling and various controls of BEV as indicated below: A. Maheshwari, S. Nageswari [70] Presents a model with an estimated state of charge of lithium-ion batteries using an improved Deep Neural Network (DNN) approach in EV to examine the training efficacy of various drive cycles, a set of DNN models with variable hidden layer counts and training algorithms are created.

Z. Guangyou, Z. Zhu [71] This paper presents the utilization of regenerative braking energy to control the speed of EV based on a Fuzzy Logic Controller (FLC). Under the conditions of stability and braking safety, the proposed strategy includes two types of braking force: regenerative and frictional.

I. Gunawan [72] Presents speed control of EV using PI and a sliding mode controller to regulate the cruise of an electric car with PMSM. As a vehicle model, the kinematic bicycle model is employed for simplicity. Vector control is used for PMSM speed control, and a sinusoidal PWM model is created to provide pulses that power the inverter. The motor's speed is changed using a gear factor to the speed needed to drive the wheels. But the drawback of this method is the weakness of performance

H. Emad [73] presents a comparative study of controllers, including the Linear Quadratic Regulator (LQR), state Observer-Based Controller (OBC), pole placement controller, and Proportional-Integral-Derivative (PID), for obtaining optimal speed control of EV. However, the same does not provide optimal and efficient system robustness.

D. Alberto, T. Bendik Nybakk [74] Proposes an efficient design for a Nonlinear PID (NPID) controller to enhance the EV dynamic responsiveness. The suggested controller's goal is to precisely monitor the reference speed that the EV driver has chosen. However, the ideal conditions of the Harmony Search (HS) optimization method, which is based on a cost function, were used to obtain the NPID and PID controllers. However, it suffers in terms of performance, the intended rising time, settling time, steady-state error, and overshoot.

A. Prashant, H. Solomon [75] Describes a Genetic Algorithm-optimized Adaptive Fuzzy Fractional Order Proportional Integral Derivative (GA-AFFOPID) controller that improves the speed control performance of Permanent Magnet Synchronous Motor (PMSM) drives in EV. However, it suffers from sensitivity and accuracy under different disturbances.

Z. Fatiha, B. Ismail [76] compares EV control design to improve behavior and stability under different road conditions. The proposed control, called backstepping control, increases efficiency by using two DC motors on the rear wheels. For high-performance motion control systems, it is recommended to replace the present PI controller with backstepping.

C. Ahmed, D. Aziz[77] present A new combination called Fuzzy Backstepping Control (FBSC) is proposed to address the optimal speed control of EV. The fuzzy algorithm inputs systematic errors and their derivatives, synthesizing the output with a reference signal. The system's stability is evaluated using the Lyapunov criterion, and performance is assessed through simulation. The proposed controller closely follows the reference value with minor errors, eliminating phase delay.

C. Kamel, S. Abdelaziz [78] compares the performance of conventional PI and sliding-mode controllers for PMSM in electric vehicle applications with single-motor drive configurations. The main topics of the comparative analysis are dynamic performance and robustness.

S. Mopidevi, D. Kiransai [79] explores the design and control of a Brushless Direct Current (BLDC) motor for speed control in EV applications, considering error as a key factor. The researchers used PI and adaptive neuro-fuzzy inference system controllers to improve steady-state and transient performance

Z. Yuefei, Z. Shushu [80] presents two adaptive PI controllers for electric drive speed control, developed using the ADALINE neural network. The controllers analyze the impact of low-pass filters

and Coulomb friction torque on parameter identification and provide a new motion equation. A parameter identification method based on unipolar speed reference is also provided

O. Bashra, K. Mohamed [81] focuses on designing linear and NPID controllers for EV speed control. The proposed controllers, including conventional, arc tan, and NPID controllers, are used in cascade with an EV model. The Aquila Optimization algorithm tunes the controller gains, reducing Integral Time Absolute Error and integral square control signal

D.Mishra, M. Kumar Maharana [82] seeks to enhance the dynamic security of microgrids by using a frequency control approach based on virtual inertia control. The proposed microgrids system includes photovoltaics, wind-generating units, thermal power units, storage units, electric vehicles (EVs), and loads. A cascaded PIDFN controller is optimized using a unique metaheuristic modified differential evolution (MDE) technique. The performance of the VIC-based MDE controller was compared to existing controllers using evolutionary optimization techniques, demonstrating that the proposed virtual inertia control strategy improves system dependability.

T.KanRoy, A.MaungThan Oo [83] introduces a cascaded controller for increasing transient and dynamic stability in load frequency regulation for low-inertia multi-area power systems (LIMAPSs) that combine solar photovoltaic and wind turbine electricity. The controller employs an adaptive neuro-fuzzy inference system (ANFIS) and a fractional-order proportional-integral-derivative (FOPI-FOPTI) control method. Simulations indicate that the controller effectively tackles load frequency control issues in LIMAPSs, surpassing existing control methods in settling time, overshoot, and defined goal functions.

Considering the instantaneous variation condition as a variable speed reference input to ensure a good running of the vehicle in terms of acceleration-deceleration relying on the classic method, such as A traditional PI controller is the familiar controller for regulating the speed of the motor. In the design of a speed controller, step response plays an important role. However, it is not able to provide quick responses for various speed references also it suffers from weakness in performance and robustness Furthermore, using the heuristics algorithms known as PSO and ACO to adjust the PI controller's parameters for controlling acceleration and deceleration of EVs during motoring and regeneration with testing the robustness under different angle road.

Structure of the thesis

This thesis is structured into five cohesive chapters, each serving a specific purpose in advancing the understanding and application of BEV and HESS.

Chapter I: State of the Art of Electric Vehicle

This chapter offers a Historical background to electric vehicles, followed by a brief definition with Various parameters that can be considered for consumer trends, providing an overview of their key components such as power sources as well as driving cycle, electric engine, energy storage system are presented, and then the static converter systems, Energy management and Regenerative braking are introduced, Topologies principles, diverse applications, the chapter end with the positive and negative impact of electric vehicle.

Chapter II: Photovoltaic Energy Conversion: Principles, Modeling and Simulation

This chapter provides the foundational knowledge necessary to delve deeper into the specific components and application of PV in the second part of the chapter, which involves mathematical and simulation-based approaches to represent the behavior of photovoltaic system under different environmental conditions, such as Variable Solar Effect, variable temperature effect and Gradual ramp evolution of irradiation.

Chapter III: Overview of energy system storage

This chapter presents a complete introduction of energy storage devices, such as mechanical, electrochemical, thermal, chemical, and electrical batteries and supercapacitors. It describes each model's specifications and attributes, and evaluates its performance, on the other hand, offers an in-depth analysis of the hybrid energy storage technologies and topologies in renewable energy systems.

Chapter IV: Modeling, Analysis and management of batteries-supercapacitors energy storage

This chapter focuses on the development of a comprehensive model for a PV connected with battery-supercapacitor system, The model outlines the system's components, behavior, and interactions, followed by a discussion of the design and optimization of PI controllers employing metaheuristic optimization methods such as GA, ACO, and GWO algorithms with deep comprehension for EMS of HESS integrating batteries and SC, as well as a new heuristic methodology for fine-tuning the parameters of a PI controller to control the power flow and performance of battery charge and discharge and SC storage.

Chapter IV: Application of metaheuristic algorithm on battery electric vehicle

Is dedicated to the modeling of the traction system components, namely vehicle dynamics, transmission, electrical machines, and energy sources, this chapter discusses the use of speed variation in optimizing acceleration and deceleration in generation systems using a conventional PI controller and metaheuristic algorithms like Particle Swarm Optimization and Ant Colony Optimization. The dynamic behavior of these systems is evaluated using simulation software, proving the effectiveness of control schemes and dynamic performance.

Conclusion and Prospects for the Future

The thesis's primary conclusions and contributions are summed up in the conclusion. It talks about how various metaheuristic algorithm approaches are integrated for photovoltaic solar connected with hybrid energy storage, and their crucial role in battery electric car systems under different conditions. Additionally, it looks at possible directions for further study and development in this area.

Chapter I
State of the art of electric vehicle

I.1.Introduction

Electric vehicle technology is moving away from mobility that relies on burning fossil fuels and toward vehicle electrification, where pollutants and CO₂ emissions are being decreased and primary energy is becoming more sustainable, this chapter presents a details historical background followed by a brief definition of the term “electric vehicle”. Then, we are interested in technology and sustainability electric vehicle articles publication in different years ,in addition ,we explore the Worldwide electric vehicle sales from 2020 to 2040 , in second part of this chapter , we considerable attention serval's topologies of electric vehicle such as : BEV, FCEV, MHEV,EREV ,PHEV and HEV ,We then explore the general description of the traction chain (driving cycle , electric machine ,energy sources, static converters, Gear box ,and regenerative braking). finally, the chapter closes with a summary conclusion.

I.2.Historical Background

The automotive sector has emerged as one of the most significant industries globally, impacting not only the economy but also the realms of research and development. Technological advancements in vehicles are being integrated more and more, aiming to enhance the safety of both passengers and pedestrians. Furthermore, the rising number of road vehicles facilitates swift and comfortable transportation. Historically, and on a global scale, EV development has known different major eras:

- In 1828, Hungarian inventor Anyos Jedlik István created a mechanism similar to a skateboard that used an electric motor [84].

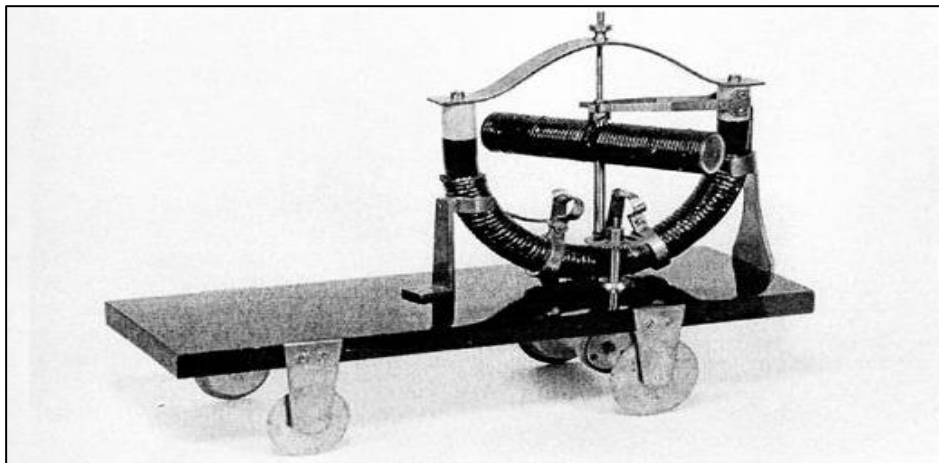


Figure I.1. Jedlik’s electric car in 1828 [85].

- In 1835, English inventor Robert Anderson introduced the first electrically propelled carriage-type vehicle at an industrial convention. It utilized a disposable battery fueled by crude oil. In the same year, Professor Sibrandus Stratingh (The Netherlands) and his colleague Christopher Becker constructed a three-wheeled electric vehicle. Where began with Sibrandus Stratingh presented "Electromagnetic Moving Force and the Use of This to an Electromagnetic Carriage" at the Royal Physics Society in Groningen. He was inspired to create a small-scale electric cart after reading about Moritz von Jacobi's work at the Academy of Sciences in St. Petersburg, Russia. After and in

the same year, Thomas Davenport, an American inventor, developed the first electric vehicles. The early electric vehicles were crude, reaching just 12 km/h [86-87].



Figure I.2. Sibrandus Stratingh 's electric horseless carriage [85].



Figure I.3. Thomas Davenport and the First Electric Car [86].

- In 1837, Scottish inventor Robert Davidson created an innovative electric motor in Scotland, which was powered by galvanic cells, commonly known as batteries. Subsequently, he constructed a larger locomotive named Galvani, which was showcased at the Royal Scottish Society of Arts Exhibition in 1841[88]. This vehicle, weighing 7,100 kilograms (7 long tons), was equipped with two direct-drive reluctance motors. These motors utilized fixed electromagnets that interacted with iron bars affixed to a wooden cylinder on each axle, along with basic commutators. The locomotive was capable of pulling a load of 6,100 kilograms (6 long tons) at a speed of 6.4 kilometers per hour (4 mph) over a distance of 2.4 kilometers (1.5 miles). It underwent testing on the Edinburgh and Glasgow Railway in September of the following year; however, the limited power supplied by the batteries hindered its widespread application. Ultimately, it was dismantled by railway workers who perceived it as a threat to their job security. Additionally, between 1832 and 1839, Robert Anderson, another Scottish inventor, developed a rudimentary electric carriage. In 1840, a patent was granted

in England for the use of rails as conductors of electric current, followed by similar patents awarded to Lilley and Colten in the United States in 1847 [89].



Figure I.4. Robert Davidson Galvani Electric locomotive [88].

- In 1860, French scientist Gaston Plante created the first rechargeable lead-acid battery [89]. In 1882, William E. Ayrtton and John Perry (England) created a three-wheeled electric vehicle (EV) with two batteries that could be switched to adjust speed [90]. Thomas Parker is credited with producing the first electric vehicle (EV) in 1884 [91], before Karl Benz's petrol-powered Motorwagen in 1886 [92]. William Morrison (US) created a six-passenger electric vehicle capable of reaching 23 km/h in 1895 or between 1887 and 1890.
- The EV "La jamais contente" surpassed 100 km/h in 1899 [93]. About 40% of US automobiles were electric battery-powered cars at the end of the 19th century; the remaining 40% were steam or gasoline-powered. Although EVs were pleasant and clean, their batteries were costly and inefficient, and they could only travel a few kilometers. They also used a battery exchange mechanism, wherein used batteries were taken out and charged at service stations. Borland Electric's EV traveled 100 miles from Chicago to Milwaukee before the turn of the century, it had Michelin tires and was fashioned like a torpedo charging its batteries overnight and making the same journey the following day.



Figure I.5. La jamais contente [93].

In the early 20th century, EVs and gasoline cars had comparable speed and range. Between 1900 and 1910, 38% of New York City's cabs were electric, with vibration-free operation and complicated recharging systems. In comparison, 40% were steam cars that required over 45 minutes to make steam and continuously poured water, while 22% were gasoline-powered cars that were difficult to start and caused smoke and vibrations. Between 1909 and 1914, the Fritchle business delivered over 200 electric buses for public transit, each capable of traveling 100 miles on a single charge. In 1912, EV sales peaked [94]. In 1914, Henry Ford and Thomas Edison collaborated to explore low-cost EV options. The discovery of big oil wells, cheaper gasoline, and improved ICEVs, including Henry Ford's Model T in 1908, led to a shift from electrical charging methods to thermal propellants. In 1912, Ford's mass production of automobiles resulted in gasoline cars costing nearly three times cheaper than electric vehicles [95]. In the same year, Charles Kettering created the first electronic starter, eliminating the need for a manual crank for running ICE vehicles. Several reasons contributed to the decline of EVs in the US during the next decade [96-99]. During the 1930-1940s, Germany used electric vehicles (EVs) [99]. The electric vehicle concept was not rethought until the 1970s oil crisis, when gasoline costs skyrocketed [100]. In 1969-1970, General Motors created the GM XP 512E EV prototype for cities.

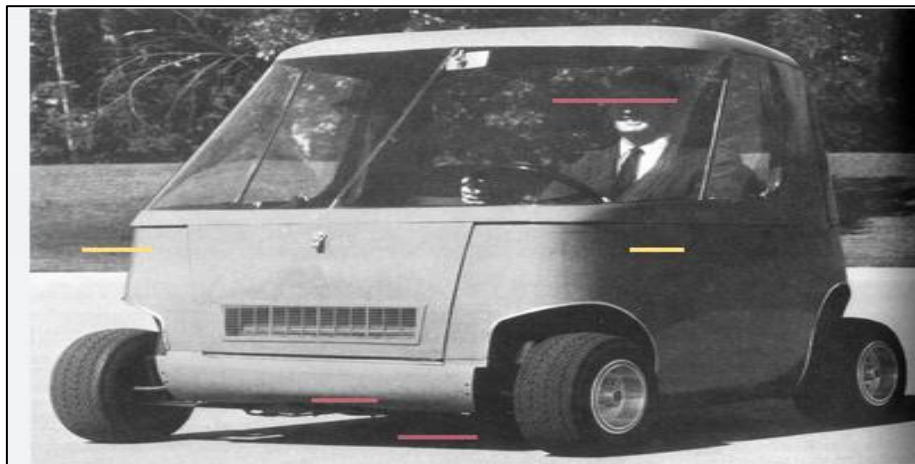


Figure I.6. GM XP 512E EV prototype [100].

- NASA's Lunar Rover EV, with a speed of 13 km/h and a range of 90 km, was utilized on the Moon's surface during the Apollo 15 mission in 1971 [101]. The 1974 Citicar is another example of an electric vehicle from the same era [102]. In 1976, Chevrolet introduced the Electrovette [103], while Volkswagen unveiled the Elektro-Golf, which resembled the original Golf GTi.
- In 1979, Chrysler introduced the ETV-1 Electric Car [104] and the Comuta EV [105]. All variants had restricted top speed (72 km/h) and autonomy (64 km). In the 1980s, environmental studies identified ICEVs as a major source of pollution in large cities [106]. In the late 1980s, Nickel Metal Hydride (Ni-MH) batteries were available, and Lithium batteries with better energy density were on the horizon (1991). Because of the pollution levels during these years, the California Air Resources Board decided that by 1998, two percent of automobiles sold should be emission-free, and by 2003, that number should rise to ten percent. General Motors started producing the all-electric GM EV1

on a large basis in 1996. However, removed all EVs from the market when the zero-emissions criterion was suddenly modified to low emissions after thousands of units had been sold. Users were formally informed that this procedure was necessary since the batteries' usable life had come to an end [107]. The creation of hybrid cars that used Ni-MH batteries to power a gasoline engine came next.

- In 1997, Toyota introduced the Prius in Japan.



Figure I.7. Toyota Prius [107].

- In 2000, it became the world's most popular hybrid model after successfully expanding its availability globally [108].
- In response to rising gasoline prices, automakers restarted EV production in 2007 [109].
- In 2008-2009, Tesla created a fully electric Tesla Roadster with a lithium battery and 320 km of autonomy [110].



Figure I.8. Tesla Roadster [110].

- With a range of more than 1003 kilometers on a single charge, the Japan Electric Vehicle Club turned a Daihatsu Mira into an EV in 2010 [111]. In that same year, the EV "Venturi Jamais Contente" achieved a top speed of 515 kilometers per hour. Meanwhile, under actual cooling/heating and traffic circumstances, the "Lekker Mobil" covered 605 kilometers from Munich to Berlin on a single 115 kWh charge.



Figure I.9. Electric car Venturi Jamais Contente [111].

- In 2010, Chevrolet announced the Volt E-REV, an extended-range electric car. This method transmits power to the wheels entirely through electricity, which originates from two sources: vehicle batteries and the conversion of fuel into electricity [112].



Figure I.10. Electric car Volt E-REV[112].

- Nissan's Nissan Leaf, a zero-emission automobile, became the best-selling vehicle worldwide. Toyota and EDF began testing a hybrid automobile based on the Prius in 2010 and 2011, with plans for eventual commercialization. The experiment took place in Strasbourg. This hybrid petrol automobile can recharge from a residential electrical plug, allowing it to run only on electricity for short trips and use fuel for longer ones [113].
- The most recent hybrid vehicle idea with PAC was on display at the 2012 Geneva Motor Show [114].
- In 2013, the Drayson Racing Technologies B12/69EV achieved 330 km/h [115].
- In 2014, Nissan's ZEOD RC achieved 300 km/h [116].
- In 2017, the Rimac Concept achieved 1088 horsepower, comparable to the famed Bugatti Veyron's 1001 hp[117].
- In 2021, the 'e-Miles' was introduced for city driving. It features a joystick, 90% 3D printed parts, smartphone control, and automated driving capabilities [118].

- The luxury "Lucid Air" was introduced in 2022 with a 520-mile range, exceeding the 500-mile range anxiety barrier that consumers had with EVs in comparison to ICEVs [119].
- In 2023 and 2024, EV advancements focused on improving autonomy, safety, and battery reliability [120], expanding the number of fast chargers available to residents [121], and lowering EV prices to encourage user adoption.

I.3. Electric vehicle

Electric vehicles (EVs) are environmentally friendly alternatives unlike combustion-engine vehicles, as they don't produce pollutants and can be powered by various sources like renewables. They can be connected to the car through electrical cables, wireless charging, or overhead power lines. EVs can recover braking energy as electricity, resulting in an efficiency of 80% compared to thermodynamic engines' 25% efficiency. Which runs on an electric motor rather than an internal combustion engine that produces power by burning a combination of fuel and gasses is known as an electric vehicle (EV) [122].

Road and rail vehicles, surface and underwater watercraft, electric aircraft, and electric spacecraft are all considered EVs.

EV's include road and rail vehicles, surface and underwater vessels, electric aircraft, and electric spacecraft. also, an electric vehicle can be self-sufficient using a battery, solar panels, fuel cells, or an electric generator to turn fuel into energy, or it can be fueled by electricity from sources outside the vehicle via a collector system [123].



Figure I.11. Electric Vehicle [123].

I.4. Descriptive analyses

Figure I.12 displays a descriptive analysis of article distribution by year, indicating a consistent increase in publications on battery technology, EVs, and sustainability, reflecting changing research and industry objectives. Earlier research (the 1970s-2000s) concentrated on fundamental battery science. In the 2000s, growth surged due to breakthroughs in lithium-ion batteries and EV adoption, which prioritized energy density and safety. Renewable energy legislation and lower battery costs led to significant growth from the 2010s to 2020, peaking in 2020-2025 [124]. The focus was on zero-emission automobiles, battery longevity, and recycling. Future developments include solid-state batteries, quick

charging, and second-life uses, with multidisciplinary research combining IA and life cycle evaluations. This progression emphasizes the importance of DTM in analyzing developing research issues. The growing interest in electric vehicles and power and energy management has led to a significant increase in publications from the electrical engineering community. Electric vehicles are now considered a new electrical equipment category with unique features, offering opportunities for research and development contributions in electrical engineering. Power and energy management of energy storage systems within vehicles is a growing area of interest. Previous studies have examined EV technology from various perspectives, providing a comprehensive picture of current EV technology and future development capabilities. Future research in the EV sector should focus on developing challenges and addressing the dynamics underlying adoption. Advanced electric machines and control strategies for electric vehicles are also being explored, as are charging systems and the integration of renewable energy sources. Future trends and challenges in EV charging and grid integration are summarized for future direction.

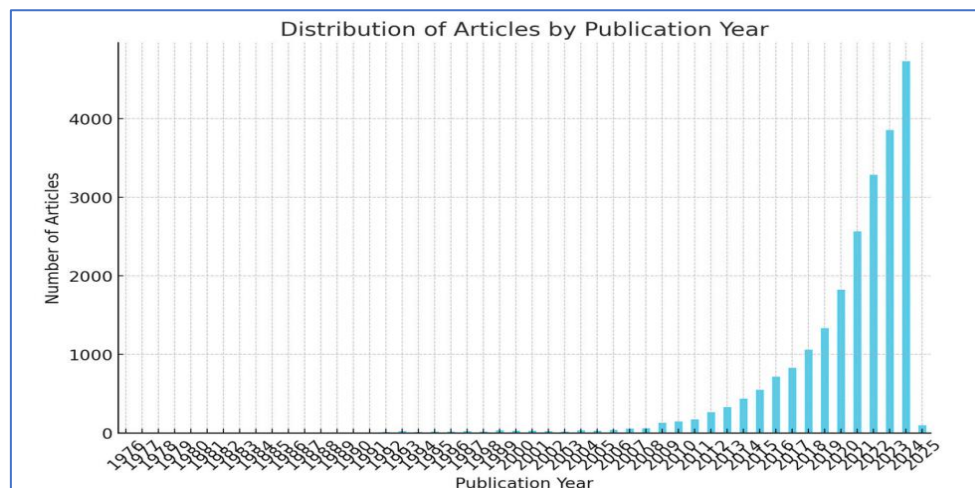


Figure I.12. Electric vehicle battery technology and sustainability articles by publication year [124].

Figure I.13 depicts a descriptive analysis of the top twenty journals in the dataset. Leading publications include *Renewable and Sustainable Energy Reviews* and the *Journal of Energy Storage*. Featuring over 1000 publications on sustainability in EV and battery research. Journals like the *Journal of Power Sources* and *Energies* specialize in energy systems, whereas *Energy Storage Materials*, integrated in EV, and the *Journal of Cleaner Manufacturing* emphasize material science and sustainable manufacturing. *World Electric Vehicle Journal* focuses on EV research and power management, but multidisciplinary journals such as *IEEE Access* and the *International Journal of Hydrogen Energy* include engineering, hydrogen, and alternative fuels. New publications, such as *Nano Energy*, focus on breakthrough battery technology connected with EVs and provide specific evaluations on sustainable and specialty themes.

Figure I.14 shows publishing patterns related to EVs, including battery technology, charging techniques, sustainable EV energy reviews, and renewable energy storage research. The *Journal of Power Sources* has a long history of advancing battery and EV technology, whereas *Energy Storage Materials* and *World Electric Vehicle Journal* have recently expanded to meet the growing need for specialized

study for electric vehicles including different energy storages. Journals such as Applied Energy and Energies focus on renewable energy and its role in electric vehicles, while interdisciplinary journals like IEEE Access, International Journal of Hydrogen Energy, and Journal of Cleaner Production bridge engineering and environmental science. Nano Energy, an emerging publication, focuses on advanced materials and showcases the field's progress toward innovative EV and battery solutions.

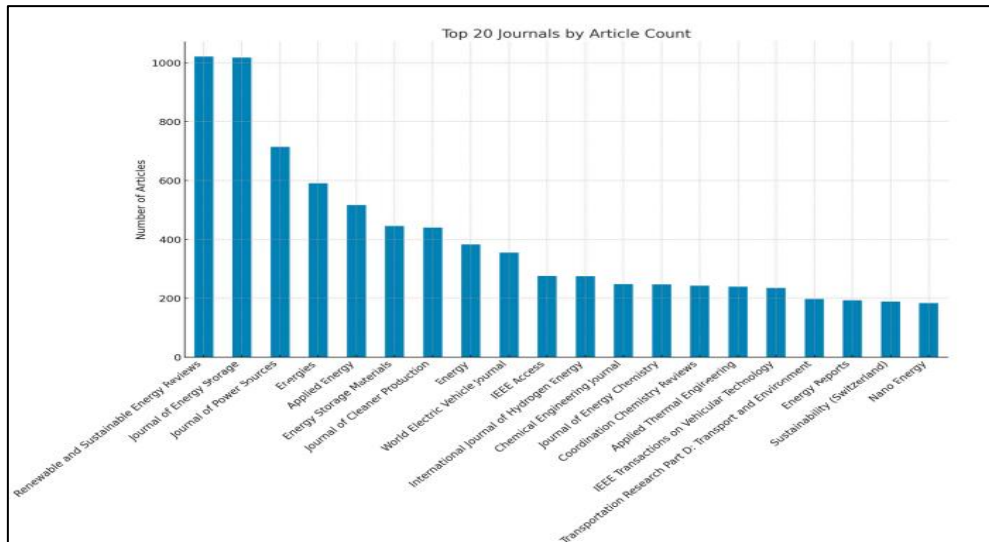


Figure I.13. Top 20 journals by EV article count [125].

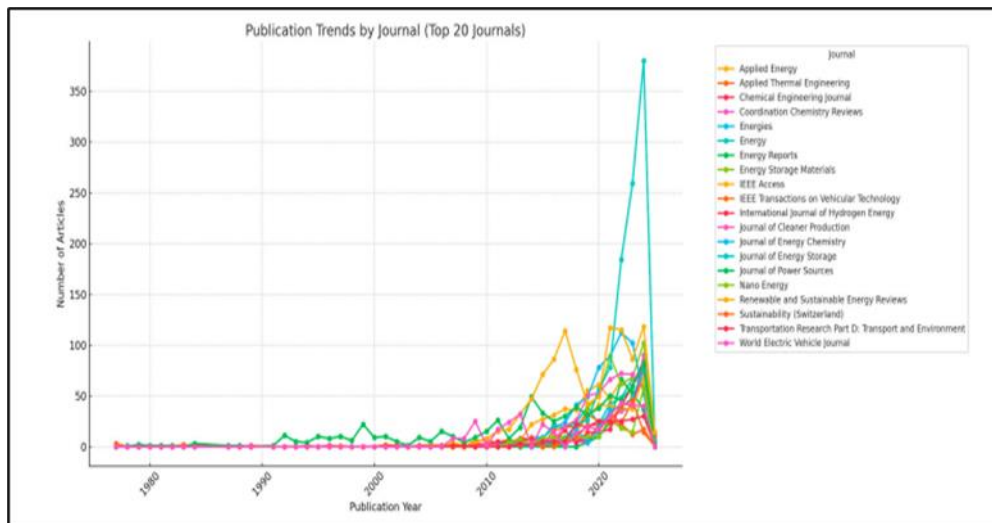


Figure I.14. EV Publication trends by journal [125].

I.5. Worldwide electric vehicle sales

A sharp rise in EV market share is seen in all areas according to Canalis, especially after 2025, as Figure I.15 illustrates the anticipated adoption of EVs in key automotive markets from 2020 to 2040. By 2040, China is expected to account for around 50% of new car sales, making it the leader in EV adoption. Europe is not far behind, while the United States has a slower but still noteworthy development trend. However, EVs currently make up a small fraction of the global vehicle fleet compared to over 1.5 billion internal combustion engine vehicles. The steep upward trends for all regions indicate a significant shift in the automotive market over the next decade. A notable inflection point occurs around 2025-2026

when the rate of EV adoption accelerates in all markets. This projected growth in EV market share represents a major transition in the automotive industry, Inequitable taxing practices that vary from nation to nation and area to area impact pricing strategies. As a result, a significant portion of the public is beginning to favor electric vehicles. A considerable change in electric mobility is shown by the composition, which has altered dramatically in favor of private and public EVs and is now on the rise [125-126].

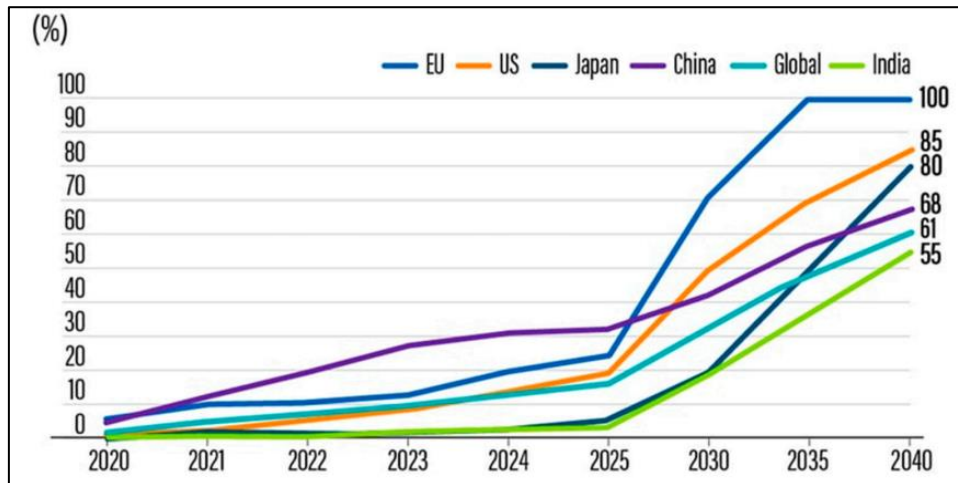


Figure I. 15. Worldwide electric vehicle sales [126].

I.6. Various parameters that can be considered for consumer trends of EVs

Currently, EV adoption is low due to its newness and limited market share. Understanding consumer needs and developing EVs to compete with ICE is crucial for EVs to gain market share and environmental benefits.

a) Price range

Electric vehicles are purchased based on their value for money, leading to a rational purchasing model. Although EVs have high initial costs, they offer the potential for fuel and efficiency savings in the future, which is a positive aspect for consumers.

b) Social and psychological acceptance

Society significantly influences the choice of goods, and information and understanding significantly influence the market of electric vehicles (EVs). Adoption depends on personal knowledge about EVs, making it crucial for the government to inform the general public about their advantages. However, "range anxiety" often arises due to EVs' limited battery range.

c) Charging station availability

The existing infrastructure for charging stations in developing countries is insufficient due to the emerging electric vehicle market. Consumers are often deterred from visiting charging stations because of their distance and limited availability. Users tend to spend more time at charging facilities compared to traditional fuel stations. The small number of stations impacts charging times and necessitates the development of more infrastructure. Setting up a home charging station requires obtaining a license,

which can be challenging, expensive, and requires a substantial investment. The chart indicates a notable increase in both the number of charging stations and electricity needs for electric vehicles from 2010 to 2025, highlighting the urgent requirement for expansion and adequate energy resources to accommodate future EV demands [126].

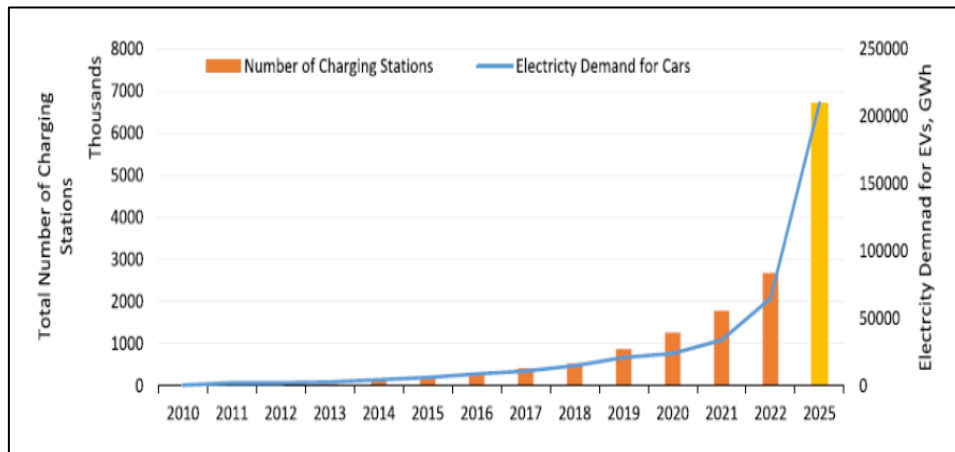


Figure I.16. Charging Station and Electricity Demand for cars increment over the years [126].

d) Technological Advancements

- Improved battery technology and range, including lithium-ion and solid-state chemistries.
- Improved energy efficiency in electric vehicle powertrains and aerodynamics.
- Software and Connectivity: AA, OTA updates, and smart features.
- Autonomous and IA Integration: Consumers are interested in self-driving electric vehicles [123-125].

I.7. Electric Vehicles Taxonomy

There are several sorts of electric vehicles based on engine technology. In general, they are divided into five categories.

I.7.1. Battery Electric Vehicles (BEVs)

Vehicles are propelled entirely by electricity. BEVs operate without an internal combustion engine or liquid fuel. BEVs often require big battery packs to provide adequate autonomy. A normal BEV has a range of 160 – 250 *km*, with some capable of traveling up to 500 *km* on a single charge [126-127]. The Nissan Leaf is an example of a fully electric car with a 62 *KWh* battery and a 360 *km* range [128].

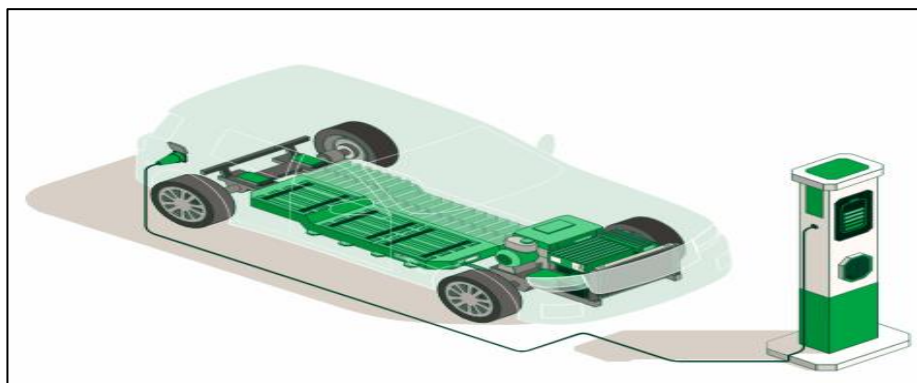


Figure I.17. Battery Electric Vehicles [128].

I.7.2. Hydrogen Fuel Cell Electric Vehicles (FCEVs)

FCEVs are driven by hydrogen fuel cells rather than batteries and are fueled by renewable energy sources. This kind of vehicle also includes an electric motor, but it uses a fuel cell to generate power when it's needed rather than a battery to store the energy. This device, typically a hydrogen cell, produces electricity by a chemical reaction known as electrolysis, in which hydrogen undergoes oxidation and loses electrons, which are then gathered to produce the electric current that permits motion. The Hyundai Nexu FCEV is an example of this type of vehicle, being able to travel 650 km without refueling [129].

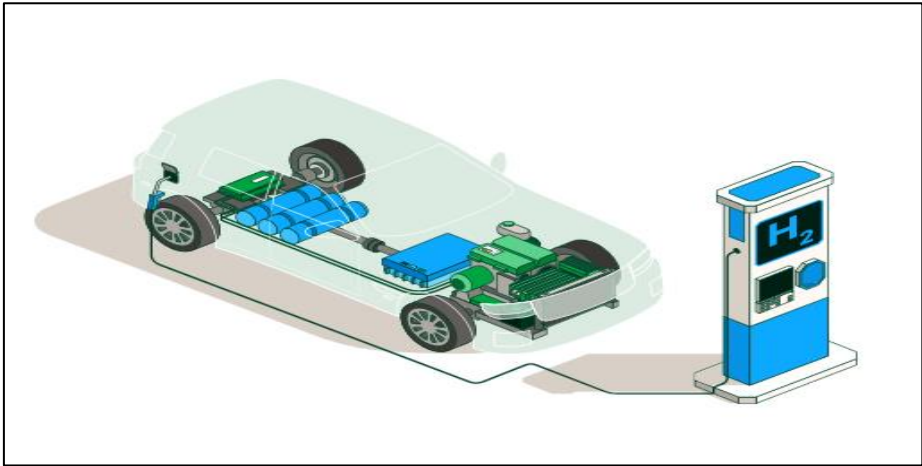


Figure I.18. Hydrogen Fuel Cell Electric Vehicles [128].

I.7.3. Mild-Hybrid Electric Vehicles (MHEVs)

Micro-hybrid automobiles are also known as MHEVs (Mild Hybrid Electric Vehicles), mild hybrids, or 48V hybrids. These cars use a mild hybrid powertrain, combining an internal combustion engine with a tiny electric motor. The battery is smaller than a standard 48V hybrid and cannot power the car alone [129]. Electric power supports the internal combustion engine during acceleration and in simpler systems like illumination and navigation. This kind of vehicle needs gasoline to move. Conversely, the battery is charged using energy produced while driving, particularly braking and decelerating, when the electric motor is a generator to collect energy and stores it in the battery.

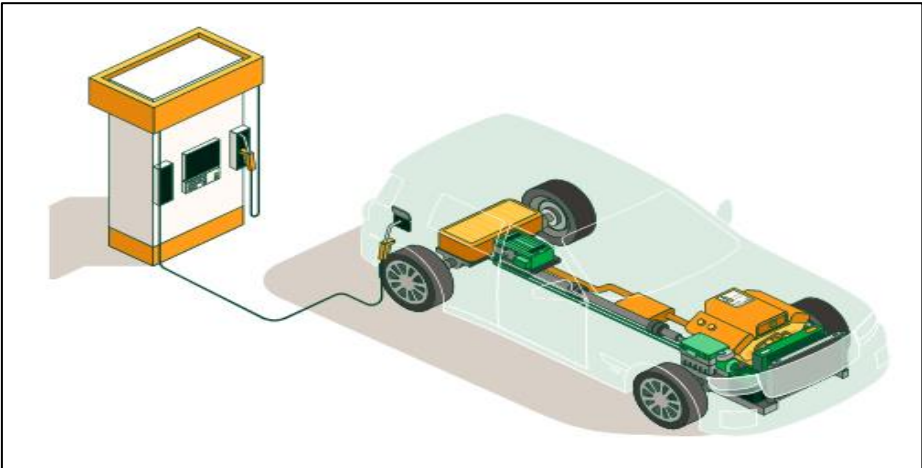


Figure I.19. Mild-Hybrid Electric Vehicles [128].

I.7.4. Extended-Range Electric Vehicles (EREVs)

Extended-Range Electric Vehicles (EREVs) combine EV and PHEV capabilities. EREVs may be charged using electricity or fuel via the internal combustion engine. EREVs offer the economy and low emissions of electric vehicles while overcoming the range restrictions of combustion engines as a backup. These cars are similar to those in the BEV category. ER-EVs have a supplemental combustion engine that can charge the vehicle's batteries as needed. Unlike PHEVs and HEVs, this engine is just used for charging and does not power the vehicle's wheels. The BMW i3 [129] is an example of this sort of car, with a 42.2 kWh battery that provides 260 km of electric autonomy and an extra 130 km in extended-range mode [130].

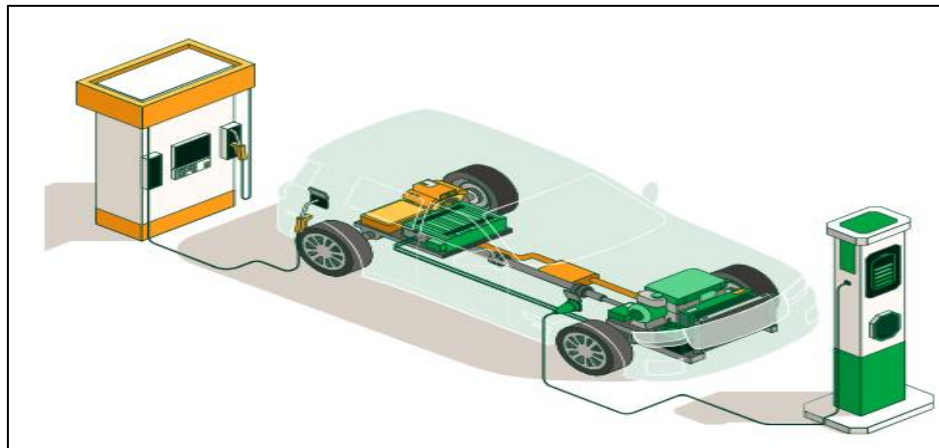


Figure I.20. Extended-Range Electric Vehicles [128].

I.7.5. Plug-in Hybrid Vehicles (PHEVs)

Plug-in Hybrid Electric Vehicles (PHEVs) have an internal combustion engine, electric motor, and battery. These models use both a combustion engine and an electric motor to drive the vehicle's wheels. They can operate in electric mode for a limited range or in hybrid mode, combining the power of both. PHEVs may store power from the grid, considerably reducing fuel use while ordinary driving. The Mitsubishi Outlander PHEV has a 12 kWh battery, allowing for about 50 km of electric driving [131-132]. However, it is important to note that PHEVs consume more gasoline than carmakers claim. The battery may be charged using an external power source or charging station. Additionally, the combustion engine can be utilized to charge the electric motor. Compared to fully battery-electric cars, these vehicles have a longer range and provide the driver more freedom to choose between using gasoline or electricity as needed.

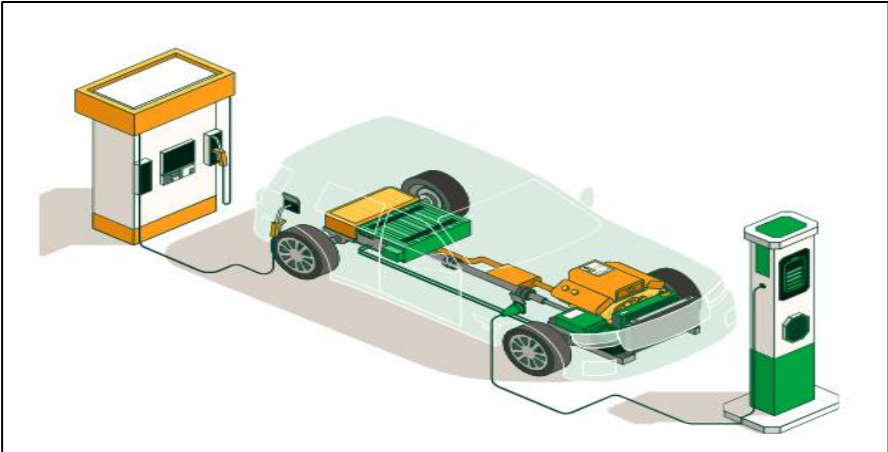


Figure I.21. Plug-in Hybrid Electric Vehicles [128].

I.7.6. Hybrid Electric Vehicles (HEVs)

Hybrid Electric Vehicles (HEVs) integrate a minimum of two energy sources for propulsion. They are propelled by a combination of an electric motor and a traditional internal combustion engine, often powered by gasoline or diesel. The internal combustion engine can be de-energized to use less fuel and get assistance from the electric motor during periods of high demand. Compared to conventional cars, HEVs offer lower pollutants and better fuel economy, particularly in conditions involving frequent stop-starts [133]. Compared to fully battery-electric cars, these vehicles have a longer range and provide the driver more freedom to choose between using gasoline or electricity as needed. Although hybrids may operate entirely on electricity, their range is constrained by tiny batteries. They frequently use internal combustion engines and regenerative braking to provide kinetic energy and charge the batteries. In more recent models, the energy produced during braking may also be used to charge the batteries by converting the kinetic energy into electrical energy. With its 1.3 kWh battery, the fourth-generation Toyota Prius hybrid car could potentially travel up to 25 kilometers on electricity alone [134].

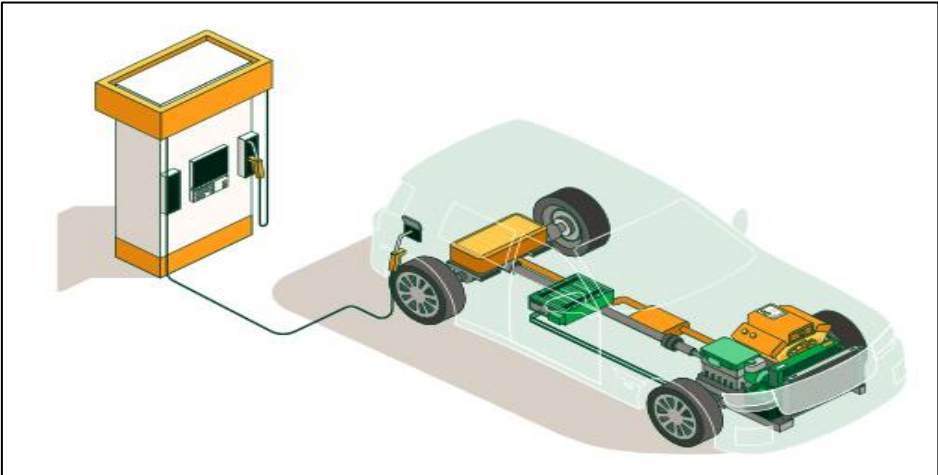


Figure I.22. Hybrid Electric Vehicles [128].

I.8. Electric car technical elements

I.8.1. Driving Cycle

The driving cycle, or graphic showing the driving vehicle's speed over time, represents the sequence of driving vehicle behavior on the specified territory. Real-time driving cycle development is crucial for several reasons, including fuel and energy consumption research and vehicle pollution management. accelerating mode, cruising mode, and decelerating mode are the various operational situations that are classified in any driving cycle.

The typical driving cycle, which consists solely of steady acceleration and speed phases, is synthesized. In contrast to the natural driving cycle, these shifts are primarily artificial. In addition, the driving cycle is the graph that shows the vehicle speed (km/h) over a journey time (s). The driving cycle pattern is used to develop the EV's components. The kind of road and its condition, traffic patterns, and driver behavior all influence driving patterns. Several typical driving cycles are dependent on various nations. Figure I.23 shows a few of the commonly used basic drive cycles.

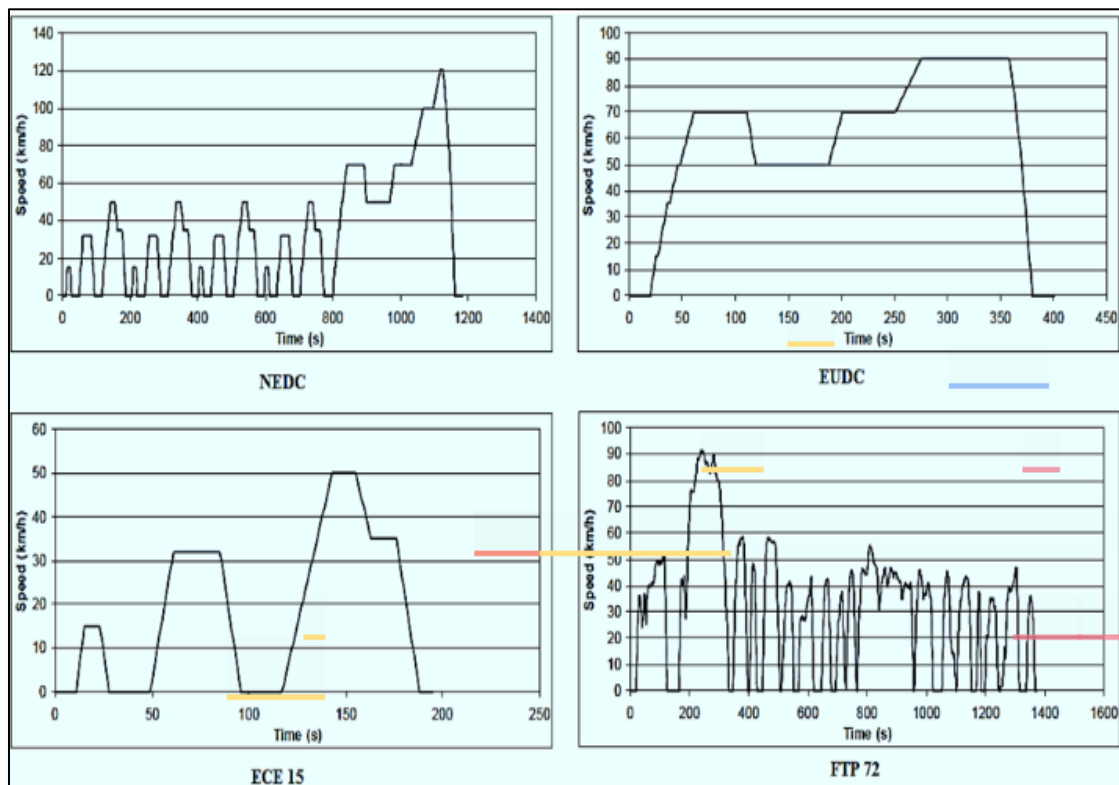


Figure I.23. Standard driving cycles [135].

I.8.2. Electric machine

1.8.2.1. AC Motors in EVs

Many contemporary electric cars depend heavily on AC motors, which provide strong performance and great efficiency, particularly at higher speeds. These alternating current motors are available in a variety of types, each with unique properties that make them suitable for a range of EV industry applications.

I.8.2.1.1. Types of AC Motors in EVs

The different types of electric motors are:

a) Synchronous motor

An electric motor that runs at a synchronous speed is called a synchronous motor. A revolving magnetic field that rotates at a synchronous speed is created when the stator windings are subjected to the AC supply voltage. The supply frequency and poles determine the synchronous speed.



Figure I.24. Asynchronous motor [136].

b) Asynchronous motor

The term "asynchronous motor" refers to motors that do not operate at synchronous speed. Another name for them is induction motors. EMF is produced in the rotor by the slip that occurs between the synchronous speed and the rotor speed. Current begins to flow in the rotor as a result of its short circuit. The rotor rotates because of the interaction between the rotor current and the revolving magnetic field, which generates torque.



Figure I.25. Synchronous motor [137]

1.8.2.2. Types of DC Motors in EVs

I.8.2.2.1. Brushed DC Motors

Brushed DC motors, the first commercial application of electric power, were used for over 100 years in commercial and industrial buildings [138]. They can be varied in speed by changing the operating

voltage or magnetic field strength. Thus, using power electronic devices has replaced brushed motors in many applications. These motors provide electrical current to their spinning component via brushes.

They are economical due to their straightforward design and ease of handling. But because of brush wear, they need to be maintained regularly.



Figure I.26. Brushed DC Motors [138]

I.8.2.2.2. Brushless DC Motors (BLDC):

Brushless DC motors use electronic communication to do away with the requirement for brushes. Longer longevity, reduced maintenance, and increased efficiency are the outcomes of this. Modern EVs frequently employ BLDC motors because of their dependability and efficiency. In addition, (BLDC) motors can function in a way that is opposite to the design of brushed motors by arranging the windings on the stator and the permanent magnets on the rotor. In place of mechanical brushes and commutators, electronic controllers manage the current flowing through the stator windings to create a rotating magnetic field that drives the rotor. The motor's functioning may be precisely controlled thanks to this electronic commutation [139].

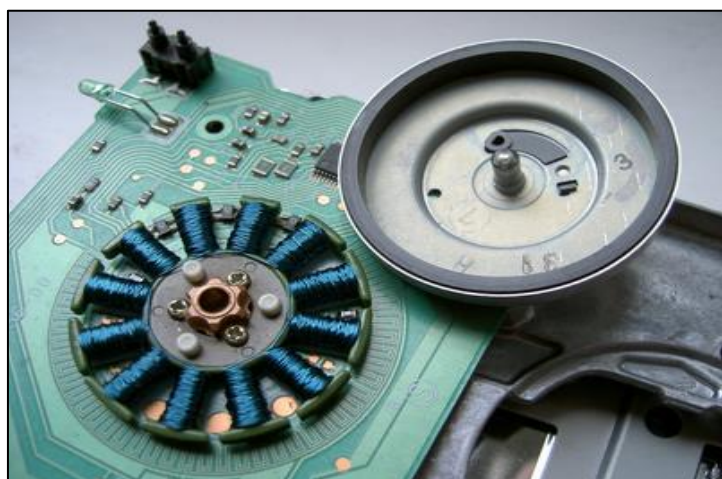


Figure I.27. Brushless DC Motors [138].

The essential requirement for EV motors is [139]:

- A wide speed range in areas with constant torque and power.
- A good torque response for dynamic operations.

- High efficiency for a wide range of speeds and torques.
- Effective regenerative braking; excellent reliability and dependability under various vehicle operating cases.
- A high power density and rapid power.
- A very high torque even at low speeds for starting and climbing.
- High power at high speeds during cruising.
- Affordable price.

1.8.2.3. Comparison between DC and AC motors

The distinctions between AC and DC motors must be taken into account when selecting the right motor for an electric vehicle. Every motor type has different advantages and disadvantages that affect things like cost, maintenance, performance, control complexity, and efficiency.

- **Performance and Efficiency**

In general, AC motors are more efficient and perform better at high speeds than DC motors. At lower speeds, DC motors especially BLDC models can offer similar efficiency and are simpler to manage.

- **Complexity and Control**

More complex and expensive EVs may result from the need for more advanced control systems for AC motors. DC motors, particularly brushed models, are easier to operate but may need more upkeep. BLDC motors are a good balance between low maintenance and moderate control complexity.

- **Upkeep and Sturdiness**

Brushless and AC motors provide greater longevity and fewer frequent maintenance requirements than DC motors with brushes, which need frequent maintenance because of wear and tear. In general, EV AC motors are more resilient and long-lasting over time.

- **Cost Factors**

AC motors provide greater long-term performance and cheaper operating costs, although potentially have higher startup costs because of their intricate control systems. Although DC motors, especially brushed ones, are initially less expensive, they may eventually require more maintenance.

1.8.3. Gearbox

The electric vehicle gearbox is a key component of the vehicle's transmission system. It guarantees that traction is effectively transmitted from the engine to the wheels. Most cars with internal combustion engines frequently feature multi-speed gearboxes that alter gear ratios [136-138]. When the electric motor generates steady power and torque. without having to change gears, the driver needs to use basic function buttons like *D* for forward, *R* for reverse, and *N* for intermediate state one level maintains the gear ratio constant, allowing the vehicle to function effectively. Additionally, shifting does not occur during abrupt acceleration or deceleration in electric vehicles with a one-level gearbox. This makes for a quiet and comfortable ride [140].



Figure I.28. Gear box in Electric Vehicles [141].

I.8.4. Energy Sources

To reduce CO₂ emissions and move toward renewable energy, electric vehicles, or EVs, are becoming more and more significant in the electrical sector. Energy density and power density are the two most crucial of these [138-142]. Indeed, additional properties like quick charging, extended service and cycle life, low cost, and simple maintenance would also be necessary for the ideal energy source. While high specific power enhances acceleration for short-range driving, high specific energy is required for long-range travel. Numerous energy storage systems (ESS) are explored, with varied combinations to fulfill different needs, because the best source requires a variety of qualities. For EVs to have a long driving range and dependable energy storage, ESS such as electrochemical, chemical, electrical, mechanical, and hybrid are necessary. The most versatile energy storage component for EVs, such as 2-wheelers, 3-wheelers, 4-wheelers, and mini-metro buses, is a battery. Auxiliary power needs in EVs are met by fuel cell, ultracapacitor, and flywheel technologies, particularly when batteries are inadequate for long driving range, low energy density, and a lack of recharging infrastructure [141]. The primary power source for fuel-cell or hydrogen-based electric vehicle (EV) technology is fuel cells (FCs). Because of their high power, ultracapacitors (UC) or supercapacitors (SC) are utilized during the initial power supply. Flywheels are also being considered as energy storage mediums due to their increased spinning speed due to torque, Flywheels are also being considered as energy storage mediums due to their increased spinning speed due to torque [143].

I.8.5. Power Electronics Converters in EV

The power electronic converters for EVs and HEV can be categorized into two groups such as unidirectional and bidirectional converters. These can also be DC–DC and DC–AC types. A brief description of each of them is given in the following:

1.8.5.1. DC-DC Converters

Figure I.29 illustrates the different types of DC-DC converters utilized in Applications of EV and HEV Unidirectional DC-DC converters are Utilized to provide power to auxiliary systems, including sensors and safety mechanisms. Utility, entertainment, and control devices, also can utilized in DC

drives for electric traction systems. Bidirectional converters are utilized during regeneration. Regenerative braking, backup power supply, and battery recharging. The Power transfer in bidirectional converters occurs from the low-voltage side to the high-voltage side, commonly referred to as commonly referred to as the boost operation. During the regenerative braking process, power transfers from the high-voltage side to the low-voltage side. Low-voltage side (used for battery charging), commonly known as the buck.

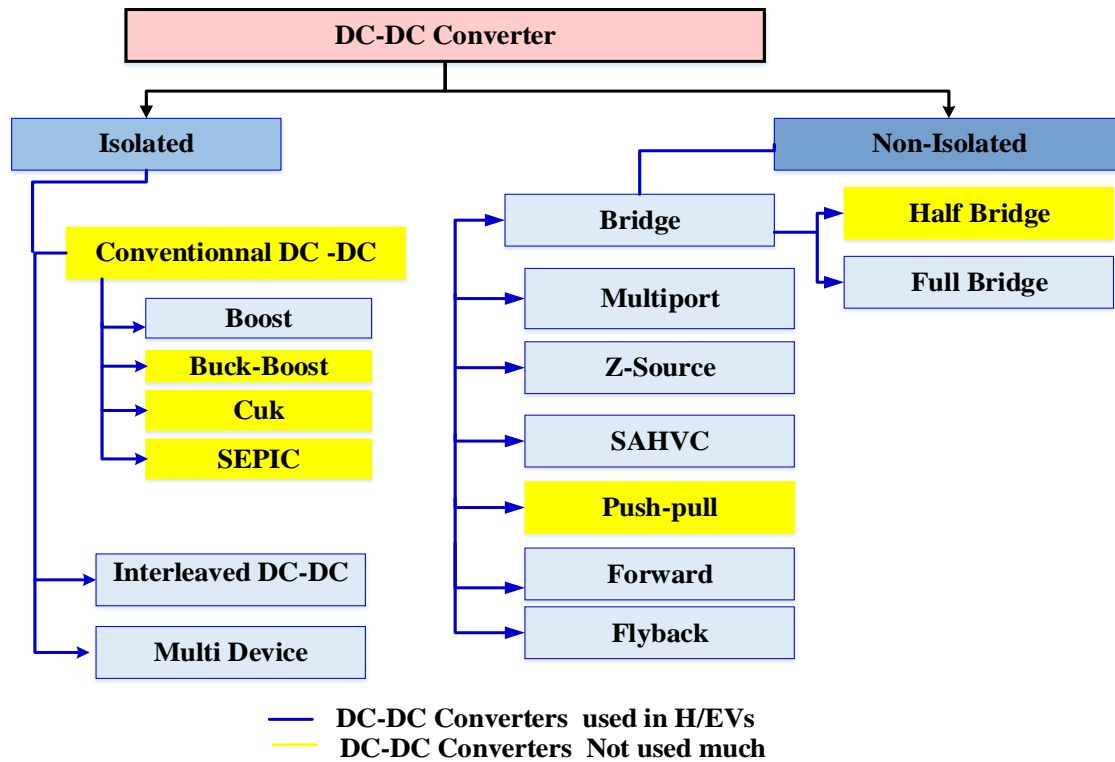


Figure I.29. DC-DC Converter in EV and HEV [144].

1.8.5.2. DC-AC Converters

A DC-AC converter, commonly referred to as an inverter, is utilized in vehicles where the propulsion motors operate on AC power. Inverters function to transform the steady DC battery voltage into a variable voltage and variable frequency AC voltage, which powers the electric traction motor. They are also employed to provide power for additional utility loads such as vehicle lighting and air conditioning. Often, a separate set of inverters is designated for this purpose. Generally, AC drives are supplied by inverters that operate using pulse width modulation (PWM). The most prevalent automotive drives are based on Voltage Source Inverters (VSI)[145]. A typical three-phase VSI comprises six bidirectional switches, each containing either an IGBT or MOSFET switch, depending on the system specifications, along with an anti-parallel diode. By regulating these switches and incorporating appropriate filters, the DC voltage input to the inverter is converted into a balanced three-phase AC output voltage with the desired magnitude and frequency[141-145]. Gallagher et al. conducted a comprehensive study focusing on the design aspects of inverters in electric vehicles, addressing switch selection, circuit design, and loss calculation. Beyond traditional PWM inverters, resonant DC link inverters, which feature series or

parallel resonant circuits, are also employed in battery-operated applications in electric vehicles. A classical review examining the development of various inverter topologies was conducted by Stemmler et al. Hoek et al. [146] discussed two topologies for traction inverters, specifically the B6C and H-bridge configurations. Jahns et al. [147] performed an extensive investigation into electric vehicles operating on rail and road systems. A novel inverter technology aimed at enhancing reliability for electric vehicles was introduced by Nakatsu et al. In addition, bidirectional DC-AC converters enhance the performance, efficiency, and controllability of hybrid electric vehicles (HEVs). These converters facilitate power transfer between the battery and the wheels through regenerative braking. Inverters used for traction in HEVs include voltage-source inverters (VSI), current-source inverters (CSI), impedance-source converters (ZSI), and soft-switching inverters. The ZSI architecture, particularly the quasi-ZSI version, offers significant advantages in terms of fuel economy and efficiency [148]. Researchers are developing innovative techniques and control algorithms to achieve zero voltage switching (ZVS) [149].

I.8.6. Energy management and Regenerative braking

Energy management in Electric Vehicles (EVs) involves a complex coordination of power flows facilitated by power electronics. This process mainly consists of channeling power from the battery to different subsystems within the vehicle, including the electric motor, heating, ventilation, air conditioning (HVAC) system, and other auxiliary systems [150]. Additionally, energy management encompasses the recovery of energy during regenerative braking. Regenerative braking is a system that transforms a vehicle's kinetic energy, which is typically wasted as heat during braking, into electrical energy that can be stored in the battery for future use. This method is an effective approach to prolong the driving range of an EV and lessen the strain on the mechanical brakes. Power electronics are crucial for facilitating regenerative braking. The procedure initiates when the driver engages the brake. The electric motor then functions as a generator, converting kinetic energy into electrical energy [151]. A power electronic converter, typically an inverter, oversees this process, managing the energy flow from the motor (operating as a generator) back to the battery.

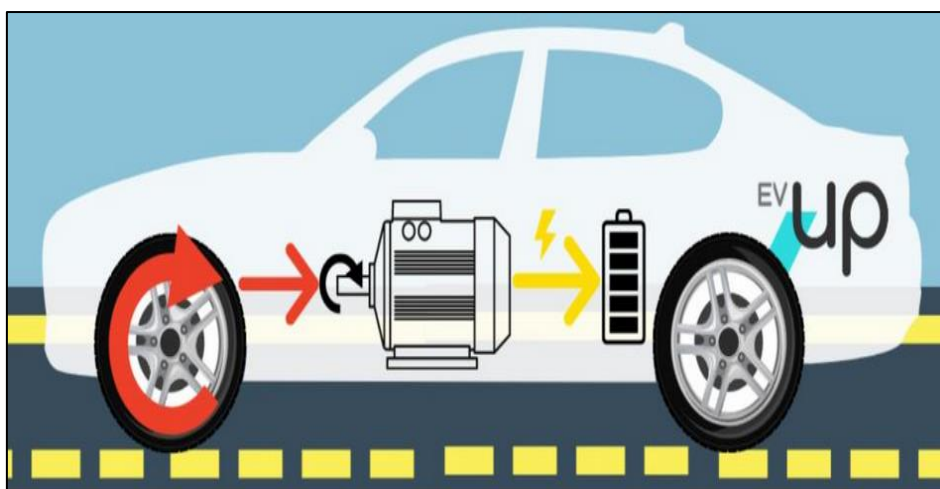


Figure I.30. Regenerative braking work in EV [150].

I.9.Charging of Electric Vehicles

There are several requirements for charging electric cars, and these are mostly determined by the area in which they are utilized. More precisely, the SAE-J1772 standard for loading electric cars is utilized throughout the Pacific and North American regions. However, the IEC-62196 standard was adopted in Europe, whereas the GB/T 20234 standard is utilized in China. The primary distinction between these three standards is that the latter group groups charging modes based on the charging power involved, whereas the first two groups them based on the power type (DC or AC power). The Tables (I.1, I.2, and I.3) establish the following Charge ratings of the SAE-J1772, IEC-62196, and GB/T 20234 [151-154].

Table I.1. Charge ratings of the SAE-J1772 [152].

Charge Method	Volts	Maximum Current (Amps-Continuous)	Maximum Power
AC Level 1	120 V AC	16 A	1.9 kW
AC Level 2	240 V AC	80 A	19.2 kW
DC Level 1	200 to 500 V DC maximum	80 A	40 kW
DC Level 2	200 to 500 V DC maximum	200 A	100 kW

Table I.2. Charge ratings of the IEC-62196 [153].

Charge method	phase	Maximum current	Maximum voltage	Maximum Power	Specific Connector
Mode 1	AC Single AC Three	16 A	230–240 V 480 V	3.8kW 7.6kW	No
Mode 2	AC Single AC Three	32 A	230–240 V 480 V	7.6kW 15.3kW	No
Mode 3	AC Single AC Three	32–250 A	230–240 V 480 V	60kW 120kW	Yes
Mode 4	DC	250–400 A	600–1000 V	400kW	Yes

Table I.3. Charging classification of the GB/T-20234 [154]

Mode	standard	Rated Voltage	Rated Current	Maximum Power
AC Charging	GB/T- 20234.2-2015	250V	10 A	27.7 kW
		250V	16A	27.7 kW
		250V	32 A	27.7 kW
		440V	16 A	27.7 kW

		440 V	32A	27.7 kW
		440 V	63 A	27.7 kW
DC Charging	GB/T-20234.3-2015	750–1000 V	80 A	250 kW
		750–1000 V	125A	250 kW
		750–1000 V	200 A	250 kW
		750–1000 V	250 A	250

I.10. Positive impact of EV

EVs are becoming a model of sustainability and environmental care due to their low emissions. They are designed to be environmentally friendly, using renewable energy sources like solar and wind power. The infrastructure required for EV deployment is being investigated for environmentally friendly solutions. Solar photovoltaic modules can lower charging costs and meet demand during high-demand periods. Recycling offers opportunities to recover valuable materials and lower life cycle costs. Battery electric vehicles (BEVs) can reduce environmental impacts by running on rechargeable batteries and reducing greenhouse gas emissions. The sustainable development of BEVs depends on circular economy strategies, focusing on resource efficiency, extending battery lifespan, and reducing reliance on virgin raw materials [156].

I.11. Negative impact of EV

Electric vehicles (EVs) have been a topic of debate due to their environmental impact and sustainability. The production technique, use over their lifetime, and disposal and recycling are the three main issues. Manufacturing EVs can demand more energy than conventional vehicles, and every kWh of battery capacity generates 150-200 kg of CO₂ emissions. The increasing demand for electricity to charge EVs also affects their environmental impact. Renewable energy is crucial for the production and charging of EVs. Proper recycling is essential for the effective application of EV technology, as batteries can cause environmental risks once they reach the end of their lifetime. The production impact of a lithium-based battery can vary depending on the chemistry used [157].

I.12. Conclusion

In summary, this chapter provides an overview of the electric vehicle. Subsequently, we introduced the significance of the electric vehicle, the bibliographical research conducted provides a comprehensive statistical and displays a descriptive analysis of EV article distribution by year. The chapter delves into a diverse understanding of the EV topologies, followed by insights into the design component and safeguarding of EVs. These fundamental insights pave the way for a deeper exploration of advanced topics and practical applications in the upcoming chapters.

Chapter II

**Photovoltaic Energy Conversion:
Principles, Modeling and Simulation**

II.1. Introduction

Photovoltaic (PV) systems are considered key technology due to sustainable power generation, local availability, environmental friendliness, simple technology, cost-effectiveness, and minimal system balancing. PV systems use solar cells to convert sunlight into electrical energy, which is based on the photovoltaic effect in semiconductors. These systems are modular, scalable, and environmentally friendly, making them suited for a wide range of applications, including small-scale residential installations and large-scale solar farms. However, the power production of PV modules is dependent on environmental conditions such as sun irradiance and temperature, which change during the day. This fluctuation poses issues in guaranteeing optimal energy extraction and distribution. To overcome these issues, innovative control tactics such as Maximum Power Point Tracking (MPPT) and efficient power electronics such as boost converters are critical components of current PV systems. In this chapter, in the first part, we will present the concept of PV solar energy and also discuss various installations, and a brief overview of Cells, Modules, Panels, and Arrays. Then we explore the modeling of the PV panels DC-DC converter, control of boost converter type perturb & observe, and also present the variable irradiation and temperature effect, the chapter examined the dynamic behavior of generation systems using MATLAB/Simulink software, presenting simulated findings to test the control scheme efficacy and system performance.

II.2. Photovoltaic Solar Energy

The photovoltaic solar energy (PV) sector is one of the most rapidly expanding in the world, to keep up with this development have been made in the areas of device design, production technologies, material use, energy consumption to manufacture these materials, and new ideas to improve the cells' overall efficiency [158]. Thus, the main goal of photovoltaic technology is to capture solar light energy and turn it straight into electrical power. Solar panels are made up of photovoltaic cells as depicted in Figure II.1, mostly silicon cells with the capacity to transform photons into electrons. Over time, PV technology has become much more efficient and cost-effective, positioning it as a major force in the solar energy sector [158]. The generated micro-power electricity can be distributed over electrical networks or used locally [159].



Figure II.1.Solar photovoltaic panels [159]

II.3. Photovoltaic Solar Effect

II.3.1. The procedure working of PV Cells

A photovoltaic cell is the fundamental component of a solar energy-generating system that converts sunlight into electrical energy quickly [160]. The p-n junction device is the solar cell. Concerning Figure II.2 of a PV structure, the terms "n-type" and "p-type" denote the negatively charged electrons contributed by donor impurity atoms and the positively charged holes produced by acceptor impurity atoms, respectively. The PV effect involves three basic steps as below [161]:

- ❖ Photons are absorbed in a $p - n$ junction semiconductor, resulting in electron-hole pairs. When a doped semiconductor material absorbs a photon with greater energy, the energy is utilized to drive an electron from the valence band to the conduction band, creating a void (hole) at the valence level. Excess photon energy increases the kinetic energy of electrons or holes. $h\nu_0$ refers to the semiconductor's minimal energy or work function needed to form an electron-hole pair. The work function represents the energy gap. Excess energy is released as heat in the semiconductor.
- ❖ The light-generated charge carriers are consequently separated. External solar circuits allow holes to flow out from the junction through the p-region, while electrons can flow out over the n-region and pass through the circuit before recombining. Ultimately, an electric circuit may be powered by split electrons. Once they have traveled across the circuit, the electrons will recombine with the holes.

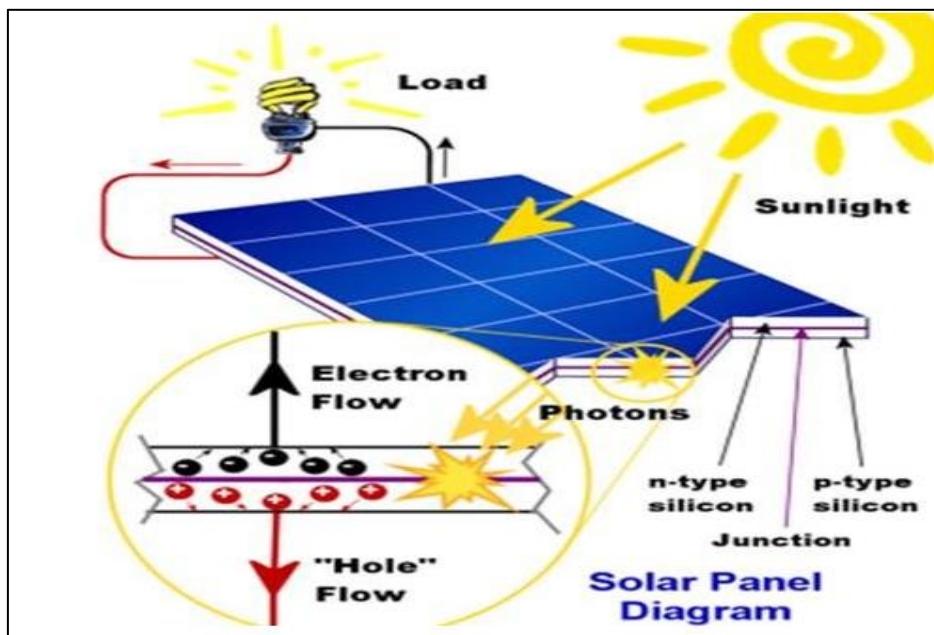


Figure II.2. Solar photovoltaic effect [161].

II.4. Different installations of solar photovoltaic

Solar photovoltaic (PV) systems come in several main types as presented in Figure II.3, each designed for specific applications and environments.

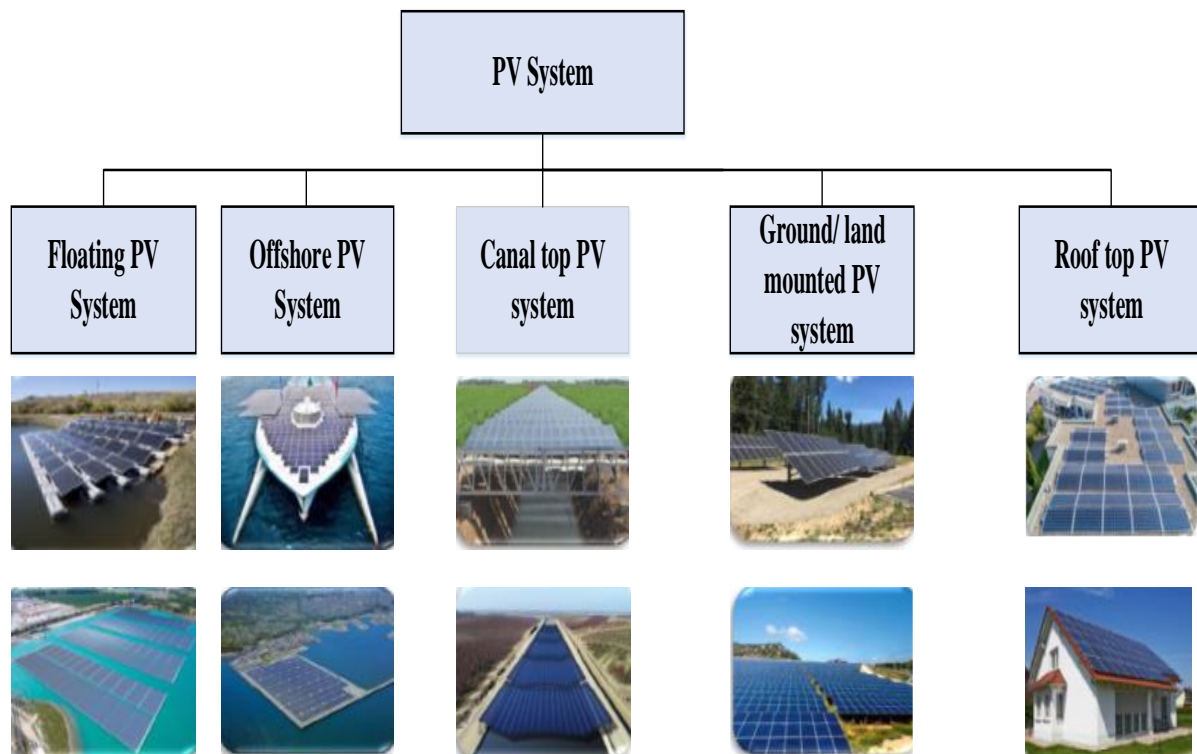


Figure II.3. Different installations of solar photovoltaic [162].

II.4. Generations of Photovoltaic Cells

A photovoltaic cell converts solar radiation into electrical energy, known as the photovoltaic effect. PV cells are manufactured using several approaches, including material modification to vary photoelectric conversion efficiencies in cell components. Figure II.4 shows that photovoltaic technology has evolved into four distinct generations [161-162].

- ❖ **First Generation:** Photovoltaic cell technology using monocrystalline, polycrystalline silicon, and gallium arsenide (*GaAs*).
- ❖ **Second Generation:** This generation includes the development of first-generation photovoltaic cell technology, as well as thin-film photovoltaic cells from microcrystalline silicon ($\mu c - Si$) and amorphous silicon ($a - Si$), copper indium gallium selenide (*CIGS*), and cadmium telluride/cadmium sulfide (*CdTe/CdS*) photovoltaic cells.
- ❖ **The third generation** of solar technology uses more current chemical components. This generation includes technologies such as nanocrystalline "films," quantum dots, dye-sensitized solar cells, and organic polymer-based solar cells.
- ❖ **Fourth Generation:** This generation combines the low flexibility and low cost of thin film polymers with the durability of innovative inorganic nanostructures like metal oxides and nanoparticles, as well as organic-based nanomaterials like graphene, carbon nanotubes, and derivatives.

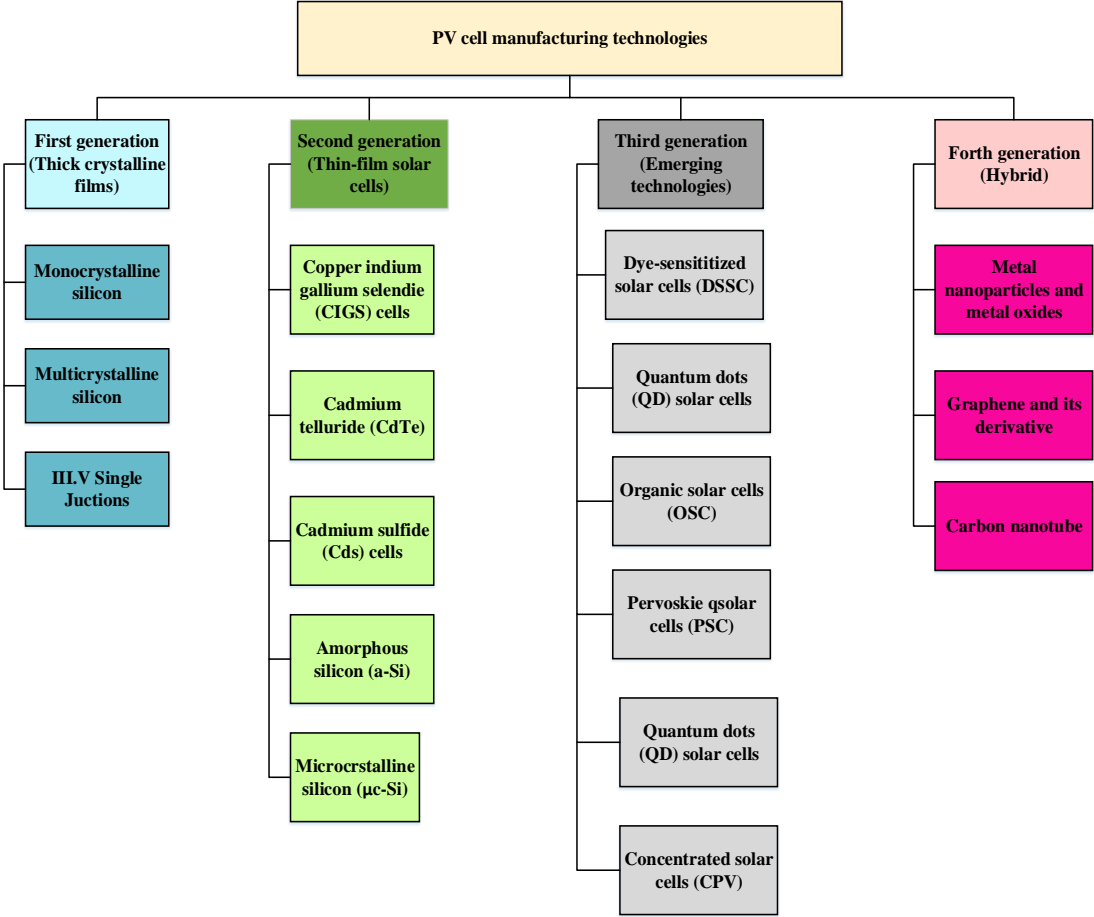


Figure II.4. Generations of Photovoltaic Cells [163].

II.6. Cells, Modules, Panels, and Arrays

PV cells are connected to electricity in series or parallel circuits to generate larger voltages, currents, and power levels. The core building blocks of PV systems are photovoltaic modules, which are made up of PV cell circuits sealed in an environmentally protected laminate. Photovoltaic panels are made up of one or more PV modules that have been pre-wired and may be installed in the field. A photovoltaic array is a full power generation unit that includes any number of PV modules and panels [161-163]. PV modules and arrays are typically rated based on their maximum DC power output (watts) under Standard Test Conditions (*STC*). Standard test conditions include a module (cell) operating temperature of 25°C (77°F), an incoming solar irradiance level of 1000 W/m², and an Air Mass 1.5 spectral distribution. Because these circumstances are not often representative of how PV modules and arrays function in the field, real performance is typically 85 to 90% of the *STC* rating[164].

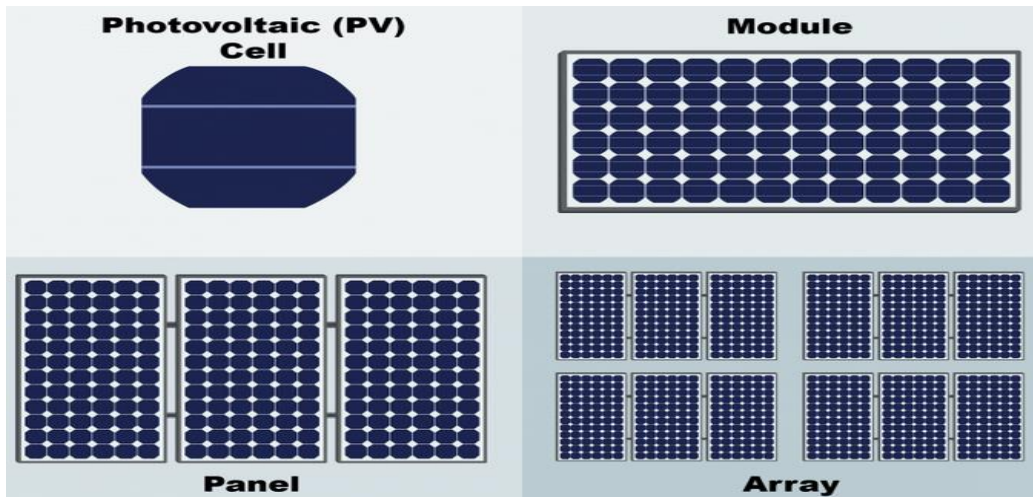


Figure II.5. Design of Cells, Modules, Panels, and Arrays [164].

II.7. Different configurations of photovoltaic array

II.7.1. Series Configuration

In a series configuration, solar cells or modules are connected end-to-end as shown in Figure II.6, with the positive terminal of one cell connected to the negative terminal of the next. The total output voltage is the sum of the voltages of all connected cells or panels, but the current remains the same across all the panels.

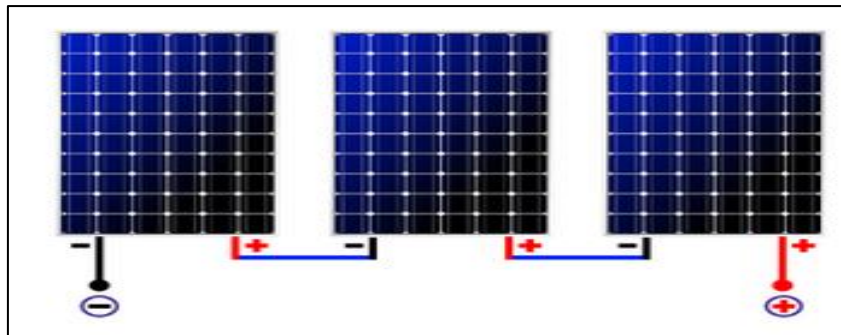


Figure II.6. Series Configuration [163].

II.7.2. Parallel Configuration

In a parallel configuration as shown in Figure II.7. The positive terminals of all the solar cells or modules are connected together as are the negative terminals. In this case, the total current is the sum of the currents from each module, while the voltage remains the same as the voltage of one module.

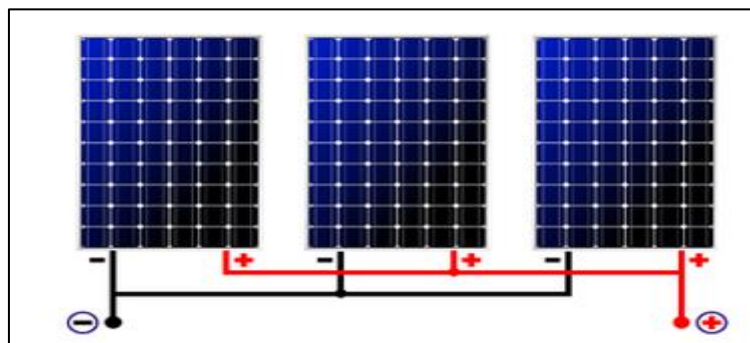


Figure II.7. Parallel Configuration [164].

II.7.3. Series-Parallel Configuration

In most practical PV systems, a **series-parallel** combination is used as shown in Figure II.8. This configuration combines the advantages of both series and parallel connections, ensuring both higher voltage and higher current for optimal power generation (The voltage of the generator rises as cells are joined in series because their voltages add together also the current rises when cells are joined in parallel). Designing solar modules and panels that can satisfy certain power and voltage needs for various applications is made possible by this mixed connection.

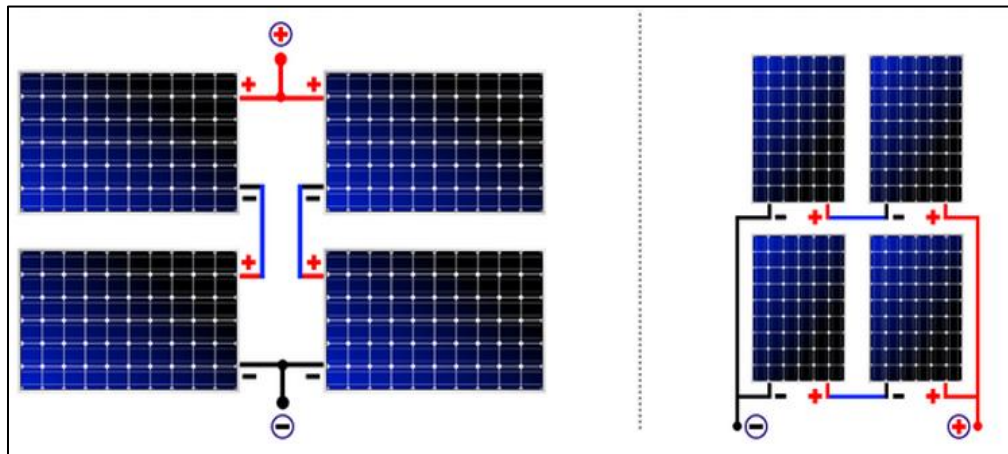


Figure II.8. Series-Parallel Configuration [164].

II.7. The major factors impacting PV electricity generation

Several variables influence the electricity generation of photovoltaic (PV) systems as depicted in Figure II.9, altering efficiency and output. These include environmental factors, system design, and operational features [165].

- ❖ **The orientation of PV modules** is crucial to increasing sunshine use and hence energy output. The optimal direction that PV modules should face varies depending on where they are put. The incorrect orientation of modules leads to a loss in output power.
- ❖ **The tilt angle** of panels may highly impact of PV system and would be increased by optimizing the tilt angle.
- ❖ **The accumulation of dust** blocks more radiation on the surface of the PV module. with a decrease in its efficiency and therefore decreases its energy production.
- ❖ **Shading** When a solar cell is shaded it consumes energy rather than producing its own and acts as a load shade can be caused by three leaves, bird droppings, snow, heavy dust, or other impurities on the surface of the PV module
- ❖ **Wind speed** Can help improve the operational efficiency of PV modules by decreasing the temperature of the solar cells due to their cooling impact.
- ❖ **Humidity** has a significant impact on the efficiency of solar cells and causes on thin layer of water to form on their surface, which can lead to a decrease in the efficiency of PV modules.

- ❖ **Temperature** The efficiency of the PV module decreases as the operating temperature increases. The temperature of the PV cells is a crucial element that reduces the PV module’s efficiency and power production.
- ❖ **Solar Irradiation** There is a direct proportionality between the solar radiation leading to decrease in the output current, and there for a decrease in the output of power of the PV module

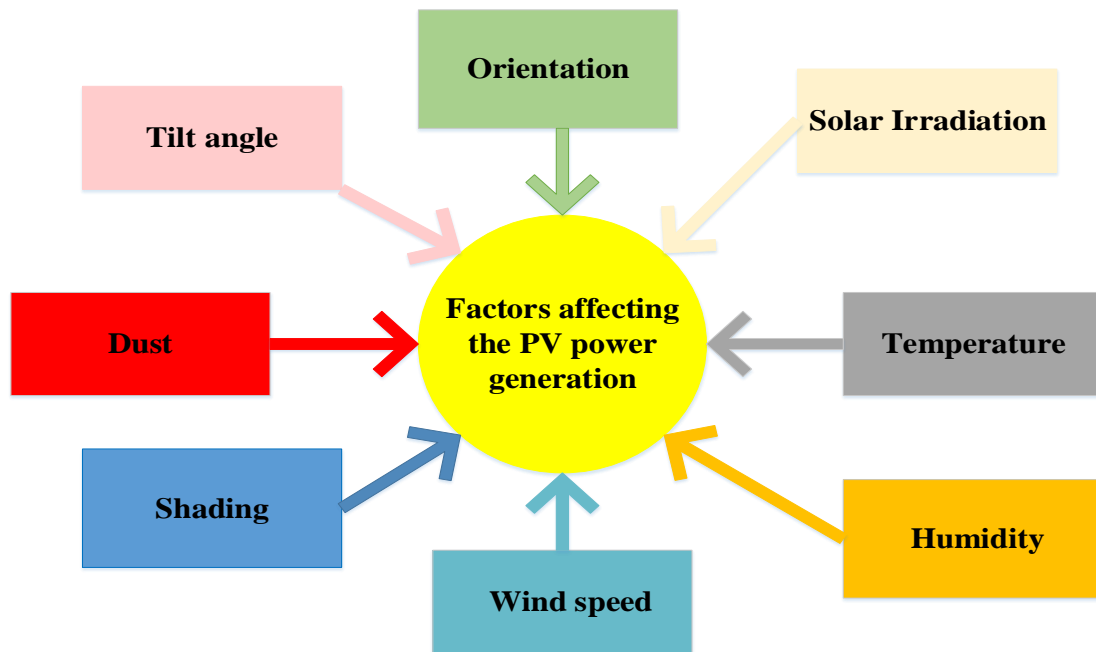


Figure II.9. The factors impacting PV electricity generation.

II.8. Sevral Types of PV systems

PV can be categorized and connected to different components and systems (stand-alone, grid-connected, and hybrid systems) as depicted in Figure II.10.

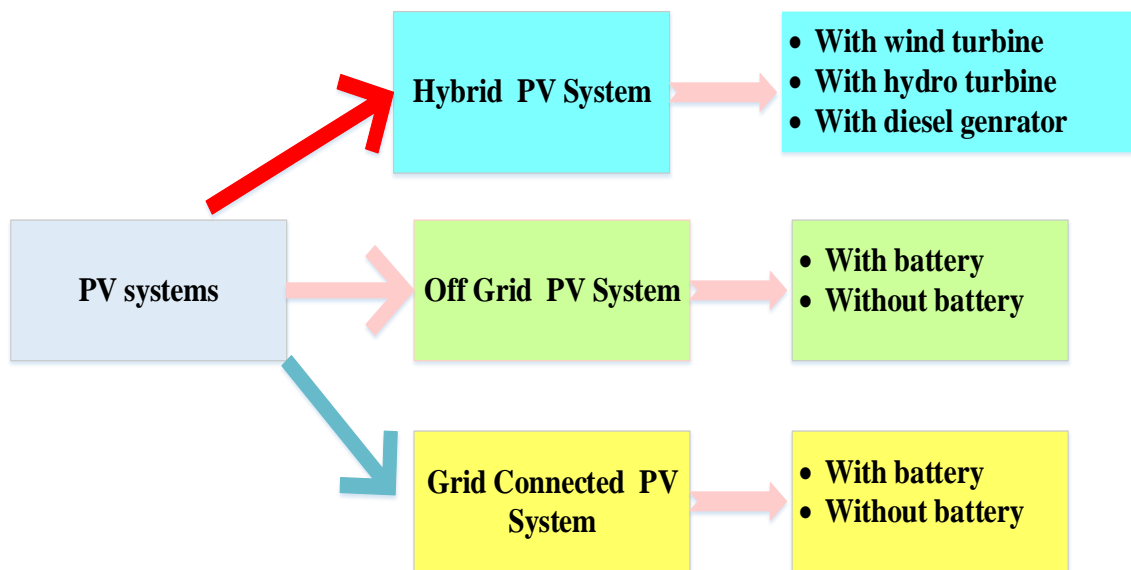


Figure II.10. The Types of PV system.

II.8.1. Off-Grid PV system (standalone)

Stand-alone PV systems are meant to function independently of the electric utility grid and are usually built and scaled to serve specific DC and/or AC electrical needs. Off-grid PV systems rely on battery energy storage to store energy, as shown in Figure II.11, providing electricity even when the sunlight isn't shining.

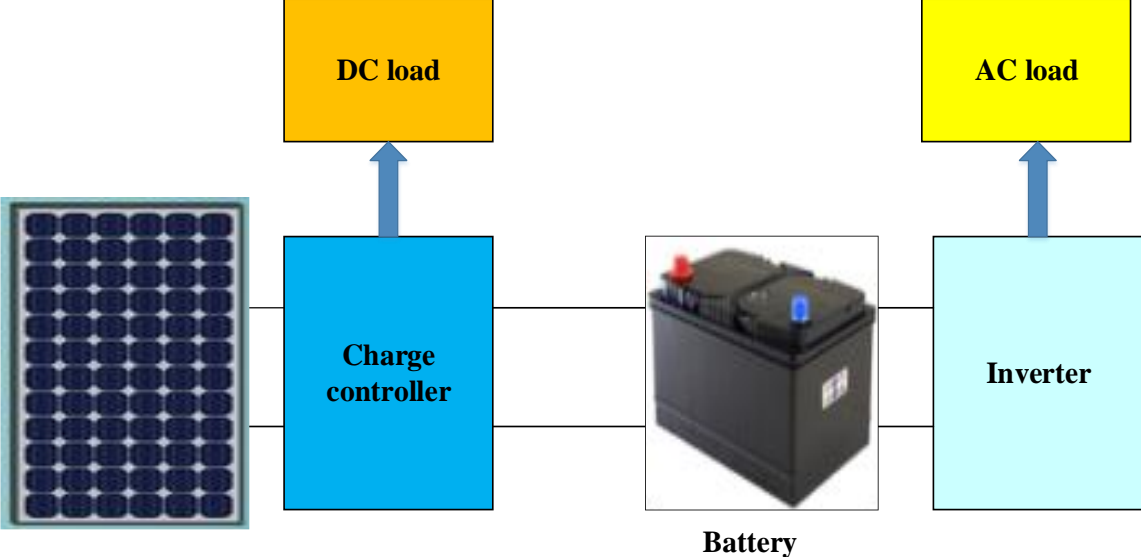


Figure II.11. Off-grid PV system.

II.8.2. Grid-connected PV system

This sort of solar power system is the most frequent. A grid-tied or grid-connected solar power system integrates extracted PV electricity into the public grid as presented in Figure II.12. As the name implies, it is connected to both the home and the standard electrical utility grid. This sort of solar power system does not have a storage battery. During blackouts and crises, such systems cannot provide local power as they must be disconnected from the grid and turned down to meet electrical safety regulations.

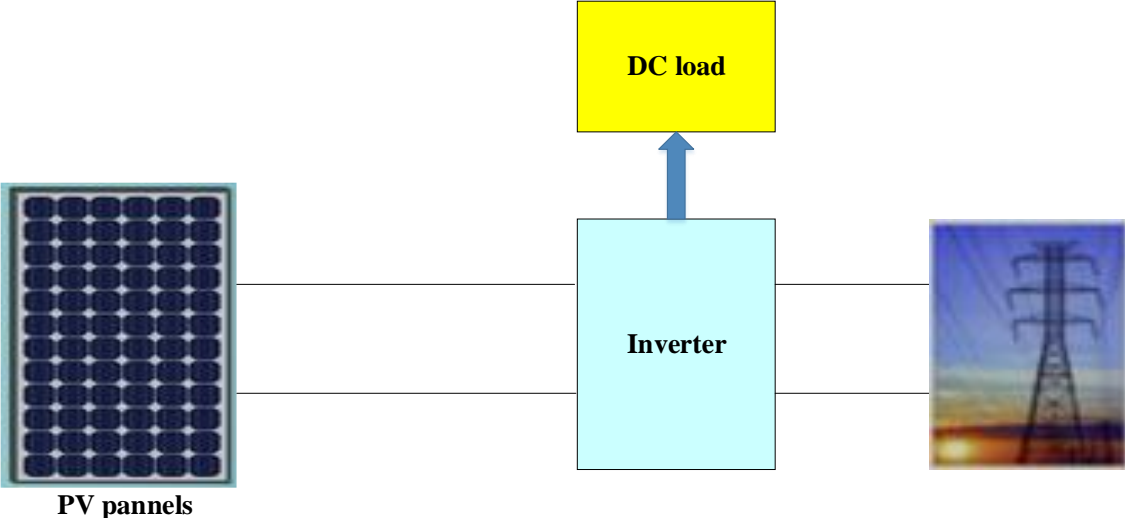


Figure II.12. Grid-connected PV system.

II.8.3. Hybrid PV system

Hybrid systems combine solar PV with other energy sources like wind, biomass, or diesel to meet demand as presented in Figure II.13. The goal of this sort of system is to increase dependability while being cost-effective by incorporating more energy sources.

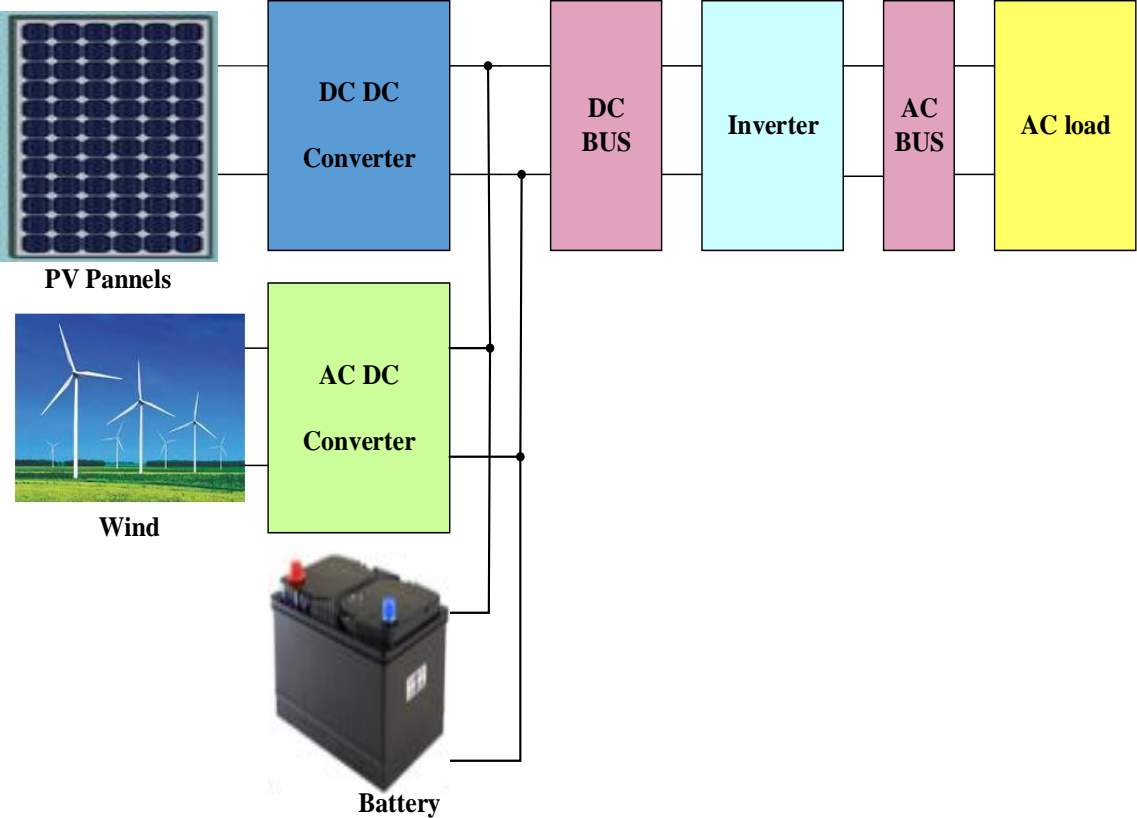


Figure II.13. Configuration Hybrid PV system.

II.9. Parameters of solar photovoltaic

Figure II.14 presents numerous factors that impact a PV cell's effectiveness and its capacity to transform sunlight into electrical power.

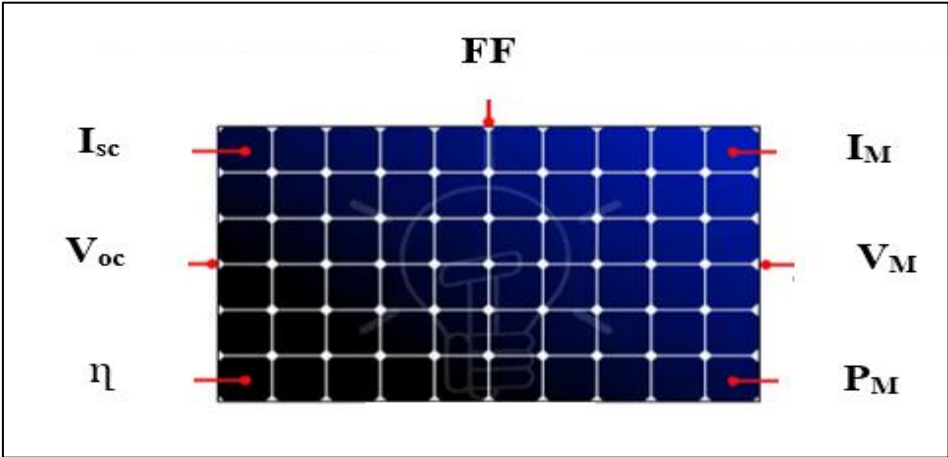


Figure II.14. Configuration Hybrid PV system [165].

The main factors that determine a PV cell's behavior, power production, and efficiency are as follows [163-166]:

- ❖ **Open Circuit Voltage (V_{oc}):** The maximum voltage a photovoltaic cell can produce when it is not connected to any load (open circuit), thus V_{oc} , depending on the amount of sunshine and the cell composition. Generally speaking, it rises with increased temperature and falls with higher irradiation.
- ❖ **Short Current Circuit Voltage (I_{sc}):** The current I_{sc} is that the Photovoltaic cell generates when its terminals are shorted, resulting in zero voltage across the cell. The value of I_{sc} depends on cell area, solar radiation falling on the cell, cell technology, etc.
- ❖ **Current and Voltage at Maximum Power Point (V_M, I_M):** The point of operation is essential for assessing the performance of a solar cell. It shows the voltage (V_M) and current (I_M) of the cell under particular operating conditions. The operating point at which the cell produces the highest power output is known as the maximum power point (P_M).
- ❖ **Maximum Power Point (P_M):** The maximum power point is the highest power a solar cell can generate at the Standard Test Condition, however, where the photovoltaic cell produces its highest power output is indicated by the current-voltage (I – V) curve, For optimal power extraction from the cell, the MPP is crucial and varies with temperature and solar intensity. PV cell operation at this point is monitored by Maximum Power Point Tracking (MPPT) devices.
- ❖ **Form Factor (FF):** A measure of the quality of the PV cell, defined as the ratio of the actual maximum power output (P_M) to the theoretical power ($V_M * I_M$) [166]:

$$FF = \frac{P_M}{(V_M * I_M)} \quad (II.1)$$

- ❖ **Energy Efficiency:** The ratio of the electrical power output to the incident solar power on the cell. Cell material, sunshine, temperature, and fill factor are some of the variables that affect efficiency. It shows how well a photovoltaic cell transforms sunlight into electrical power. The energy efficiency is calculated in equation (II.2) [166].

$$\eta = \frac{P_M}{G * A} \quad (II.2)$$

II.10. Modeling of Photovoltaic (PV)

The equivalent electrical circuit, which has several variable characteristics, describes the solar cell. Mathematical equations using external factors like temperature and irradiance can be used to calculate these parameters. The analytical techniques are explained below:

II.10.1. Electrical Equivalent Circuit for One-Diode Photovoltaic Cell Model

A popular depiction of a photovoltaic cell in the form of an electrical equivalent circuit is the one-diode model. The usual equivalent circuit used for this model is shown in Figure II.15 that includes a diode, a shunt, a series resistance, and a photosensitive current source.

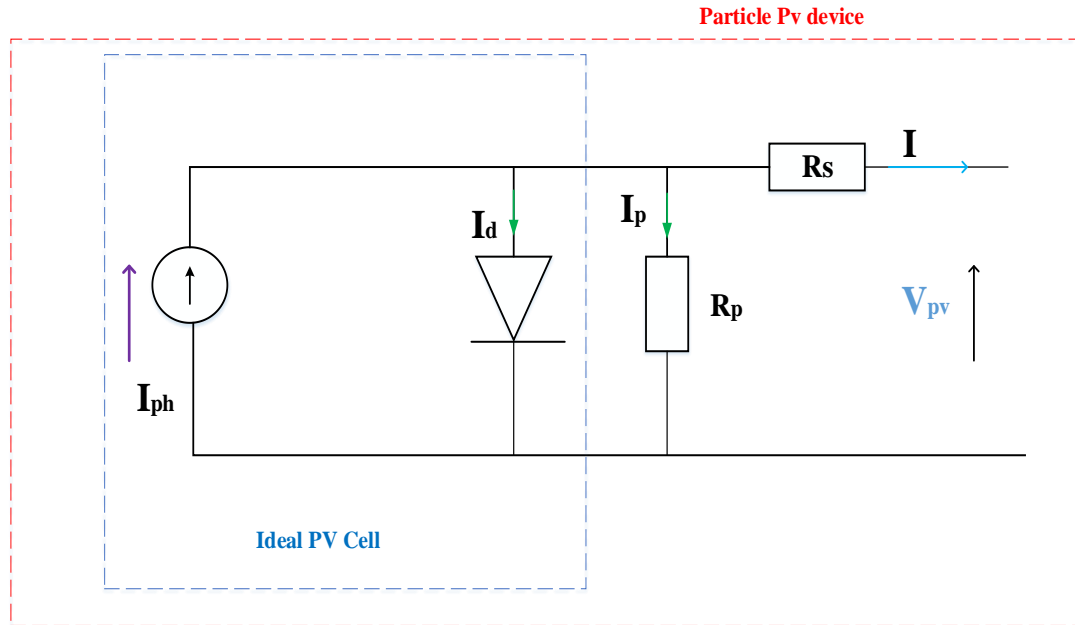


Figure II.15 :Electrical Equivalent Circuit of a One-Diode Photovoltaic Cell Model.

- ❖ The expression of the current I

$$I = I_{ph} - I_d - I_p \quad (II.3)$$

- ❖ The expression of the current I

$$V_{ph} = V_d - IR_s \quad (II.4)$$

- ❖ The equation provides the mathematical description of the one-diode model. [167]

$$I = I_{ph} - I_s \left[\exp\left(\frac{q \cdot V_{pv} + R_s \cdot I}{K \cdot T \cdot n}\right) - 1 \right] - \frac{(V_{pv} + I \cdot R_s)}{R_p} \quad (II.5)$$

II.10.2. Electrical Equivalent Circuit for Two-Diode Photovoltaic Cell Model

The impact of recombination current loss in the depletion area is intrinsically ignored by the single-diode models that have been covered up to this point. The two-diode model is a more accurate solution considering this loss, especially at low voltage. The model is displayed in Figure II.16.

- ❖ The equation provides the one-diode model's mathematical description [167].

$$I = I_{ph} - I_{s1} \left[\exp\left(\frac{q \cdot V_{pv} + R_s \cdot I}{K \cdot T \cdot n_1}\right) \right] - I_{s2} \left[\exp\left(\frac{q \cdot V_{pv} + R_s \cdot I}{K \cdot T \cdot n_2}\right) \right] - \frac{(V_{pv} + I \cdot R_s)}{R_p} \quad (II.6)$$

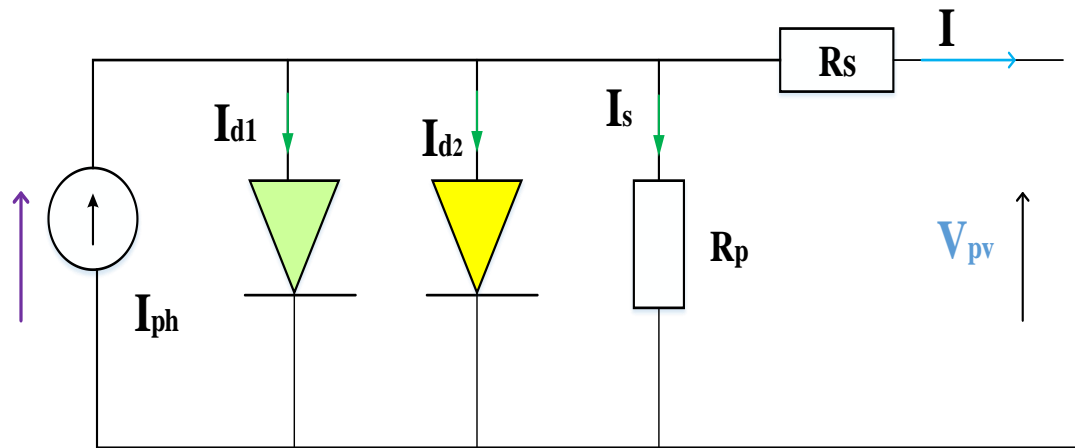


Figure II.16. Electrical Equivalent Circuit: Two-Diode Photovoltaic Cell Model [167].

II.11. Proposed Modeling of the system (PV connected to DC-DC converter with DC load)

Figure II.17 illustrates the configuration of the PV panels connected to the DC load. This model is composed of the following elements:

- ❖ photovoltaic panels generate the supplied power.
- ❖ DC-DC converter type boost.
- ❖ Control of boost via Maximum power point (MPPT).
- ❖ DC load type resistance.

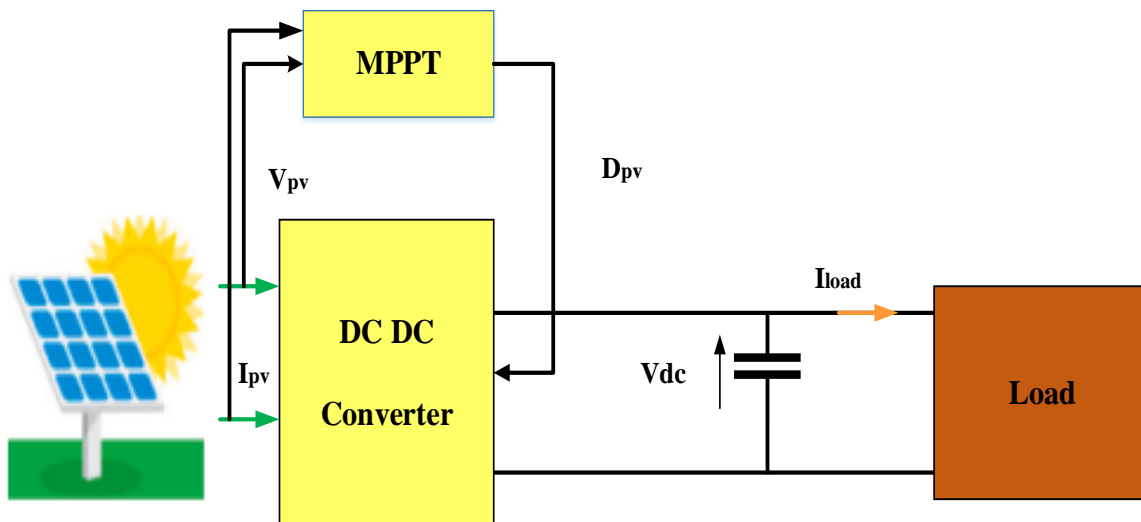


Figure II.17. Scheme DC load connected with PV panels.

II.11.1. DC-DC converter model

DC/DC converters regulate the voltage or current at the load by adjusting the switching times between the input (DC source) and output. This allows photovoltaic panels to supply uncontrolled voltage to a regulated DC voltage at the output. On the next page, we present a brief description with explanations of models for boost converters.

II.11.1.1. Boost converter model

Figure II.18 depicts the construction of the boost converter. The direct current input of this converter

is powered by DC sources like photovoltaic panels. In this system, the input voltage is raised through three primary components: an inductor, a diode, and a power switch. The boost converter's output is coupled to a capacitor, which reduces and stabilizes output voltage ripples. Lastly, an output capacitor is linked to a load as an adjustable resistor. Below, several equations describing the connections between parameters make up the mathematical model of a boost converter.

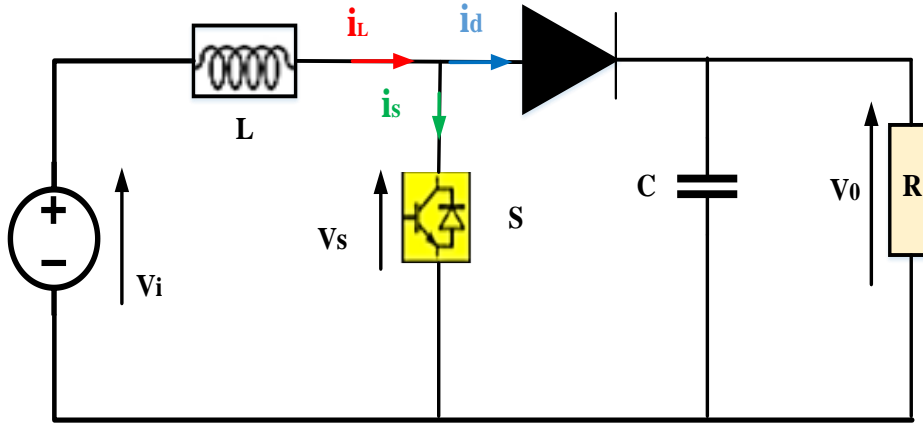


Figure II.18. Boost converter.

❖ **Phase 1 : $0 < \alpha < \alpha T$**

When the switch is in position 1 ($S = 1$) as shown in Figure II.19, it causes the current to increase in the inductance, indicating that L stores a quantity of energy in the form of magnetic energy. The diode D is then blocked ($D = 0$) and the Charge is disconnected from the power.

$$V_s = 0, i_d = 0 \tag{II.7}$$

$$V_i = V_L = L \frac{di_L}{dt} \tag{II.8}$$

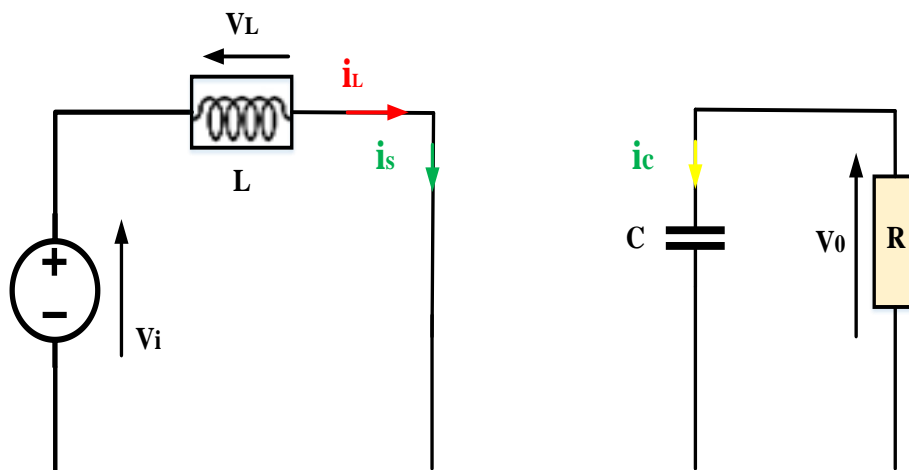


Figure II.19. Boost converter in First Phase (when S is open).

❖ **Phase 2 : $\alpha T < \alpha < T$**

When the switch in position 2 is open ($S = 0$), ($D = 1$), the inductance is then in series with the generator and its fem. Adds to the generator's (boost effect). The current is through the inductance, then through the diode D , capacitor C , and resistor R . It results in a transfer of the energy accumulated in the

inductance to the capacitance.

$$V_i = V_L + V_0 \tag{II.9}$$

$$V_i = L \frac{di_L}{dt} + V_0 \tag{II.10}$$

$$V_L = V_i - V_0 \tag{II.11}$$

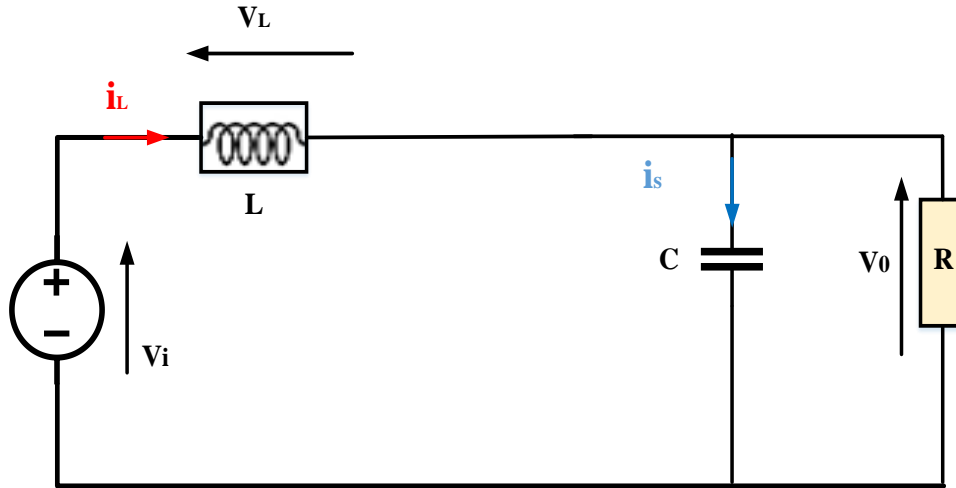


Figure II.20. Boost converter in First Phase (when S is close).

❖ **The average value of the output voltage V_0**

On a full-time permanent, the mean value of the voltage at the inductance terminals is zero, which imposes the following relationship:

$$V_L = -\frac{1}{T} \int_0^{\alpha T} V_i(t) dt - \frac{1}{T} \int_{\alpha T}^T (V_i(t) - V_0) dt \tag{II.12}$$

$$V_0 = \frac{1}{1 - \alpha} V_i \tag{II.13}$$

❖ **The value of the inductance L**

Accurate inductor estimation is crucial in electronic design, as it ensures the stability and efficiency of the converter, ensuring it operates within the desired performance. This estimation process involves parameters like output voltage, switching frequency, duty cycle, and inductor current ripple.

$$L = \frac{V_i(V_0 - V_i)}{\Delta i_L * F_{sw} * V_0} \tag{II.14}$$

II.11.2. The Control of DC-DC converter

The most difficult aspects of solar energy are dynamic power and voltage generation, which vary according to external conditions [166]. Solar energy generation is influenced by several conditions, including wind speed, shadow, and sun insolation angle. Thus, maximum power generation is not guaranteed for all electrical loads. To improve the effectiveness of those specific cells, precise tracking of incident light on the PV cells is crucial; this is known as MPPT. Optimizing the match between the

generator and load for maximum power transfer is the main objective of MPPT. Additionally, MPPT constantly aims to operate solar PV systems at peak or values near peak power from incident radiation on solar cells under various environmental conditions. Many research efforts are underway in MPPT to track the maximum power from the PV cells and boost efficiency as well, taking into account the present research condition [166-167].

The literature has a variety of algorithms for MPPT that have been developed recently (Mohapatra, 2017) [167]. These techniques adjust input factors, including temperature, voltage, current, solar irradiation, and PV panel power. Table II.2 illustrates several MPPT methodologies for maximizing PV module power output. The efficacy of these systems depends on their ability to follow quickly changing meteorological conditions such as temperature and Irradiation.

Table II. 2 : Several basic classifications of MPPT methods[166].

Classic Methods	Optimization Methods	Advanced Methods	• Hybrid methods
<ul style="list-style-type: none"> • Perturb &observe. • Modified Perturb. &observe • Incremental Conductance. • Ripple Correlation Control • Hill climbing • Short Circuit Current • Open Circuit Voltage 	<ul style="list-style-type: none"> • Particle Swarm Optimization • Grey Wolf Optimization • Cukoo Search • Articial Bee Colony • Gauss Newton 	<ul style="list-style-type: none"> • Artificial Neural Network • Fibonacci Series based MPPT • Sliding Mode Control • Double Integral Sliding Mode Control • Fuzzy Logic Controller 	<ul style="list-style-type: none"> • Fuzzy Particle Swarm Optimization • Adaptive Neuro Fuzzy Inference System • Grey Wolf Optimization with Perturb &observe • Particle Swarm Optimization with Perturb &observe

This chapter focuses on the MPPT type Perturb & Observe algorithm to control the boost converter.

II.11.2.1. Perturb and Observe (P&O) methods

(P&O) Methods is a popular algorithm for MPPT in PV systems. This algorithm changes the PV system's operating point to the maximum of power generation by continually perturbing (slightly adjusting) the system's voltage or current and monitoring the effect on output power.

II.11.2.1.1. Functional characteristics of the P&O Algorithm

The P&O control process is presented in Figure II.21. The P&O approach tracks the MPP by continually perturbing the PV generator's output voltage and measuring the ensuing power changes. The algorithm adjusts the operating voltage depending on observed power variations during each iteration. If the power increases ($\Delta P > 0$), it indicates that the system is approaching its ideal condition. When ΔV is positive, the algorithm increases the voltage, whereas if ΔV is more than 0, it decreases the voltage. If the power change is negative ($\Delta P < 0$), it indicates a divergence from the optimum and calls for corrective action. The algorithm reverses the direction of changes, boosting voltage if ΔV is negative and decreasing it if ΔV is greater than 0 [166-169].

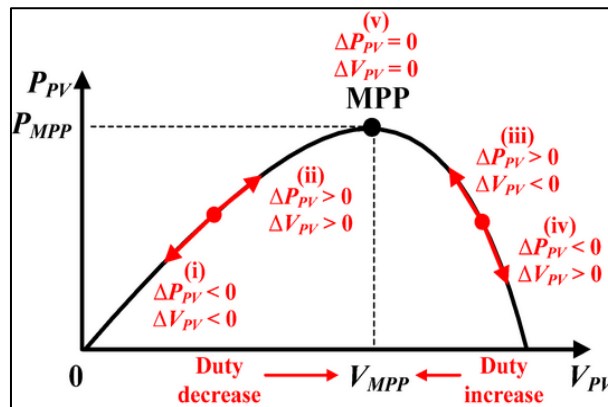


Figure II.21. Functional characteristics of the P&O Curve [169].

II.11.3. Performance Effect of Photovoltaic Panels

The performance of a photovoltaic module is determined by its materials, manufacturing technology, and operating circumstances (solar irradiation and temperature).

❖ Variable Solar Effect

Solar irradiation values significantly influence a solar cell's P-V and I-V curves. Environmental changes fluctuate solar irradiation, but control mechanisms can track and adjust the cell's operation to meet load demands. Higher irradiation increases solar input, power magnitude, and open circuit voltage as depicted in Figure II.22.

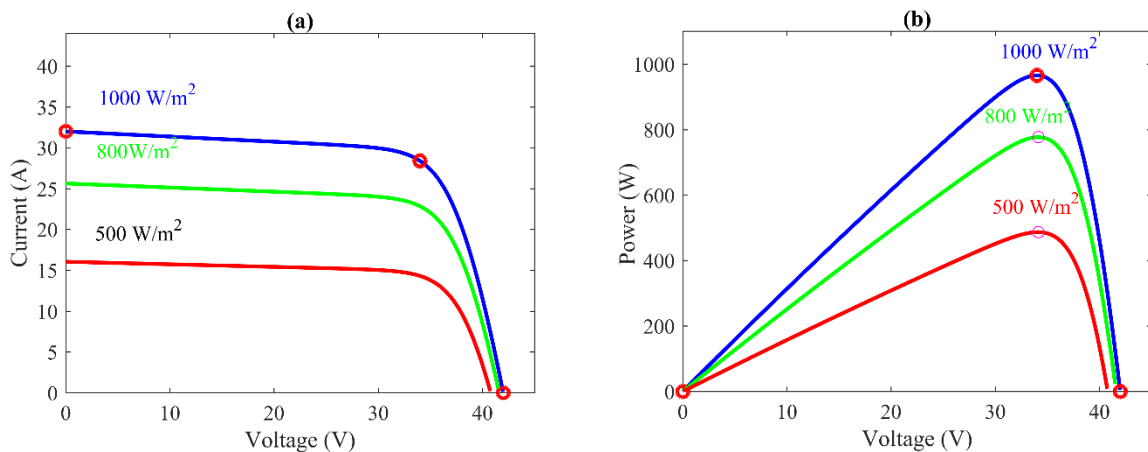


Figure II.22. Variation of I – V and P – V curve with solar irradiation.

❖ Variable Temperature Effect

Figure II.23 presents the $I - V$ and $P - V$ characteristics of the PV panels at a constant irradiation of 1000 W/m^2 and a variable range of temperature. The curve indicates that temperature has no significant impact on the current value. Nonetheless, the voltage lowers dramatically as the temperature rises. On the other hand, the amount of power generated decreases.

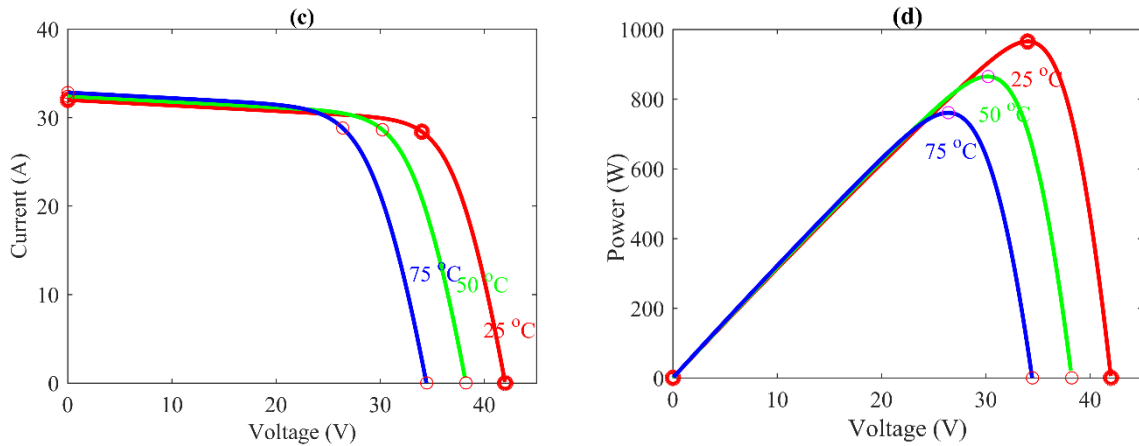


Figure II. 23. Variation of $I - V$ and $P - V$ curve with solar temperature.

II.12. Simulation results

The suggested PV system was validated by connecting solar panels to a DC load and observing its behavior using an MPPT-controlled boost converter. The system was simulated using the MATLAB/Simulink system.

• Test 1: Abrupt irradiation changes

A simulation of the First test was conducted with dynamic weather, such as fixed temperature input and abrupt irradiation changes, as depicted in Figure II.24 was conducted to validate the effectiveness of the control strategy. Figures II.25, II.26, and II.27 show the dynamic characteristics of the voltage, current, and power outputs. The simulation results demonstrate that the systems can quickly adjust to sudden changes in irradiation. Analyzing the current, voltage, and power outputs into algorithm performance amid variable irradiation shifts for tracking maximum power.

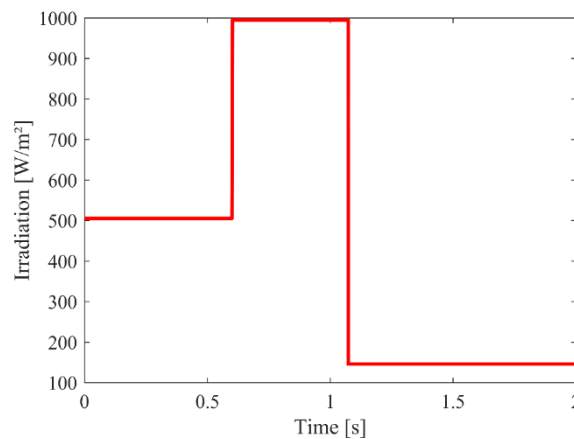


Figure II.24. Abrupt irradiation changes input.

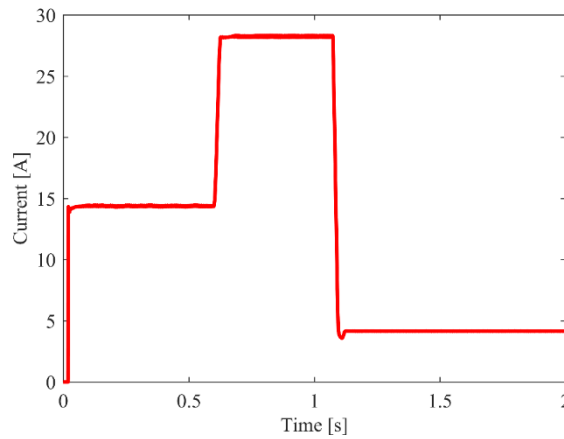


Figure II.25. Solar Output Current.

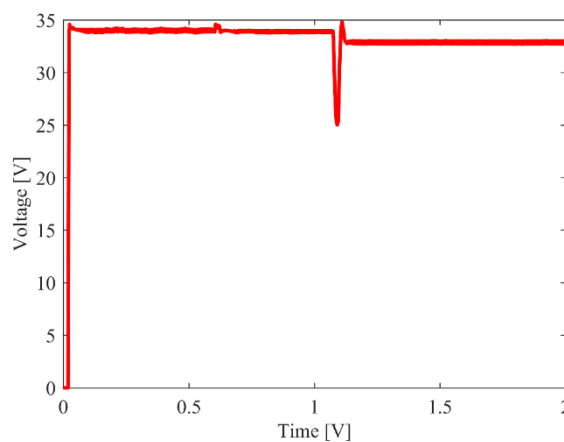


Figure II. 26. Solar Output Voltage.

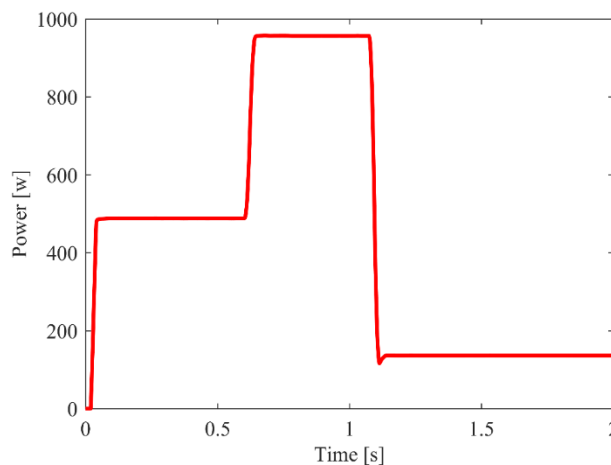


Figure II.27. Solar Photovoltaic Power.

- **Test 2: Gradual ramp evolution of irradiation**

In the second simulation test, a meticulously crafted irradiation profile featuring a gradual ramp progression was employed as depicted in Figure II.28. This design aimed to emulate the subtle and smooth transitions in solar intensity that occur in nature, thereby mirroring realistic environmental changes. The MPPT algorithms were fine-tuned to respond to this intricate modeling and control of the photovoltaic system linked to the DC load, showcasing a progressive evolution of irradiation, as

illustrated in the simulation results.

This scenario holds significant relevance in real-world contexts where solar intensity fluctuates gently, such as during the enchanting moments of sunrise or sunset. A thorough analysis of the current, voltage, and power is shown in Figure II.29, II.30 and II.31 outputs reveal the algorithm's remarkable ability to optimize power generation, even amidst less abrupt variations in irradiation, underscoring the adaptability and sophistication of the MPPT type perturb and observe.

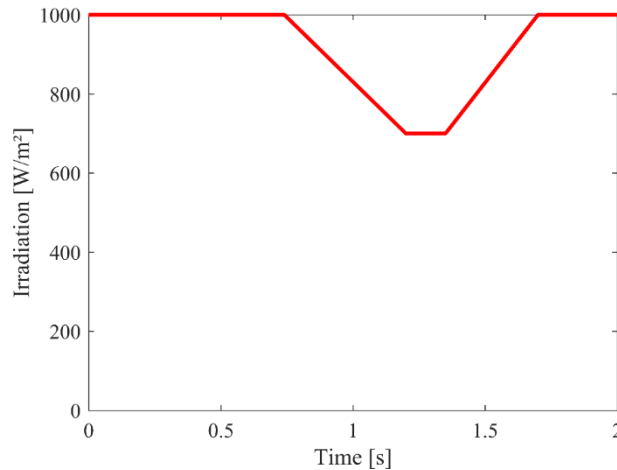


Figure II. 28 .Gradual ramp evolution of irradiation.

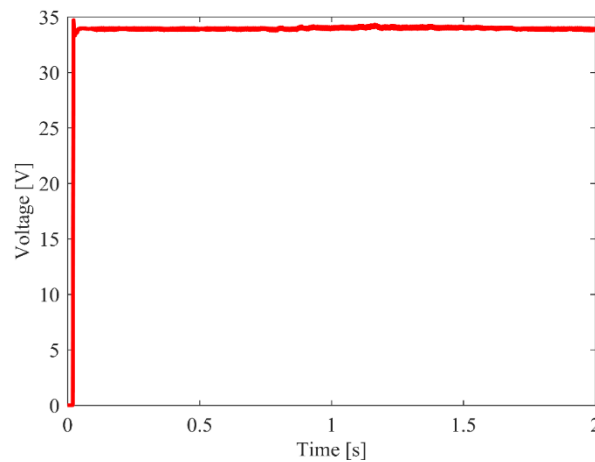


Figure II. 29.PV Voltage.

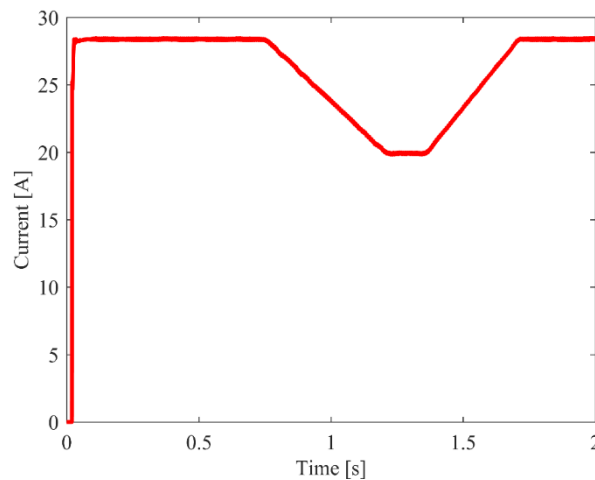


Figure II. 30.PV Current.

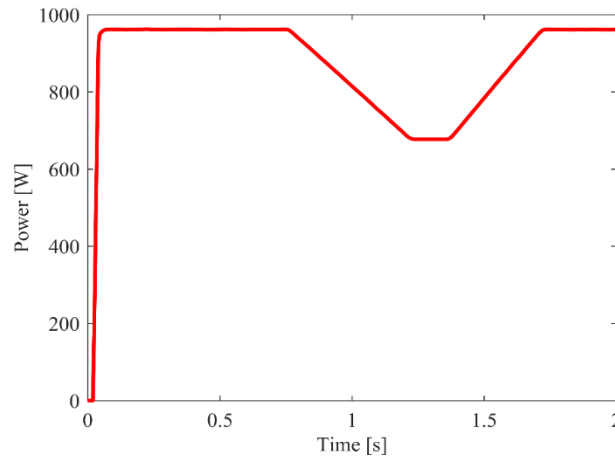


Figure II.31.PV Power.

II.13. Conclusion

In this chapter, we delved deeply into the technical aspects of PV systems such as different generations, serval installations, and types of PV solar systems. mathematical models for PV panels accurately estimate energy generation under various environmental circumstances. We modeled crucial components including DC- DC converters type boost, and the control, these models revealed dynamic interactions between components, leading to a thorough knowledge of the system. Additionally, it showed the complexities of system control, highlighting how crucial control strategies are to maximizing system performance. We investigated MPPT approaches, such as P&O, to optimize PV array efficiency and performance. The Effect of photovoltaic panels was simulated under variable values of temperature and irradiation that confirm that the photovoltaic voltage was influenced by temperature, on the other hand, the current was affected with serval irradiation levels. Thorough simulation tests have confirmed the effectiveness of the P&O approach in enhancing the reliability and efficiency of the overall system under scenario of irradiation.

Chapter III

Overview of energy system storage

III.1. Introduction

As the world moves towards a low-carbon future, ESS are becoming more important in power systems. A recent advancement in energy storage is the HESS, which combines several ESSs to enhance system performance.

These HESS, which can incorporate batteries and supercapacitors are designed to balance cost-effectiveness, efficiency, and energy and power density. HESS can provide high power output, fast response times, and long-term energy storage capacity by integrating several types of ESS.

This chapter offers a comprehensive overview of ESS with different topologies and will focus on different batteries and several types of supercapacitor storage presented/ Moreover, the chapter delves into the Comparison between battery and supercapacitor energy storage via Ragone diagram, Subsequently, we explore a detailed hybrid energy storage with its Classification.

III.2. Overview of Energy Storage

ESS has recently gained importance in modern energy systems and has been the subject of intense research, however, it offers an alternate means of meeting peak energy demands during peak energy use. because it ensures stability, increases efficiency, and allows for the integration of renewable energy sources [170].

It refers to capturing energy generated at one moment and using it later, which is critical for balancing demand and supply in centralized and distributed environments [171].

To lower peak energy loads, close the gap between supply and demand for energy, lower costs, and lessen the effects of global warming, Additionally, energy storage facilitates auxiliary grid functions like voltage and frequency management, which are critical to grid stability.

ESS improves power quality and avoids interruptions by reacting rapidly to variations in voltage or frequency [172].

Additionally, it reduces the need for costly transmission and distribution upgrades, optimizes energy usage patterns, and provides backup power during outages [173]. Emerging technologies like vehicle-to-grid systems further contribute to grid flexibility.

Figure III.1 includes power quality, power reliability, load demand profile with energy storage system, energy arbitrage, peak shaving, load flowing, spinning reserve, voltage support, black start, and frequency regulation are all applications for ESS.

ESS include shifting, smoothing and firming, deferral of transmission and distribution upgrading, congestion alleviation, and off-grid service.

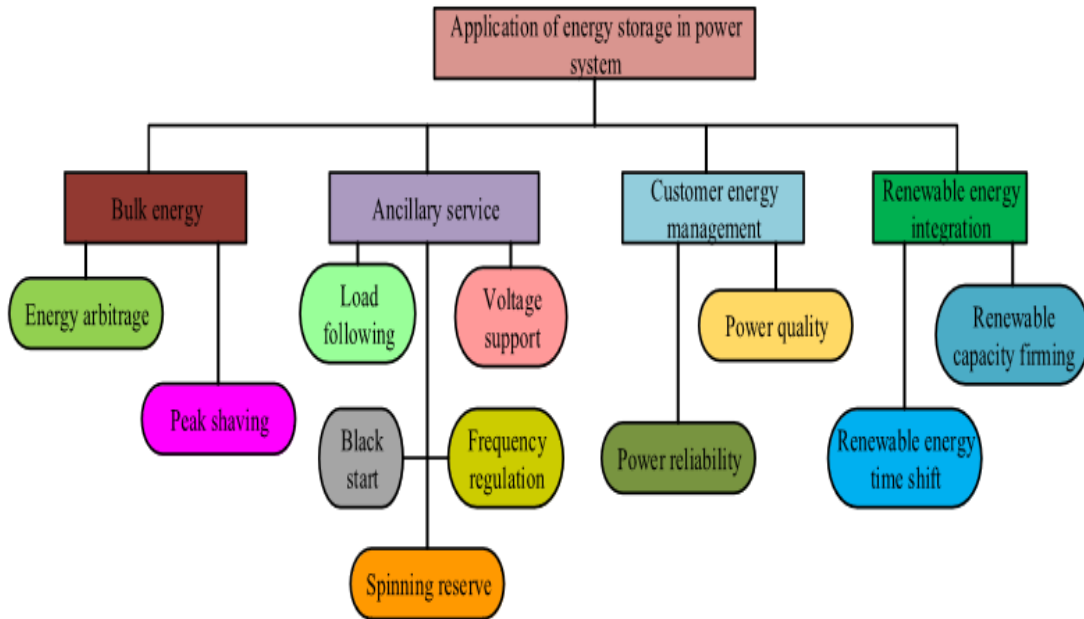


Figure III.1.Application of Energy storage system [173].

III.3. Technologies of energy storage

ESS encompasses a variety of systems, which can be classified into Five broad categories, these are: mechanical, electrochemical, thermal, chemical, and electrical energy storage, as shown in Figure III.2.

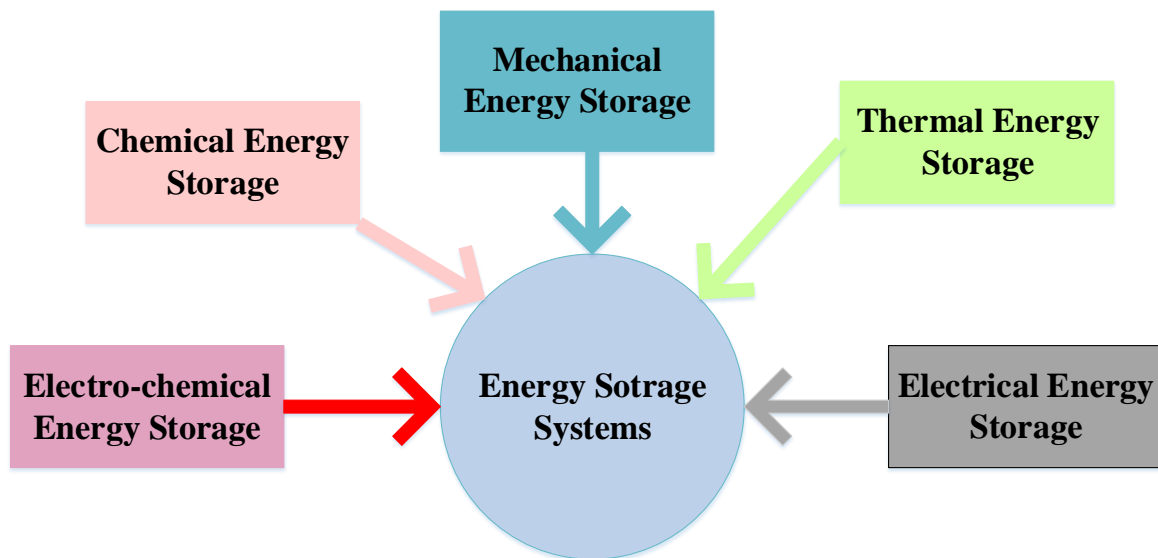


Figure III.2.Technologies of electrical energy storage .

III.3.1. Thermal energy storage

TES systems store heat energy as depicted in Figure III.3 through a substance's cooling, heating, melting, condensation, or vaporization. Materials are stored in an insulated repository at high or low temperatures [174]. The energy recovered is used for residential and industrial applications, such as space heating, cooling, hot water production, or electricity generation, depending on the operating temperature range. Although TES systems come in various forms, they all operate on the same fundamental idea: heat is transferred into a storage medium and kept there until it is required [175].

There are several ways to keep the storage medium, including in a tank, subterranean reservoir, or phase transition material. It can be a solid, liquid, or gas [173-175]. TESs have two types: sensible heat storage and latent heat storage.



Figure III.3. Thermal energy storage [175].

III.3.2. Mechanical energy storage

MES systems are critical components of modern energy solutions because they efficiently store and release energy using mechanical forces such as compression, motion, or gravity. These systems are sustainable and dependable, particularly for large-scale and long-term applications. Pumped hydro storage (PHS), compressed air energy storage (CAES), flywheel energy storage, and gravitational energy storage devices are among the most popular technologies. MES systems are noted for their durability, quick response times, and low environmental effect, making them perfect for incorporating renewable energy sources such as wind and solar [175]. However, such problems as site reliance, expensive initial infrastructure expenditures, and energy efficiency losses during conversion operations can jeopardize their success. Despite these obstacles, MES continues to evolve with advances in materials and hybrid systems, increasing efficiency and application [176].



Figure III.4. Mechanical energy storage [174].

III.3.3. Chemical energy storage (CES)

Chemical energy storage systems use chemical bonds to store energy, which can then be released through chemical processes to give useful energy [175-177]. These systems are adaptable, scalable, and

critical for dealing with the difficulties of energy demand, supply fluctuation, and sustainability. Chemical energy storage is essential for integrating renewable energy sources, balancing the grid, and enabling a wide range of applications, including portable devices and grid-scale energy systems. Both the production of energy and the global transportation sector are today dominated by chemical fuels. Common chemical fuels include coal, gasoline, diesel fuel, natural gas, liquefied petroleum gas (LPG), propane, butane, ethanol, and hydrogen. To create electricity, these molecules are first transformed into mechanical energy and then into electrical energy [178]. In addition; solar fuel storage, synthetic natural gas, and hydrogen are the three primary components of CES systems. the most popular types of CES are: Hydrogen storage ,Fuel cells and Biofuels[176-178].



Figure III.5.Chemical energy storage [177].

III.3.4. Electrical energy storage (EES)

Rapid energy transfer and discharge are made possible by EES systems, which directly store energy as electric fields or charges. Unlike mechanical or chemical storage, these systems function without transforming energy between forms, making them extremely effective for applications that need quick reactions, such as grid stabilization and power quality enhancement. Powering sophisticated electronic devices, improving grid dependability, and facilitating the incorporation of renewable energy all depend on electrical energy storage technology [180].



Figure III.6.Electrical energy storage [180].

III.3.5. Electrochemical energy storage (ECES)

A key component of contemporary energy systems is electrochemical energy storage, which

effectively stores and releases electrical energy through chemical reactions, for a sustainable energy transition, electrochemical energy storage systems are essential because they integrate renewable energy sources like wind and solar power while maintaining dependability [177-181]. They promote decarbonization, improve energy security, and enable mobility and technological improvements through continuous innovation.



Figure III.7.Electrochemical energy storage [181].

III.4. Battery energy storage

The vital technologies known as BESS store electrical energy in chemical form for later use [182]. Batteries are widely employed across numerous applications, ranging from extensive grid energy systems to compact consumer devices, due to their ability to provide scalable, dependable, and efficient energy storage solutions. Energy is stored through reversible chemical reactions between the anode, cathode, and electrolyte within a battery's electrochemical cells. Numerous battery varieties are appropriate for distinct uses as follows [183]:

- Lead-acid
- Nickel-cadmium
- Nickel-metal hydride
- Sodium-sulfur
- Vanadium-redox flow
- Lithium-ion

III.4.1. Lead-Acid (LA)

The lead-acid (LA) battery, as depicted in Figure III.8 was the first type of rechargeable battery used in both residential and commercial applications [183-184]. In addition, they can perform deep discharges, although their performance is significantly affected by temperature. It includes low cost, high cell voltage, appropriateness for intermittent charge applications, and recycling capabilities. On the other hand, (LA) has negative aspects, including a lower lifetime cycle count than other technologies and a reduced energy density. Table III.1 provides comprehensive details about the (LA) battery technology [185].



Figure III.8.Lead-Acid Battery [185].

Table III.1:Features of Lead-Acid[185]

Characterizes	Value
Cell voltage	2 - 2.1 V
Specific energy	25 - 50 Wh/kg
Specific power	150 - 400 W/kg
Energy density	25 - 90 kWh/m ³
Power density	100 - 400 kWh/m ³
Efficiency	63 - 90 %
Working temperature	18 - 45 °C
Lifetime cycles	250 - 2000
Lifetime	2 - 15 years
Max. depth of discharge	80 %
Self-discharge rate	0.1 - 0.3 % per day
Power rating	0 - 20 MW
Energy cost	40 - 170 €/kWh
Power cost	250 - 500 €/kW

III.4.2. Nickel-Cadmium

A nickel-cadmium battery is a type of rechargeable battery as shown in Figure III.9 that uses respectively nickel oxide and metallic cadmium as positive and negative electrodes, it was one of the first commercially available rechargeable batteries and has been widely used in various applications, such as portable electronics, power tools, medical equipment, military devices, and aerospace systems. Nickel-cadmium batteries offer high power, long life, low self-discharge rate, low maintenance cost, resistance to extreme temperatures and overloads, and are available and affordable. However, in contrast, Ni-Cd has several disadvantages such as low energy density. Self-discharge fairly

fast (20% *per month*). Sensitivity to memory effect [185-187]. Contains hazardous substances (6% *cadmium*) which means that it must be collected at the end of its life for recycling. The table III.2 below provides features about the (Ni-Cd) battery [187].



Figure III.9. Nickel-Cadmium Battery [187].

Table III.2 : Features of Nickel-Cadmium (Ni-Cd)[187]

Characterizes	Value
Cell voltage	1.2 – 1.3 V
Specific energy	30 – 80 Wh/kg
Specific power	80 – 300 W/kg
Energy density	15 – 150 kWh/m ³
Power density	100 – 400 kWh/m ³
Efficiency	60 – 90%
Working temperature	–40 – 50 °C
Lifetime cycles	1000 – 5000
Lifetime	10 – 20years
Max. depth of discharge	80 %
Self-discharge rate	0.2 – 0.6 % <i>per day</i>
Power rating	0 – 40 MW
Energy cost	680 – 1300€/kWh
Power cost	420 – 1300€/kW

II.4.3. Nickel-metal hydride

NiMH or Ni-MH presented in Figure III.10 is an electric accumulator (therefore rechargeable) using a positive electrode in nickel oxyhydroxide and a negative electrode in metal hydride (compound to store hydrogen), Ni-MH batteries can have two to three times the capacity of Ni-Cd batteries of the same size, as well as a substantially better energy density, albeit only approximately half that of lithium-ion batteries [185-187]. They initially react very well to use at very low temperatures and do not suffer from loss of efficiency, which can be a problem with NiCad batteries, strong resistance to battery overcharging and over-discharging, as well as good recycling capabilities. Ni-MH has drawbacks the high cost is in contrast to lead-acid technology and poor performance [188]. Table III.3 displays certain features of Ni-MH battery technology.



Figure III.10. Nickel-metal hydride Battery [188].

Table III.3: Features of Nickel-metal hydride (Ni-MH)[188]

Characterizes	Value
Cell voltage	1.2 - 1.35V
Specific energy	40 - 110 Wh/kg
Specific power	200 - 300 W/kg
Energy density	40 - 300 kWh/m ³
Power density	10 - 600 kWh/m ³
Efficiency	50 - 80%
Working temperature	- 30 - 70 °C
Lifetime cycles	300 - 1800
Lifetime	2 - 15years
Max. depth of discharge	100 %
Self-discharge rate	5 - 20% per day
Power rating	0.01 - 3 MW

Energy cost	170 – 640€/kWh
Power cost	200 – 470 €/kW

III.4.4. Sodium-Sulfur

Sodium-sulfur (Na-S) battery technology shown in Figure III.11 is ideal for energy storage because of its high energy density. The electrolyte is beta alumina ceramics, and the anode and cathode are sodium and sulfur. This type of battery has low internal cell resistance, which improves power-to-weight ratio and reduces heat production when charging[187-188]. The normal operating temperature for Na-S batteries is between 300°C and 350°C, which maintains the electrodes wet and reduces cycle efficiency while increasing operation cycles. Na-S batteries are flexible, and modular, and can withstand deep drains without substantial deterioration, making them ideal for grid stabilization, renewable energy integration, peak load shifting, and backup power. They are environmentally friendly and provide steady performance at high working temperatures. On the other side,(Na-S) includes high costs and high temperatures for battery operation[189].



Figure III.11.Sodium-Sulfur Battery [189].

Table III.4: Features of Sodium-Sulfur (Na-S)[189]

Characterizes	Value
Cell voltage	1.8 – 2.71V
Specific energy	150 – 240 Wh/kg
Specific power	90 – 230 W/kg
Energy density	150 – 350 kWh/m ³
Power density	1.2 – 50 kWh/m ³
Efficiency	75 – 90 %
Working temperature	300 – 350 °C
Lifetime cycles	2500 – 40000
Lifetime	10 – 15 years
Max. depth of discharge	100 %
Self-discharge rate	0 per day

Power rating	0.05 – 34 MW
Energy cost	250 – 420 €/kWh
Power cost	850 – 2500 €/kW

III.4.5. Vanadium-Redox Flow

VRF batteries are rechargeable batteries as depicted in Figure III.12, which are generally based on two liquid electrolytes. These electrolytes contain the redox species in the form of dissolved salts, carriers of the electric charge. A VRF is composed of a central electrochemical cell (or stack) and two storage tanks, each containing one of the electrolytes. During battery operation, electrolytes are directed from storage tanks to the electrochemical cell, where electron exchanges occur and then return to the storage tank. Thus, the battery is progressively charged or discharged as the electrolytes are converted. The main benefits of VRF batteries are their capacity, adjustable at will, using tanks of varying sizes, filled to a greater or lesser extent; they can also be left uncharged for long periods without degradation. The electrolyte can also be recharged if no power source is available. This battery allows a quick recharge by replacing the electrolyte through a pump, or a slow recharge by connecting to an energy source; in addition, the battery VFR is not permanently harmed if the electrolytes are inadvertently combined. The disadvantages of the VRF consist of a low energy density and a large space needed for technology placement. Table III.5 presents certain features of VRF battery technology [184-190].



Figure III.12. Vanadium-Redox Flow Battery [189].

Table III.5: Features of Nickel-metal hydride (Ni-MH)[189]

Characterizes	Value
Cell voltage	1.2 – 1.4 V
Specific energy	10 – 130 Wh/kg
Specific power	50 – 150 W/kg
Energy density	10 – 33 kWh/m ³
Power density	2.5 – 33 kWh/m ³
Efficiency	75 – 90 %

Working temperature	5 – 45 °C
Lifetime cycles	10000 – 16000
Lifetime	5 – 15years
Max. depth of discharge	100 %
Self-discharge rate	0 per day
Power rating	0.03 – 3MW
Energy cost	130 – 850 €/kWh
Power cost	500 – 1300 €/kW

III.4.6. Lithium-ion

LIBs are presented in Figure III.13 were made in 1991 and have since evolved primarily to serve as a power source for portable electronics, especially mobile phones and laptops. Today, the use of LIBs is broadening to include large-scale power solutions and energy storage systems, like electric vehicles and renewable energy technologies. The way a lithium battery works involves the movement of electrons, which is made possible by establishing a potential difference between two electrodes one negative and the other positive [188-189]. These electrodes are placed in a liquid known as an electrolyte that conducts ions. The lithium-ion battery exhibits significant autonomy, capable of storing a substantial amount of energy within a compact structure. Its high energy density allows it to retain three to four times more energy per unit mass compared to alternative battery types. One downside is that lithium-ion batteries are more expensive than other technologies. They also don't perform well at high temperatures and need protective circuits to function properly. Table III.6 shows more specific details about lithium-ion battery technology [190].



Figure III.13. Lithium-ion Battery [190].

Table III.6: Features of lithium-ion battery [190]

Characterizes	Value
Cell voltage	2.5 – 5V

Specific energy	80 – 250 Wh/kg
Specific power	200 – 2000 W/kg
Energy density	95 – 500 kWh/m ³
Power density	50 – 800 kWh/m ³
Efficiency	75 – 97%
Working temperature	20 – 65 °C
Lifetime cycles	100 – 10000
Lifetime	5 – 15years
Max. depth of discharge	100 %
Self-discharge rate	0.1 – 0.3 per day
Power rating	0 – 0.1MW
Energy cost	500 – 2100 €/kWh
Power cost	1000 – 3400 €/kW

III.5. Supercapacitor Energy Storage

Supercapacitors are well-suited for scenarios that demand rapid energy release and absorption, including regenerative braking in electric vehicles, power stabilization in renewable energy systems, and providing backup power for essential infrastructure. These devices store electricity and consist of two typically identical electrodes, which are separated by an electrolyte. Similar to batteries, they are rechargeable systems, often referred to as secondary generators, in contrast to primary generators that cannot be recharged, as well as fuel cells that convert chemical energy directly into electrical energy [190-191]. Three main types of supercapacitors depicted in Figure III.14 can be distinguished due to the unique architecture and storage methods characteristic of these devices.

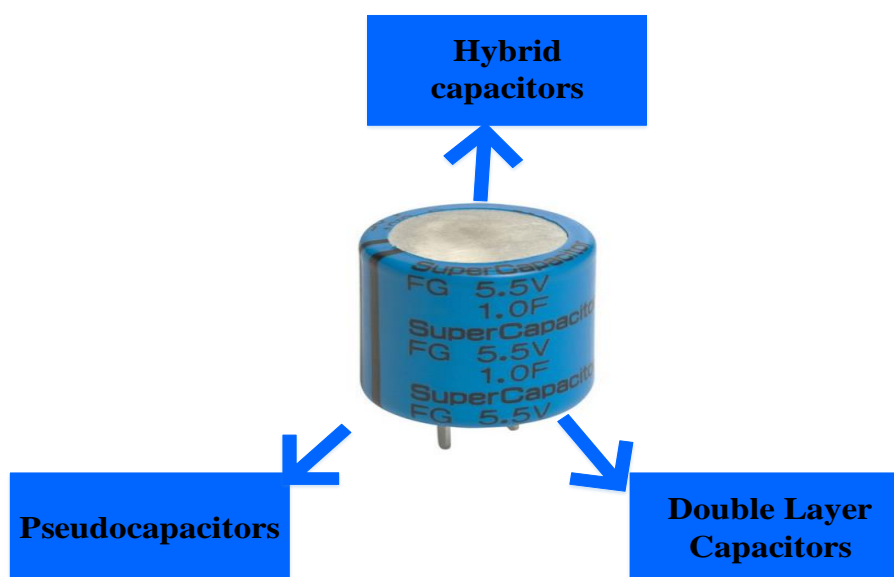


Figure III. 14. Supercapacitors types [191].

III.5.1. Pseudo-capacitors

The term '**Pseudo**' finds its roots in the Greek word 'pseuds.' A pseudocapacitor, while resembling a traditional capacitor, does not conform to its strict definition. A pseudocapacitor engages in rapid and reversible electrochemical reactions, known as Faradaic reactions, to facilitate energy storage. This mechanism utilizes near-surface charge transfer, complementing the electrostatic charge storage. The charge transfer occurs at the interface between the electrode and electrolyte, where Faradaic reactions take place at or near the electrode material's surface, involving a limited number of electrons transitioning between the valence states of the electrode materials [190].

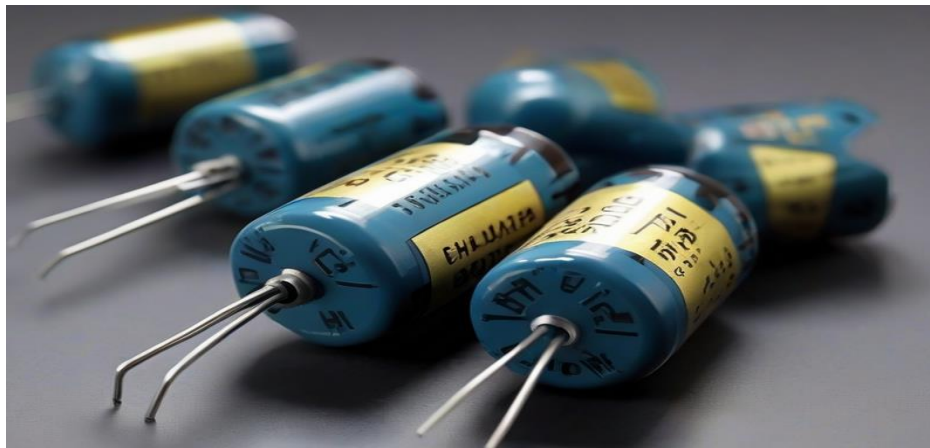


Figure III.15.Pseudo-capacitors[191].

III.5.2. Electric Double Layer Capacitors

Electrical capacitors are exceptional energy-storage solutions, renowned for their remarkable power density and extended cycle life[191]. These sophisticated devices can be classified into two categories based on their energy-storage mechanisms: electrochemical double-layer capacitors and redox supercapacitors. The former, known as electric double-layer capacitors (EDLCs), leverage the double-layer capacitance formed at the interface of high-surface-area materials and the electrolyte solution. Here, energy is primarily stored through separating electronic and ionic charges at this interface, a process fundamentally rooted in electrostatics. Conversely, redox supercapacitors engage in rapid Faradic reactions at the electrode materials under specific potentials, akin to the behavior of batteries, resulting in a phenomenon referred to as pseudo-capacitance[192].



Figure III.16.Electric Double Layer Capacitors[192].

III.5.2. Hybrid Capacitors

Hybrid supercapacitors, often referred to as asymmetric supercapacitors, elegantly address the inherent limitations of both electric double-layer capacitors (EDLCs) and pseudocapacitors, resulting in superior performance attributes. These sophisticated devices function through a harmonious blend of pseudocapacitance, which involves a faradaic process, and double-layer capacitance, characterized by a nonfaradaic process, to effectively store energy. In this configuration, one electrode is composed of a material that facilitates the pseudocapacitive process, while the second electrode relies solely on charge separation through the formation of a double layer. As a result, hybrid capacitors achieve remarkable energy and power densities, surpassing those of traditional EDLCs, all while maintaining exceptional long-term stability[193].



Figure III.17. Hybrid capacitors[193].

III.6. Performance of different types of Supercapacitors Energy Storage

The efficacy of superior supercapacitors can be assessed through a variety of criteria as depicted in Table III.7, including[194-195]:

- Storage Mechanism
- Specific Capacitance
- Energy density
- Cycle Life/stability

Table III.7: Performance of several supercapacitors

Parameters	Pseudocapacitors	Electric Double Layer Capacitors	Hybrid Capacitors
Storage mechanism	Faradic, reversible redox reaction	Non-faradic/electrostatic, electrical charge stored at the metal/electrolyte interface	Both faradic and non-faradic
Energy density	High	Low	High

Cycle Life/stability	Low	High	High
-----------------------------	-----	------	------

III.7. Comparison between battery and supercapacitor energy storage via diagram Ragone

ESS are available in various sizes, including fuel cells, batteries, capacitors, SCs, and superconducting magnetic energy storage (SMES) systems. In evaluating the overall performance of these systems, two critical specifications are commonly referenced: **energy density and power density**. To assess and compare the capabilities of different energy delivery options, a Ragone plot, created by David V. Ragone, is frequently employed as depicted in Figure III.18. Supercapacitors are energy storage devices that have a large power density and a long cycle life. Compared with batteries, in addition to remarked the supercapacitors have hundreds of times longer cycle lives and over 10 times larger power densities, leading also to much shorter charging times. Also, note that the supercapacitors have approximately 10 times lower energy density compared to batteries. The application scope of both components can be established based on these essential factors.

- Capacitors are advantageous when there is a need to store or release a charge rapidly within a brief period. Common examples include the flash mechanism in mobile phones, which utilizes an LED capable of handling a significant current for a very short duration.
- Batteries are preferred when a substantial amount of charge is required over an extended period, which is typical for most Smart Objects.
- Recent advancements in electrochemical energy storage technologies have resulted in hybrid designs that integrate batteries and supercapacitors, aiming to leverage the benefits of both types of devices simultaneously[194].

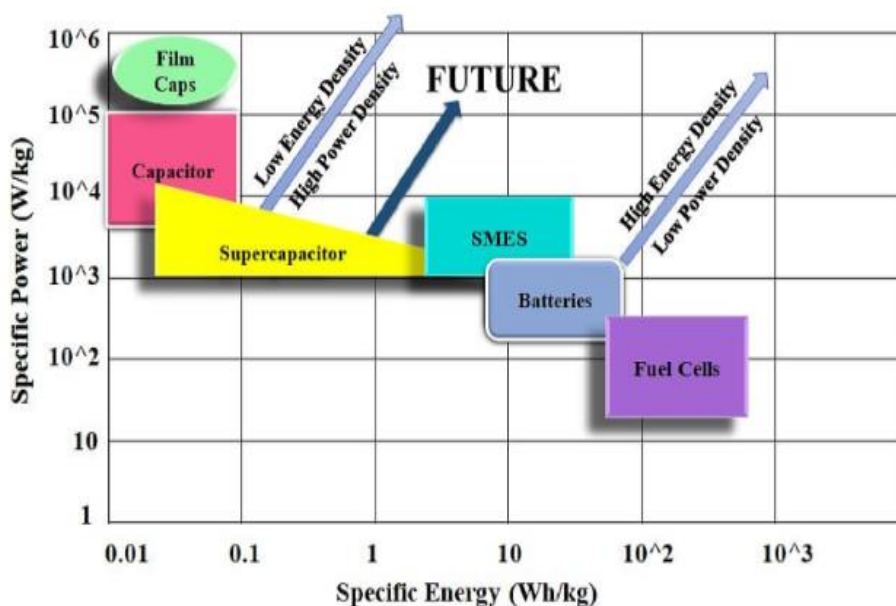


Figure III.18.Ragone Diagram [195].

III.7. Hybrid energy storage

HESS is formed by effectively integrating two or more ESSs as depicted in Figure III.19 with complementary characteristics, such as energy efficiency, power density, self-discharge rate, and longevity. Each storage technology has its advantages and disadvantages; therefore, combining different storage technologies can enhance the overall performance of energy storage systems. In an HESS, one unit may be specifically designed to handle high power demands, rapid fluctuations, and transient events, necessitating a quick response time, high efficiency, and extended cycle life. Conversely, the second unit may focus on providing substantial energy capacity while maintaining a low self-discharge rate. For example, integrating flywheel and battery technologies within a smart grid can significantly mitigate fluctuations at the point of common coupling, achieving reductions of over 80% in the output profile of renewable energy sources[196]. The advantages of an HESS include:

- The decoupling of energy and power components leads to reduced overall investment costs.
- The energy efficiency of the HESS surpasses that of any individual component.
- The energy storage capacity and operational lifespan of the system are both enhanced in an HESS [195].

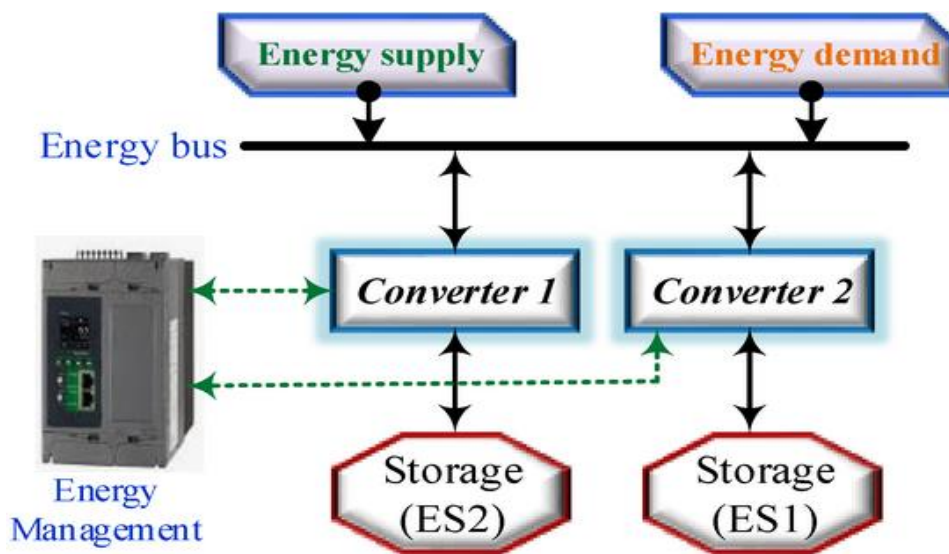


Figure III.19. structure of HESS [196].

III.8. Classification of Hybrid energy storage

Figure III.20 demonstrates the integration of multiple storage systems to fulfill diverse functions across various renewable energy applications [197]. The most commonly utilized types of hybrid energy storage systems in renewable energy systems include SC/battery, battery/SMES, flywheel/battery, battery/FC, SC/FC, FC/flywheel, and CAES/battery. It is crucial to note that the selection of appropriate hybrid energy storage system combinations depends on numerous factors, including the specific hybridization objectives, storage costs, geographical location, and the availability of storage capacity.

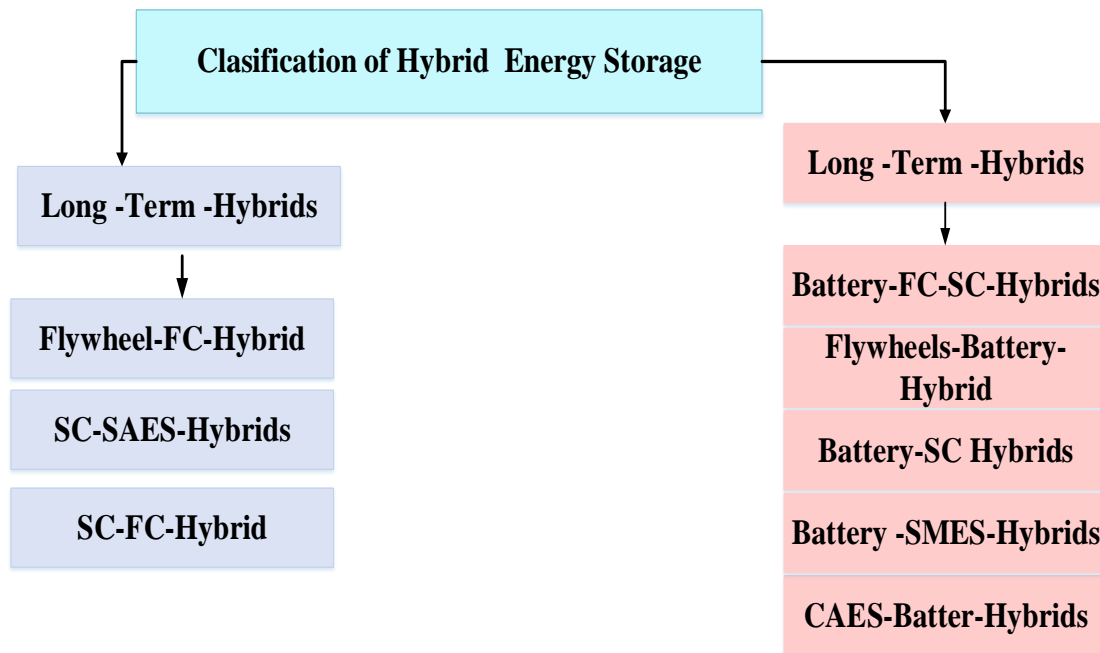


Figure III.20. Classification of HESS[198].

III.7.1. Different configurations used for batteries/supercapacitors Hybrid energy storage

The combination of batteries and SC is an ideal fit that can fulfill a wide range of energy and power demands for renewable energy systems, particularly solar power systems [4]. As a consequence, there are several HESS configurations, and the most popular ones as shown in Figure III.21 [198-199].

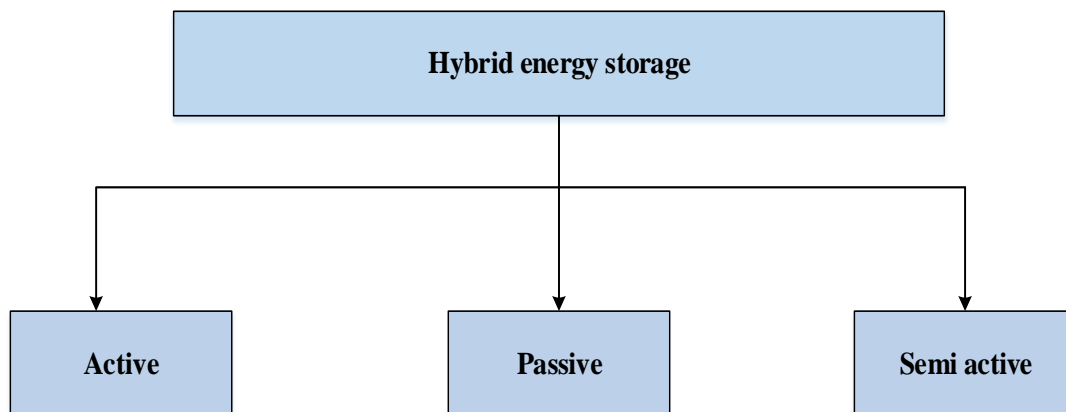


Figure III.21. Different configurations of HESS.

III.7.2. Basic passive parallel hybrid configuration

In a passive HESS design, the integration of the two energy sources, batteries, and SC, are connected directly without the use of a power converter, as depicted in Figure III.22. Due to the parallel connection of the two sources, the voltage across the DC link remains essentially the same [200]. Passive integration requires the utilization of a regulated power system. Furthermore, the buck-boost converter needs to be larger to manage the power of the SC [200], [201]. The primary advantage lies in the increased reliability resulting from a reduced number of elements prone to failure. However, the drawback of this

configuration is that the power distribution between the SC and batteries is not controlled, but rather dependent on the internal resistance of both the batteries and SC [201].

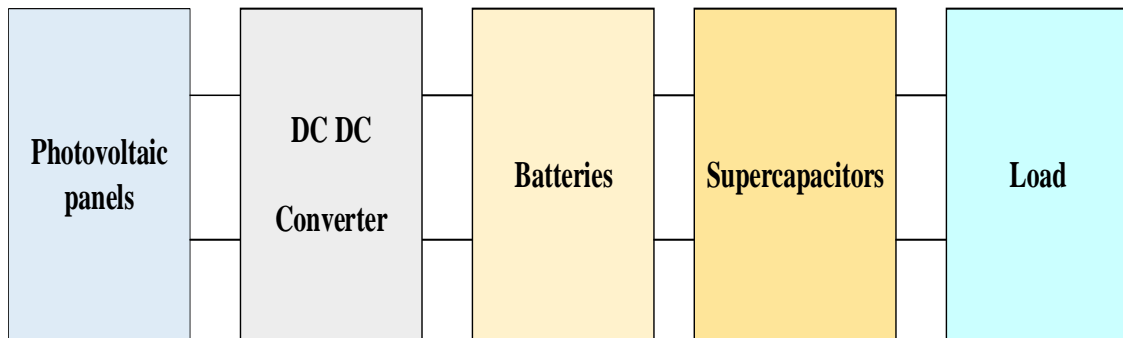


Figure III.22.Basic passive parallel hybrid configuration.

III.7.3. Basic semi-active parallel hybrid configuration employing batteries

Figure III.23 illustrates the arrangement of the SC and batteries for the semi-active configuration. In this setup, the battery's voltage can be maintained higher than that of the SC [201-202]. The SC is directly connected to the DC bus, while the battery power is regulated. The control strategy employed in this configuration allows for the fluctuation of the DC link voltage within a specified range. The primary advantage of this approach is the reduced sizing and mass cost compared to configurations employing multiple converters. However, a drawback of this arrangement is the insufficient control of the DC bus voltage due to the direct connection of the SC to the DC bus [202].

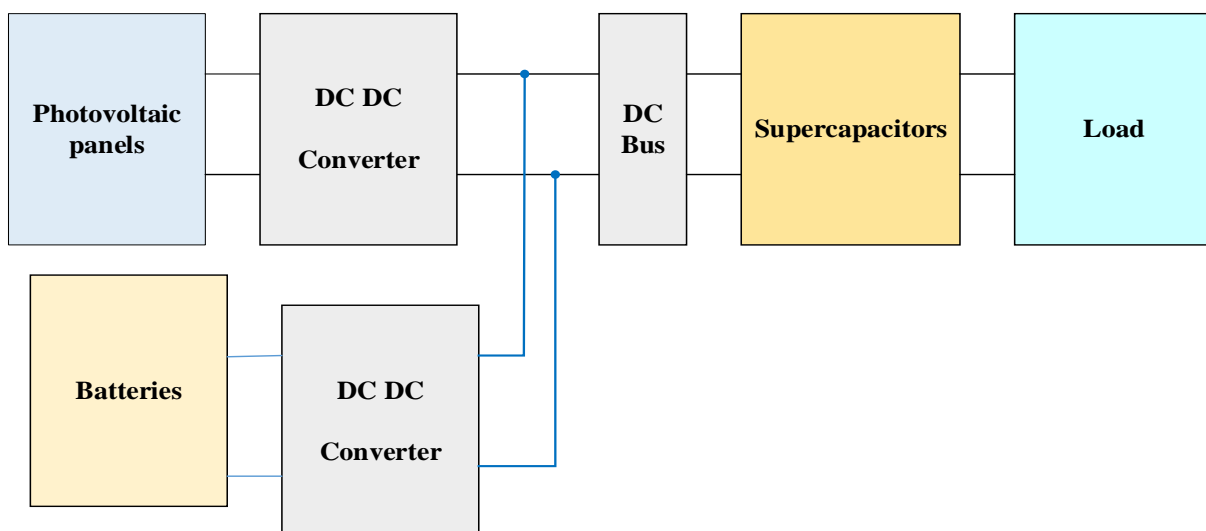


Figure III. 23.Basic semi-active parallel hybrid configuration employing batteries.

III.7.4. Basic semi-active parallel hybrid configuration employing SC

Figure III.24 illustrates the configuration of a HESS featuring a BDC that interfaces with the SC to enable a broader range of voltage utilization. This setup includes only one controllable power source. However, to effectively manage the power of the SC, the BDC must be upsized [203-204]. Furthermore, the nominal voltage of the SC bank may be lower. Since the battery is directly linked to the DC bus, the

voltage of the DC bus remains fixed. The primary advantage of this arrangement is the relatively constant voltage of the DC bus, which is adjusted by the SOC of the batteries due to their direct connection.

Nevertheless, the main drawback is the need to regulate the voltage of the DC bus since, in this configuration, the batteries are directly connected to the bus [205].

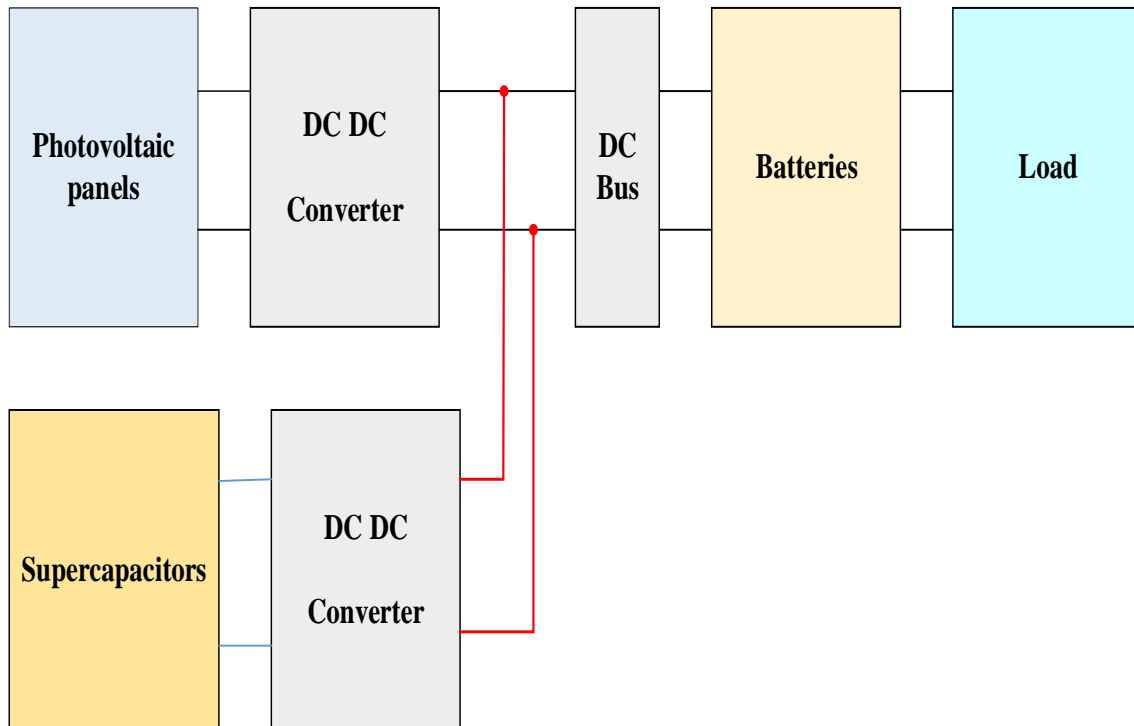


Figure III. 24. Basic semi-active parallel hybrid configuration employing SC.

III.7.5. HESS using multiple converters hybrid configuration

The optimal solution, depicted in Figure III.25, involves a multiple converter architecture utilizing two separate bidirectional buck-boost converters. It involves maintaining the voltage of both batteries and the SC lower than that of the DC bus [204-206]. By doing so, the capacitor can be fully utilized, given the potential wide range of voltage for the SC. This configuration enables independent management of power from the batteries and SC, allowing for tailored control based on their supply requirements and their SOC [207].

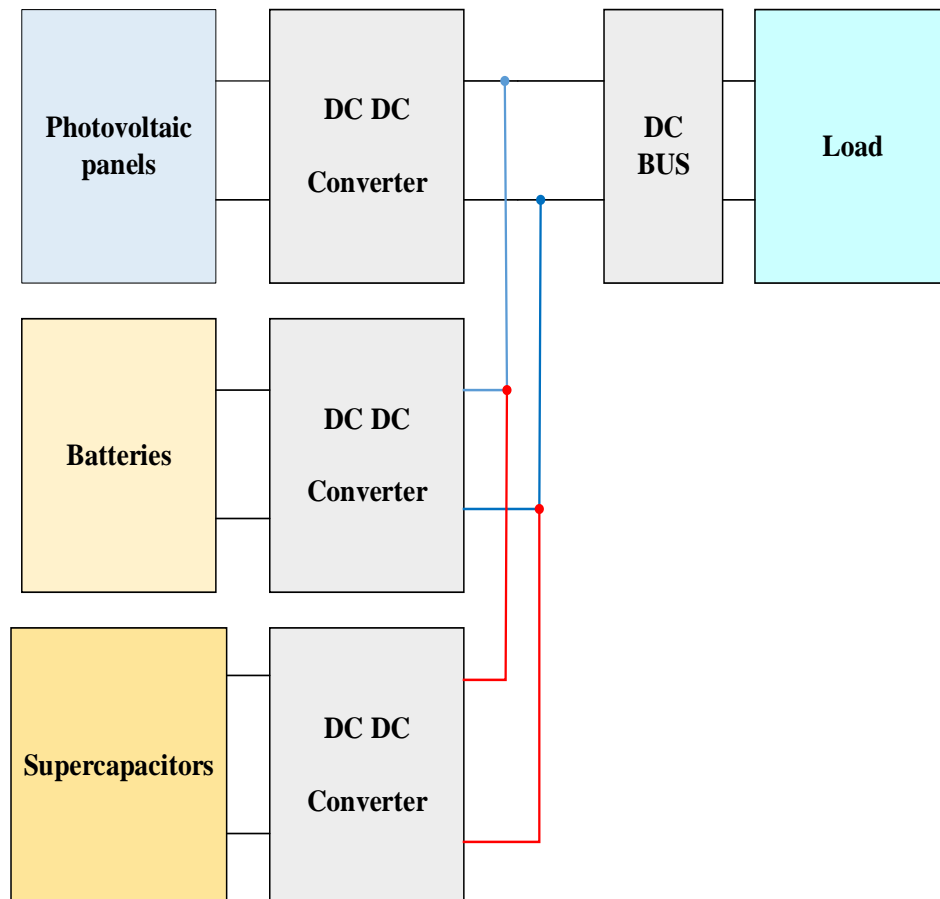


Figure III.25. Basic, several converters, parallel hybrid configuration.

III.8. Conclusion

The chapter culminates by elucidating the overview of the energy storage system, encompassing critical technologies such as mechanical, electrochemical, thermal, chemical, and electrical energy storage batteries/SCs with different types of details the characters on every model of batteries/SCs requirement. Additionally, to evaluate the overall performance of these storages systems, two critical specifications are commonly referenced: energy density and power density by using a diagram, Ragone. Overall, this chapter equips readers with a comprehensive understanding of hybrid energy storage technologies and topologies' pivotal association and role in renewable energy systems. In conclusion, a sustainable energy future depends on the development and application of sophisticated energy storage and hybrid systems. These technologies contribute to a cleaner, more efficient energy environment, greater utilization of renewable resources, and increased energy security. By comprehending the principles of batteries SCs we are better equipped with the control and management that will be present in chapter 4 to enhance the reliability and efficiency of these systems and tackle the challenges posed by energy in different scenarios.

Chapter IV

Modeling, Analysis, and management of batteries- supercapacitors energy storage

IV.1. Introduction

Chapter 4, titled “Modeling, Analysis, and management of batteries-supercapacitors energy storage” a pivotal section in exploring photovoltaic systems connected to batteries-supercapacitors. We begin by providing a thorough overview of our suggested system, which includes solar panels, a boost converter, and an EES made up of a supercapacitor and batteries. A DC-DC type buck-boost converter connects each ESS to the DC bus. Moreover, we present the design and optimization of PI controllers using metaheuristic optimization methods such as GA, ACO, and GWO algorithms for EMS of HESS combining batteries and SC, as well as an innovative heuristic approach for fine-tuning the parameters of a PI regulator to control the power flow and performance of battery charge and discharge and SC storage.

IV.2. System Description

Figure IV.1 illustrates a HESS that combines batteries and SC, with all resources connected in parallel across the load. The PV panel is connected to a DC/DC boost converter regulated by Maximum Power Point Tracking (MPPT) to extract maximum power from the PV panels. The HESS effectively smooths out power fluctuations, while the SC handles rapid dynamic power fluctuations. Unlike batteries, which operate in a stable state, SC functions in a transient state. This HESS utilizes a buck-boost converter to connect batteries and SC to the DC bus, enabling charge and discharge control for each storage element.

A DC link ensures power allocation between the load, the primary PV source, and the two energy storage devices (batteries and SC).

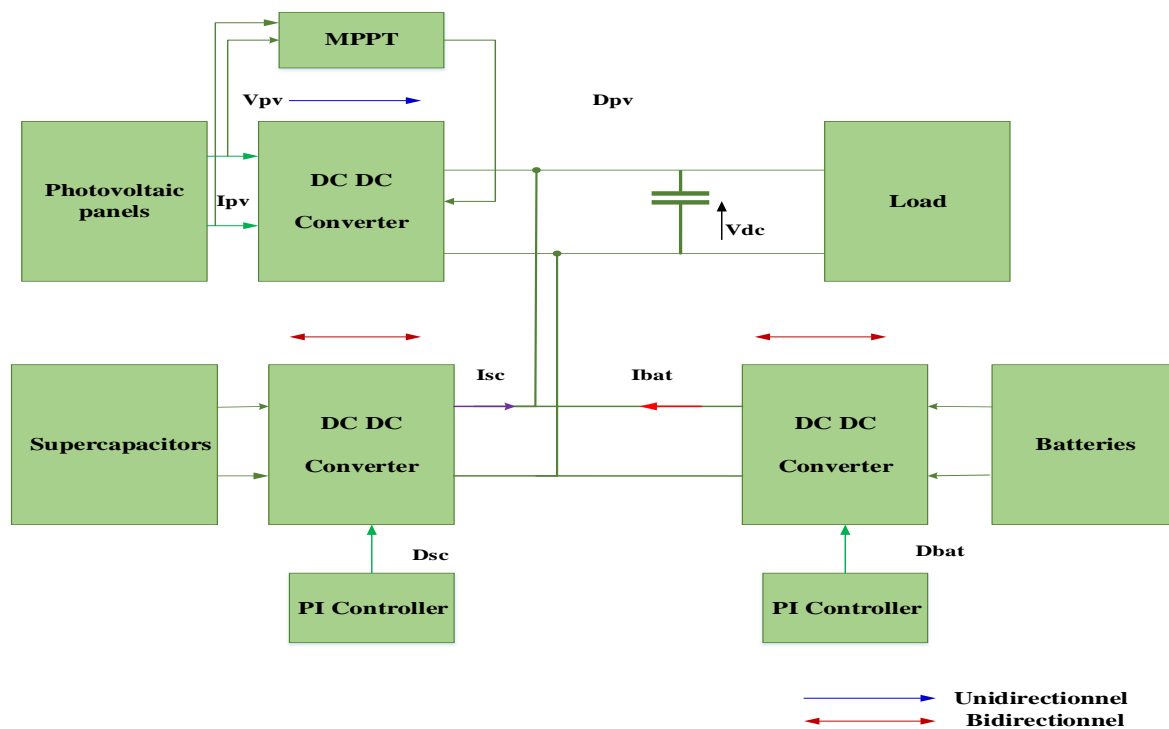


Figure IV.1. PV system with HESS.

IV.2.1. Electrical Model of Battery

Batteries are the basic storage technology in PV systems. Battery cells are connected in series to increase pack voltage, whereas parallel cell connections increase current and power capabilities and, hence, pack capacity. This model is used to examine the impacts of variable load and SOC.

The equivalent circuit parameters can be modified to represent a particular type of battery based on its charge/discharge characteristics [208].

The battery model used in this study is depicted in Figure IV.2 [209]:

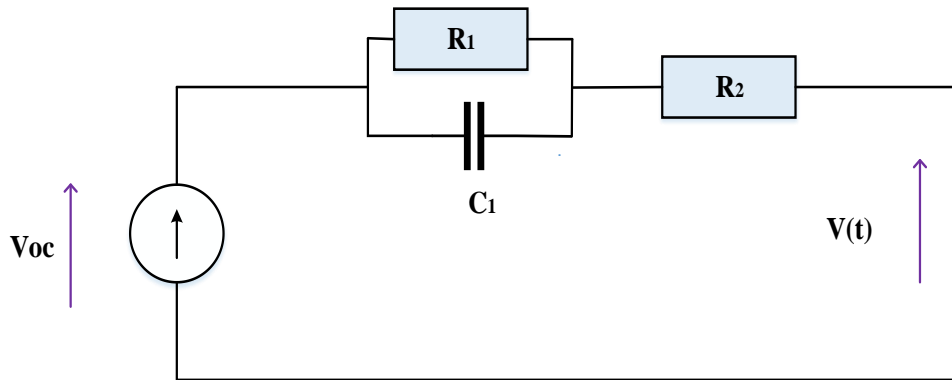


Figure IV.2. Battery cell model.

- The SOC of the battery is expressed as [208]:

$$SOC = SOC_{init} - \int \frac{I_b}{C_{bu}} dt \quad (IV.1)$$

Where :

$$C_{bu} = 3600 * C_{BN} * f_1(CN) * f_2(T) \quad (IV.2)$$

The most common operational constraint for a BESS is related to the battery's charge and discharge or SOC limits.

The SOC expressed as a percentage, represents the energy remaining in the storage system relative to its total capacity.

Battery deterioration is a critical factor to consider in power system planning. With each charge and discharge cycle, the battery energy storage capacity decreases slightly and irreversibly [209-211]. Battery capacity depends on several operating variables, such as charge, discharge rate, depth of discharge, cut-off voltage, temperature, and the number of cycles recorded by the battery [212]. To ensure optimal performance, the energy charged and discharged daily must be balanced, considering the efficiency of ESS.

The defined bound conditions are as follows [213]:

$$SOC_{min} < SOC < SOC_{max} \quad (IV.3)$$

IV.2.2. Electrical Model of Supercapacitors

SC also known as ultracapacitors or electrochemical double-layer capacitors, are regarded as

promising technologies with beneficial properties. Energy is stored as an electric field between the two electrodes, with no chemical reaction [214-215].

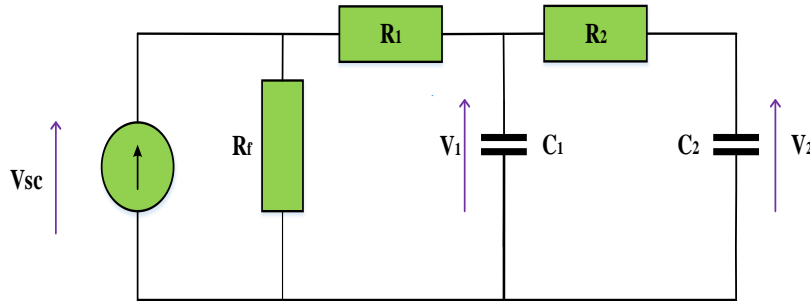


Figure IV.3. SC cell model.

- The voltage V_2 can be expressed by [214-216]:

$$V_2 = \frac{1}{C_2} \int i_2 dt \tag{IV.4}$$

- The voltage V_1 across the main cell's capacitor C_1 is provided by:

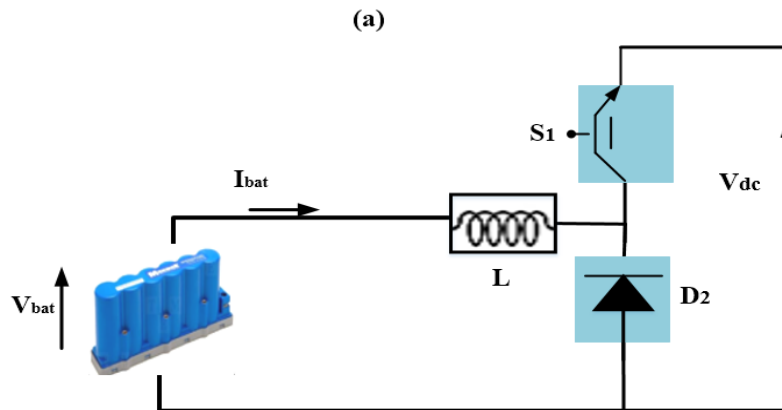
$$V_1 = \frac{-C_k + \sqrt{C_k^2 + 2C_p Q_1}}{C_p} \tag{IV.5}$$

where Q_1 is the instantaneous charge of capacitor C_1 and is calculated as follows:

$$Q_1 = C_k V_1 + \frac{1}{2} C_p V_1^2 \tag{IV.6}$$

IV.3. DC-DC Bidirectional Converter

Figure IV.4 shows the buck-boost converter for the battery, while the converter for the SCs is shown in Figure IV.5. These converters adjust the voltage level according to the system requirements. The HESS is connected to the high-voltage DC bus in PV systems through a bidirectional converter. This allows the load power supply to be controlled to meet the required power demand. The converter consists of $VESS$, an inductor L and switches (S_1, S_2) for the battery, and (S_3, S_4) for the SC. The values of these parameters are described in detail in [217].



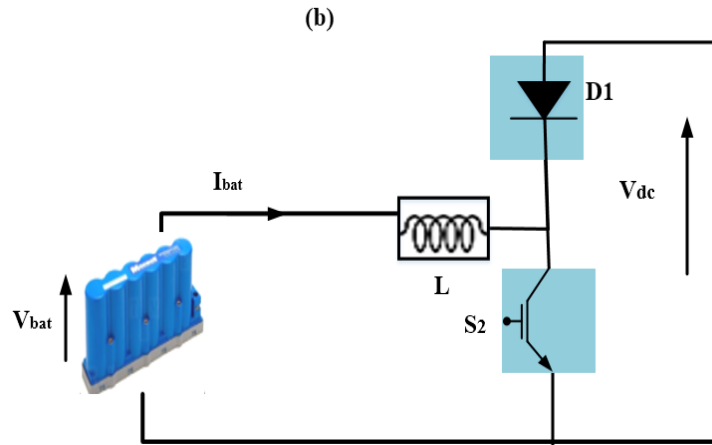


Figure IV.4. Circuit for the Buck-Boost in two transfer directions (a) From V_{bat} to V_{dc} (forward mode), (b) From V_{dc} to V_{bat} (reverse mode) converter of the battery

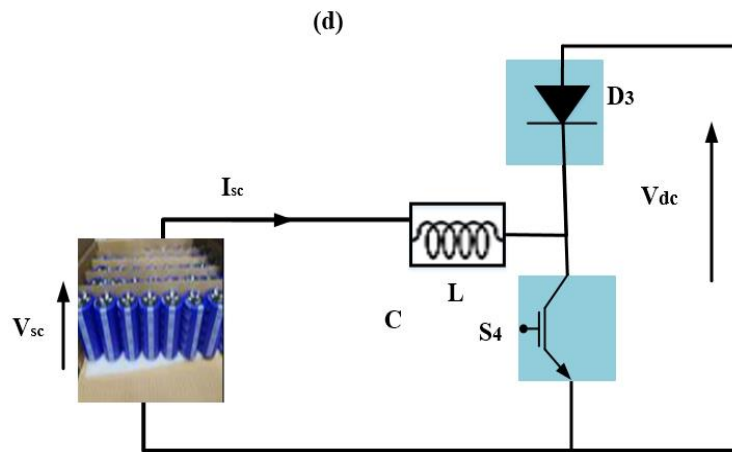
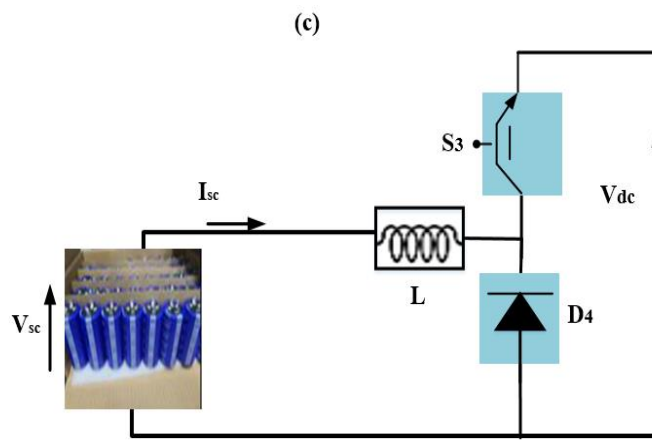


Figure IV. 5. Circuit for the Buck-Boost converter in two transfer directions (c) From V_{sc} to V_{dc} (forward mode), (d) From V_{dc} to V_{sc} (reverse mode) converter of the supercapacitor.

The bidirectional converter allows power transfer in both directions, allowing energy to flow from the load to the battery /Supercapacitor Energy Storage System and vice versa [217].

- The buck-boost converter operates in two modes:

When the storage system (battery / SC) is in charging mode, in this case, the converter works in Buck mode:

$$D = \frac{V_{dc}}{V_{bat/sc}} \quad (IV.7)$$

When the storage system (battery / SC) is in discharge mode, in this case, the converter operates in boost mode:

$$D = 1 - \frac{V_{bat/sc}}{V_{dc}} \quad (IV.8)$$

IV.4. Control Strategy of HESS

The control scheme is illustrated by the block diagram shown in Figure IV.6. A PI controller keeps the DC link voltage V_{dc} at the reference voltage ($V_{dc\ ref} = 50V$).

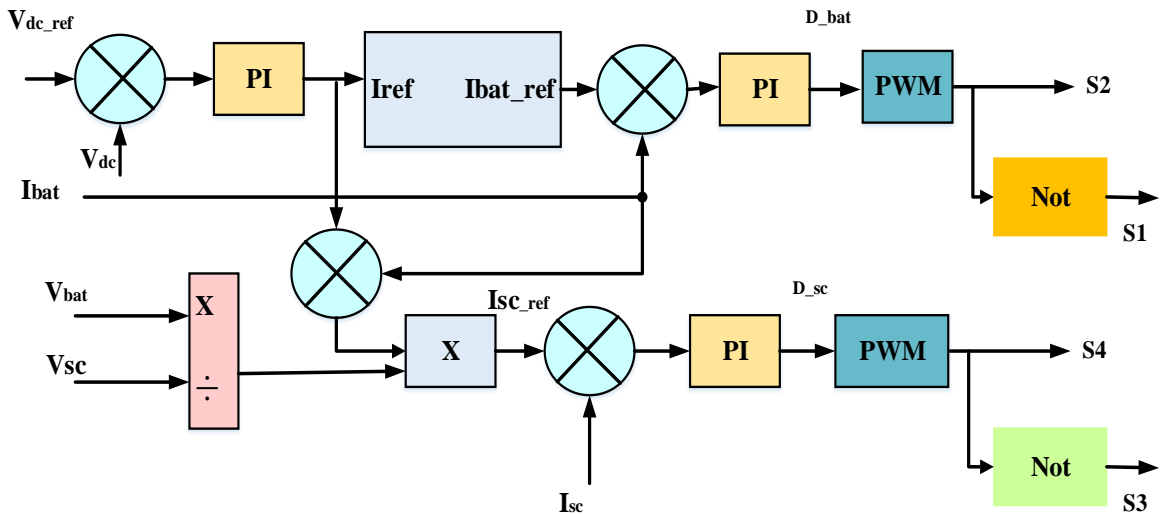


Figure IV.6. Control scheme of HESS.

The voltage error is given by:

$$\Delta V = V_{dc\ ref} - V_{dc} \quad (IV.9)$$

- The transfer function of the DC link (V_{dc}) is given by:

$$\frac{V_{dc}}{I_{dc}} = \frac{1}{Cs} \quad (IV.10)$$

- The transfer function of the battery is given by:

$$G_{bat}(s) = \frac{I_{bat}}{D_{bat}} = \frac{V_{bat}Cs + 2V_{bat}}{R \cdot L_{bat}Cs^2 + L_{bat}s + (1 - D_{bat})^2} \quad (IV.11)$$

- The transfer function of the SC is given by:

$$G_{sc}(s) = \frac{I_{sc}}{D_{sc}} = \frac{V_{sc}Cs + 2 \cdot V_{sc}}{R \cdot L_{sc} \cdot C \cdot s^2 + L_{sc} \cdot s + (1 - D_{sc})^2} \quad (IV.12)$$

The sum of the reference currents, $I_{bat\ ref}$ and $I_{sc\ ref}$, must be equal to the total current I_{dc} [41]:

$$I_{dc} = I_{bat\ ref} + I_{sc\ ref} = I_{PV} - I_L \quad (IV.13)$$

The following equation describes the DC bus voltage:

$$C \frac{dV_{dc}}{dt} = I_{bat} + I_{sc} + I_{PV} - I_L \quad (IV.14)$$

The difference between the battery current (I_{bat}) with its reference (I_{bat_ref}) is fed to the PI regulator, which then generates the duty cycle (D_{bat}) of the PWM control signal for the converter's switches (S_1) and (S_2).

In case the batteries cannot supply the required power, the SC compensates for the leftover power. As a result, the SC reference current is provided by the equation below [218]:

$$I_{sc_ref} = \frac{P_{bat}}{V_{sc}} = (I - I_{bat}) \frac{V_{bat}}{V_{sc}} \quad (IV.15)$$

Similarly, after comparing the SC current (I_{sc}) with its reference (I_{sc_ref}) then the difference is passed to the PI regulator to calculate the duty cycle (D_{sc}) of the PWM control signal for the converter's switches (S_3) and (S_4) [219].

IV.5. Energy Management System of HESS

Figure IV.7 depicts the flowchart for the EMS implementation for the standalone PV connected with the HESS.

Initially, the load power (P_L) is compared with the power generated from the PV system (P_{PV}).

If the PV power is greater than the load power ($P_{PV} > P_L$), then the PV will provide the necessary power to the load. Here, the SC starts charging from the excess of PV power. However, Batteries cannot hold excess power for such a short time.

If the PV power is less than the load power ($P_{PV} < P_L$), the energy deficit between the load power and the PV will be supplied from the battery's energy storage ($P_{bat} = P_L - P_{PV}$). Here, the SOC of the batteries will also decrease; in the meantime, the SC is fully charged and ready to discharge to provide the energy to the load to support the power delivered by the PV.

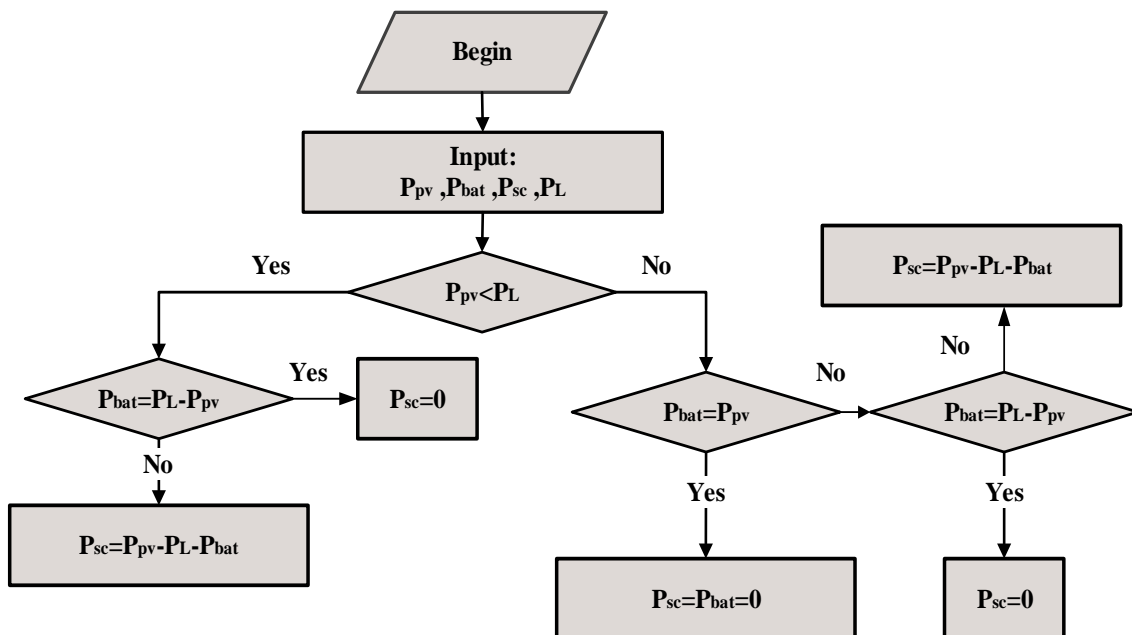


Figure IV.7. Flowchart of the EMS.

IV.6. Generality of optimization

Optimization has been thoroughly investigated and garnered significant research attention over the last few decades. Algorithm validation, complexity assessment, and optimization are pivotal areas of inquiry within theoretical computer science, each contributing to our understanding of how computational processes can be effectively designed and implemented. These domains enhance our theoretical knowledge and have practical implications in various fields, including software development, data analysis, and artificial intelligence. The complexity associated with various computational tasks is meticulously analyzed through the lens of computational resources, which encompass execution time and memory usage [220-223].

This analysis is crucial because it allows researchers and practitioners to gauge the feasibility of solving specific problems within given constraints. By determining which problems can be resolved efficiently, meaning within specified time and space limits, significant savings can be realized in both time and financial resources during the algorithm design phase. Optimization entails the process of minimizing or maximizing a particular function [224].

IV.7. Classification of Optimization Problems

Since algorithms are suited to particular problem types and classifications differ among authors, solving optimization problems necessitates identifying problem categories.

- **Single-objective or multi-objective optimization problems**

Single-objective problems are characterized by a single objective function, whereas multi-objective problems necessitate a balance among conflicting objectives. Reformulating multi-objective problems into a single objective function or transforming objectives into constraints is not always an effective approach.

- **Deterministic and stochastic optimization problems**

Deterministic optimization problems assume that all data is fully known, while stochastic optimization problems incorporate uncertainty into the model. This is particularly useful when considering variables like future product sales, as it enables more precise forecasting.

- **Continuous versus discrete optimization problems**

In certain scenarios, the decision variables manifest as discrete entities, typically represented as integers or binary values, thereby categorizing the optimization challenge as discrete. Conversely, in continuous optimization, the variables are free to assume any real value, rendering these problems generally more straightforward to resolve. When an optimization problem intertwines continuous and discrete variables, it is elegantly referred to as a mixed optimization problem.

- **Constrained and unconstrained optimization problems**

Distinguishing between problems with constraints on decision variables, which can be bounds or equations of equality and inequality, is crucial. Equality constraints can be eliminated by substitution in the objective function, while constraints require dedicated algorithms.

IV.8. Different Optimization methods

Figure IV.8 illustrates various optimization methods, divided into exact algorithms and approximate algorithms, where approximate algorithms include heuristics and meta-heuristics algorithms.

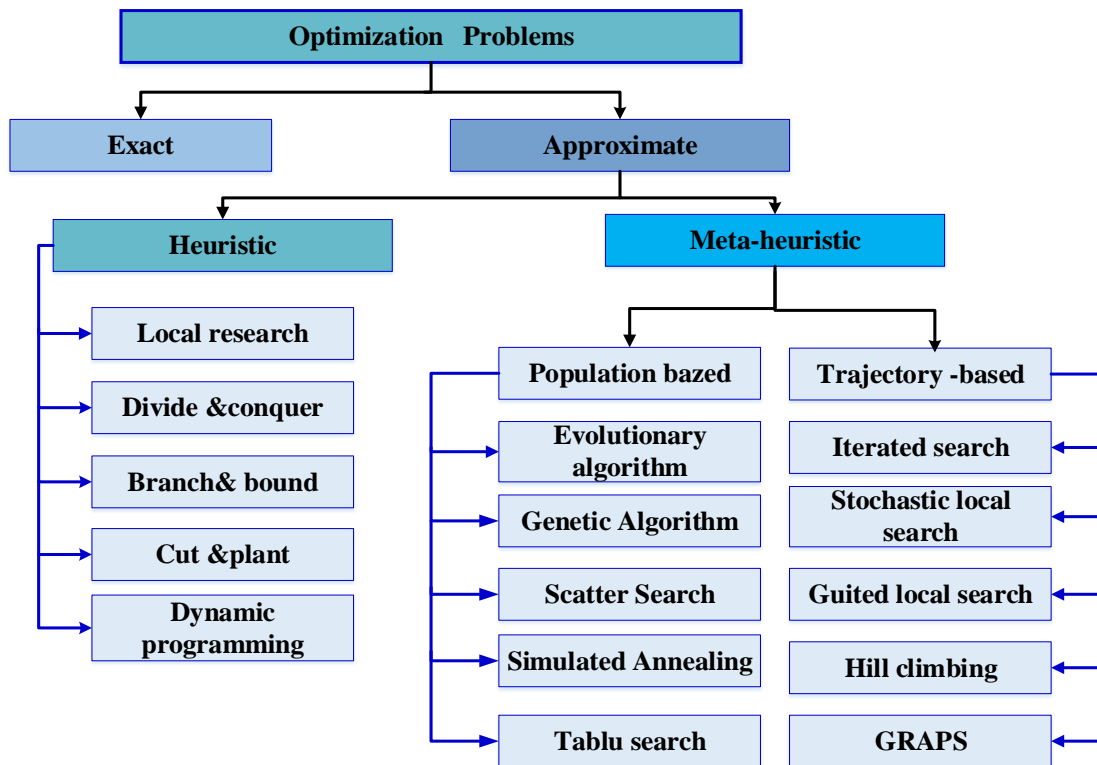


Figure IV.8. Optimization methods [225].

IV.8.1. Heuristic algorithm

Heuristics refer to experience-driven methods employed for problem-solving, learning, and exploration. These techniques facilitate the rapid identification of satisfactory solutions by leveraging rules of thumb, informed estimates, intuitive reasoning, or practical wisdom. Heuristics are strategies that utilize readily available information to guide problem-solving processes in humans and machines. They find applications in computer science, artificial intelligence, and mathematical optimization, enabling quicker resolutions when traditional methods are inefficient or when seeking approximate solutions. Although heuristics may be viewed as imprecise and not entirely accurate algorithms, they typically yield solutions that are close to the optimal ones swiftly and straightforwardly.

IV.8.2. Meta-heuristic algorithm

Metaheuristics represent an advanced category of heuristics, derived from the combination of the terms "meta" and "heuristic," signifying a level that transcends traditional approaches. Traditionally, algorithms employing stochastic processes were referred to as heuristic algorithms. Metaheuristic algorithms serve to guide and enhance other heuristic methods, aiming to yield solutions that surpass those usually obtained in the pursuit of local optimality. While these algorithms can generate highly effective solutions, they do not ensure the discovery of optimal solutions [226].

They work well for a variety of problems since they don't assume anything about the issue at hand.

Metaheuristics can find good solutions in combinatorial optimization with less processing effort than optimization algorithms, iterative approaches, or simple heuristics. They frequently employ stochastic optimization, which is based on generated random variables. They are efficient methods for resolving optimization problems.

The following are characteristics that define the majority of metaheuristics [227]:

- Metaheuristics serve as strategies that direct the search process.
- Their primary objective is to navigate the search space to identify near-optimal solutions effectively.
- The methods that make up metaheuristic algorithms vary from straightforward local search techniques to intricate learning processes.
- Metaheuristic algorithms are typically approximate and often non-deterministic.
- Metaheuristics are not tailored to specific problems.

IV.9. Optimized PI Controller Tuning

Three different metaheuristic algorithms, GA, ACO, and GWO, are used to optimize the gains of the PI controllers for the HESS. The control structures are briefly explained below.

IV.9.1. Optimization criteria for a PI controller

In this chapter, the objective is to determine optimal gains for a PI controller to improve the performance of the HESS. In this case, the objective is to minimize the error. For this purpose, each individual in the population of solutions is sent to the evaluation unit, and its fitness is calculated to determine its performance as a controller for the given process. The performance of the system is calculated using the criterion ITAE. The performance criterion is related to the fitness function, and the optimal PI parameters are derived by minimizing an objective.

IV.9.2. Classic PI Controller Pole Placement Optimization Application to PI Controller Tuning

Pole placement, also called full-state feedback, is a technique for controlling various closed-loop parameters such as overshoot, peak time, rising time, and settling time.

These parameters are then used to calculate the relative damping δ and frequency ω of the closed-loop characteristic polynomial. The closed-loop transfer function can be expressed as:

$$G_{pp} = \frac{D(1 - D)}{LCs^2 + \frac{L}{R}s + (1 - D)^2} \quad (IV.16)$$

The transfer function of the PI controller is given by:

$$G_{pi_pp}(s) = \frac{K_p(1 + s T_i)}{T_i} \quad (IV.17)$$

The closed-loop transfer function of the system is:

$$H(S) = \frac{G_{pi_pp}(s)G_{pp}(s)}{1 + G_{pi_pp}(s)G_{pp}(s)} \quad (IV.18)$$

The characteristic equation is as follows:

$$1 + G_{pi_pp}(s)G_{pp}(s) = 0 \quad (IV.19)$$

$$1 + \frac{K_p(1 + s T_i)}{T_i} \frac{D(1 - D)}{LCs^2 + \frac{L}{R}s + (1 - D)^2} = 0 \quad (IV.20)$$

$$LCT_i s^3 + \frac{L}{R}T_i s + T_i(1 - D)^2 + K_p(1 + s T_i)(1 + s T_i) = 0 \quad (IV.21)$$

A third-order reference model generally provides a good approximation of the closed-loop system

$$(s + \alpha\omega)(s^2 + 2\xi\omega s + \omega^2) = 0 \quad (IV.22)$$

$$s^3 + 2\xi\omega s^2 + \omega^2 s + \alpha\omega s^2 + 2\alpha\xi\omega s + \alpha\omega^3 = 0 \quad (IV.22)$$

$$s^3 + (2\xi\omega + \alpha\omega)s^2 + (\omega^2 + 2\alpha\xi\omega)s + \alpha\omega^3 = 0 \quad (IV.23)$$

Subsequently, the PI controller parameters K_p and T_i are calculated by making Equating (14) with the denominator of Equation (17) gives:

$$\begin{cases} LCT_i = 1 \\ K_p D(1 - D) = \alpha\omega^3 \end{cases} \quad (IV.24)$$

Solving for the PI controller parameters K_p and T_i gives:

$$K_p = \frac{\alpha\omega^3}{D(1 - D)_i} \quad (IV.25)$$

$$T_i = \frac{1}{LC}$$

Table IV.1 shows the PI controller gains values for the HESS.

Table IV. 1 : Parameters of HESS tuned by conventional PI

Parameters	K_{p_bat}	K_{i_bat}	K_{p_sc}	K_{i_sc}	ITAE
PI	4.76	21.8	0.85	30	0.456

IV.9.3. Optimization of PI parameters using GA heuristic algorithms

IV. 9.3.1. Overview of genetic algorithm

GA is a stochastic global optimization method inspired by natural selection processes. J. Holland developed the GA in 1975 as a tool for adaptation modeling and working in a bit string space. It is most popular among researchers in different disciplines. D.E. Goldberg widely used and developed it in 1989 [226-230]. Their role is to search for the global extremum of a defined function in a data space, and their fields of application are extensive. In addition to economics, they are used for optimizing functions in finance, optimal control theory, and repeated play theory. The reason for this large number of applications is their simplicity and efficiency. It has gained popularity for its efficiency in solving optimization problems [228-230]. GA operates iteratively by maintaining a population of potential solutions at a constant size. At each iteration or generation, three genetic operators, selection, crossover, and mutation, are applied to generate new populations. The fitness of the chromosomes in these new populations is evaluated based on specific cost functions.

IV.9.3.2. Details of Different Steps in the GA Process

1) Initial population

The initial step in implementing genetic algorithms is to generate a population of N individuals, each representing one possible solution to the given issue. Individual selection has a significant impact on algorithm speed. If the optimum position in the search space is unknown, seeing how the population is dispersed over the whole space is fascinating. Additionally, selecting the population size poses a significant challenge. Large population sizes need more computing time and memory space, whereas lower population sizes result in a local optimum. On the other hand, if there is prior information about the situation.

2) Encoding

Encoding techniques are critical for computational issues because they turn data into specified bit strings. Common encoding systems include binary, octal, hexadecimal, permutation, value-based, and tree. Binary encoding depicts each gene or chromosome as a string of 1s or 0s, allowing for speedier implementation of crossover and mutation operators. However, because of epistasis and natural representation, it takes additional work and is inappropriate for many technical design issues. Other encoding systems are octal, hexadecimal, permutation, value-based, and tree. Each approach has advantages and limitations, with binary encoding best suited for engineering design challenges and permutation encoding for ordering difficulties.

- **Binary-coded GA**

Goldberg's genetic technique demands that users choose the smallest alphabet that allows for the natural representation of problem parameters. The binary alphabet (0 and 1) is appropriate for expressing parameters since it adheres to the principle of minimal alphabets. Binary encoding is a common way of describing alternative solutions in GA, particularly for discrete optimization problems.

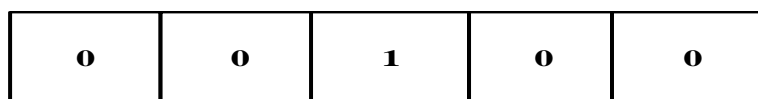


Figure IV.9. Binary coding scheme.

- **Real-coded GA**

In real-world applications, real-coded GAs (RGAs) are reliable, effective, and accurate representations of chromosomes. However, they suffer from premature convergence. Thus, Researchers are attempting to enhance their performance by altering crossover, mutation, and selection operators.

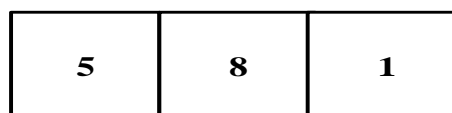


Figure IV.10. Real coding scheme.

3) Evaluation Function

Individuals are evaluated using function, fitness, or selective value, which allows one to associate a

value with each individual. These values will be used to select suitable breeding candidates.

GA three basic functions are selection (reproduction), crossover, and mutation. They choose excellent strings, change a string locally, and then recombine good substrings. The mutation operator stresses excellent strings, whereas the reproduction operator rids the following generation of poor strings. These operators make it simpler to handle mathematical problems and enable quicker convergence to real-world issues.

4) Selection

Selection or (Reproduction) is the first operation performed on a population, selecting suitable strings and creating a mating pool. The proportionate selection operator is often employed, which selects a string in the current population based on its fitness. indicate that those with high relative fitness are more likely to be picked. The well-known selection techniques are:

- Roulette wheel.
- Rank.
- Tournament.
- Boltzmann.
- Stochastic universal sampling.

5) Crossover

Recombination is a genetic operator used in evolutionary computing and algorithms that combines the genetic information of two parents to create new offspring. It is one method of randomly producing new solutions from an existing population. Crossing is a process where the bits of two selected chains are exchanged, allowing information exchange between chromosomes (individuals) in the genetic language. Recombination aims to provide one child with positive traits from two separate parents.

The commonly recognized crossover operators include single-point, two-point, k-point, uniform, partially matched, order, precedence preserving crossover, shuffle, reduced surrogate, and cycle. Figures IV.11, IV.12, and IV.13 below illustrate some of these techniques:

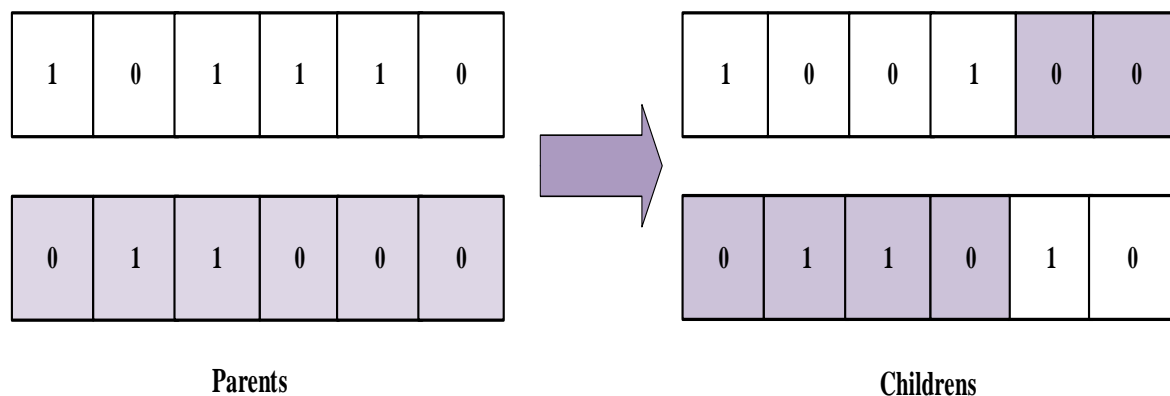


Figure IV.11. single-point crossover.

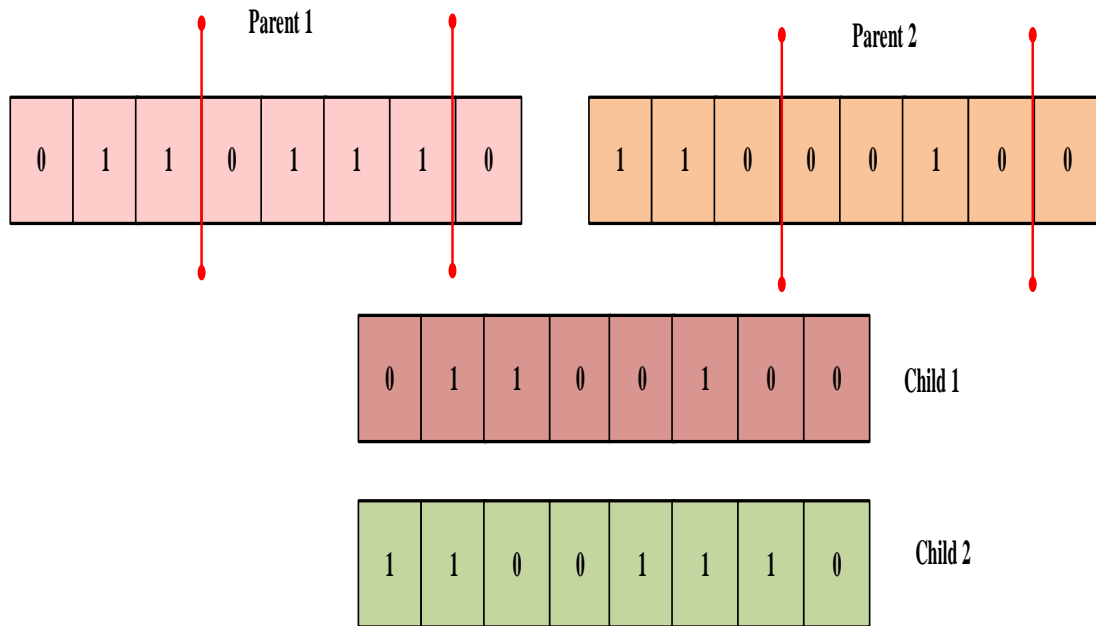


Figure IV.12. Two-point crossover.

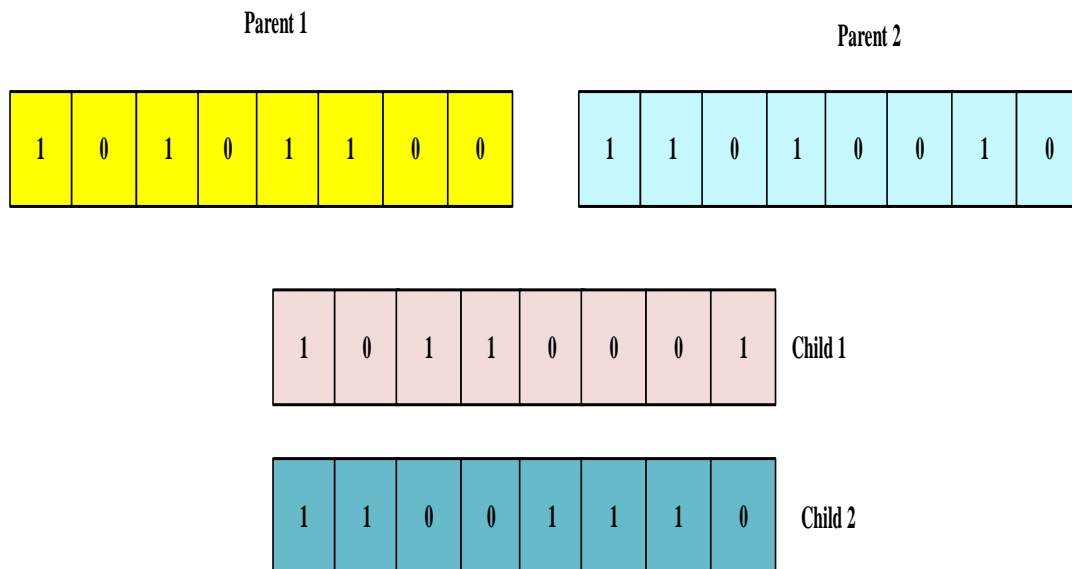


Figure IV.13. Uniform crossover.

6) Mutation

A mutation is a probabilistic genetic operator that prevents population stagnation and promotes variation. This issue was solved using three forms of mutations: bit inversion, mutation by exchange, and mutation by reversion. Inversion of bits is a simple and effective way to work with binary chromosomes. The challenge intends to use mutation as part of the mutation operator for population diversity and to search for a larger solution space. Figures IV.14, IV.15, and IV.16 below, illustrate some of this mutation technique:

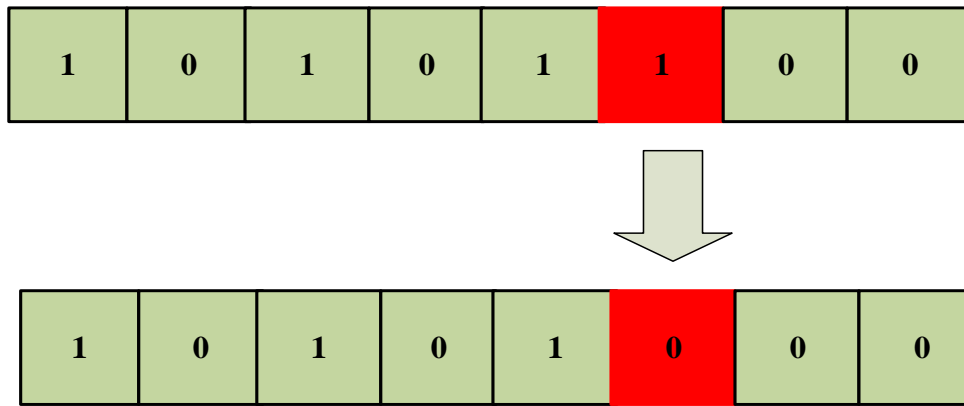


Figure IV.14.bit inversion.

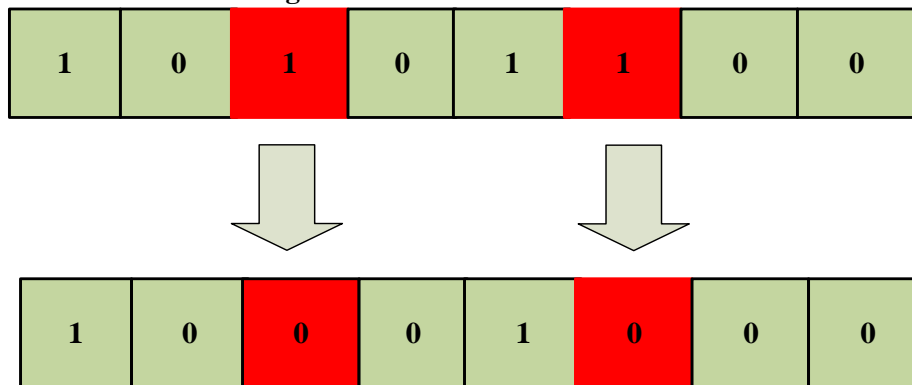


Figure IV.15.mutation by the exchange.

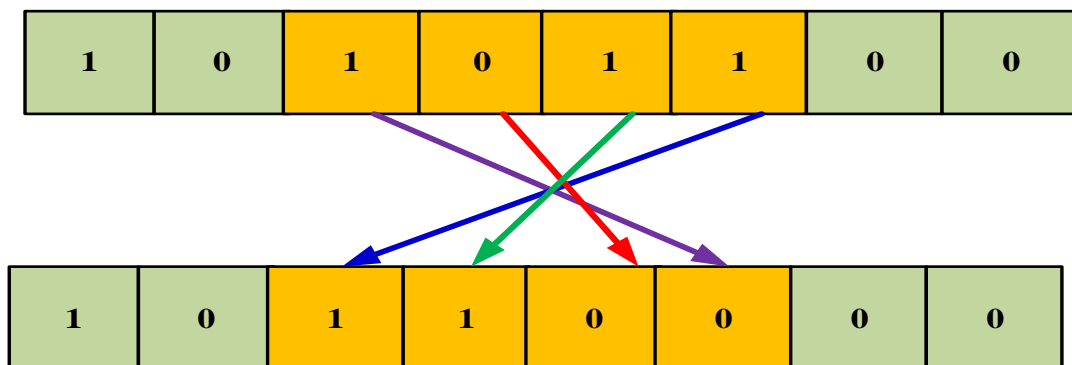


Figure IV. 16. Mutation by reversion.

7) Elitist Operation

To prevent the greatest accomplishment from being lost throughout genetic operations, the elitist operation [8, 9, 10, 21] maintains the best chromosome acquired thus far at any stage (i.e., the iteration) of the GA and passes that on to the following generation.

In this work, GA is employed for the optimal tuning of PI parameters.

The main benefit of GA is that, by using mutation, it can prevent itself from falling into a local optimum [230].

The main drawback of GA is that the optimal solution is difficult to achieve since GA is prone to early convergence, as a result, various enhancements to the underlying algorithm have been developed.

The GA steps for tackling the optimization are presented below:

1. **Start:** introduce the transfer function $F(s)$.
2. Generate a random population $[a b]$ of N chromosomes
3. **Fitness:** Evaluate the objective function $ITAE$ of each chromosome x in the population.
4. **New population:** Create a new population by repeating the following steps until the new population is complete:
 - i. **Selection:** Select two parent chromosomes K_p and K_i from a population according to their $ITAE$ fitness.
 - ii. **Crossover:** With a crossover probability crossover the parents to form new offspring. If no crossover was performed, the offspring is the exact copy of the parents.
 - iii. **Mutation:** With a mutation probability, mutate new offspring at each locus.
 - iv. **Accepting:** Place new offspring in the new population K_p and K_i .
5. **Replace:** Use the newly generated population for a further run of the algorithm
6. Check if the end condition is satisfied by getting the optimal parameters K_p and K_i to stop the algorithm.
7. **Return to step 3.**

Table IV.2 presents the PI controller gains values for the HESS obtained through GA optimization.

Table IV.2: Parameters of HESS tuned by GA.

Parameters	k_{p_bat}	k_{i_bat}	k_{p_sc}	k_{i_sc}	ITAE
PI-GA	1.5	15.7	0.17	7.62	0.083

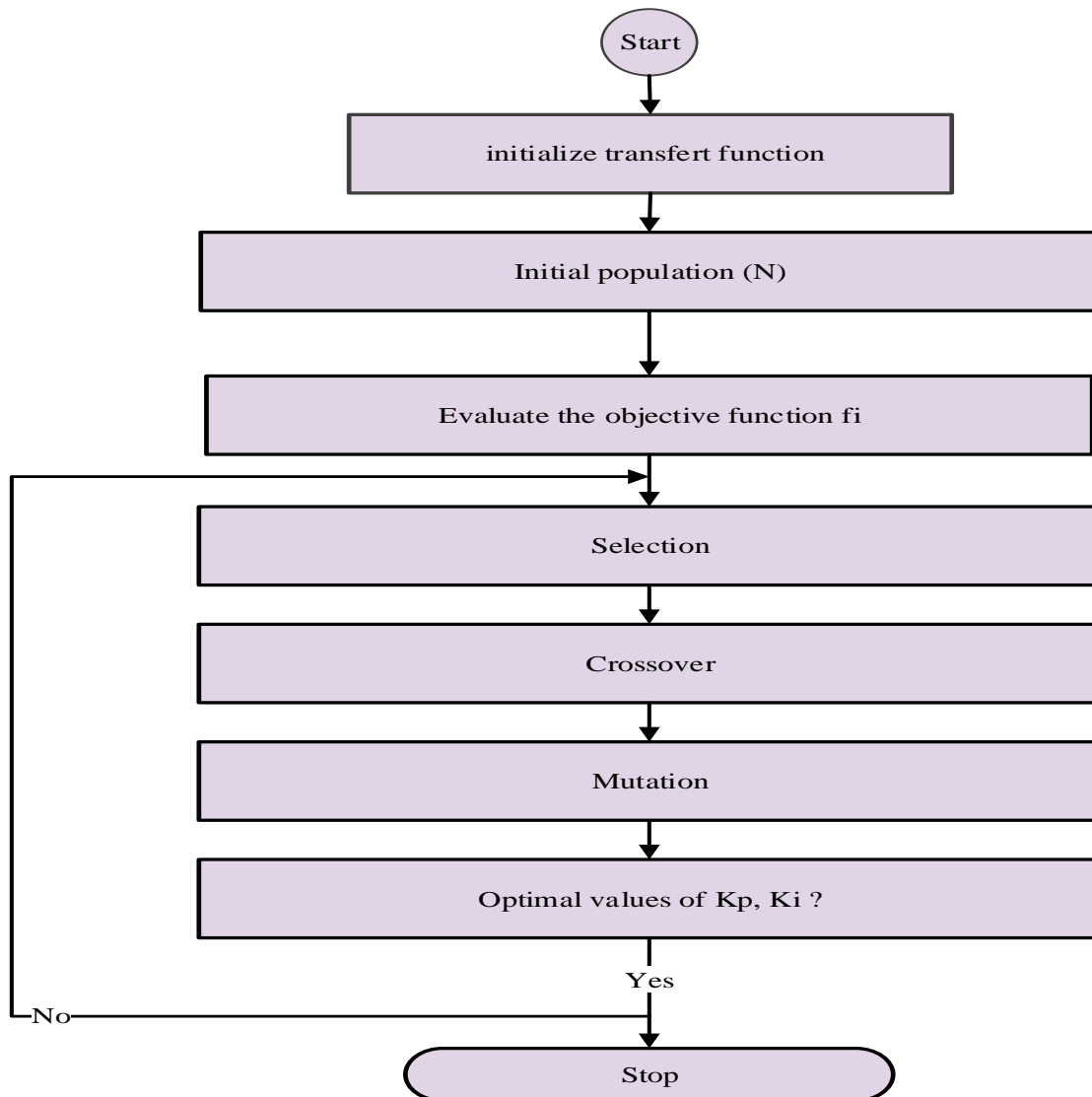


Figure IV.17.The PI-GA flowchart.

IV.9.4. Background of ACO

ACO is a swarm intelligence inspired by how ants indirectly transmit directions to one another. The most intriguing part of ant species' collaborative behavior is their ability to determine the shortest pathways between the ants' nest and food sources [230-232]. Ants leave chemical molecules called pheromones on the ground that other ants may detect and visit in the future. When ants find a food supply, they examine its amount and quality before transporting any back to the nest. The quantity and quality of the meal determine how much pheromone is left on the ground. The more intense the trail, the more likely an ant would follow it, enriching the path with its pheromone [233]. The pheromone trails of the longest pathways vanish. Pheromones, being chemical substances, evaporate after time, with longer paths having a higher evaporation rate. Shorter paths are more rapidly refreshed, increasing the likelihood of other ants selecting them. The simple scheme for ants searching for food is described in Figure IV.18 where all ants are in the nest and no pheromone exists [234].

- 1) All ants are in the nest, there is no pheromone in the environment.

- 2) During foraging, 50% of ants take the short way (circles) and 50% take the lengthy approach to the food source (rectangles).
- 3) The ants who took the shorter route arrived at the food source earlier. Returning to the short path increases the likelihood probability to take it again.
- 4) The pheromone trail on the short path receives more pheromones, so higher probability of taking the shortest way.

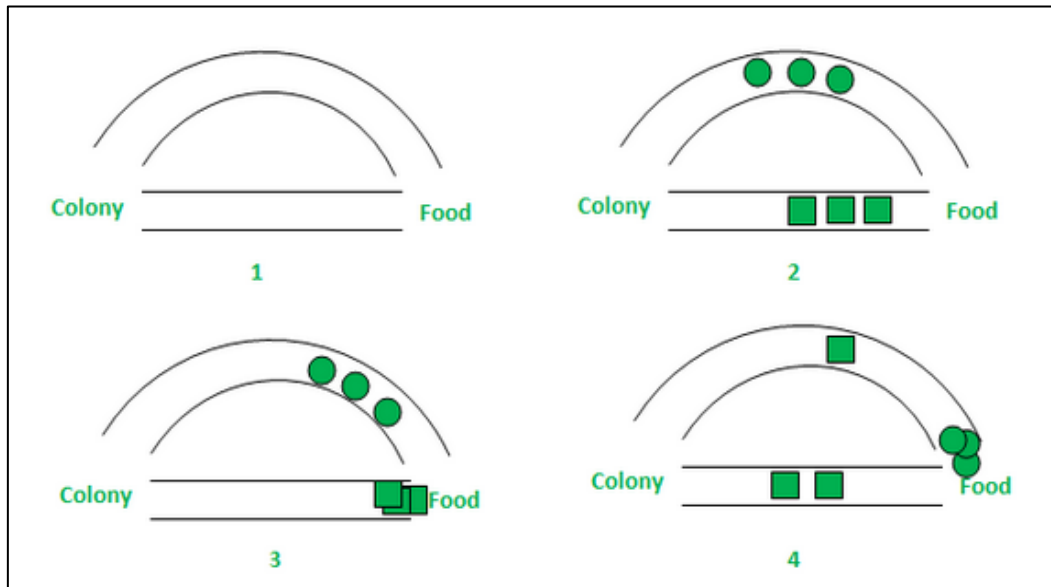


Figure IV.18. Ants' foraging activity for food [235].

IV.9.4. Optimization of PI parameters using ACO heuristic algorithms

In this part, the ACO algorithm is used for the optimal tuning of PI parameters K_p and K_i as shown in Figure IV.19.

The benefits of the ACO approach include [236]:

- Positive Feedback allows for the quick finding of excellent solutions
- Distributed computation minimizes premature convergence.

The outline of the basic steps of ACO is given as follows:

1. First, enter the transfer function of the system
2. Select the following parameters:
 - population size (N).
 - upper bound (ub).
 - lower bound (lb).
 - scaling parameter.
 - evaporate rate.
 - several iterations (T).
 - step size (h).
3. Enter the fitness objective function ITAE.
4. Initialize pheromone and probability.

a. Pheromone

$$\Delta\tau_j^{(k)} = \frac{\rho f_{best}}{f_{worst}} \quad (IV.26)$$

b. Probability

$$p_j^{(k)} = \frac{\tau_j}{\sum_{j=1}^m \tau_j} \quad (IV.37)$$

Where: Rand is a randomly generated number with a range of [0,1].

5. Update the pheromone
6. Update the probability
7. Determine the parameters for the PI controller.
8. Stop the algorithm if the overall iteration and optimum parameters are obtained.

Table IV.3 presents the PI controller gains values for the HESS obtained through ACO.

With: $N = 47$; $ub = 0$; $lb = 100$; $\delta = 2$; $\rho = 0.5$; $T = 50$; $h = 0.2$.

Table IV.3:Parameters of HESS tuned by the Ant colony algorithm.

Parameters	k_{p_bat}	k_{i_bat}	k_{p_sc}	k_{i_sc}	ITAE
PI-ACO	0.455	2.5	0.16	0.9	0.0076

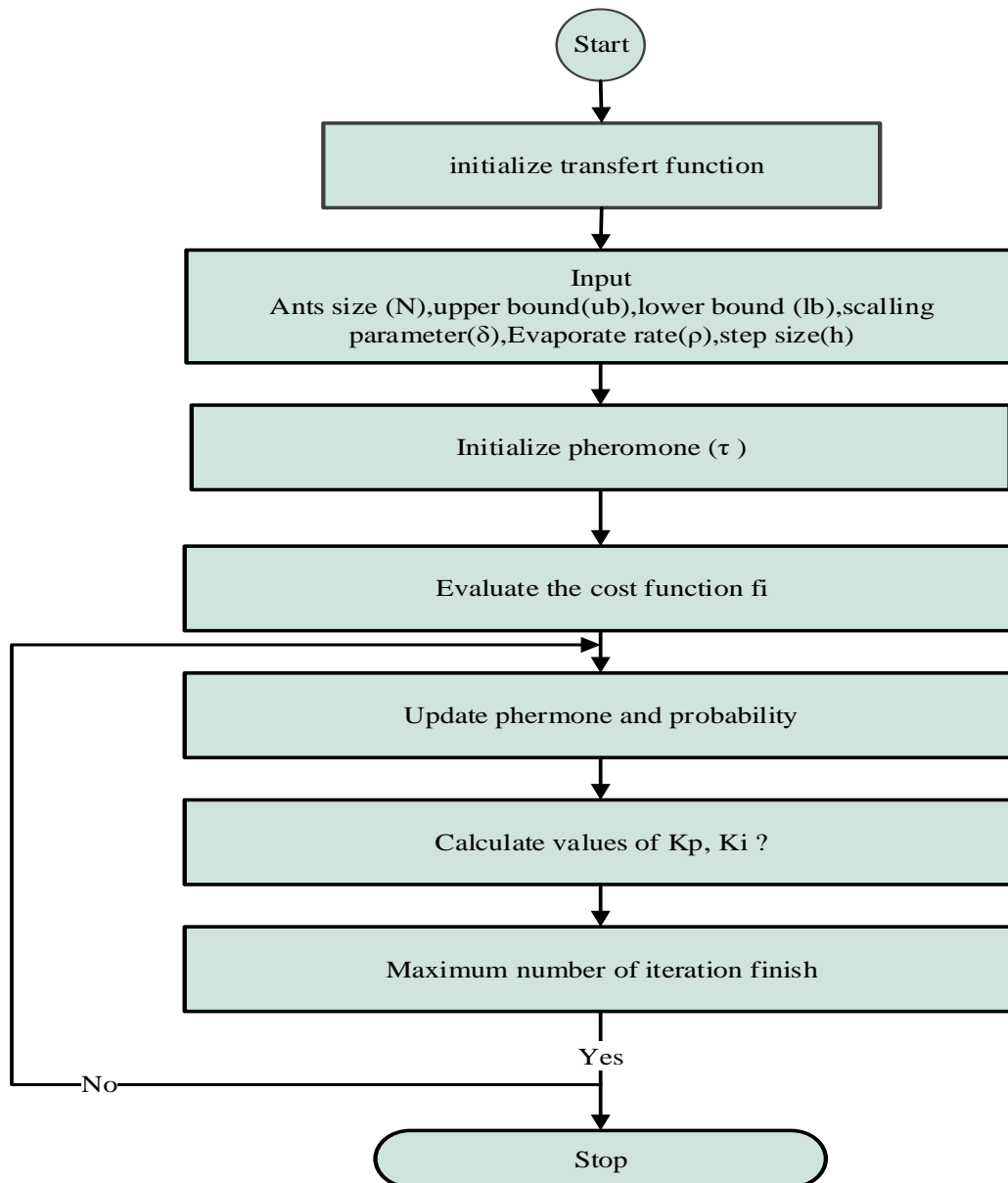


Figure IV.19.PI-ACO flowchart.

IV.9.5.Optimization of PI parameters using GWO heuristic algorithms

The GWO is a metaheuristic optimization technique based on the natural hunting behavior of grey wolves. Canidae is the family name of the grey wolf (*Canis lupus*) [237-240]. Since they occupy the highest position in the food chain, grey wolves are called apex predators. In this algorithm, a group of wolves comprises alpha, beta, and omega wolves' functions [241]. The alpha wolf is the pack's leader and the other wolves follow it. The alpha wolf is superior to the beta, and omega wolves, who have a lesser pack rank. The social hierarchy of grey wolves is shown in Figure IV.20.

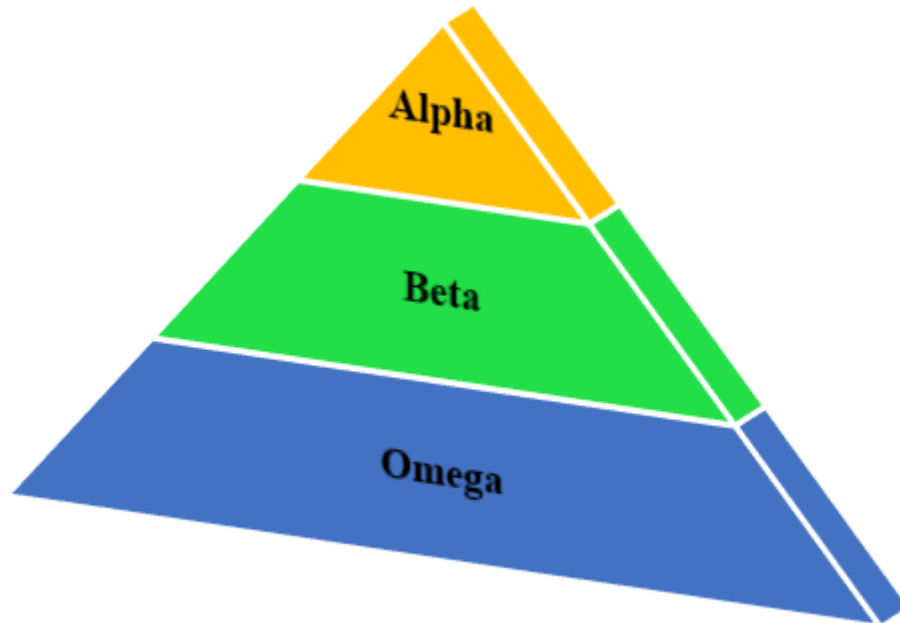


Figure IV.20. Social hierarchy of grey wolves [241].

Muro et al. identified three primary periods of grey wolf hunting, as seen in Figure IV.21). The phases are: **tracking, chasing, and approaching the prey**. Grey wolves hunt by chasing, cornering, and tormenting their victims, eventually attacking them. The mathematical model is used to predict and optimize grey wolf behavior.



Figure IV.21:The hunting behavior of the grey wolves A chasing, approaching, and tracking the prey B-D pursuing, harassing, and encircling the prey E attacking when the prey stops moving[242].

IV.9.5.1. Basic of GWO

The next section goes into additional detail about the mathematical model or algorithm structure,

which includes social hierarchy, tracking, surrounding, and attacking prey.

1) Encircling

According to Equation IV.31, GWO takes into account two wolves in an n dimensional space during the encircling phase and modifies their placement depending on the second one[243].

$$X(t + 1) = X(t) - A \cdot D \quad (\text{IV.28})$$

Where:

$X(t + 1)$: represents the next location of the wolf.

$X(t)$: represents the current location.

A : is a coefficient matrix.

D : is a vector that is determined by the prey's position (X_p) and is computed as shown in equation (IV.33).

$$X(t + 1) = X(t) - A \cdot D \quad (\text{IV.29})$$

$$D = |C \cdot X_p(t) - X(t)| \quad (\text{IV.30})$$

Where C is a randomly generated vector in the interval $[0,1]$. A solution can move around another solution by utilizing these two equations. Because vectors are used in the equations, this may be applied to any number of dimensions.

Figure IV.22 illustrates an example of a grey wolf's potential location concerning prey.

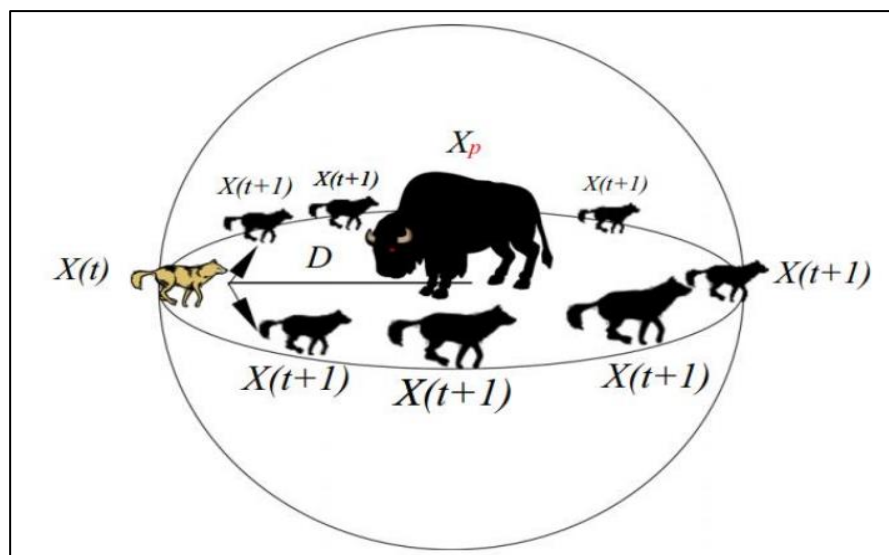


Figure IV. 22.Updates on Wolf's location[244].

The equations in the above simulate different step sizes and movement speeds of grey wolves, with random components defining their value.

$$A = 2a \cdot r_1 - a \quad (\text{IV.31})$$

The elements of the set a will linearly decrease from 2 to 0 throughout an iteration, with r_1 and r_2

being random vectors between 0 and 1.

$$a = 2 - t \left(\frac{2}{T} \right) \quad (\text{IV.34})$$

where T is the maximum number of iterations and t is the current iteration.

2) Hunting

Grey wolves instinctively sense their prey's position and surround it, headed by the alpha, the beta, and the omega. Some of the prey's ideal places are unknown to humans. To further comprehend their behavior, a mathematical equation was developed, assuming alpha and beta had more information about their prey's position. The first two wolves were saved as the best candidates, while the remaining wolves (omega) adjusted their places based on the best search candidate. Therefore, other wolves should be obliged to update their positions as follows [245]:

$$X(t+1) = \frac{1}{3}X_1 + \frac{1}{3}X_2 + \frac{1}{3}X_3 \quad (\text{IV.35})$$

With the Equation below calculate X_1 , X_2 and X_3 :

$$X_1 = X_\alpha(t) - A_1 \cdot D_\alpha \quad (\text{IV.36})$$

$$X_2 = X_\beta(t) - A_2 \cdot D_\beta \quad (\text{IV.37})$$

$$X_3 = X_\delta(t) - A_3 \cdot D_\delta \quad (\text{IV.38})$$

The Equations IV.30, IV.31, and IV.32 below calculate D_α , D_β and D_δ :

$$D_\alpha = |C_1 \cdot X_\alpha - X| \quad (\text{IV.39})$$

$$D_\beta = |C_2 \cdot X_\beta - X| \quad (\text{IV.40})$$

$$D_\delta = |C_3 \cdot X_\delta - X| \quad (\text{IV.41})$$

3) Attacking prey (exploitation)

The grey wolves will end their hunt by attacking the victim after it stops moving. A is a random variable in the interval $[-\alpha, \alpha]$ that will limit the wolves' mobility while searching for prey. The search is controlled by decreasing the intervals in α and A . As α decreased from 2 to 0, it drew closer to the prey over iterations.

4) Search for prey (exploration)

The algorithm searches for and converges on prey using alpha, beta, and delta locations. The parameter A is set to 1 or -1 to signify divergence and convergence, with a focus on exploration and global GWO search. The method begins with assessing the prey's location and updating their position and distance. The parameter α is reduced to focus on exploration and exploitation. Wolves advance to the prey, diverge and converge, and then remove the algorithm after the prey's position is known and recognized by all wolves. As seen in Figure IV.23, the GWO method is employed to optimize the tuning of the proportional (K_p) and integral (K_i) gains.

The grey wolf's hunting method includes the following steps:

1. First, enter the transfer function of the system

2. Select the following parameters:
 - Initial population (N);
 - upper bound (ub).
 - lower bound (lb).
 - coefficient value (a).
 - several iterations (T).
 - variable number (Var).
3. Define the objective function.
4. Calculate X_α , X_β , and X_δ .
5. Update the position of the population.
6. Evaluate the objective function
7. Update X_α , X_β , and X_δ
8. Determine the parameters for the PI controller.
9. Stop the algorithm if the overall iteration and optimum parameters are obtained.

Table 5 presents the gains K_p and K_i components of the HESS (battery and SC) stunned by Grey Wolf optimization.

With: $N = 47$; $ub = 0$; $lb = 100$; $a = 2$; $T = 50$; $Var = 2$.

Table IV.4: Parameters of HESS tuned by the GWO.

Parameters	k_{p_bat}	k_{i_bat}	k_{p_sc}	k_{i_sc}	ITAE
PI-GWO	0.13	1.2	0.1	0.3	0.0021

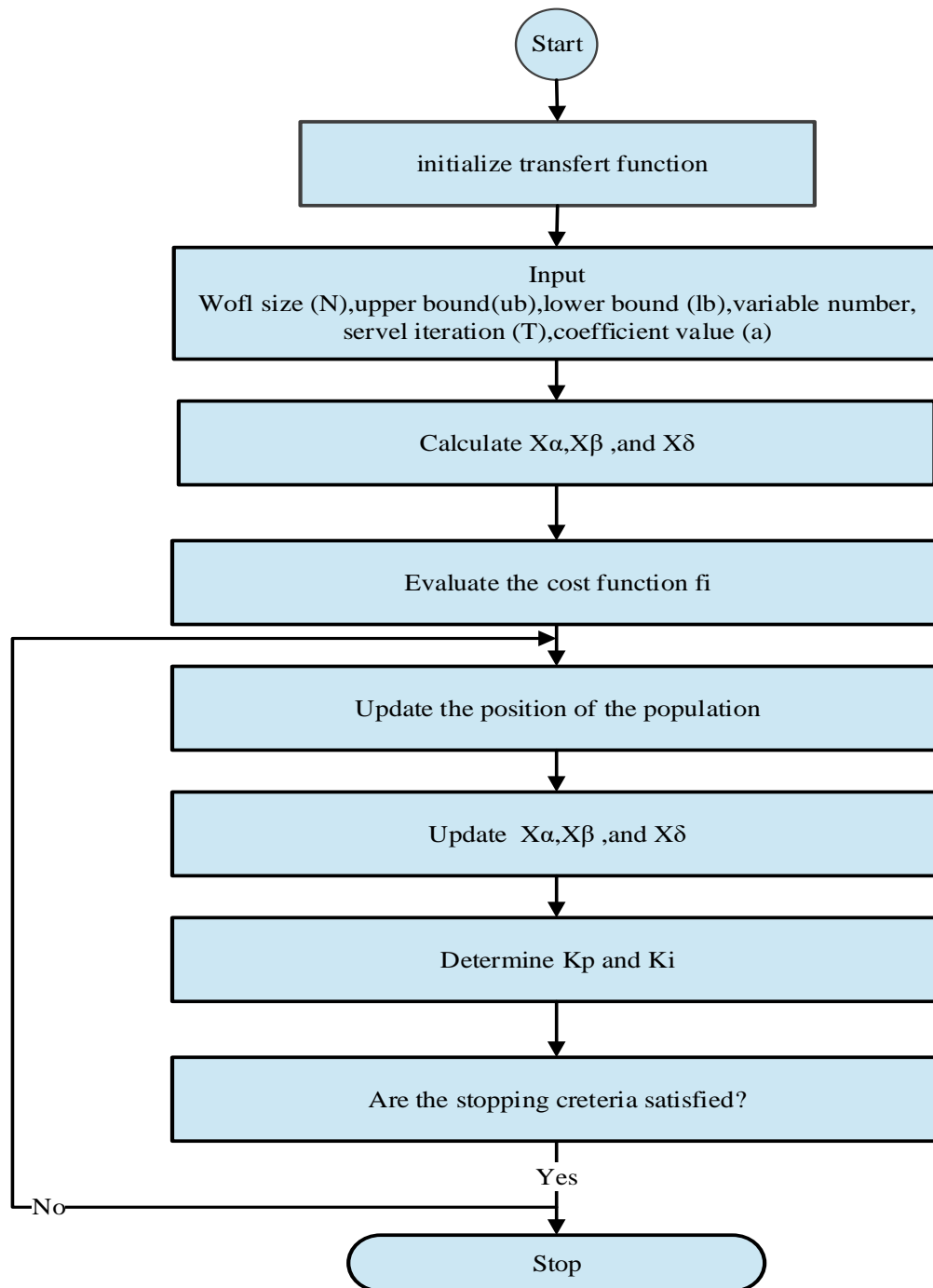


Figure IV.23.PI-GWO flowchart.

IV.10. Implementation of different algorithms (GA, ACO and GWO) in Simulink

Figures IV.24 and IV.25 illustrate the relationship between the proposed algorithms (*GA, ACO, and GWO*) within the Simulink model concerning the battery and supercapacitor integration. As indicated in Figure IV.24, the input to the PI controller for the battery is the discrepancy between the actual current (I_{bat}) and the reference current. At the same time, the output corresponds to the duty cycle (D_{bat}) of the converter. Conversely, the input for the PI controller remains the same scenario, the comparison between the actual current (I_{sc}) and the reference current (I_{sc_ref}), with the output also

being the duty cycle (D_{sc}) of the converter side supercapacitor, as shown in the accompanying figure IV.25. Furthermore, this supercapacitor and battery are defined by a transfer function, a fundamental component of the several metaheuristic algorithms implemented in MATLAB to determine the optimal gains for the regulator. Ultimately, this calculated value of gains is utilized in the PI controller associated with the battery /SC.

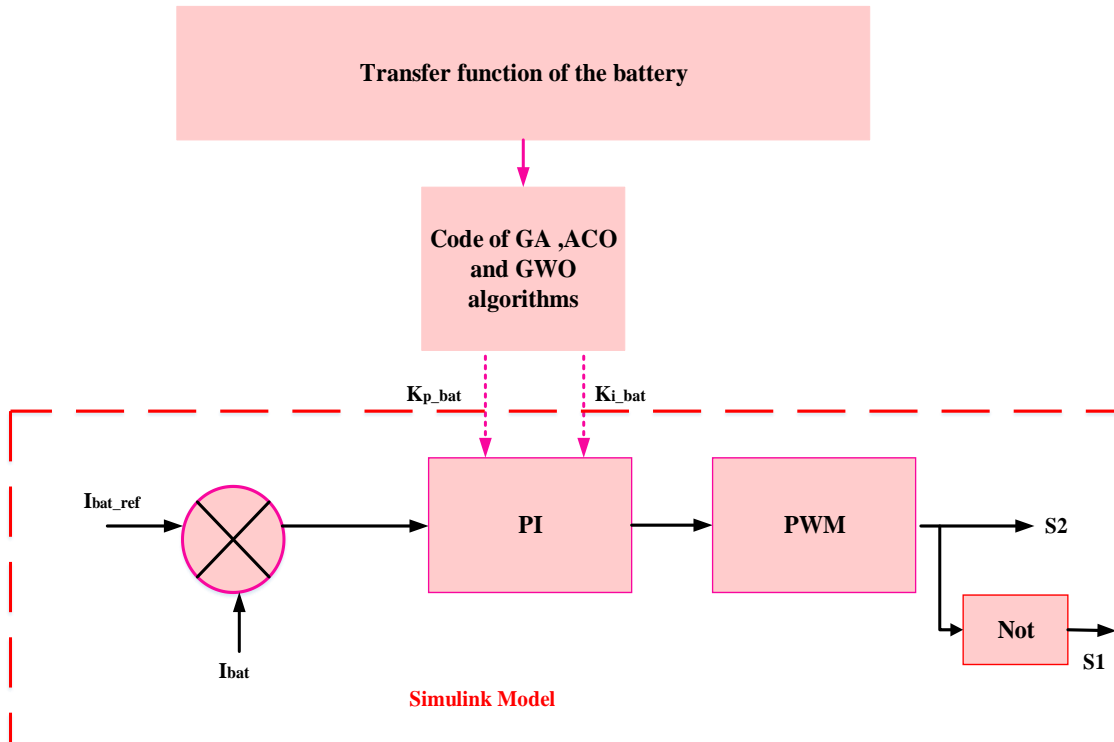


Figure IV.24. Implementation of several algorithms (GA, ACO, and GWO) in Simulink side battery.

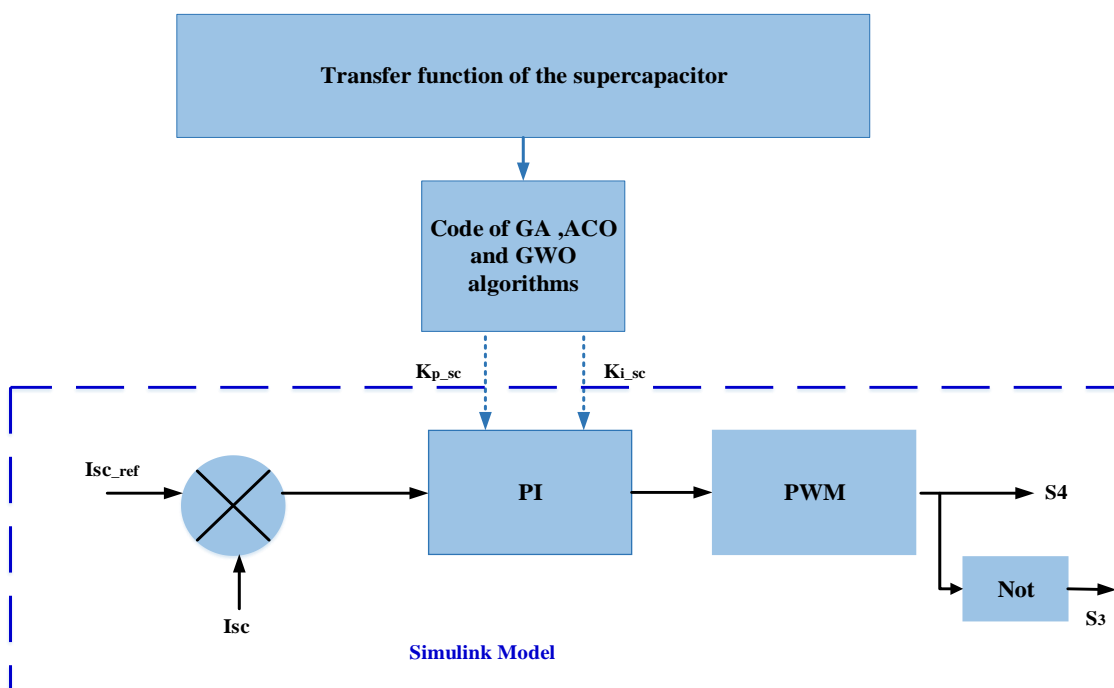


Figure IV.25. Implementation of several algorithms (GA, ACO, and GWO) in Simulink side SC.

IV.11. RESULTS AND DISCUSSION

The overall system and its control scheme were simulated using MATLAB/Simulink and Sim Power Systems toolbox.

Two simulation scenarios were considered to evaluate the performances of the proposed controllers (conventional PI, PI-GA, PI-ACO, and PI-GWO).

IV. 11.1. Test 1: Variable solar irradiation and constant load

In this scenario, the system was simulated with a continuous load power ($P_L = 500\text{ W}$) as depicted in Figure IV.26, while the solar irradiation varies, as shown in Figure IV.27.

Figures IV.28 highlight the evolution of the DC voltage with the reference equal to 50 v, however, they validate the performance of the regulator in terms of quick response, good convergence to the reference with optimal overshoot, and zero error, which provides stability of the system

Figures IV.29, IV.30, and IV.31 depict the voltage, Current, and state of charge of the battery. Following an initial transient reaction, the battery voltage remains generally steady at around 25V, suggesting that the battery produces a consistent voltage output despite fluctuations in current demand. The battery current has abrupt peaks and transitions, indicating charging and discharging cycles based on the load's power consumption or energy transfer to the SC. In another hand, the status of charge SOC displays the battery's charge and discharge, confirming that energy is continually supplied to the system.

Figures IV.32 and IV.33 depict the voltage, Current of the supercapacitor. SC voltage responds dynamically, with an early dip followed by a quick increase before stabilizing, showing that it charges and discharges faster than a battery. The supercapacitor current has several abrupt peaks, indicating a quick reaction to transitory power demands. This pattern verifies the supercapacitor's significance in managing high-frequency oscillations and minimizing battery stress. The combination of these answers indicates the success of the HESS system, in which the battery delivers consistent energy while the supercapacitor handles unexpected power needs, maintaining system stability and efficiency.

Figures IV.34, IV.35, and IV.36 show the profiles of the power generated by the PV system, the power of the battery, and that of the SC, respectively.

In the time interval between 0 and 0.4 seconds, the power generated by the PV system is lower than that required by the load. In this case, the EMS quickly requests the storage system to supply the energy deficit. The SC intervenes quickly during the transient regime, allowing the batteries to operate steadily.

In the time interval between 0.4 and 0.7 seconds, the power generated by the PV system is higher than that requested by the load. In this case, the EMS quickly intervenes to ensure battery charging by using the excess power generated by the PV system compared to that requested by the load.

A similar scenario is observed in the time interval between 0.7 and 2 seconds as in the first-time interval. It is important to note that the variation of the solar irradiance also causes a variation of the power generated by the PV system. The EMS responds to each change, thus ensuring the proper

operation of the power system.

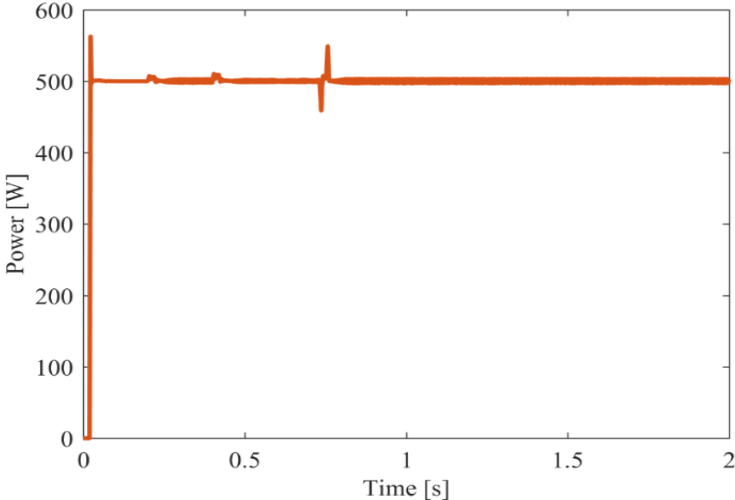


Figure IV.26. Power of load.

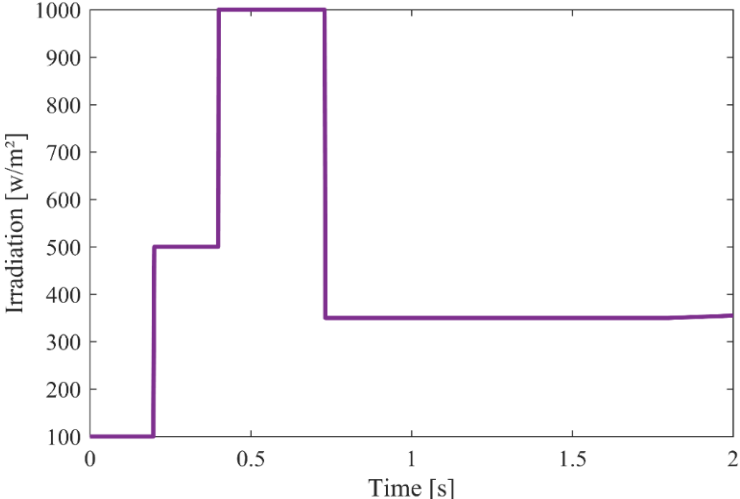


Figure IV.27. Variable irradiation

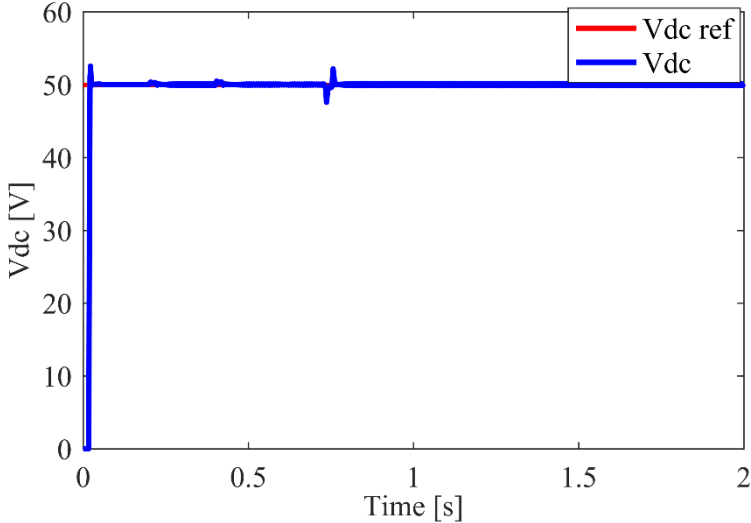


Figure IV.28. The DC voltage with the reference voltage.

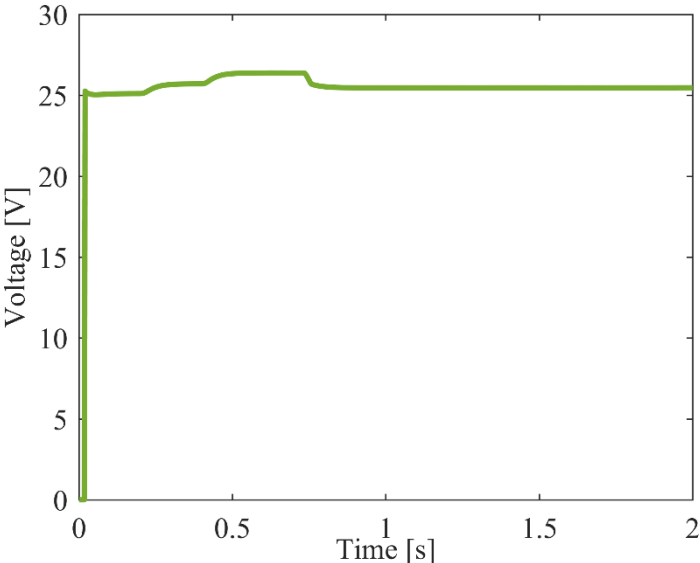


Figure IV.29.The voltage of Battery.

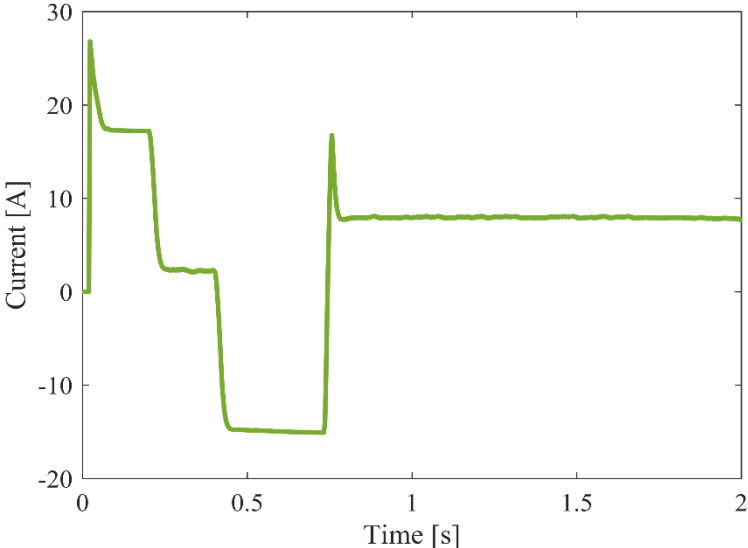


Figure IV.30.Current of battery .

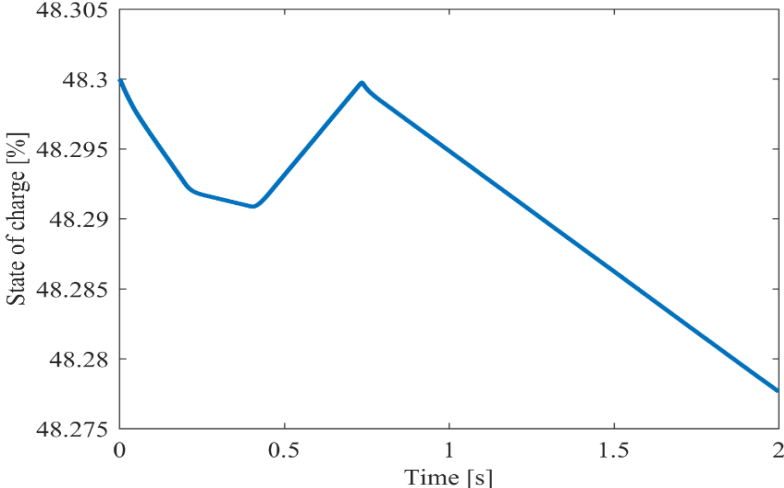


Figure IV.31. Sate of Charge of the battery.

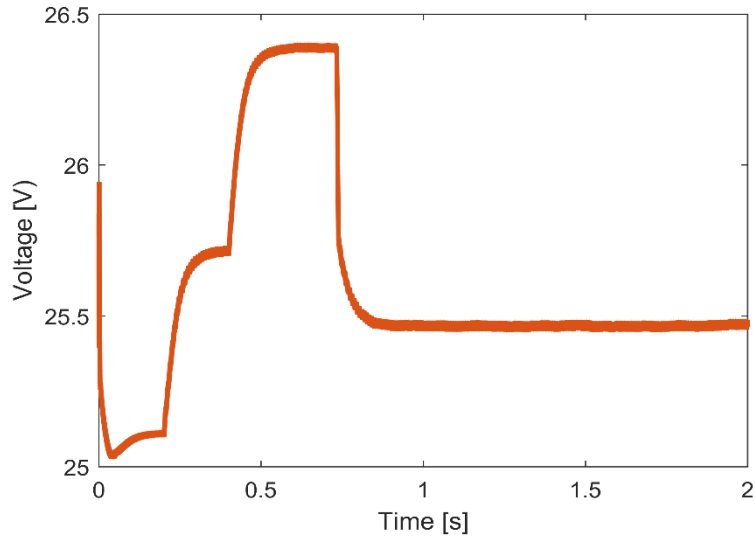


Figure IV.32. Voltage of Supercapacitor.

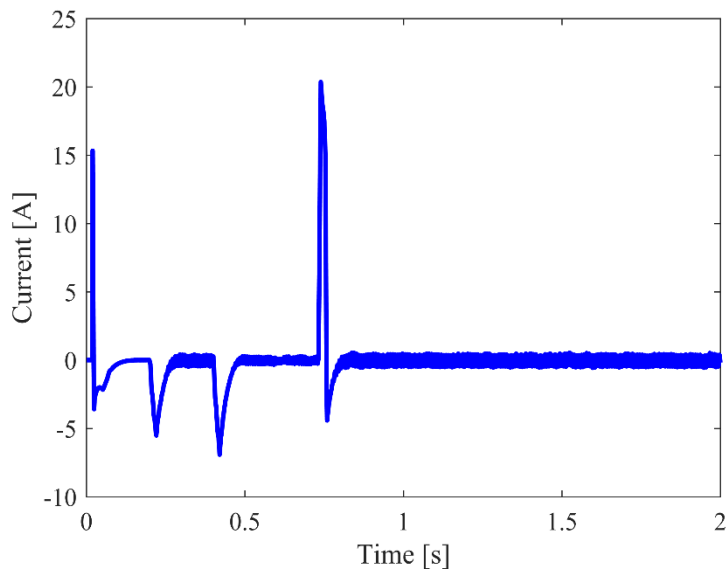


Figure IV.33. current of supercapacitor.

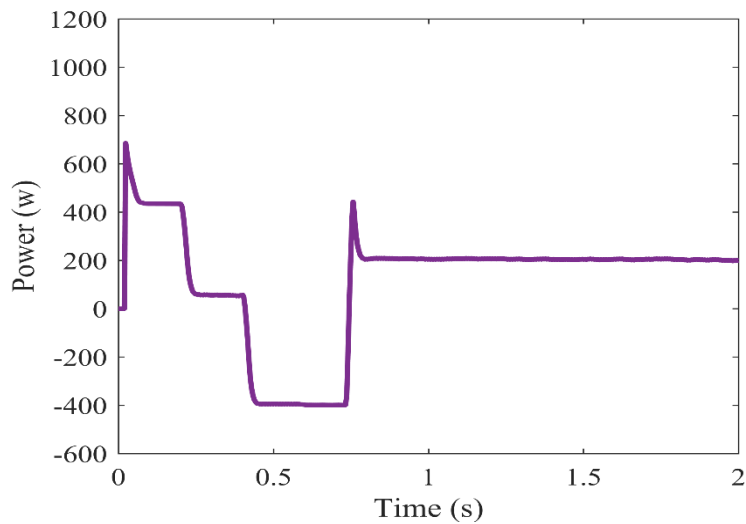
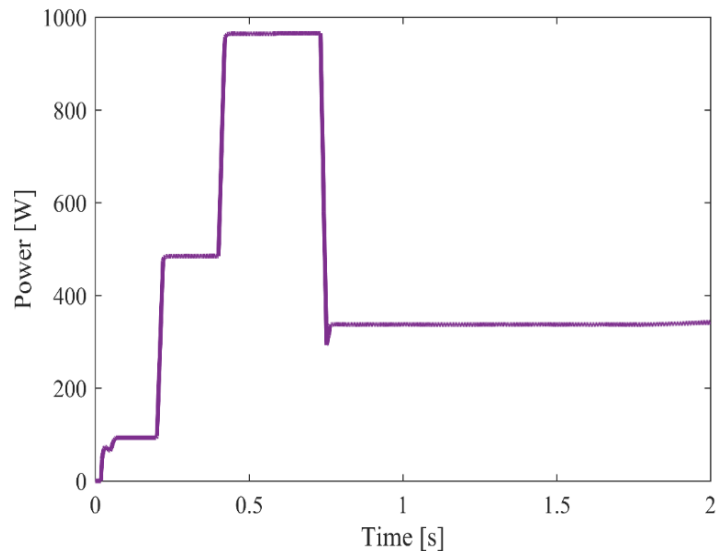
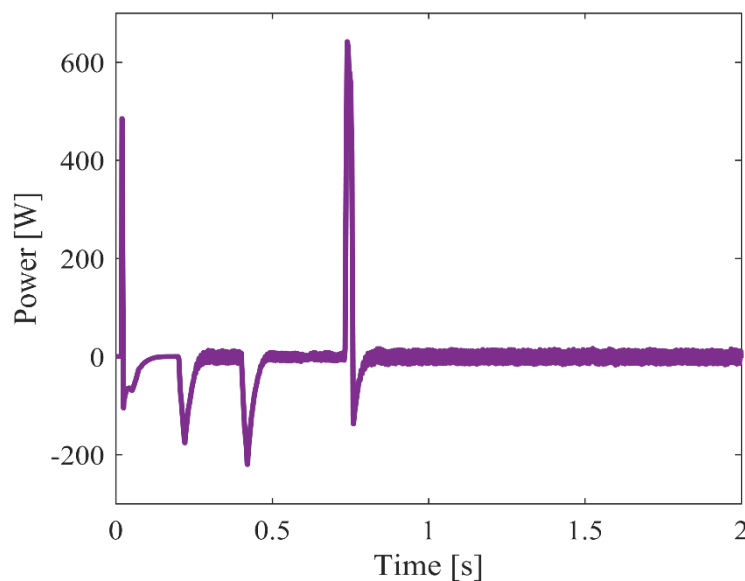


Figure IV. 34.Power of battery**Figure IV.35.**Power of PV.**Figure IV.36.** Power of supercapacitor.

Figures IV.37, IV.38, IV.39, and IV.40 present the dynamic responses of the current and battery side batteries and SC during the charging and discharging phases using GA, ACO, and GWO optimization algorithms for the PI controller and how well each method follows this reference. An extensive simulation study has been conducted to evaluate the effectiveness of the proposed controllers in various operational scenarios, with a special focus on rapid fluctuations in solar irradiance. The graphical representations demonstrate the superior performance of the GA-PI, ACO-PI, and GWO-PI controllers over the conventional PI controller in the lateral HESS. Notably, the figures illustrating the settling time, overshoot, and rise time reveal the effectiveness of the metaheuristic-based controllers, highlighting their dynamic responsiveness under varying conditions .

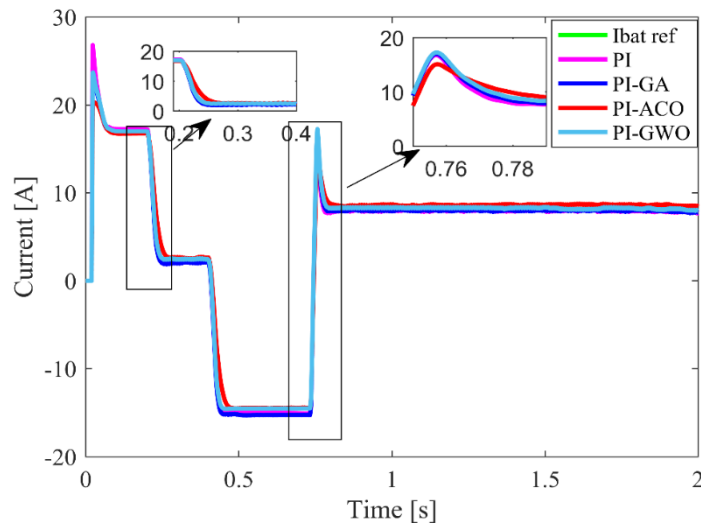


Figure IV.37. Battery Current with different optimization methods of the PI controller (scenario1)

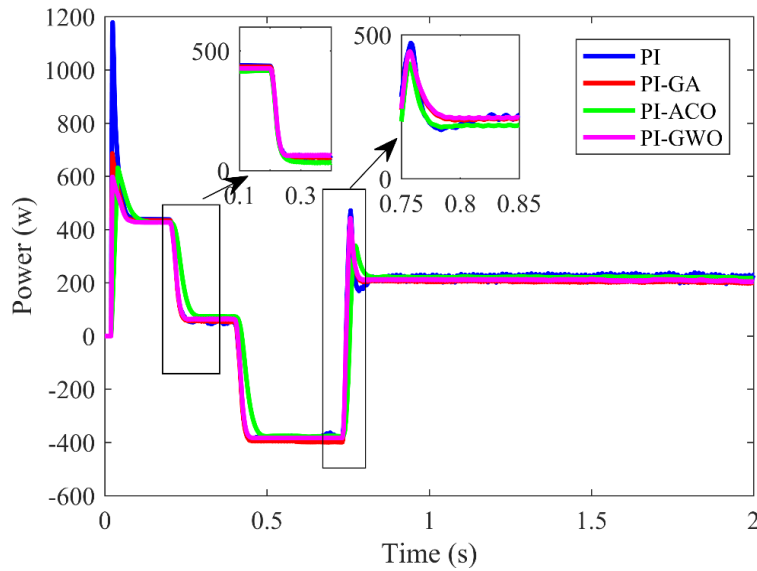


Figure IV.38. Battery Power with different optimization methods of the PI controller (scenario1)

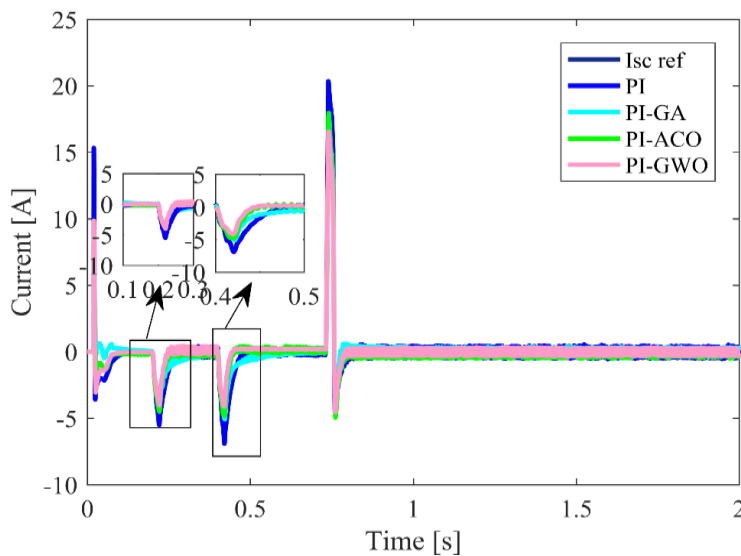
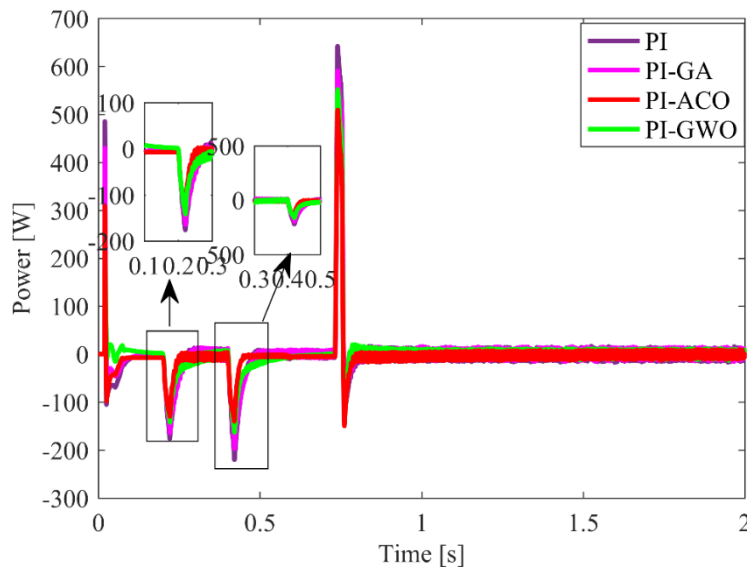
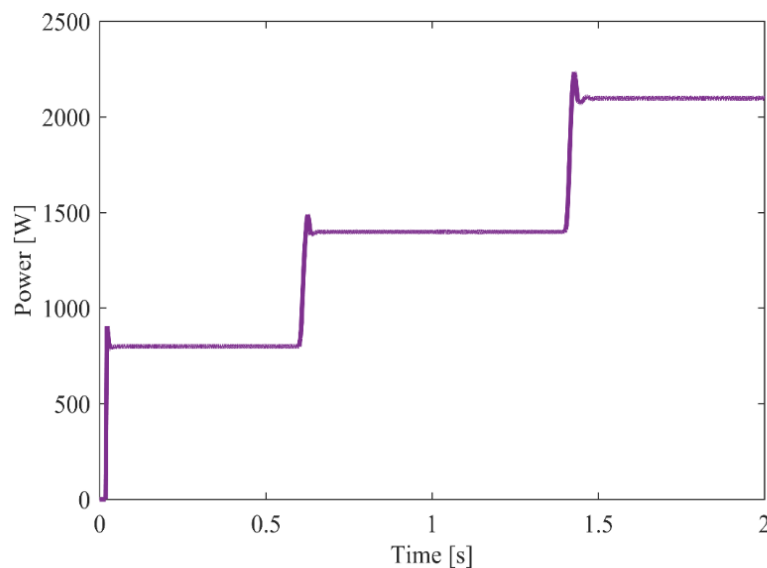


Figure IV.39. SC current with different optimization methods of the PI controller (scenario1)**Figure IV.40.** SC power with different optimization methods of the PI controller (scenario 1)

IV. 11.2. Test 2: Variable load and constant irradiation

The second scenario is proposed to test the performance of the optimized PI controllers when the power requested by the load varies. The load power profile is shown in Figure IV.41.

**Figure IV.41.** Power of variable load.

The system was simulated with a nominal and constant solar irradiation of 1000 W/m^2 . The PV system generates an almost continuous power with this irradiation value, as shown in Figure IV.42.

By analyzing the power required by the load, the power generated by the PV system, and the energy stored in the battery and SC, as shown in Figures IV.44, and IV.45, three distinct intervals can be distinguished.

- Between $t = 0 \text{ s}$ and $t = 0.6 \text{ s}$, the power generated by the PV system exceeds the load demand. The excess power is sent there is a surplus of power that is stored in the SC also the battery During

this short time, the battery remains in charge mode as depicted in Figure IV.45, thereby maintaining the balance.

- From $t = 0.6$ s to $t = 1.4$ s, the power generated by the PV system is not enough to meet the load power requirement. To maintain a stable energy supply and fulfill the demand of the load, the SC promptly compensates for the power deficit of the PV system.
- Between $t = 1.4$ s and $t = 2$ s, the power generated by the PV system consistently remains below the load power requirement. Consequently, the battery supplies power to the load, ensuring a stable energy balance between the power generation of the PV system and the power consumption of the load.

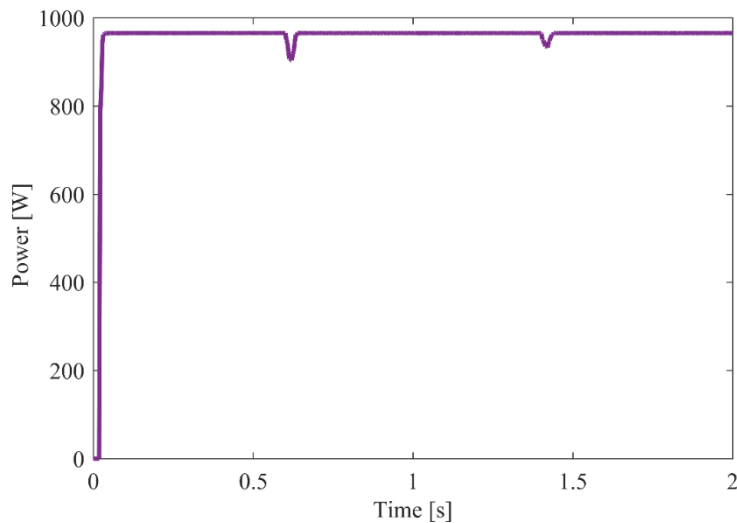


Figure IV.42.Power of PV.

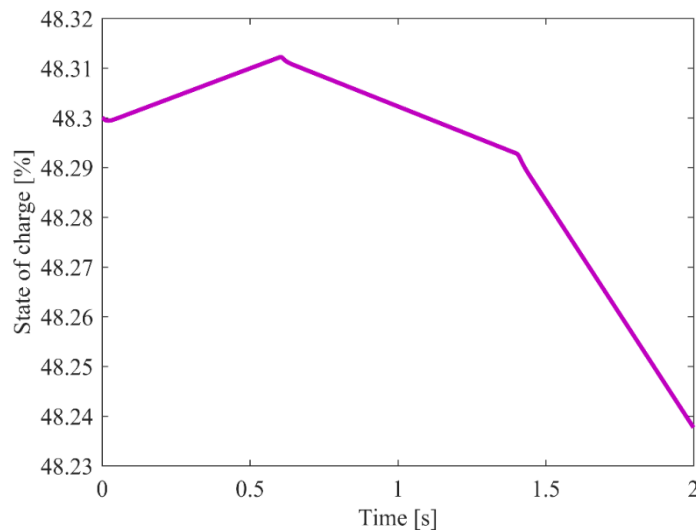


Figure IV.43.State of charge of the battery (scenario2)

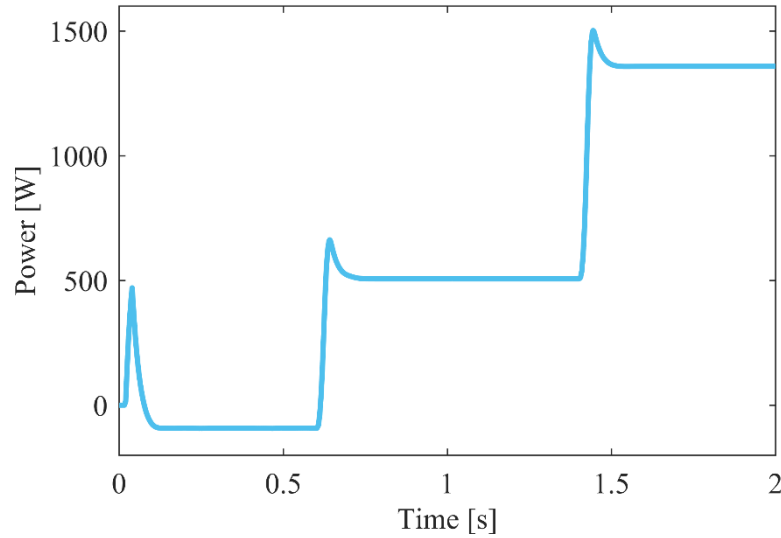


Figure IV.44.Power of battery.

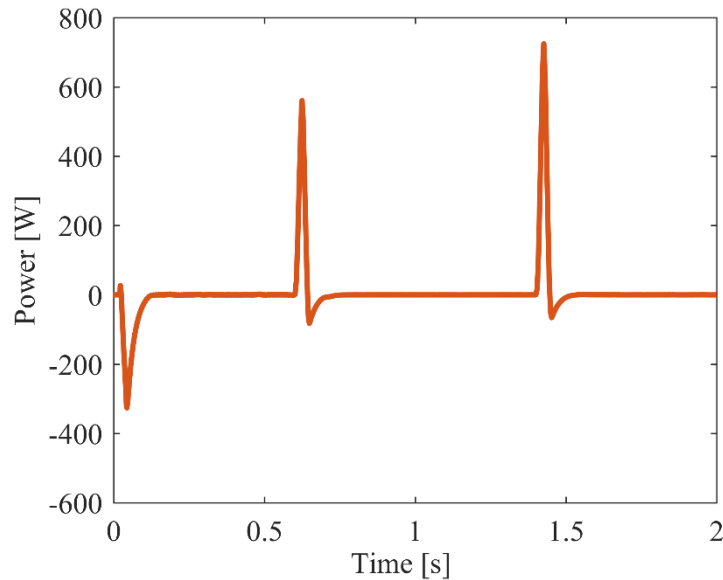


Figure IV.45.Power of supercapacitor.

Figures IV.46, IV.47, IV.48 and IV.49 show the current power profiles of the batteries and SC, respectively. Depending on the power generated by the PV system, the power required by the load, and the EMS, the HESS operates properly and successfully. The optimized PI tuned by the GWO controller exhibits good performance in terms of response time and overshoot, which results in a satisfactory result for the operation of the batteries and SC

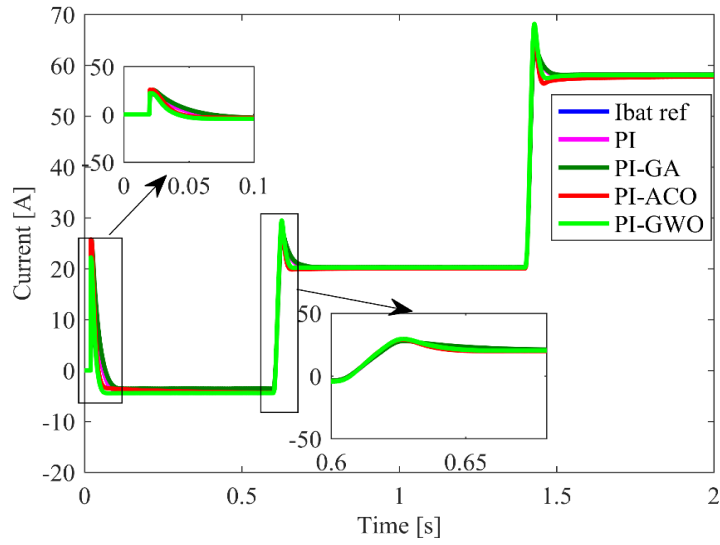


Figure IV. 46.Current of battery under different optimization methods of the PI controller under variable load.

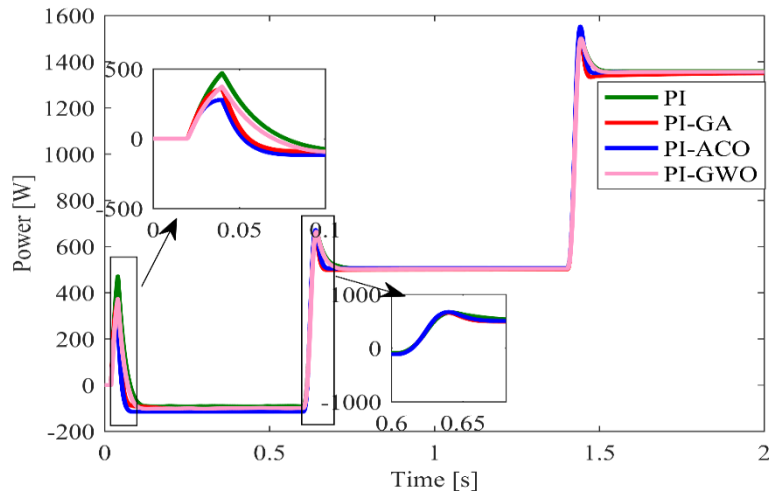


Figure IV. 47.Power of battery under different optimization methods of the PI controller under variable load.

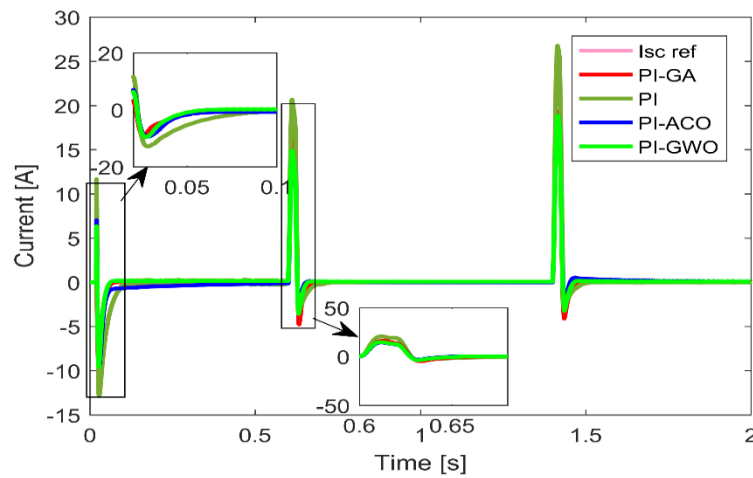


Figure IV.48.SC current under different optimization methods of the PI controller under variable load.

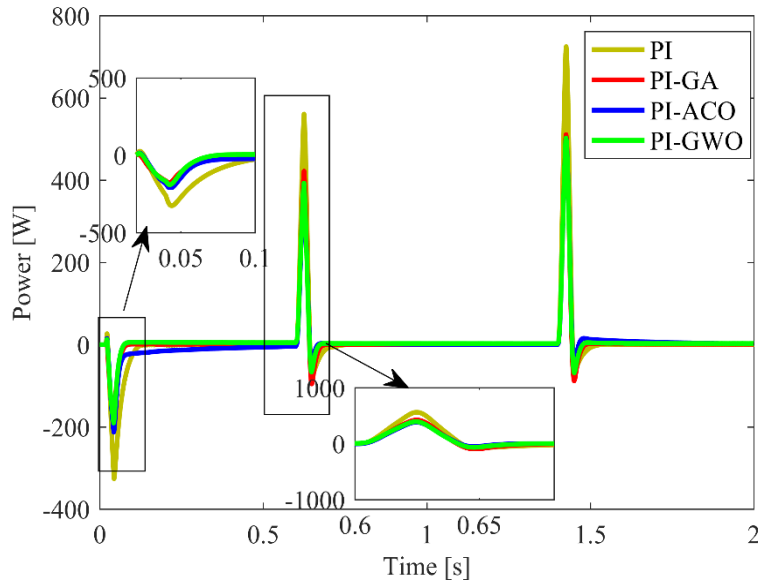


Figure IV.49. SC power under different optimization methods of the PI controller under variable load.

IV.12. The Performance evaluation of the controllers

This section aims to demonstrate the effectiveness of the proposed controllers on the performance of the battery and SC. Tables IV.5 and IV.6 present the SC and battery performances, respectively. The results show that the ACO technique offers an additional advantage over the GA approach in terms of performance. This reduces the stress on the batteries and extends their lifetime.

Table IV.5: Performance of the SC with the various optimization algorithms of the PI controller.

Controllers	Rise time	Peak overshoot in [%]	Settling time in [sec]
PI conventional	$2.9 \cdot 10^{-3}$	30.56	2.47
GA	$3.98 \cdot 10^{-4}$	18.91	2.39
ACO	$5.89 \cdot 10^{-4}$	6.15	2.1
GWO	$5.12 \cdot 10^{-4}$	5.89	1.9

Table IV.6: Performance of the batteries with the various optimization algorithms of the PI controller.

Controllers	Rise time	Peak overshoot in [%]	Settling time in [sec]
PI conventional	$9.5 \cdot 10^{-3}$	42.41	3.78
GA	$6.57 \cdot 10^{-3}$	28.89	2.85
ACO	$4.34 \cdot 10^{-3}$	5.98	1.96
GWO	$3.87 \cdot 10^{-3}$	4.67	1.45

IV.13. Conclusion

This chapter focuses on the application of HESS with effective controls to guarantee stability and autonomous backup for intermittent and unpredictable energy sources such as solar PV systems. In terms of control strategies, both the conventional PI controller and optimized PI controllers using metaheuristic optimization techniques, including GA, ACO, and GWO, have been investigated. The results confirm the limitation of the conventional GA and ACO approaches in terms of the rate of charge and discharge performance of batteries-SC and also affirm and showcase the robustness and effectiveness of the PI controller fine-tuned by GWO with optimal performance under varying irradiation and load conditions. The outcomes highlight a notable reduction in peak dynamic response on the battery- SC, thus reducing the stress on the battery, consequently enhancing overall system performance, and extending the lifetime of the components. Additionally, the GWO-optimized control strategy leads to a more efficient management of the batteries charge, thereby reducing discharge rates and ultimately contributing to an extended battery lifespan. Looking forward, this research opens avenues for further exploration and development.

Chapter V
**Application of metaheuristic
algorithm on battery electric vehicle**

V.1. Introduction

This chapter presents the design, modeling, and simulation validation of an electric vehicle system, to develop a control strategy and estimate the energy consumption of an electric vehicle, it is very important to have a suitable vehicle model. The EV model is very complex because it contains many components, such as vehicle dynamics, transmission, electrical machines, power electronics, and energy sources. Each component must be correctly modeled to avoid wrong conclusions. The design or modeling of each element is a difficult task because the parameters of one component affect the power level of another. There is therefore a risk that a component will be considered inappropriate, which could make the vehicle unusable, expensive, or ineffective. To do this, we draw up a balance sheet of the forces applied to the vehicle. After having developed the dynamic model, the second step consists of modeling the internal elements of each subsystem, which will give us an approximate view of the nature of the control strategy to be carried out, in the second part of the chapter we will use speed variation as a reference to ensure optimal operation in terms of acceleration and deceleration regulated with a conventional PI controller and different metaheuristic algorithms, such as Particle Swarm Optimization (PSO), and Ant Colony Optimization (ACO) followed with test of robustness. The dynamic behavior of the generation systems studied was evaluated by simulation using MATLAB/Simulink software. Simulation results are presented to validate the effectiveness of the control schemes and evaluate the dynamic performance of the systems examined.

V.2. Description of the traction system of BEV with DC motor

An electric vehicle (EV) consists of five main parts: electric motor drive, ESS, controller, Body vehicle, and auxiliary systems. Figure V.1 shows a schematic diagram of a model EV with battery components. The system comprises the car's body, electrochemical battery, electric motor, drive line, braking system, and regulator for controlling the velocity (acceleration /brake). However, electrically driven material systems include vehicle control, electronic power, electric motors, mechanical gears, and drive wheels. Power supply subsystems (body vehicle) include power supply units, power management units, and power supply units. The auxiliary subsystem includes a power steering unit, a hotel air conditioning system, and an auxiliary power supply unit. This type of BEV model, powered by a DC motor, operates using electrical energy stored in a rechargeable battery pack, which serves as the primary energy source for propulsion. When the driver accelerates, the battery supplies direct current (DC) electricity to the DC motor through a power electronic controller, which regulates the voltage and current based on the required speed and torque. The DC motor converts this electrical energy into mechanical energy, driving the wheels via a drivetrain or direct coupling. The controller ensures smooth acceleration and efficient power distribution by adjusting the motor's speed according to the driver's input and road conditions. Regenerative braking plays a crucial role in energy efficiency, where, during deceleration or braking, the motor acts as a generator, converting kinetic energy back into electrical

energy, which is then fed back to recharge the battery. The state of charge (SOC) of the battery is continuously monitored to optimize energy usage and prevent deep discharge, ensuring longevity. The power electronics also manage auxiliary systems such as lighting, climate control, and infotainment using a DC-DC converter to step down the high-voltage battery output for low-voltage components. Charging the battery is done externally by plugging the vehicle into an electric charging station or a household power outlet, where an onboard charger converts AC power into DC for storage.

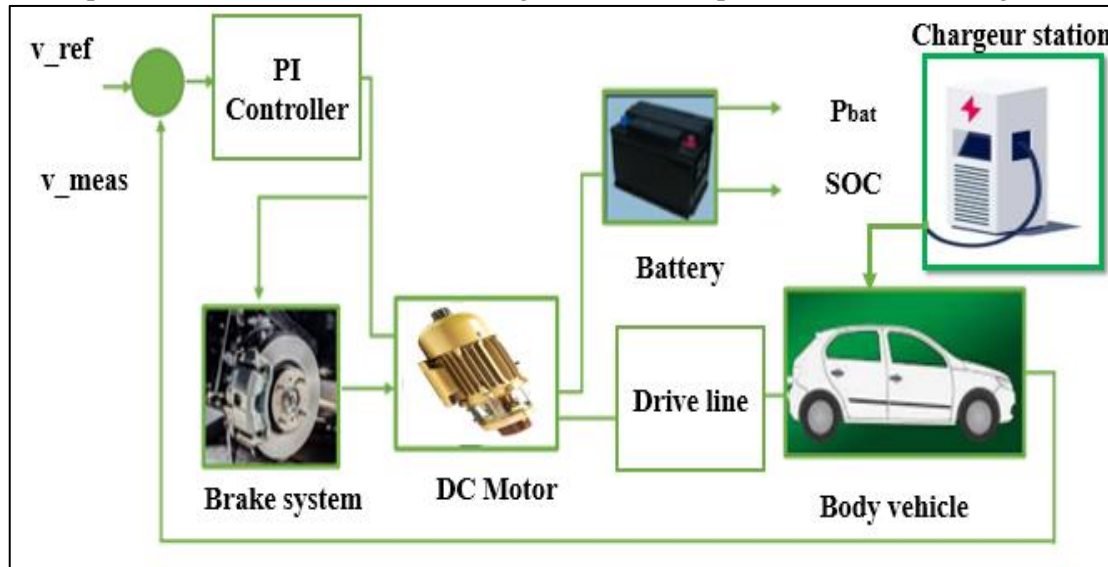


Figure V.1. BEV components.

V.3. Modeling of EV

Vehicle behavior may be described quantitatively using fundamental physics ideas. Modeling an automobile, a very complex system with several subsystems, requires advanced mechanical and mathematical knowledge. The following sections include descriptions of the fundamental vehicle types that were created using the most fundamental mechanical ideas. All-wheel automobiles are covered by the same fundamental dynamic models as vehicles. Together with the proper accessories to substitute for other powertrain components covered in the upcoming sections, this might fairly depict the EV

V.3.1. Dynamic Modeling of the Electric Vehicle

The propulsion system generates mechanical energy that is supposed to be stored momentarily in the vehicle. The motor resistors are assumed to supply the energy for this tank. The energy in the vehicle is stored[246]:

- Kinetic energy is when the vehicle is accelerated.
- in the form of potential energy when the vehicle reaches higher altitudes.

The amount of mechanical energy supplied by a vehicle while driving depends mainly on five effects:

- Aerodynamic Resistance
- Tire Rolling Resistance
- Gradient Resistance
- Acceleration forces

- Inertia resistance

The mechanical model covered in this part, as shown in Figure V.2, is used to determine the driving force necessary for the vehicle to function. The vehicle's power system must deliver a tractive effort at the wheel equal to the sum of the forces required to overcome rolling resistance, aerodynamic drag, and road inclination. Additionally, it must provide the force required to move the vehicle. The force required to pull the automobile at its wheels is defined by equation V.1 [247].

$$F_{\text{total}} = F_{\text{aero}} + F_{\text{rol}} + F_{\text{acce}} + F_{\text{grad}} \quad (\text{V.1})$$

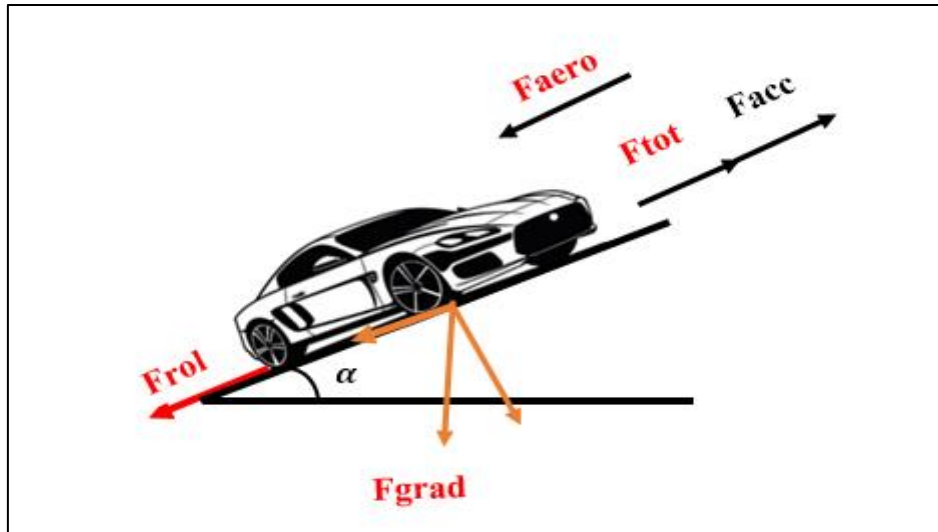


Figure V.2. Basic forces applied on an electric vehicle.

V.3.1.1. Rolling resistance force

The rolling resistance force is caused by the friction between the tires and the driving surface. In addition, when the vehicle is stopped, the rolling resistance force equals zero. The rolling resistance force, which acts in the opposite direction when the automobile starts moving, may be calculated by multiplying the rolling resistance coefficient C_r by the normal force between the vehicle and the road. The vehicle mass (m) times the standard gravity is the normal force on a level surface. Equation (V.2) is used to calculate the tire rolling resistance [248]:

$$F_{\text{rol}} = m * g * C_r * \cos \theta \quad (\text{V.2})$$

V.3.1.2. Aerodynamic drag forces

The aerodynamic resistance that is acting on a moving vehicle is caused by the viscous friction of the surrounding air on the surface of the vehicle [249]. On the other hand, losses are caused by the difference in pressure between the front and rear of the vehicle, generated by a separation of the airflow. For idealized vehicle shapes, the calculation of an approximate pressure field and the resultant force is possible using numerical methods. A detailed analysis of the particular effects (engine ventilation, turbulence in wheel arches, sensitivity to wind, etc.) is only possible with specific measurements in the wind tunnel. Usually, the aerodynamic strength is approximated by simplifying the vehicle into a front surface prismatic body A_f . The force caused by the stagnation pressure is multiplied by an aerodynamic

drag coefficient C_d which models the actual flow conditions[250].

The C_d parameter shall be estimated using CFD programs or wind tunnel experiments. For the estimation of the mechanical energy required to drive a typical test cycle, this parameter can be assumed constant.

The aerodynamic drag force opposes vehicle motion as speed increases because it forces air to flow around the moving vehicle [251]. Here is how the aerodynamic drag resistance is presented in equation V.3:

$$F_{aero} = \frac{1}{2} * \rho * C_d * A_f * V_f^2 \quad (V.3)$$

V.3.1.3. Acceleration forces

The force due to acceleration F_{acc} ensures the dynamic behavior supported by the driver. This force is obtained by the product of vehicle mass and driver acceleration [252].

$$F_{acc} = m * \frac{dv}{dt} \quad (V.4)$$

V.3.1.4. Gradient forces

The gradient force that a car experiences when traveling up or down a road. The longitudinal component of gravitational force, or mg , is what causes the gradient force, where theta is the inclination angle of the road. As mentioned earlier, the normal force and associated rolling resistance force are influenced by the cosine component of gravity [251-252].

The gradient force and angle theta are negative when driving downhill and positive when driving uphill. Road gradients typically fall between plus and minus 10% and are expressed as a percentage in terms of tangent theta.

$$F_{grad} = m * g * \sin \theta \quad (V.5)$$

V.3.1.5. Inertia forces

The inertia of the vehicle and all the rotating parts inside the vehicle generate fictitious forces (Alembert). The inertia force induced by the vehicle mass. The inertia of the rotating masses of the power train may be taken into account in the respective sub models. Nevertheless, sometimes for a quick calculation it may be useful to add the inertia of the rotating masses to the mass of the vehicle. Such an analysis usually takes into consideration a main engine and a transmission with a total ratio. The total inertia torque of the wheels is given by [253]:

$$T_{m,\omega}(t) = \theta_{m,\omega} \frac{d}{dt} \omega_{m,\omega}(t) \quad (V.6)$$

and it acts on the vehicle as an additional inertia force:

$$F_{m,\omega}(t) = \frac{T_{m,\omega}}{r_\omega} \quad (V.7)$$

Usually, wheel slippage is not taken into account in the first approximation:

$$v = r_{\omega} * \omega_{\omega} \quad (\text{V.8})$$

In this case:

$$F_{m,\omega}(t) = \frac{\theta_{m,\omega}}{r_{\omega}^2} \frac{d}{dt} v(t) \quad (\text{V.9})$$

V.3.2. Electric Engines Modeling

The vehicle mass, highway grade, rolling resistance, aerodynamic drag coefficients, vehicle velocity, and acceleration all affect the road load that the electric motor of the automobile must overcome. The motor should have a wide operating speed range to enable single-gear transmission, a high power density and efficiency to increase battery range, and a strong starting torque for early acceleration. Three areas make up the torque-speed profile of an electric motor: natural characteristics, constant torque, and constant power. The constant torque area reaches the motor's rated or base speed when the rated power condition is satisfied [251],[253].

V.3.2.1. PMDC motor

Permanent magnet dc motor that is type of dc motor which converts the electrical energy in to mechanical energy, to produce the field in stator using permanent magnet also PMDC motor is used in battery operated toys to drive the toys cars, used in industrial motion control systems such as the electric vehicle, electric wheelchair, etc. Figure V.3 depicts the schematic block of the PMDC motor.

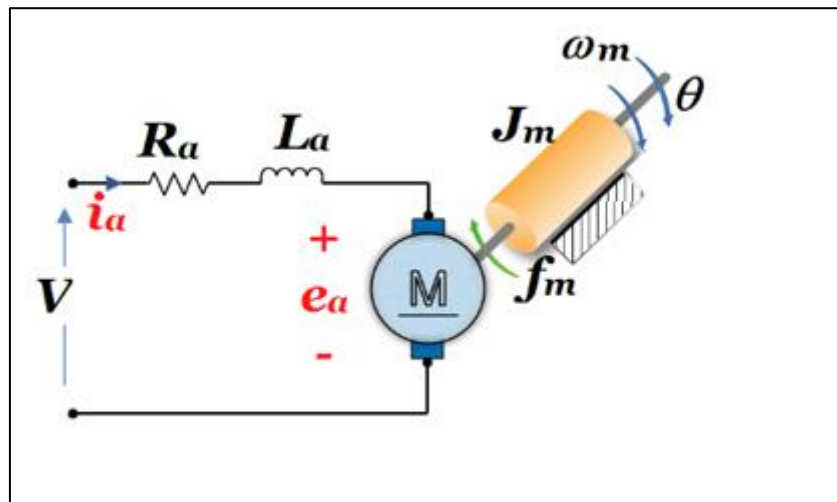


Figure V.3. Block diagram of the PMDC motor[254].

a) The dynamic equations of a PMDC motor are [254]:

$$V(t) = R_a i_a(t) + L_a \frac{di_a}{dt} + e_a(t) \quad (\text{V.10})$$

$$T(t) = J_m \frac{d\omega_r}{dt} + f_m \omega_m + T_L \quad (\text{V.11})$$

- **PMDC motor with PI controller**

The transfer function defining the PMDC motor can be written as follows:

$$G(s) = \frac{K_m}{LJs^2 + (RJ + Lf)s + Rf + K_e + K_m} \quad (\text{IV.12})$$

The transfer function of the PI controller is given by:

$$F(s) = K_p + \frac{K_s}{s} \quad (IV.13)$$

$$TF = G(s).F(s) = \frac{K_m}{LJs^2 + (RJ + Lf)s + Rf + K_e + K_m} \cdot \left(K_p + \frac{K_s}{s}\right) \quad (IV.14)$$

The closed-loop transfer function of the system is:

$$H(S) = \frac{G(s)F(s)}{1 + G(s)F(s)} \quad (IV.15)$$

$$D(s) = \frac{\omega^2}{s^3 + 2\xi\omega s^2 + \omega^2} \quad (IV.16)$$

Following identification, the controllers' parameter expressions are provided by:

$$\begin{aligned} K_p &= J\omega^2 \\ K_I &= 2\xi J\omega - f \end{aligned} \quad (IV.17)$$

V.3.3. Driveline model

The motor provides the whole tractive force necessary at the wheel via a series of gears. These gears are used to raise or reduce torque and wheel speed. Even transmission spin losses are evaluated and modeled, lowering the torque transferred from motor to wheel by a set amount. Another technique to model is to include transmission efficiency. Total tractive torque at the wheel is determined from the total tractive force required at the wheel by [255]:

$$T = F_{total} * r_w \quad (V.18)$$

V.3.4. Brake system

The speed of the vehicle is fed into the braking system. Based on the motor and system regen power limitations, the brake pedal position signal is utilized to calculate the braking force the driver intends to apply to the vehicle and divides this force into a frictional brake output and a regenerative braking force output. The application of regen braking is contingent upon the vehicle speed exceeding a certain threshold, which is ascertained from the vehicle speed input.

V.3.5. Driver model

The vehicle driver is modeled using a PI controller, with the input error being the difference between the desired drive cycle speed and the actual vehicle speed. The PI output is the demand for power to move the vehicle, with a positive signal representing the power necessary for vehicle acceleration and a negative signal representing the power essential for braking.

V.3.6. Batteries

Batteries are ESS devices that are made up of one or more electrochemical cells that transform the

chemical energy contained inside them into electrical energy. Primary batteries are distinguished from secondary batteries. Secondary batteries are rechargeable, but main batteries are not. The battery's capacity is measured in ampere-hours (Ah), while its energy is measured in watt-hours (Wh). It is important to remember that the energy stored in the battery must be accurately approximated in Wh . The battery's useable SOC stated as a percentage, is very important since it reflects the level of charge available in the battery [256-258].

The typical battery lifespan in EVs is 8 to 10 years, which is defined by a 20% – 30% decline in battery capacity relative to its initial capacity. In actuality, the high-power profile of the vehicle during acceleration and braking, which can be more than 10 times greater than the average power, reduces battery longevity. To overcome this limitation, not only battery technological improvement to boost specific energy is required, but also better control and optimization approaches. In this scenario, the adoption of a dependable model of the battery becomes a critical aspect in boosting performance [258]. The Equivalent circuit model is presented in Figure V.4.

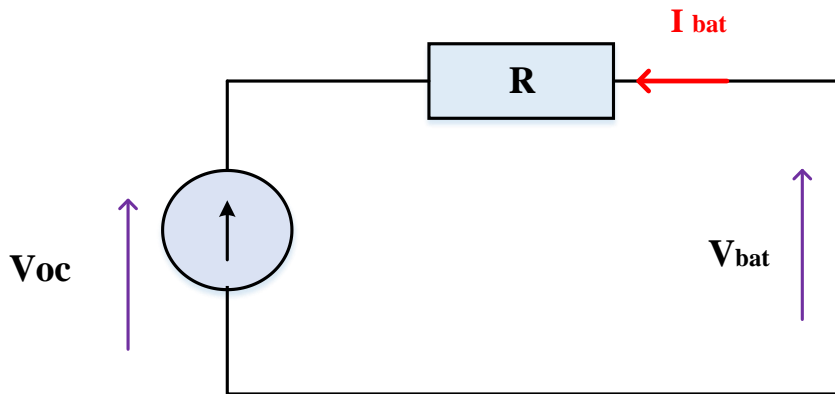


Figure V.4. Equivalent circuit of batterie component.

Where:

$$V_{bat} = E + R * I_{bat} \quad (V.19)$$

The equation is used to compute the battery current [258]:

$$I_{bat} = \frac{\sqrt{V_{oc} + V_{oc}^2 - 4R}}{2R} \quad (V.20)$$

The state of the charge of the battery is expressed [258]:

$$SOC = SOC_{init} - \int \frac{I_{bat}}{C_{bu}} dt \quad (V.21)$$

V.4. Optimization of PI parameters using conventional method and meta-heuristic PSO and ACO algorithms

This part of the chapter describes the tuning of PI controllers using the suggested technique, including the standard way and meta-heuristic type PSO and ACO algorithms for achieving optimal gains.

V.4.1. PI using conventional method

PI controllers are widely used in power electronics due to their simple design and implementation.

Also used to manage constant or gradually changing numbers. In actuality, this controller is a mix of proportional and integral action, as seen in Figure V.5 that is employed to provide optimal control. However, it oscillates significantly, performs poorly in transitory situations, and takes longer to settle. They are also not compatible with nonlinear systems. The transfer function is as follows [230]:

Table (V.1) presents the PI controller gains values for EVs obtained through the PI conventional.

Table V.1: Parameters of EV tuned by PI conventional.

Parameters values	k_p	k_i	ITAE
Conventional PI	0.567	123.5	1.2

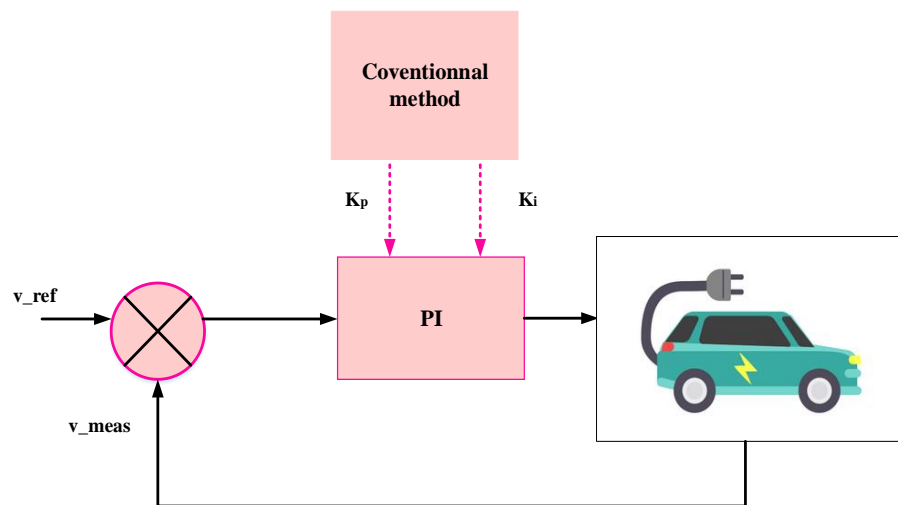


Figure V.5.Block diagram of conventional PI.

V.4.2. PI using Particle swarm optimization

Particle swarm optimization (PSO) is a population-based metaheuristics technique that mimics the social behavior of flocking birds as depicted in Figure V.6 to obtain food destinations [259]. The approach, developed by Russell Eberhart and James Kennedy, optimizes continuous nonlinear functions. Particle swarm optimization (PSO), a collection of particles explores potential solutions to a specified continuous optimization challenge, with each particle representing a candidate solution and utilizing both its own prior experiences and those of neighboring particles to navigate the search space. During the initialization phase, each particle is assigned a random starting position and an initial velocity [260-261]. The position of each particle indicates a potential solution to the problem and is evaluated using the objective function. As particles traverse the search space, they keep track of the position of the best solution they have discovered thus far. In every iteration of the algorithm, each particle updates its velocity based on a weighted combination of three factors: its previous velocity, a velocity component that directs it towards the location of its personal best solution found up to that point, and a velocity component that guides it towards the best solutions identified by neighboring particles. PSO has been implemented in a variety of applications and serves as a notable example of an effective

artificial/engineering swarm intelligence system[259-262].



Figure V.6.Particle Swarm Optimization.

V.4.2.1. Core Components of PSO

V.4.2.1.1. Overview of Key Elements

Particles, population, locations, velocities, and the objective function are the basic building components of particle swarm optimization (PSO). These essential elements allow the swarm to search the space efficiently and converge on the best answers. Let us examine each of these components in further depth [262-264].

a) Particles and Population

In a swarm's search space, particles are essential entities that might be used to solve optimization issues. Every particle in the swarm contributes to the group's collective intellect as an agent or person. Position and velocity are the two main characteristics of particles. The issue variables that define a solution are defined by a particle's position, which is its present location in the search space. A particle's velocity, which is impacted by the swarm's global best and the particle's personal best, dictates its speed and direction of travel. Particles in PSO are arranged into a population that communicates and exchanges information. To keep the balance between exploration and exploitation, population diversity is essential. The swarm can efficiently explore various areas of the search space and hone in on interesting answers by having particles with varying locations and velocities.

b) Position and Velocity

By transferring the values of the issue variables from the search space to the solution space, a particle's location in the search space indicates a possible solution to an optimization problem. An objective function, which gauges how well a certain solution performs about the optimization aim, is used to assess the quality of a particle's location. By giving each location a fitness value, this function makes it possible to compare and rank various solutions. Particles are directed toward more promising areas of the search space by the objective function.

A particle's velocity plays a critical role in establishing its direction and magnitude as it moves across

the search space. Its velocity depends on several factors, including the swarm's global best and the particle's personal best. The PSO optimization process is driven by the interaction between location and velocity. Particles travel to new locations in the search space when their velocities are updated. These places are assessed using the objective function and contrasted with both the global best of the swarm and the particle's personal best. Particles may learn from both their own and other experiences thanks to this feedback loop, which helps them find the best solutions.

c) number of iterations

The number of iterations required to arrive at a satisfactory solution also depends on the nature of the problem. The search may end too soon if there are too few iterations. If the number of iterations is the only limiting factor, an excessively high number of repetitions results in needless additional computing complexity.

d) Weight of inertia

The particle's propensity to continue traveling in the same direction is controlled by its inertia weight. Particles are encouraged to explore additional areas of the search space by a larger inertia weight. A reduced inertia weight, on the other hand, encourages exploitation by concentrating the search on potential regions. Using a constant amount, reducing it linearly over time, or adjusting it in response to the swarm's performance are several methods for determining the inertia weight.

e) Acceleration Coefficients

- The coefficient of cognitive acceleration (c_1) indicates how inclined a particle is to head towards its own best position. When the (c_1) value is elevated, it highlights the particle's unique experiences and promotes exploration in the area surrounding its personal best.
- The coefficient of social acceleration (c_2) regulates the inclination of the particle to navigate towards the global best position. An increased (c_2) value focuses on the collective experiences within the swarm, drawing particles closer to the optimal solution discovered by the group as a whole.

f) Objective function

Each particle's performance in the optimization process is determined by the objective function, a fitness evaluation criterion unique to the task. In machine learning and neural network training, the objective function may be an error function, a cost function in engineering applications, or a mathematical function. It is intended to capture the key features of the system being optimized and can be maximized or lowered based on the issue. For the PSO method to be successful overall in resolving complicated optimization problems, the objective function must be properly formulated to prevent difficulties such as sluggish convergence, premature convergence, and local optima entrapment.

In this chapter, the block diagram with the flowchart of the PSO algorithm is used for the optimal tuning of PI parameters K_p and K_i as shown in Figure V.7 and Figure V.8 .

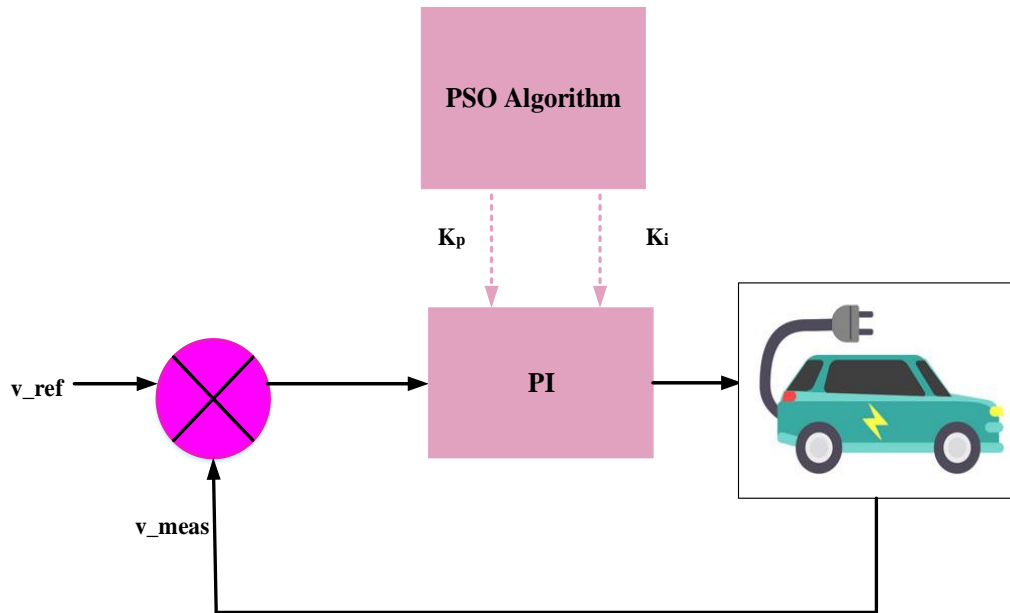


Figure V.7. Block diagram of PI tuned by PSO algorithm.

The implementation of the PSO algorithm in MATLAB is based on the following steps :

1. Definition of PSO parameters:
 - Number of variables (Var = 2).
 - Population size (N) .
 - Upper bound (ub).
 - Lower bound (lb).
 - Inertia weight (w).
 - Individual and social cognitive (c).
 - Number of iterations (T).
2. Selection of velocity and position

- a. Velocity

$$V_m^n = (w \times V_m^n) + (c \times rand \times (Xp_m^n - X_m^n)) + (\times rand \times (Xg_n - X_m^n)) \quad (V.22)$$

- b. Position

$$X_m^n = X_m^n - V_m^n \quad (V.23)$$

With: $m = 1$: Particles; $n = 1$: Var

Where *rand* is a randomly generated number in the range [0,1]

9. The fitness function is used to determine and minimize the fitness value of each particle as below:

$$f_f = \int_0^t t|e|dt \quad (V.24)$$

10. Update both the global optimal solution and the individual optimal solution.

11. Determine the parameters for the *PI* controller.
12. If the overall ideal solution has been reached, stop iterating.

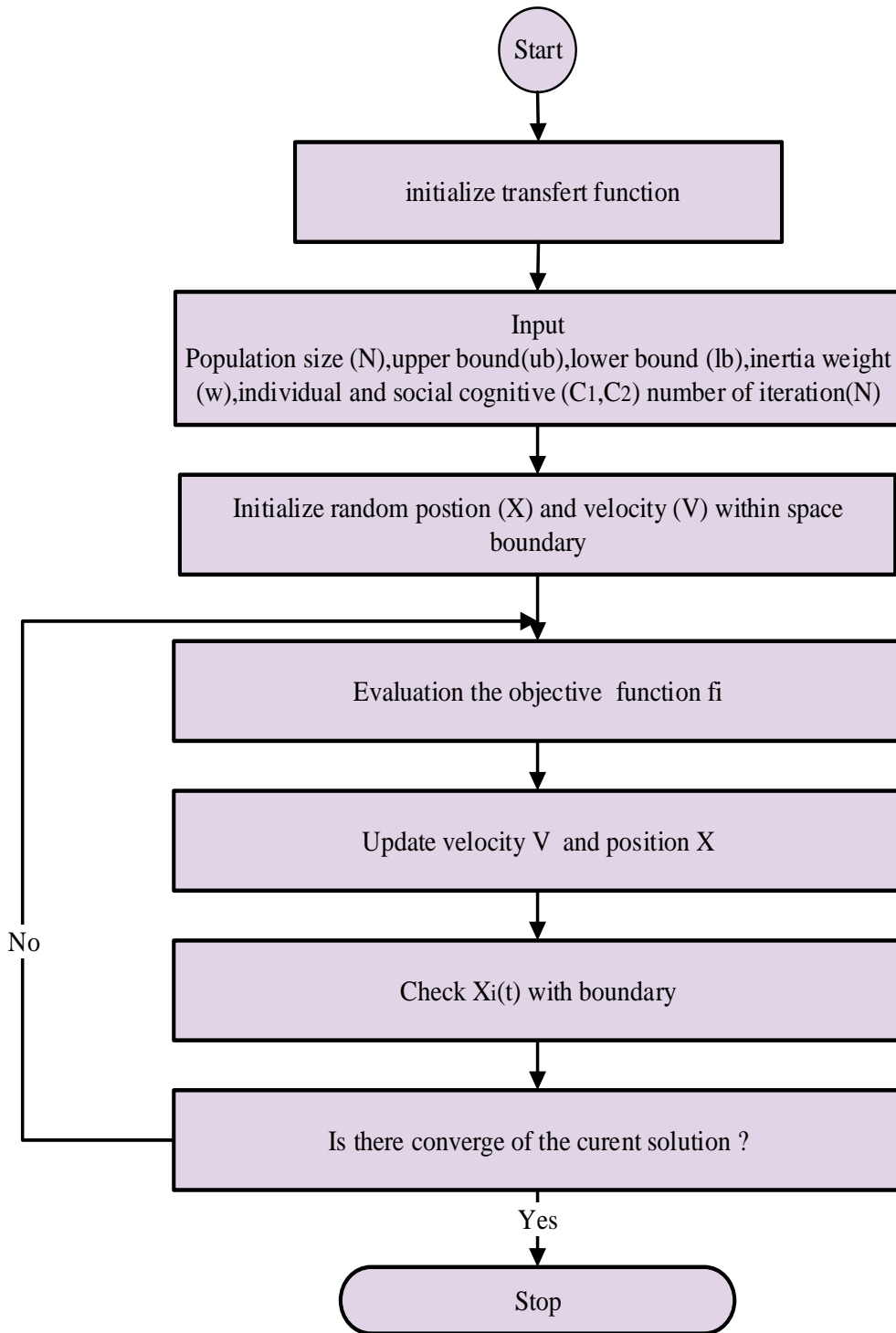


Figure V.8. PI-PSO flowchart.

Table V.2 presents the PI controller gains with the objective function values for the EVs obtained through PSO optimization.

Table V.2: Parameters of EV tuned by PSO.

Parameters	k_p	k_i	ITAE
------------	-------	-------	------

PI-PSO	0.476	87.6	0.921
---------------	-------	------	-------

Figure V.9 depicts the evolution of the objective function with the PSO algorithm across 20 iterations at the beginning of the algorithm. As depicted in the figure below, we remarked that the first objective function equals 1.24, which suggests a less optimal solution. Between iterations 1 and 4. The graph shows a sharp drop, indicating that as the swarm of particles efficiently searches the search space, the quality of the answer will rapidly improve. After iteration 5, the curve flattens and the pace of progress slows down. By iteration 16, the objective function value stabilizes around 0.921, this result indicates and confirms the slow convergence of PSO to achieve the best solution.

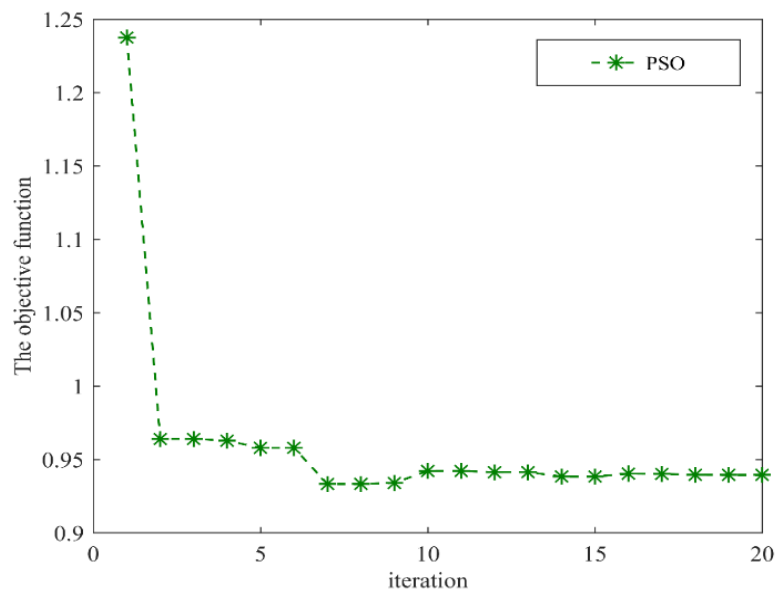


Figure V.9.Convergence of the objective function of PSO.

V.4.3. PI using Ant colony optimization

The figure V.10 shows a closed-loop control system for EV speed regulation using a Proportional-Integral (PI) controller optimized by an Ant Colony Optimization (ACO), this algorithm is detailed in chapter 4. The system compares a reference speed with the actual measured speed, generating an error signal. The PI controller adjusts the control input to minimize speed deviation. The ACO algorithm optimizes gains to enhance performance, reduce steady-state error, and ensure stability. The controlled output is applied to the EV, and the actual speed is fed back into the system, forming a closed-loop structure. This approach optimizes speed control, energy usage, and driving dynamics.

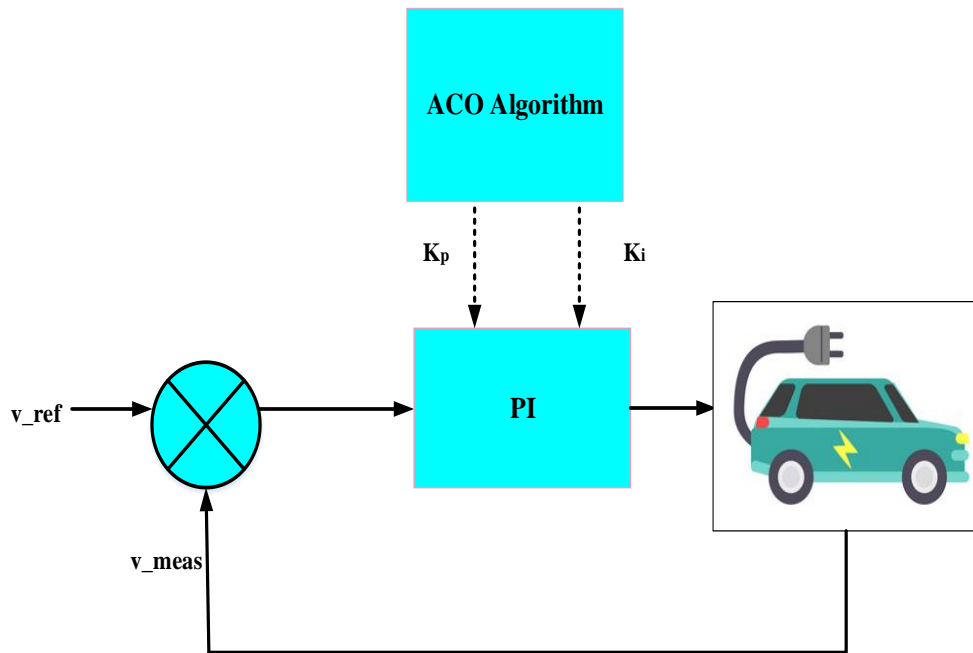


Figure V.10. Block diagram of PI tuned by ACO algorithm.

Table V.3 presents the PI controller gains values for the EV obtained through ACO optimization with the objective function.

Table V.3: Parameters of EV tuned by ACO.

Parameters	k_p	k_i	ITAE
PI-ACO	0.326	35.7	0.3345

Figure V.11 presents the evolution of the objective function value under a series of iterations, initially, we observed the curve decrease rapidly. This rapid improvement is a feature of ACO algorithms. Identify the solution space by leaving pheromone trails on promising pathways. The increase of the iteration results in a swift initial alignment toward more optimal solutions. Towards the end of the iterations, exactly $T = 10$ indicates that the algorithm has reached the optimal solution equal to 0.3345.

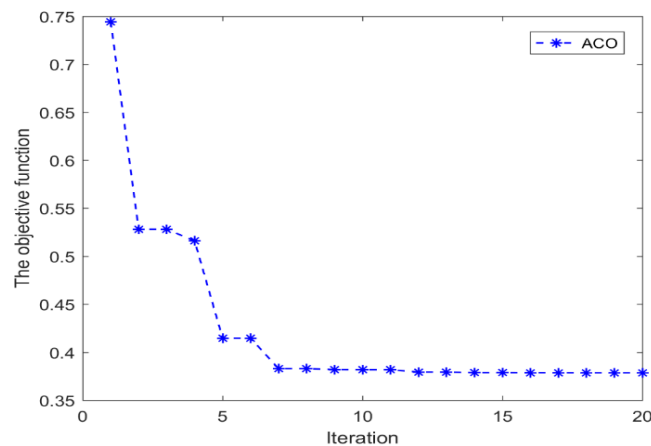


Figure V.11. Convergence of the objective function of ACO algorithm.

V.4.5. Statistical analysis and robustness between PSO and ACO

As explained in the following sections, this study aims to compare and assess the statistical analysis and robustness of PSO and ACO algorithms with different parameter values, such as the number of iterations (T), population size (N), inertia weight (w) in PSO, and evaporate rate ρ in ACO.

a) Comparison of iteration

Table V.4 shows the analysis of the statistical results under different values of iterations, concerning the maximum number of iterations of 100. This study compares the performance of PSO and ACO algorithms, focusing on the impact of the maximum number of iterations to achieve the global minimum solution. The results show that PSO attracts the optimal solution at $T = 80$, while ACO achieves the optimal objective function at $T = 60$. This result demonstrates ACO's robustness in terms of convergence and performance.

Table V. 4: Sensitivity analysis result – maximum number of iterations for PSO and ACO algorithms

Iterations	The best solution with PSO	The best solution with ACO
10	0.25	0.129
20	0.198	0.043
30	0.198	0.043
40	0.198	0.043
50	0.198	0.043
60	0.167	0.031
70	0.155	0.031
80	0.110	0.031
90	0.110	0.031
100	0.110	0.031

b) Comparison of population (N)

Table V.5 shows the results of the different population sizes for the Particle Swarm Optimization (PSO) and Ant Colony Optimization (ACO) algorithms. The results show that PSO is extremely sensitive to changes in swarm size (N), resulting in a slower convergence rate to the ideal particle. This means that PSO particles have a lower chance of discovering the objective function's global minimum. Furthermore, when the ant's size increases, the concentration of pheromones rises proportionally, and the probabilities increase, in ACO algorithms, reaching a better convergence rate.

Table V.5: Statistical analysis result for Population size (N) for PSO and ACO algorithm

N	The best solution with PSO	The best solution with ACO
54	0.867	0.248

88	0.257	0.045
135	0.098	0.034

c) Comparison of inertia weight (W) for the PSO algorithm and evaporation rate for the ACO algorithm

Table V.6 shows the results of the different values of inertia weight (W) for the PSO algorithm and evaporate rate for the ACO algorithm to achieve the best objective function. From PSO, the increases in inertia weight provide further swarm particles to the previous velocity that explore a larger bound of search space, proportionally increasing exploration, consequently leading to an improved performance equal to 0.122. From ACO, a higher value of evaporation rate makes the older pheromone lose its influence faster, which indicates that the ants explore the novel solution that leads to good convergence to the optimal solution equal to 0.010.

Table V. 6: Statistical analysis result – inertia weight (W) for PSO algorithm and evaporate rate for ACO algorithm

W	The best solution with PSO	ρ	The best solution with ACO
0.4	0.968	0.3	0.342
0.8	0.456	0.5	0.094
1.2	0.122	0.8	0.010

V.4.5. Computational Cost

Table V.7 presents a comparative examination of the computing cost incurred while changing the several parameters of two optimization algorithms proposed: Particle Swarm Optimization (PSO) and Ant Colony Optimization (ACO).

a) The computational cost of PSO and ACO under varying iterations and population sizes

The result of the table in the case of the PSO algorithm demonstrates that the computing overhead gradually increases with the number of iterations, referred to as the Average time repetitions. However, the basic nature of PSO allows for quick updates of particle locations, thus, the effect of more iterations is very modest. Additionally, when the population changes or increases, PSO has computational cost referred to as "Average time which signifies demanding more updates to their locations (X) and velocities (V) with each iteration. This indicates that the computation requirements will increase dramatically as the number of repeats grows. However, this effect is considered insignificant due to the relatively basic nature of the computations in PSO. On the other hand, ACO classifies changing the number of iterations and population (ants size) as "Long time.". ACO's iterative and population nature involves frequent adjustments to pheromone trails and recalculation of ant paths, resulting in a higher

overhead than PSO. This result validates and demonstrates the accuracy of the ACO algorithm to achieve the best and optimal solution.

b) The computational cost of ACO under varying Evaporate rate

The result of the table below that the computational cost of the ACO takes average time under the changing the evaporating rate However this parameter offers a crucial role in the algorithm that encourages exploration, forcing ants to seek new paths this operation is the main reason for the extension the running period that ensures the accuracy and robustness of ACO algorithms

c) The computational cost of PSO under varying inertia weight

The result of the table below shows that the computational cost of the PSO takes a "Short time under the changing of the inertia weight, however, this parameter influences. The balance between exploration and exploitation in PSO, also affects how particles modify their velocities. The "Short time" classification results from the fact that altering this parameter requires only minor computational changes.

Table V.7:The Computational cost for PSO algorithm and ACO algorithm

Computational of cost when change :	PSO	ACO
iteration	Average time	Long time
Population size	Average time	Long time
Evaporate rate	/	Average time
inertia weight	Short time	/

V.5. Results and Discussion

In this section, we verify the effectiveness and dynamic performance of the proposed strategies. The Matlab / Sim Power System software environment was employed to conduct numerical simulations on a BEV.

Figure V.12 illustrates the driving cycle profile type US06 considerable variation over time reflecting different acceleration-deceleration driving conditions.

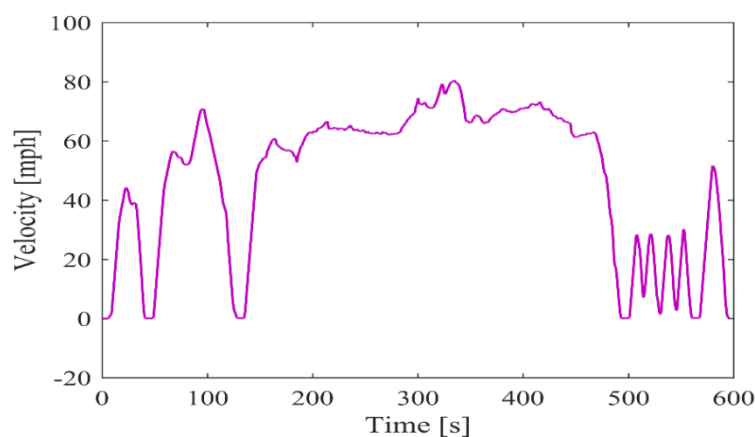


Figure V.12.Driving cycle profile type US06.

Figure V.13 progression of mechanical speed with the reference speed which is essential for supporting the demanding motor during charge and discharge cycles.

The findings indicate that the traditional PI method exhibits performance deficiencies, particularly overshoot and rise time. In contrast, implementing the PSO and ACO algorithms to enhance the PI controller yields significantly improved results. Especially. This optimization ACO effectively manages the dynamic variations, maintaining reference values without exceeding limits or introducing dynamic errors. A comparative analysis between the conventional PI method and the PI-ACO approach reveals the advantages of the ACO in delivering superior dynamic performance, characterized by reduced overshoot and rise time, as well as decreased sensitivity to load power during acceleration and braking.

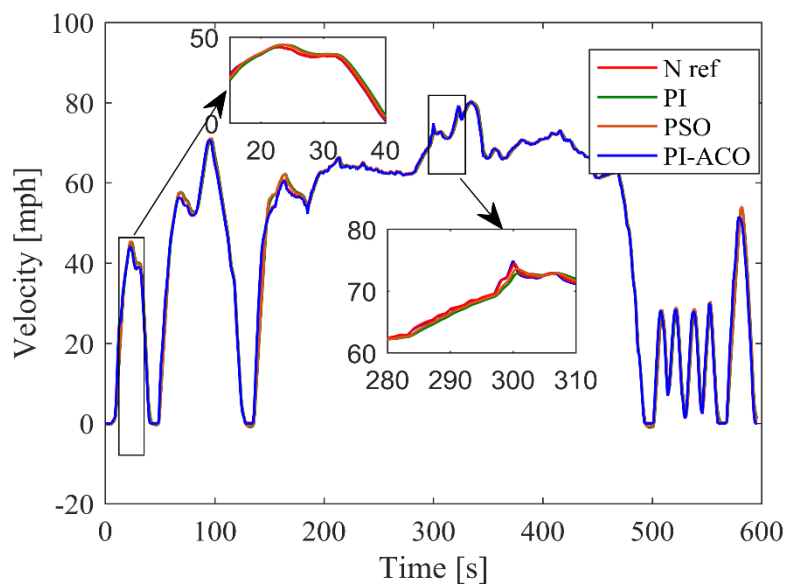


Figure V.13. Vehicle speed tuned with conventional PI, PSO, and ACO algorithms.

The graph depicted in Figure V.14 reflects the varying intensity of the current, suggests different driving behaviors, with sections of high power demand interspersed with energy recovery phases under a realistic driving cycle characterized by a mix of acceleration and regenerative braking this type of Analyzing such current behavior helps optimize energy efficiency, extend battery life, and improve the overall performance of the EV.

As seen are frequent current spikes, indicating a high power consumption when driving uphill or during acceleration. These peaks show when energy is being released from the battery to run the electric motor. These spikes vary in amplitude, most likely as a result of altered driving circumstances such as speed fluctuations or inclination in the road.

From 200s to 280s, indicate that the current swings but remain in a reasonable range, indicating steady-state driving circumstances with reasonably consistent energy consumption. However, sudden drops indicate regenerative braking, coasting, or unexpected power usage reductions.

From 460s to 480s indicates that the current rapidly drops. These dips might signify energy recovery via regenerative braking, in which the car turns kinetic energy into stored electrical energy, essentially recharging the battery.

Figure V.15 illustrates the progression of the motor's power with the battery BESS across various driving cycle scenarios. During acceleration, the battery provides a lot of power to the motor, but during braking or deceleration, the power drops dramatically owing to energy recovery. The variety of power use during the time implies a realistic driving cycle in which energy demand fluctuates based on speed variations, driver behavior, road conditions, and any external loads impacting the system.

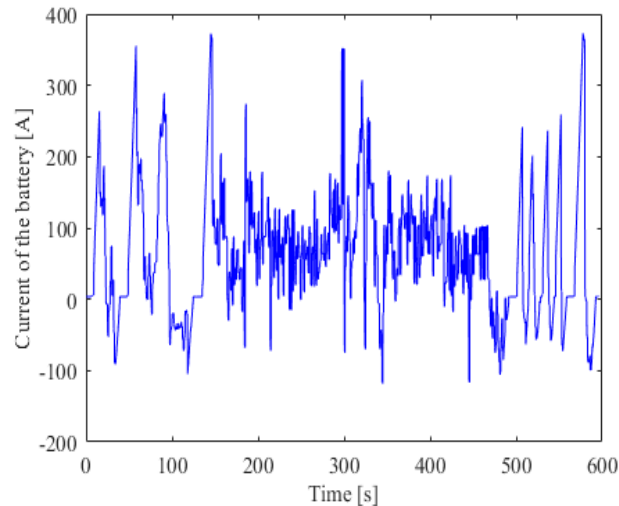


Figure V.14. Current of the battery.

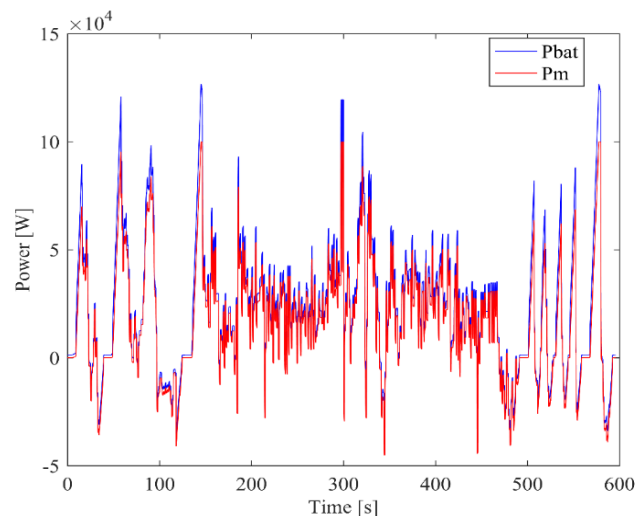


Figure V.15. Power of motor and battery.

The torque-time plot in Figure V.16 highlights the vehicle's dynamic reaction to acceleration, deceleration, cruising, and perhaps regenerative braking phases by displaying how torque changes across various driving cycles. Frequent torque spikes during the first phase (0 – 100s) signify quick acceleration occurrences. Less drastic torque variations are shown throughout the mid-range (100– 400 s) period, indicating a shift into moderate acceleration and deceleration that most likely reflects mixed road conditions. A high-performance driving cycle is suggested by the last phase (400– 600s), which exhibits a more dynamic torque requirement with numerous surges back to the 500 Nm limit. Frequent acceleration followed by slowdown is indicated by the frequent switch between maximum torque and near-zero readings.

This is a result of high-speed test cycles, or intense driving situations that call for constant power changes. The torque profile points to a varied driving cycle that includes periods of quick deceleration, and acceleration-heavy situations. Heavy acceleration is indicated by high torque peaks, whereas coasting, stopping, or energy recovery via regenerative braking systems are shown by intervals of nearly zero torque.

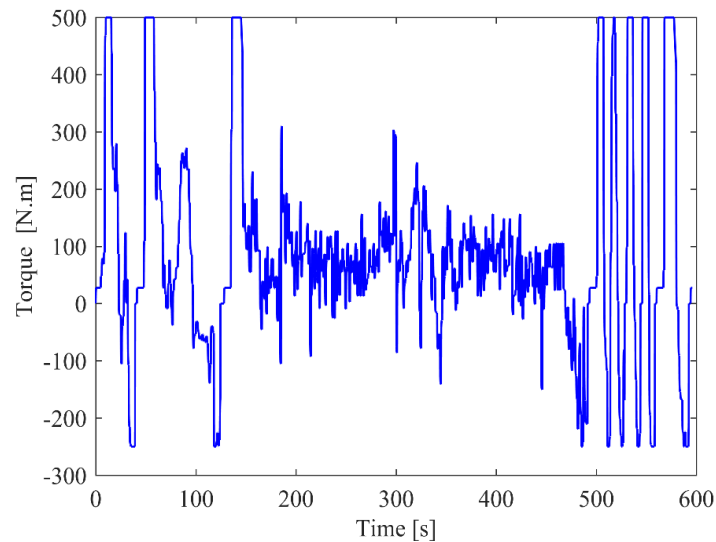


Figure V.16.Motor Torque.

In this section, an extensive analysis is performed to study the impact of the angle road on the performance of the proposed controllers (PI, PSO, ACO) and evaluate their influence on the vehicle dynamic response.

The system's velocity response while traversing a road with various angles and disturbances while using various control algorithms is depicted in several figures V.17, V.18, V.19 and V.20. A conventional proportional-integral (PI) controller, a PI controller optimized using particle swarm optimization (PI-PSO), a PI controller optimized using ant colony optimization (PI-ACO), and the reference velocity are among the several velocity profiles in the figure that correspond to various control strategies. The reference velocity serves as a standard by which the performance of the controllers can be assessed since it depicts the optimal speed trajectory. By decreasing deviations from the reference velocity, the PI-PSO controller shows improved tracking performance, proving that Particle Swarm Optimization has successfully adjusted the controller's parameters to enhance response time and reduce overshoot. The standard PI controller follows the reference velocity but shows deviations. By reducing oscillations, the PI-ACO controller performs at its peak, offering a more responsive and stable control action even in difficult driving situations. These findings highlight the value of intelligent optimization methods in control system design by showing how evolutionary algorithms like PSO and ACO can improve performance in practical settings where dynamic challenges are introduced by environmental variations like changes in road inclination.

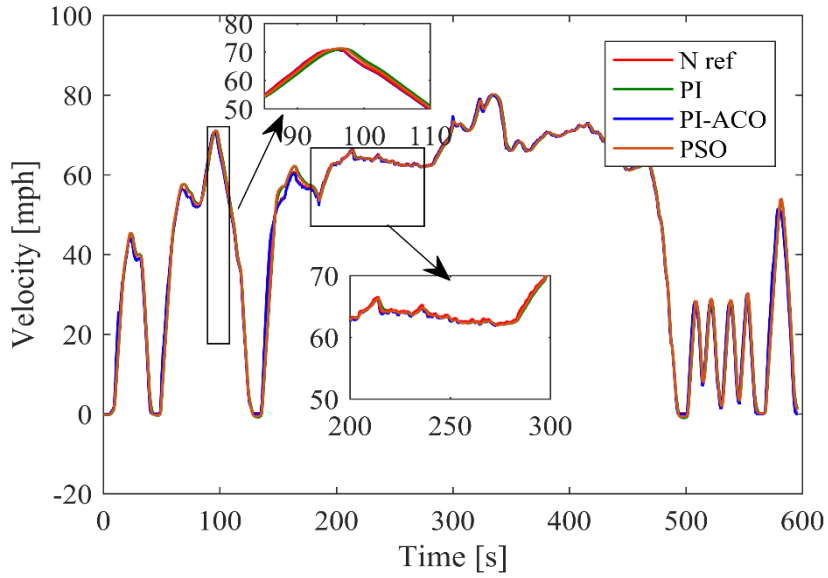


Figure V. 17. Vehicle speed tuned with conventional PI, PSO, and ACO at 5 degrees' road angle.

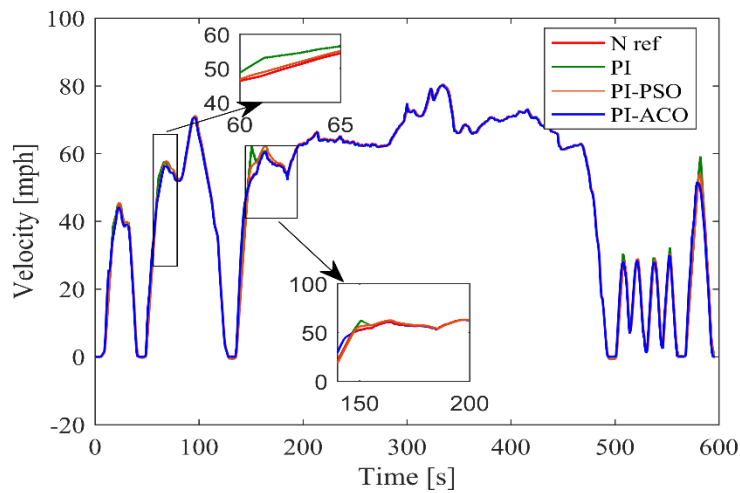


Figure V.18. Vehicle speed tuned with conventional PI, PSO, and ACO 15 degrees' road angle

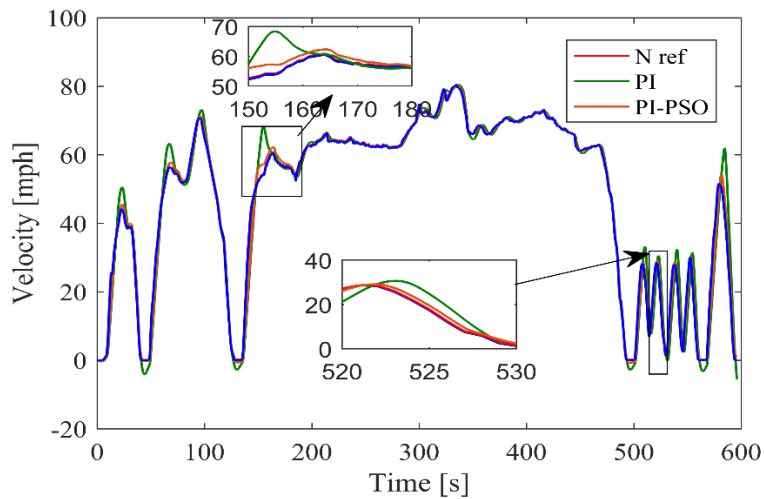


Figure V. 19. Vehicle speed tuned with conventional PI, PSO, and ACO at 28 degrees' road angle.

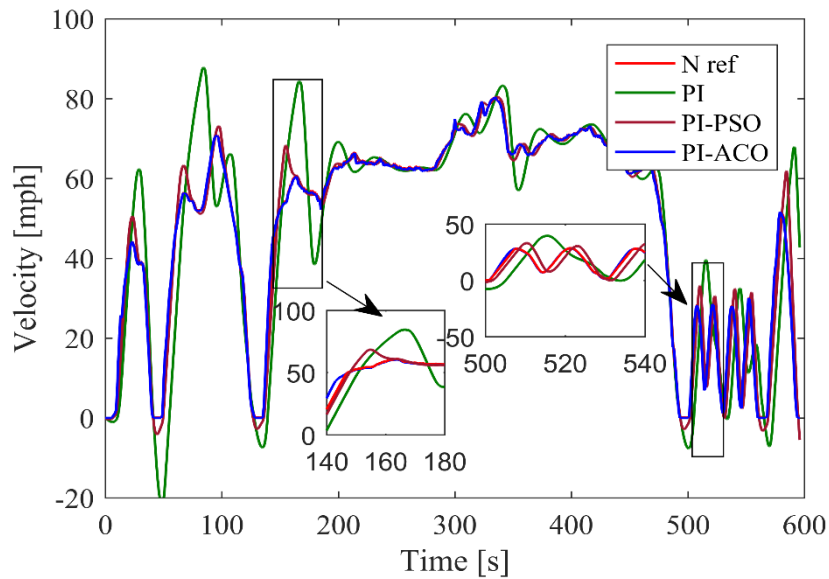


Figure V. 20. Vehicle speed tuned with conventional PI, PSO, and ACO at 40 degrees' road angle.

From these figures, the results were analyzed and summarized in Table V.5 to evaluate the performance of the proposed controllers against angle load variations. It was found that beyond 28 *degree* angle, the PI controller causes system instability, while the system remains stable with the PSO and ACO controllers.

For 5 and 28 angle increase, the system based on a regulator tuned by PI becomes unstable, on the other hand, when the angle equals 40, the PI-PSO turns into Unstable. However, the system tuned by ACO maintains stability. This allows us to conclude that the optimization of settings via ACO offers superior robustness and efficiency compared to the other methods examined in this study.

Table VI. 7: Test of the robustness of the conventional PI ,PSO, and ACO.

Tunnig approaches	5 degree	15 degree	28 degree	40 degree
PI Classic	Stable	Stable	Unstable	Unstable
PI-PSO	Stable	Stable	Stable	Unstable
PI-ACO	Stable	Stable	Stable	Stable

V.6. Conclusion

In this chapter, two novel techniques for improving the speed control motor in EV with BESS application, PSO and ACO controllers, are presented. Comparing the PI-ACO controller to more traditional controllers like PI and particle swarm optimization, extensive simulations and statistical analyses reveal that it performs better than other methods in terms of speed regulation, minimizing overshoot, removing undershoot, improving rise time, settling time, and steady-state error, and exhibiting robustness under varying road. These findings are especially promising for BEV drive systems, where precise speed control is critical for improving efficiency and performance.

General Conclusion

With the evolution of technologies, electrical energy sources are taking an increasingly important role in today's industrial world. The current technology of batteries ensures that the system that they feed has a very limited autonomy. In addition, the batteries must be subjected to high power fluctuations, greatly impairing their reliability and service life. These drawbacks can be reduced by inserting a new reliable energy source capable of providing the power peaks at the right time. Supercapacitors, given their good service life, their strong power density, and their great ability to charge and discharge quickly, are a plausible candidate for the position. The energy management of sources in EV is now a high-profile research.

The development of research focuses, among other things, on new sources of ESS such as batteries and the implementation of advanced control and energy management to optimize the performance (life and cost) of the EV.

The first part of the contribution addressed in this thesis allowed us to study the operation of a photovoltaic system connected to a battery-supercapacitor system, focusing on the integration of different advanced algorithms such as genetic algorithm, ant colony optimization, and Grey wolf optimization. The outcome of this novel application is to contribute to advancements in the design and operation of ESS systems, fostering improvements in overall system performance and reliability. The performance of these controllers is evaluated under different solar irradiation and load situations. Different simulation scenarios are presented to analyze the system response. The results indicate that the GWO-based PI control technique demonstrates superior performance in terms of settling time, overshoot, and rise time. Additionally, from the result, the proposed control scheme improves power quality by minimizing the ripples of the power, which can harm sensitive loads, thereby improving power quality.

In the second part, allowed the deep modeling of BEV followed by uses a speed variation as a reference to ensure optimal operation in terms of acceleration and deceleration regulated with a conventional PI controller and different metaheuristic algorithms, such as Particle Swarm Optimization (PSO), and Ant Colony Optimization (ACO) followed, A comparative study with other tuning methods is presented to provide empirical evidence on the superiority of the proposed PP_PSO controller in enhancing the performance of the overall system. This comparative study serves to demonstrate the feasibility and effectiveness of the algorithms introduced to optimize the PI controller, resulting in improved system performance and robustness under different conditions such as variation of the degree angle of the road. Through diverse simulation tests, ACO methodologies have demonstrated robust performance and efficacy.

Limitations of this work.

Due to the lack of necessary experimental materials, this work is limited to simulation-based analysis. The study focuses on modeling and simulating PV, HESS, EV, BEV, conventional methods, and metaheuristic algorithm systems to evaluate their performance. Validation is carried out by comparing

simulation results with data from existing literature, ensuring accuracy and reliability.

Perspectives and Future Directions

This research opens avenues for further exploration and development. Future work could delve into the integration of advanced algorithms for real-time adaptation to varying environmental conditions. Moreover, the study paves the way for incorporating other energy sources and ESS technologies to ensure a continuous and stable power supply to the load. In addition to optimizing the hybrid system for broader applications, such as in microgrids and smart grid configurations. Our work has limitations in terms of the GWO algorithm may struggle to converge to the global optimum in complex problem spaces with multiple local optima. It should include Hybrid controls such as Adaptive Neuronal Network-Harris Hawks Optimization (ANN-HHO), and implement other robust commands like PSO-optimized infinite H. The proposed control scheme can also be applied to other HESS using Machine Learning (ML) and deep RL approaches. for the design of the control strategy to solve the optimization problem.

- The different approach proposed in this thesis can be adopted to a medium and high power experimental configuration by using easily available platforms equipped with DSpace boards.
- Integration of Hydrogen power generation systems in the electric car, in addition to wireless and fast-charging technologies, which can shorten charging periods and improve user convenience, is another exciting field. Bidirectional energy flow will be made possible by more research on vehicle-to-grid (V2G) and vehicle-to-everything (V2X) technologies, enabling EVs to assist the power grid during periods of high demand. Additionally, autonomous driving and artificial intelligence (AI)-based energy management may maximize route planning and driving economy.
- Test the BEV with other driving profiles such as WLTP, NEDC, SORDS .

Appendix A

Parameters of the PV cell (Model WU-120)

P_{PV}	W	120.7
$V_{oc,n}$	V	21
$I_{sc,n}$	A	8
I_{mp}	A	7.1
R_p	Ω	31.6334
R_s	Ω	0.196
K_V	V/K	-0.358
K_I	A/K	0.052
N_s	-	72

The technical characteristics of the battery (Lithium-Ion)

I_n	A	32.5
V_n	V	24
C	Ah	14
soc	%	50
R	Ω	12.6609

The technical characteristics of the Supercapacitor

I_n	A	20
V_n	V	32
V_i	V	32
C	F	29

The technical characteristics of the DC bus

C	F	$300 \cdot 10^{-6}$
P	W	500
V_{dc}	V	50

Appendix B

The Parameters of the Battery electric vehicle

G	m/s^2	9.81
P	kg/m^3	1.23
r_w	m	0.254
A_f	m^2	2.1
C_d	/	0.38
C_f	/	0.01
M	Kg	1616.15
θ	Degree	0
P_m	Kw	150
T_M	N.m	360
V_bat	V	240
R	Ω	20
SOC_init	%	60

The Parameters of the ACO algorithm for electric vehicles

Var	/	2
Ants	/	45
Iteration	/	20
Ub	/	0
Lb	/	100
H	/	0.2
P	/	0.6
Δ	/	2

The Parameters of the PSO algorithm for electric vehicles

W	/	0.7
Var	/	2
Particles	/	35
c	/	2
Iteration	/	20

Bibliography

- [1] M. Haghani, F. Sprei, K. Kazemzadeh, Z. Shahhoseini, and J. Aghaei, "Trends in electric vehicles research," *Transportation Research Part D: Transport and Environment*, vol. 123, pp. 103881–103881, Oct. 2023, doi: <https://doi.org/10.1016/j.trd.2023.103881>.
- [2] T.-Z. Ang, M. Salem, M. Kamarol, H. S. Das, M. A. Nazari, and N. Prabakaran, "A Comprehensive Study of Renewable Energy sources: Classifications, Challenges and Suggestions," *Energy Strategy Reviews*, vol. 43, p. 100939, Sep. 2022, doi: <https://doi.org/10.1016/j.esr.2022.100939>.
- [3] D. Zbroński, H. Otwinowski, A. Górecka-Zbrońska, D. Urbaniak, and T. Wyleciał, "Analysis of Changes in Electricity Generation from Renewable Energy Sources after Poland's Accession to Structures of the European Union," *Energies*, vol. 16, no. 12, p. 4794, Jun. 2023, doi: <https://doi.org/10.3390/en16124794>.
- [4] Y. Wang, Z. Pan, W. Zhang, T. N. Borhani, R. Li, and Z. Zhang, "Life cycle assessment of combustion-based electricity generation technologies integrated with carbon capture and storage: A review," *Environmental Research*, p. 112219, Oct. 2021, doi: <https://doi.org/10.1016/j.envres.2021.112219>.
- [5] J. Das, A. Ur Rehman, R. Verma, G. Gulen, and M. H. Young, "Comparative Life-Cycle Assessment of Electricity-Generation Technologies: West Texas Case Study," *Energies*, vol. 17, no. 5, p. 992, Jan. 2024, doi: <https://doi.org/10.3390/en17050992>.
- [6] P. Garia, A. Mittal, A. Singh, N. Kumar, and S. Oli, "A Study and Performance Review of an On-Grid PV Solar Plant Using Artificial Intelligence," *2023 International Conference on Power Energy, Environment & Intelligent Control (PEEIC)*, pp. 484–489, Dec. 2023, doi: <https://doi.org/10.1109/peeic59336.2023.10451368>.
- [7] S. M. Alawad, R. B. Mansour, F. A. Al-Sulaiman, and S. Rehman, "Renewable energy systems for water desalination applications: A comprehensive review," *Energy Conversion and Management*, vol. 286, p. 117035, Jun. 2023, doi: <https://doi.org/10.1016/j.enconman.2023.117035>.
- [8] M. Khalid, "Smart grids and renewable energy systems: Perspectives and grid integration challenges," *Energy Strategy Reviews*, vol. 51, pp. 101299–101299, Jan. 2024, doi: <https://doi.org/10.1016/j.esr.2024.101299>.
- [9] C. Breyer *et al.*, "On the History and Future of 100% Renewable Energy Systems Research," *IEEE Access*, vol. 10, pp. 78176–78218, 2022, doi: <https://doi.org/10.1109/access.2022.3193402>.
- [10] S. Heroual, B. belabbas, T. Allaoui, "A stand-alone PV system with pi controller for battery (charging/discharging)", conference: national conference on industrial engineering and sustainable (ciesd'23), relizane, 2023.
- [11] I. E. Atawi, A. Abuelrub, A. Q. Al-Shetwi, and O. H. Albalawi, "Design of a wind-PV system integrated with a hybrid energy storage system considering economic and reliability assessment," *Journal of Energy Storage*, vol. 81, pp. 110405–110405, Mar. 2024, doi:

<https://doi.org/10.1016/j.est.2023.110405>.

- [12] A. G. Abo-Khalil, K. Sayed, A. Radwan, and Ibrahim I. A. El-Sharkawy, "Analysis of the PV system sizing and economic feasibility study in a grid-connected PV system," *Case Studies in Thermal Engineering*, vol. 45, p. 102903, May 2023, doi: <https://doi.org/10.1016/j.csite.2023.102903>.
- [13] M. Baqir and H. K. Channi, "Analysis and design of solar PV system using Pvsyst software," *Materials Today: Proceedings*, Sep. 2021, doi: <https://doi.org/10.1016/j.matpr.2021.09.029>.
- [14] A. Banik, A. Shrivastava, R. Manohar Potdar, S. Kumar Jain, S. Gopal Nagpure, and M. Soni, "Design, Modelling, and Analysis of Novel Solar PV System using MATLAB," *Materials Today: Proceedings*, vol. 51, pp. 756–763, Jan. 2022, doi: <https://doi.org/10.1016/j.matpr.2021.06.226>.
- [15] J.N. Anang, S. N. A. Syd Nur Azman, W. M. W. Muda, A. N. Dagang, and M. Z. Daud, "Performance analysis of a grid-connected rooftop solar PV system in Kuala Terengganu, Malaysia," *Energy and Buildings*, vol. 248, p. 111182, Oct. 2021, doi: <https://doi.org/10.1016/j.enbuild.2021.111182>.
- [16] J. Mitali, S. Dhinakaran, and A. A. Mohamad, "Energy storage systems: A review," *Energy Storage and Saving*, vol. 1, no. 3, Jul. 2022, doi: <https://doi.org/10.1016/j.enss.2022.07.002>.
- [17] Shaik Nyamathulla and C. Dhanamjayulu, "A review of battery energy storage systems and advanced battery management system for different applications: Challenges and recommendations," *Journal of Energy Storage*, vol. 86, pp. 111179–111179, May 2024, doi: <https://doi.org/10.1016/j.est.2024.111179>
- [18] A. G. Olabi *et al.*, "Battery energy storage systems and SWOT (strengths, weakness, opportunities, and threats) analysis of batteries in power transmission," *Energy*, vol. 254, p. 123987, Sep. 2022, doi: <https://doi.org/10.1016/j.energy.2022.123987>.
- [19] T. Zhu, R. G. A. Wills, R. Lot, H. Ruan, and Z. Jiang, "Adaptive energy management of a battery-supercapacitor energy storage system for electric vehicles based on flexible perception and neural network fitting," *Applied Energy*, vol. 292, p. 116932, Jun. 2021, doi: <https://doi.org/10.1016/j.apenergy.2021.116932>.
- [20] Q. Hassan, M. Jaszczur, A. M. Abdulateef, J. Abdulateef, A. Hasan, and A. Mohamad, "An analysis of photovoltaic/supercapacitor energy system for improving self-consumption and self-sufficiency," *Energy Reports*, vol. 8, pp. 680–695, Nov. 2022, doi: <https://doi.org/10.1016/j.egy.2021.12.021>.
- [21] X. Lin and R. Zamora, "Controls of hybrid energy storage systems in microgrids: Critical review, case study and future trends," *Journal of Energy Storage*, vol. 47, p. 103884, Mar. 2022, doi: <https://doi.org/10.1016/j.est.2021.103884>.
- [22] H. Xu and M. Shen, "The control of lithium-ion batteries and supercapacitors in hybrid energy storage systems for electric vehicles: A review," *International Journal of Energy Research*, Aug. 2021, doi: <https://doi.org/10.1002/er.7150>.
- [23] A. Bharatee, P. K. Ray, and A. Ghosh, "A Power Management Scheme for Grid-connected PV

Integrated with Hybrid Energy Storage System,” *Journal of Modern Power Systems and Clean Energy*, vol. 10, no. 4, pp. 954–963, 2022, doi: <https://doi.org/10.35833/mpce.2021.000023>.

[24] M. M. Gulzar, A. Iqbal, D. Sibtain, and M. Khalid, “An Innovative Converterless Solar PV Control Strategy for a Grid Connected Hybrid PV/Wind/Fuel-Cell System Coupled with Battery Energy Storage,” *IEEE Access*, pp. 1–1, 2023, doi: <https://doi.org/10.1109/access.2023.3252891>.

[25] L. Zhang *et al.*, “Hybrid electrochemical energy storage systems: An overview for smart grid and electrified vehicle applications,” *Renewable and Sustainable Energy Reviews*, vol. 139, p. 110581, Apr. 2021, doi: <https://doi.org/10.1016/j.rser.2020.110581>.

[26] A. K. Podder, O. Chakraborty, S. Islam, N. Manoj Kumar, and H. H. Alhelou, “Control Strategies of Different Hybrid Energy Storage Systems for Electric Vehicles Applications,” *IEEE Access*, vol. 9, pp. 51865–51895, 2021, doi: <https://doi.org/10.1109/ACCESS.2021.3069593>.

[27] M. C. Argyrou, C. C. Marouchos, S. A. Kalogirou, P. Christodoulides, “Modeling a residential grid-connected PV system with battery–supercapacitor storage: Control design and stability analysis”, *Energy Reports*, 2021, Vol. 7, pp. 4988-5002, <https://doi.org/10.1016/j.egy.2021.08.001>.

[28] M. A. Zdiri *et al.* “Design and analysis of sliding-mode artificial neural network control strategy for hybrid PV-battery-supercapacitor system”. *Energies*, 2022, vol. 15, no. 11, p. 4099, <https://doi.org/10.3390/en15114099>.

[29] K. Javed, H. Ashfaq, R. Singh, S. S. Hussain, T. S. Ustun, “Design and performance analysis of a stand-alone PV system with hybrid energy storage for rural India”. *Electronics*, 2019, vol. 8, no. 9, p. 952, <https://doi.org/10.3390/electronics8090952>.

[30] S. Aggarwal, M. Alam, J. Kumar, “Sliding Mode Control Scheme for Hybrid Energy Storage Technologies in a DC Microgrid,” *International Mobile and Embedded Technology Conference (MECON), IEEE, 2022, pp. 486–489, https://ieeexplore.ieee.org/abstract/document/9751987/*.

[31] A. U. Rahman, S. S. Zehra, I. Ahmad, H. Armghan, “Fuzzy super twisting sliding mode-based energy management and control of hybrid energy storage system in electric vehicle considering fuel economy”. *Journal of Energy Storage*, 2021, vol. 37, p. 102468, <https://doi.org/10.1016/j.est.2021.102468>.

[32] S. Patel, A. Ghosh, P. K. Ray, “Efficient power management and control of DC microgrid with supercapacitor-battery storage systems”. *Journal of Energy Storage*, 2023, vol. 73, p. 109082, <https://doi.org/10.1016/j.est.2023.109082>.

[33] M. Mossadak, A. Chebak, N. Ouahabi, A. Rabhi, A. A. Elmahjoub, “A novel hybrid PI–backstepping cascade controller for battery–supercapacitor electric vehicles considering various driving cycle scenarios”. *IET Power Electronics*, 2024, vol. 17, no. 9, pp. 1089–1105, <https://doi.org/10.1049/pel2.12697>.

[34] S. Pattnaik, M. R. Kumar, S. K. Mishra, S. P. Gautam, B. Appasani, T. S. Ustun, “DC Bus Voltage Stabilization and SOC Management Using Optimal Tuning of Controllers for Supercapacitor

Based PV Hybrid Energy Storage System". *Batteries*, 2022, vol. 8, no. 10, p. 186, <https://doi.org/10.3390/batteries8100186>.

[35] N.-D. Nguyen, C. Yoon, and Y. I. Lee, "A standalone energy management system of battery/supercapacitor hybrid energy storage system for electric vehicles using model predictive control", *IEEE Transactions on Industrial Electronics*, 2022, vol. 70, no. 5, pp. 5104–5114, <https://doi.org/10.1109/TIE.2022.3186369>.

[36] F. A. Yusvianti, V. Lystianingrum, M. F. Romlie, "Neural-Network Based Energy Management System for Battery-Supercapacitor Hybrid Storage". 6th Global Power, Energy and Communication Conference (GPECOM), IEEE, 2024, pp. 411–416, <https://ieeexplore.ieee.org/abstract/document/10582642/>.

[37] M. M. Hasan, A. H. Chowdhury. "An improved adaptive hybrid controller for battery energy storage system to enhance frequency stability of a low inertia grid". *Journal of Energy Storage*, 2023, vol. 58, p. 106327, <https://doi.org/10.1016/j.est.2022.106327>.

[38] A. S. Mohammed, S. M. At Naw, A. O. Salau, J. N. Eneh, "Review of optimal sizing and power management strategies for fuel cell/battery/supercapacitor hybrid electric vehicles". *Energy Reports*, 2023, vol. 9, pp. 2213–2228, <https://doi.org/10.1016/j.egy.2023.01.042>.

[39] A. Aghmadi, O. Ali, H. Hussein, O. A. Mohammed, "Dynamic Pulsed Load Mitigation in PV-Battery-Supercapacitor Systems: A Hybrid PI-NN Controller Approach," *IEEE Design Methodologies Conference (DMC), IEEE, 2023*, pp. 1–6, <https://ieeexplore.ieee.org/abstract/document/10412563/>.

[40] F. Kang, X. Zhang, Z. Wang, Y. Luo, H. Zhai, H. Yi, "An SOC-based Adaptive Control Strategy for Pulsed Power Elimination in Hybrid Energy Storage System," *10th International Power Electronics and Motion Control Conference (IPEMC2024-ECCE Asia)*, IEEE, 2024, pp. 627–632, <https://ieeexplore.ieee.org/abstract/document/10567493/>.

[41] K. Deepak, R. K. Mandal, V. Verma, "Improvement of power quality by using a novel controller for hybrid renewable energy sources based microgrid". *International Emerging Electric Power Systems*, 2024, vol. 25, no. 3, pp. 289-303, <https://doi.org/10.1515/ijeeps-2023-0020>.

[42] H. Maghfiroh, O. Wahyunggoro, A. I. Cahyadi, "Energy Management in Hybrid Electric and Hybrid Energy Storage System Vehicles: A Fuzzy Logic Controller Review". *IEEE Access*, 2024, vol. 12, pp. 56097-56109, <https://ieeexplore.ieee.org/abstract/document/10504274/>.

[43] A. I. Zermane and T. Bordjiba, "Optimizing energy management of hybrid battery-supercapacitor energy storage system by using PSO-based fractional order controller for photovoltaic off-grid installation". *Européen des Systèmes Automatisés*, 2024, Vol. 57, no. 2, pp. 465-475. <https://doi.org/10.18280/jesa.570216>.

[44] J. Zhang, B. Xiao, G. Niu, X. Xie, S. Wu, "Joint estimation of state-of-charge and state-of-power for hybrid supercapacitors using fractional-order adaptive unscented Kalman filter". *Energy*, 2024, vol. 294, p. 130942, <https://doi.org/10.1016/j.energy.2024.130942>.

- [45] M. Hilmi, V. Lystianingrum, M. F. Romlie, "Energy Management System Based on Finite State Machine for Battery-Supercapacitor Hybrid Energy Storage System on Standalone Photovoltaic". 4th International Conference in Power Engineering Applications (ICPEA), IEEE, 2024, pp. 91–96, <https://ieeexplore.ieee.org/abstract/document/10498346/>.
- [46] T. K. Roy, A. M. T. Oo, and S. K. Ghosh, "Designing a High-Order Sliding Mode Controller for Photovoltaic-and Battery Energy Storage System-Based DC Microgrids with ANN-MPPT". *Energies*, 2024, vol. 17, no. 2, p. 532, <https://doi.org/10.3390/en17020532>.
- [47] J. Rocabert, R. Capó-Misut, "Control of Energy Storage System Integrating Electrochemical Batteries and Supercapacitors for Grid-Connected Applications". *IEEE Transactions on Industry Applications*, 2018. 55(2): p. 1853-1862. doi: [10.1109/ECCE.2016.7854966](https://doi.org/10.1109/ECCE.2016.7854966)
- [48] V. jaarsveld, G. Rupert. "An active hybrid energy storage system utilizing a rule-based fuzzy logic control strategy" *World Electric Vehicle Journal*, 2020, vol. 11, no. 2, p. 34.
- [49] S. Augustine, M.K. Mishra and N. Lakshminarasamma, "A Unified Control Scheme for a standalone solar PV low voltage DC microgrid system with HESS". *IEEE Journal of Emerging and Selected Topics in Power Electronics*, 2020. 8(2): p. 1351-1360.
- [50] M. Khalid, "A Review of the Selected Applications of Battery-Supercapacitor Hybrid Energy Storage Systems for Microgrids". *Energies*, 2019. 12(23): p. 4559.
- [51] S. Xie Liu, L. Yang, "Analysis Modeling and Implementation of a Switching Bidirectional Buck-Boost Converter Based on Hybrid Electric Vehicle Energy Storage for the V2G System". *IEEE Access*, 2020. 8: p. 65868-65879.
- [52] B. Ravada, N. Tummuru. "Control of a stand-alone DC-Microgrid based on a supercapacitor battery PV". *IEEE Transactions on Energy Conversion*, 2020. 35(3): p. 1268-1277.
- [53] G. Husein, A. Tayeb. "Power management and control of a photovoltaic system with hybrid battery-supercapacitor energy storage based on heuristics methods". *Journal of Energy Storage*, 2021. 39: p. 102578.
- [54] Z. Abbasali, S. Masoud. "Design of a fractional order PID controller using the GBMO algorithm for load–frequency control with consideration of governor saturation". *ISA transactions*, 2022, vol. 64, p. 56-66.
- [55] C. Siyuan, Y. Qiufan. "A model predictive control method for hybrid energy storage systems". *CSEE Journal of Power and Energy Systems*, 2020, vol. 7, no. 2, p. 329-338.
- [56] P. Srinivas, M. Udaya, "A comparative analysis of PI and predictive control strategy for HESS-based bidirectional DC-DC converter for DC microgrid applications". In: *Next-Generation Smart Grids: Modeling, Control, and Optimization*. Singapore: Springer Nature Singapore, 2022. p. 181-220.
- [57] K. Akhil, MANTHATI, U. Bhasker. "Predictive power management scheme for the hybrid energy storage system in electric vehicles". *International Journal of Circuit Theory and Applications*, 2021, vol. 49, no. 11, p. 3864-3878.

- [58] S.Imran, H.FAROOQ. "An Artificial Neural Network-Based Approach for Real-Time Hybrid Wind–Solar Resource Assessment and Power Estimation". *Energies*, 2023, vol. 16, no 10, p. 4171
- [59] Z. Mohamed,A. GUESMI,. "Design and analysis of the sliding mode artificial neural network control strategy for the hybrid photovoltaic battery-supercapacitor system". *Energies*, 2022, vol. 15, no. 11, p. 4099.
- [60] N. Namala, K. NAIDU. "Energy management for PV-powered hybrid storage system in electric vehicles using artificial neural network and the Aquila Optimizer algorithm". *Energies*, 2022, vol. 15, no. 22, p. 8540.
- [61] K. Mohamed, Y.Zyodulla. "Enhancing Microgrid Performance through Integration of Hybrid Energy Storage System: ANFIS and GA approaches". *Int. J. Electr. Eng. and Sustain.*, 2023, p. 38-48.
- [62] F.Fareesa, S.REDDY. "A hybrid energy storage system using GA and PSO for islanded microgrid applications". *Energy Storage*, 2023, vol. 5, no 7, p. e460.
- [63] B.Badis, G., Hatem, D.Habiba, "Optimal sizing of a hybrid microgrid system using solar, wind, diesel, and battery energy storage to alleviate energy poverty in a rural area of Biskra," Algeria. *Journal of Energy Storage*, 2024, vol. 84, p. 110651
- [64] R Santosh S., Raghuwanshi . "Modeling and optimization of hybrid renewable energy with storage system using flamingo swarm intelligence algorithms ". *Energy Storage*, 2023, vol. 5, no. 7, p. e470.
- [65] M. Vijayan," Optimal PI-Controller-Based Hybrid Energy Storage System in DC Microgrid," *Sustainability*,2022, vol. 14, no. 22, p. 14666
- [66] A. Annamalaichamy, P. David, P. Balachandran, and I. Colak, "Performance evaluation of PI and FLC controller for shunt active power filters," *Electrical Engineering* ,2024,doi: <https://doi.org/10.1007/s00202-024-02546-x>
- [67] R. Arun, R.Muniraj, N.Karuppiah, B. Kumar, and K. Murugaperumal, "Automated approach to design predictive PI control scheme for gain margin specification," *International Journal of Systems Assurance Engineering and Management*,2024, vol. 15, no. 6, pp. 2230–2237
- [68] L. He, H. Jing, Y. Zhang, P. Li, and Z. Gu, "Review of thermal management system for battery electric vehicle," *Journal of Energy Storage*, vol. 59, p. 106443, Mar. 2023, doi: <https://doi.org/10.1016/j.est.2022.106443>.
- [69] H. Yuan et al., "Battery electric vehicle charging in China: Energy demand and emissions trends in the 2020s," *Applied energy*, vol. 365, pp. 123153–123153, Jul. 2024, doi: <https://doi.org/10.1016/j.apenergy.2024.123153>.
- [70] M. Adaikkappan and N. Sathiyamoorthy, "Modeling, state of charge estimation, and charging of lithium-ion battery in electric vehicle: A review," *International Journal of Energy Research*, Oct. 2021, doi: <https://doi.org/10.1002/er.7339>.

- [71] G. Zhou, Z. Zhu, and S. Luo, "Location optimization of electric vehicle charging stations: Based on cost model and genetic algorithm," *Energy*, vol. 247, p. 123437, May 2022, doi: <https://doi.org/10.1016/j.energy.2022.123437>.
- [72] I. Gunawan, A. Redi, A. Santosa, M. F. N. Maghfiroh, A. H. Pandyaswargo, and A. C. Kurniawan, "Determinants of Customer Intentions to Use Electric Vehicle in Indonesia: An Integrated Model Analysis," *Sustainability*, vol. 14, no. 4, p. 1972, Feb. 2022, doi: <https://doi.org/10.3390/su14041972>.
- [73] E. Hadian, H. Akbari, M. Farzinfar, and S. Saeed, "Optimal Allocation of Electric Vehicle Charging Stations With Adopted Smart Charging/Discharging Schedule," *IEEE Access*, vol. 8, pp. 196908–196919, 2020, doi: <https://doi.org/10.1109/access.2020.3033662>.
- [74] A. Danese, B. N. Torsæter, A. Sumper, and M. Garau, "Planning of High-Power Charging Stations for Electric Vehicles: A Review," *Applied Sciences*, vol. 12, no. 7, p. 3214, Jan. 2022, doi: <https://doi.org/10.3390/app12073214>.
- [75] T. L. sime, P. Aluvada, S. Habtamu, and Z. Tolosa, "Modeling of Genetic Algorithm Tuned Adaptive Fuzzy Fractional Order PID Speed Control of PMSM for Electric Vehicle," Apr. 2024, doi: <https://doi.org/10.21203/rs.3.rs-4234710/v1>.
- [76] F. Zaghrat, "A comparison study using backstepping and PI controllers for Electric Vehicle," *PRZEGLĄD ELEKTROTECHNICZNY*, vol. 1, no. 3, pp. 214–217, Mar. 2024, doi: <https://doi.org/10.15199/48.2024.03.37>.
- [77] A. Chantoufi et al., "Direct Torque Control-Based Backstepping Speed Controller of Doubly Fed Induction Motors in Electric Vehicles; Experimental Validation," *IEEE Access*, pp. 1–1, Jan. 2024, doi: <https://doi.org/10.1109/access.2024.3462821>.
- [78] K. Cherif, Abdelaziz Sahbani, and K. B. Saad, "Performance Evaluation of PI and Sliding Mode Control for PMSM in Applications for Electric Vehicles," *Engineering Technology & Applied Science Research*, vol. 14, no. 4, pp. 15464–15470, Aug. 2024, doi: <https://doi.org/10.48084/etasr.7172>.
- [79] M. Subbarao, K. Dasari, S. S. Duvvuri, K. R. K. V. Prasad, B. K. Narendra, and V. B. Murali Krishna, "Design, control and performance comparison of PI and ANFIS controllers for BLDC motor driven electric vehicles," *Measurement: Sensors*, vol. 31, p. 101001, Feb. 2024, doi: <https://doi.org/10.1016/j.measen.2023.101001>.
- [80] Y. Zuo, S. Zhu, Y. Cui, C. Liu, and X. Lin, "Adaptive PI Controller for Speed Control of Electric Drives Based on Model Reference Adaptive Identification," *Electronics*, vol. 13, no. 6, p. 1067, Jan. 2024, doi: <https://doi.org/10.3390/electronics13061067>.
- [81] B. Oleiwi and M. J. Mohamed, "Optimal design of linear and nonlinear PID controllers for speed control of an electric vehicle," *Journal of Intelligent Systems*, vol. 33, no. 1, Jan. 2024, doi: <https://doi.org/10.1515/jisys-2024-0028>.
- [82] D. Mishra, Manoj Kumar Maharana, M. K. Kar, A. Nayak, and M. Cherukuri, "Modified Differential Evolution Algorithm for Governing Virtual Inertia of an Isolated Microgrid Integrating

Electric Vehicles,” *International Transactions on Electrical Energy Systems*, vol. 2023, pp. 1–14, Sep. 2023, doi: <https://doi.org/10.1155/2023/8950650>.

[83] T. K. Roy and A. M. T. Oo, “Virtual inertia and damping-based cascaded control approach for enhancing load frequency control in low-inertia multi-area power systems,” *The Journal of Engineering*, vol. 2025, no. 1, Jan. 2025, doi: <https://doi.org/10.1049/tje2.70054>

[84] S. C. de Lima, A. S. Rodrigues, V. A. N. Magalhães, and I. Â. P. Lopes, “challenges of the deployment of electric cars in BRAZIL,” *Journal of Engineering Research*, vol. 2, no. 17, pp. 2–21, Aug. 2022, doi: <https://doi.org/10.22533/at.ed.3172172202085>.

[85] N. Burton, “History of Electric and Hybrid Vehicles,” *Engineering & Technology Reference*, Jan. 2015, doi: <https://doi.org/10.1049/etr.2014.0040>.

[86] M. Guarnieri, “Looking back to electric cars,” 2012 Third IEEE history of electro-technology conference (HISTELCON), Sep. 2012, doi: <https://doi.org/10.1109/histelcon.2012.6487583>.

[87] M. Henderson, “Developments in lead-acid batteries,” *Electronics and Power*, vol. 23, no. 6, p. 491, 1977, doi: <https://doi.org/10.1049/ep.1977.0260>.

[88] G. Ren, J. Wang, C. Chen, and H. Wang, “A variable-voltage ultra-capacitor/battery hybrid power source for extended range electric vehicle,” *Energy*, vol. 231, p. 120837, Sep. 2021, doi: <https://doi.org/10.1016/j.energy.2021.120837>.

[89] A. O. Kiyaklı and H. Solmaz, “Modeling of an Electric Vehicle with MATLAB/Simulink,” *International Journal of Automotive Science And Technology*, pp. 9–15, Jan. 2019, doi: <https://doi.org/10.30939/ijastech.475477>.

[90] J. Styczyński, “A brief history of CAR-T cells: from laboratory to the bedside,” *Acta Haematologica Polonica*, vol. 51, no. 1, pp. 2–5, Mar. 2020, doi: <https://doi.org/10.2478/ahp-2020-0002>.

[91] N. Patel, A. K. Bhoi, S. Padmanaban, and J. B. Holm-Nielsen, Eds., *Electric Vehicles*. Singapore: Springer Singapore, 2021. doi: <https://doi.org/10.1007/978-981-15-9251-5>.

[92] A. Upadhyay et al., “Electric Vehicles over Contemporary Combustion Engines,” *IOP Conference Series: Earth and Environmental Science*, vol. 635, p. 012004, Jan. 2021, doi: <https://doi.org/10.1088/1755-1315/635/1/012004>.

[93] P. K. Joseph, E. Devaraj, and A. Gopal, “Overview of wireless charging and vehicle-to-grid integration of electric vehicles using renewable energy for sustainable transportation,” *IET Power Electronics*, vol. 12, no. 4, pp. 627–638, Apr. 2019, doi: <https://doi.org/10.1049/iet-pel.2018.5127>.

[94] A. Burkert, “Electric Motor in Pole Position,” *MTZ worldwide*, vol. 80, no. 9, pp. 6–7, Aug. 2019, doi: <https://doi.org/10.1007/s38313-019-0073-5>.

[95] Q. Skrabec, “The green vision of Henry Ford and George Washington Carver: two collaborators in the cause of clean industry,” *Choice Reviews Online*, vol. 51, no. 02, pp. 51-085551-0855, Sep. 2013, doi: <https://doi.org/10.5860/choice.51-0855>.

[96] C. C. Chan and K. T. Chau, “Modern Electric Vehicle Technology,” Oxford University Press eBooks, Oct. 2001, doi: <https://doi.org/10.1093/oso/9780198504160.001.0001>.

- [97] D. W. Kurtz, T. W. Price, and J. A. Bryant, "Performance Testing and System Evaluation of the DOE ETV-1 Electric Vehicle," SAE Technical Paper Series, Feb. 1981, doi: <https://doi.org/10.4271/810418>.
- [98] P. Banerjee et al., "Advancement in Electrolytes for Rechargeable Batteries," pp. 87–98, Apr. 2020, doi: <https://doi.org/10.1002/9781119714774.ch5>.
- [99] F. Dulcich, F. Porta, M. Ubogui, and G. Baruj, "The transition to electric mobility: opportunities for the automotive value chain in Argentina," *International Journal of Automotive Technology and Management*, vol. 22, no. 3, p. 374, 2022, doi: <https://doi.org/10.1504/ijatm.2022.124829>.
- [100] G. Rizzoni, D. Cooke, and G. Pastor, "The fastest electric vehicles on earth: A history of electric land speed racing and of the Venturi Buckeye Bullet program," *Proceedings*, pp. 1129–1130, Jan. 2015, doi: https://doi.org/10.1007/978-3-658-08844-6_77.
- [101] A. N. Duhon, K. S. Sevel, S. A. Tarnowsky, and P. J. Savagian, "Chevrolet Volt Electric Utilization," *SAE International Journal of Alternative Powertrains*, vol. 4, no. 2, pp. 269–276, Apr. 2015, doi: <https://doi.org/10.4271/2015-01-1164>.
- [102] A. Zentani, A. Almaktoof, and M. T. Kahn, "A Comprehensive Review of Developments in Electric Vehicles Fast Charging Technology," *Applied Sciences*, vol. 14, no. 11, p. 4728, Jan. 2024, doi: <https://doi.org/10.3390/app14114728>.
- [103] D. Chunhu Li, J. Felix, "Integrated Extended Kalman Filter and Deep Learning Platform for Electric Vehicle Battery Health Prediction," *Applied Sciences*, vol. 14, no. 11, pp. 4354–4354, May 2024, doi: <https://doi.org/10.3390/app14114354>.
- [104] W. Lewicki, M. Niekurzak, and E. Sendek-Matysiak, "Electromobility Stage in the Energy Transition Policy—Economic Dimension Analysis of Charging Costs of Electric Vehicles," *Energies*, vol. 17, no. 8, p. 1934, Jan. 2024, doi: <https://doi.org/10.3390/en17081934>.
- [105] J. M. Desantes, S. Molina, R. Novella, and M. Lopez-Juarez, "Comparative global warming impact and NOX emissions of conventional and hydrogen automotive propulsion systems," *Energy Conversion and Management*, vol. 221, p. 113137, Oct. 2020, doi: <https://doi.org/10.1016/j.enconman.2020.113137>.
- [106] D. Savio Abraham et al., "Electric Vehicles Charging Stations' Architectures, Criteria, Power Converters, and Control Strategies in Microgrids," *Electronics*, vol. 10, no. 16, p. 1895, Aug. 2021, doi: <https://doi.org/10.3390/electronics10161895>.
- [107] F. Un-Noor, S. Padmanaban, L. Mihet-Popa, M. Mollah, and E. Hossain, "A Comprehensive Study of Key Electric Vehicle (EV) Components, Technologies, Challenges, Impacts, and Future Direction of Development," *Energies*, vol. 10, no. 8, p. 1217, Aug. 2017, doi: <https://doi.org/10.3390/en10081217>.
- [108] R. Xiong, J. Cao, Q. Yu, H. He, and F. Sun, "Critical Review on the Battery State of Charge Estimation Methods for Electric Vehicles," *IEEE Access*, vol. 6, pp. 1832–1843, 2018, doi: <https://doi.org/10.1109/ACCESS.2017.2780258>.

- [109] B. Belabbas, “Gestion des Flux Energétiques d’un Système de Production d’Energie de Sources Renouvelables avec Stockage en Vue de la Conception des Réseaux Electriques Intelligents “Smart GRID”,” Ph.D. dissertation, Université de Tiaret, 2018.
- [110] R. R. Kumar and K. Alok, “Adoption of electric vehicle: A literature review and prospects for sustainability,” *Journal of Cleaner Production*, vol. 253, no. 1, p. 119911, Apr. 2020, doi: <https://doi.org/10.1016/j.jclepro.2019.119911>.
- [111] A. König, L. Nicoletti, D. Schröder, S. Wolff, A. Waclaw, and M. Lienkamp, “An Overview of Parameter and Cost for Battery Electric Vehicles,” *World Electric Vehicle Journal*, vol. 12, no. 1, p. 21, Mar. 2021, doi: <https://doi.org/10.3390/wevj12010021>.
- [112] C. Liu, K. T. Chau, C. H. T. Lee, and Z. Song, “A Critical Review of Advanced Electric Machines and Control Strategies for Electric Vehicles,” *Proceedings of the IEEE*, vol. 109, no. 6, pp. 1–25, 2020, doi: <https://doi.org/10.1109/jproc.2020.3041417>.
- [113] T. R. Hawkins, O. M. Gausen, and A. H. Strømman, “Environmental Impacts of Hybrid and Electric Vehicles—a Review,” *The International Journal of Life Cycle Assessment*, vol. 17, no. 8, pp. 997–1014, May 2012, doi: <https://doi.org/10.1007/s11367-012-0440-9>.
- [114] A. Daanoune, “Contribution à l’étude et à l’optimisation d’une machine synchrone à double excitation pour véhicules hybrides,” Ph.D. dissertation, Université de Grenoble, 2012.
- [115] M. Kremer. Electromagnetic Design of a Disc Rotor Electric Machine as Integrated Motor-Generator for Hybrid Vehicles. Ph.D. Thesis, Université de Haute Alsace-Mulhouse, France, 2016.
- [116] K. Okba, “Control and energy management of an electrical vehicle,” Ph.D. dissertation, 2015.
- [117] S. Akhegaonkar, “Development of a safe and efficient driving assistance system for electric vehicles,” Ph.D. dissertation, Université Paris-Saclay (ComUE), 2015.
- [118] W. Zong, C. Zhang, Z. Wang, J. Zhu, and Q. Chen, “Architecture Design and Implementation of an Autonomous Vehicle,” *IEEE Access*, vol. 6, pp. 21956–21970, 2018, doi: <https://doi.org/10.1109/access.2018.2828260>.
- [119] J. Y. Yong, V. K. Ramachandaramurthy, K. M. Tan, and N. Mithulananthan, “A review on the state-of-the-art technologies of electric vehicle, its impacts and prospects,” *Renewable and Sustainable Energy Reviews*, vol. 49, pp. 365–385, Sep. 2015, doi: <https://doi.org/10.1016/j.rser.2015.04.130>.
- [120] J. Du and M. Ouyang, “Review of Electric Vehicle Technologies Progress and Development Prospect in China,” *World Electric Vehicle Journal*, vol. 6, no. 4, pp. 1086–1093, Dec. 2013, doi: <https://doi.org/10.3390/wevj6041086>.
- [121] J. A. P. Lopes, F. J. Soares, and P. M. R. Almeida, “Integration of Electric Vehicles in the Electric Power System,” *Proceedings of the IEEE*, vol. 99, no. 1, pp. 168–183, Jan. 2011, doi: <https://doi.org/10.1109/jproc.2010.2066250>.
- [122] V. Monteiro, J. Afonso, J. Ferreira, and J. Afonso, “Vehicle Electrification: New Challenges and Opportunities for Smart Grids,” *Energies*, vol. 12, no. 1, p. 118, Dec. 2018, doi: <https://doi.org/10.3390/en12010118>.

- [123] K.-T. Chau, C. Jiang, W. Han, and C. H. T. Lee, "STATE-OF-THE-ART ELECTROMAGNETICS RESEARCH IN ELECTRIC AND HYBRID VEHICLES (INVITED PAPER)," *Progress In Electromagnetics Research*, vol. 159, pp. 139–157, 2017, doi: <https://doi.org/10.2528/pier17090407>.
- [124] K. V. Singh, H. O. Bansal, and D. Singh, "A Comprehensive Review on Hybrid Electric vehicles: Architectures and Components," *Journal of Modern Transportation*, vol. 27, no. 2, pp. 77–107, Mar. 2019, doi: <https://doi.org/10.1007/s40534-019-0184-3>.
- [125] S. Jamshed Rind, Y. Ren, "Configurations and control of traction motors for electric vehicles: A review," *Chinese Journal of Electrical Engineering*, vol. 3, no. 3, pp. 1–17, Dec. 2017, doi: <https://doi.org/10.23919/cjee.2017.8250419>.
- [126] F. Arena and G. Pau, "An Overview of Vehicular Communications," *Future Internet*, vol. 11, no. 2, p. 27, Jan. 2019, doi: <https://doi.org/10.3390/fi11020027>.
- [127] I. W. Damaj, D. K. Serhal, L. A. Hamandi, R. N. Zantout, and H. T. Mouftah, "Connected and Autonomous Electric Vehicles: Quality of Experience survey and taxonomy," *Vehicular Communications*, vol. 28, p. 100312, Apr. 2021, doi: <https://doi.org/10.1016/j.vehcom.2020.100312>.
- [128] I.-S. Sorlei *et al.*, "Fuel Cell Electric Vehicles—A Brief Review of Current Topologies and Energy Management Strategies," *Energies*, vol. 14, no. 1, p. 252, Jan. 2021, doi: <https://doi.org/10.3390/en14010252>.
- [130] H. Tu, H. Feng, S. Srdic, and S. Lukic, "Extreme Fast Charging of Electric Vehicles: A Technology Overview," *IEEE Transactions on Transportation Electrification*, vol. 5, no. 4, pp. 861–878, Dec. 2019, doi: <https://doi.org/10.1109/tte.2019.2958709>.
- [131] Y. Tahir *et al.*, "A state-of-the-art review on topologies and control techniques of solid-state transformers for electric vehicle extreme fast charging," *IET Power Electronics*, May 2021, doi: <https://doi.org/10.1049/pel2.12141>.
- [132] M. Khalid, F. Ahmad, B. K. Panigrahi, and L. Al-Fagih, "A comprehensive review on advanced charging topologies and methodologies for electric vehicle battery," *Journal of Energy Storage*, vol. 53, p. 105084, Sep. 2022, doi: <https://doi.org/10.1016/j.est.2022.105084>.
- [133] M. İnci, M. Büyük, M. H. Demir, and G. İlbey, "A review and research on fuel cell electric vehicles: Topologies, power electronic converters, energy management methods, technical challenges, marketing and future aspects," *Renewable and Sustainable Energy Reviews*, vol. 137, no. 1, p. 110648, Mar. 2021, doi: <https://doi.org/10.1016/j.rser.2020.110648>.
- [134] T. Hofman, S. Ebbesen, and L. Guzzella, "Topology Optimization for Hybrid Electric Vehicles With Automated Transmissions," *IEEE Transactions on Vehicular Technology*, vol. 61, no. 6, pp. 2442–2451, Jul. 2012, doi: <https://doi.org/10.1109/tvt.2012.2196299>.
- [135] H. Gong, Y. Zou, Q. Yang, J. Fan, F. Sun, and D. Goehlich, "Generation of a driving cycle for battery electric vehicles : A case study of Beijing," *Energy*, vol. 150, pp. 901–912, May 2018, doi: <https://doi.org/10.1016/j.energy.2018.02.092>.

- [136] N. Ding, K. Prasad, and T. T. Lie, “The electric vehicle: a review,” *International Journal of Electric and Hybrid Vehicles*, vol. 9, no. 1, p. 49, 2017, doi: <https://doi.org/10.1504/ijehv.2017.082816>.
- [137] R. Basso, B. Kulcsár, and I. Sanchez-Diaz, “Electric vehicle routing problem with machine learning for energy prediction,” *Transportation Research Part B: Methodological*, vol. 145, pp. 24–55, Mar. 2021, doi: <https://doi.org/10.1016/j.trb.2020.12.007>.
- [138] K. Senda, M. Uesaka, S. Yoshizaki, and Y. Oda, “Electrical Steels and Their Evaluation for Automobile Motors,” *World Electric Vehicle Journal*, vol. 10, no. 2, p. 31, May 2019, doi: <https://doi.org/10.3390/wevj10020031>.
- [139] A. Di Gioia et al., “Design and Demonstration of a Wound Field Synchronous Machine for Electric Vehicle Traction With Brushless Capacitive Field Excitation,” *IEEE Transactions on Industry Applications*, vol. 54, no. 2, pp. 1390–1403, Mar. 2018, doi: <https://doi.org/10.1109/tia.2017.2784799>.
- [140] M. S. Kumar and S. T. Revankar, “Development scheme and key technology of an electric vehicle: An overview,” *Renewable and Sustainable Energy Reviews*, vol. 70, pp. 1266–1285, Apr. 2017, doi: <https://doi.org/10.1016/j.rser.2016.12.027>.
- [141] C. Liu, K. T. Chau, C. H. T. Lee, and Z. Song, “A Critical Review of Advanced Electric Machines and Control Strategies for Electric Vehicles,” *Proceedings of the IEEE*, vol. 109, no. 6, pp. 1–25, 2020, doi: <https://doi.org/10.1109/jproc.2020.3041417>.
- [142] A. Colmenar-Santos, A.-M. Muñoz-Gómez, E. Rosales-Asensio, and Á. López-Rey, “Electric vehicle charging strategy to support renewable energy sources in Europe 2050 low-carbon scenario,” *Energy*, vol. 183, pp. 61–74, Sep. 2019, doi: <https://doi.org/10.1016/j.energy.2019.06.118>.
- [143] M. A. Hannan, M. M. Hoque, A. Mohamed, and A. Ayob, “Review of energy storage systems for electric vehicle applications: Issues and challenges,” *Renewable and Sustainable Energy Reviews*, vol. 69, pp. 771–789, Mar. 2017, doi: <https://doi.org/10.1016/j.rser.2016.11.171>.
- [144] R. Islam, S. M. S. H. Rafin, and O. A. Mohammed, “Comprehensive Review of Power Electronic Converters in Electric Vehicle Applications,” *Forecasting*, vol. 5, no. 1, pp. 22–80, Dec. 2022, doi: <https://doi.org/10.3390/forecast5010002>
- [145] A. Ali, H. Mousa, M. F. Shaaban, M. A. Azzouz, and Ahmed, “A Comprehensive Review on Charging Topologies and Power Electronic Converter Solutions for Electric Vehicles,” *Journal of Modern Power Systems and Clean Energy*, vol. 12, no. 3, pp. 675–694, Jan. 2024, doi: <https://doi.org/10.35833/mpce.2023.000107>.
- [146] F. Blaabjerg, H. Wang, I. Vernica, B. Liu, and P. Davari, “Reliability of Power Electronic Systems for EV/HEV Applications,” *Proceedings of the IEEE*, vol. 109, pp. 1–17, 2020, doi: <https://doi.org/10.1109/jproc.2020.3031041>.
- [147] M. S. Hossain Lipu et al., “Power Electronics Converter Technology Integrated Energy Storage Management in Electric Vehicles: Emerging Trends, Analytical Assessment and Future Research Opportunities,” *Electronics*, vol. 11, no. 4, p. 562, Feb. 2022, doi: <https://doi.org/10.3390/electronics11040562>.

- [148] A. Sharma and S. Sharma, "Review of power electronics in vehicle-to-grid systems," *Journal of Energy Storage*, vol. 21, pp. 337–361, Feb. 2019, doi: <https://doi.org/10.1016/j.est.2018.11.022>.
- [149] R. Kotb, S. Chakraborty, D.-D. Tran, E. Abramushkina, M. El Baghdadi, and O. Hegazy, "Power Electronics Converters for Electric Vehicle Auxiliaries: State of the Art and Future Trends," *Energies*, vol. 16, no. 4, p. 1753, Feb. 2023, doi: <https://doi.org/10.3390/en16041753>.
- [150] Ibrahim Sengor, Hasan Can Kiliçkiran, Hüseyin Akdemir, Bedri Kekezoğlu, Ozan Erdinc, and Joao, "Energy Management of a Smart Railway Station Considering Regenerative Braking and Stochastic Behaviour of ESS and PV Generation," *IEEE Transactions on Sustainable Energy*, vol. 9, no. 3, pp. 1041–1050, Jul. 2018, doi: <https://doi.org/10.1109/tste.2017.2759105>.
- [151] V. Vodovozov, Z. Raud, and E. Petlenkov, "Review on Braking Energy Management in Electric Vehicles," *Energies*, vol. 14, no. 15, p. 4477, Jul. 2021, doi: <https://doi.org/10.3390/en14154477>.
- [152] S. Hemavathi and A. Shinisha, "A study on trends and developments in electric vehicle charging technologies," *Journal of Energy Storage*, vol. 52, p. 105013, Aug. 2022, doi: <https://doi.org/10.1016/j.est.2022.105013>.
- [153] R. P. Narasipuram and S. Mopidevi, "A technological overview & design considerations for developing electric vehicle charging stations," *Journal of Energy Storage*, vol. 43, p. 103225, Nov. 2021, doi: <https://doi.org/10.1016/j.est.2021.103225>.
- [154] B. Al-Hanahi, I. Ahmad, D. Habibi, and M. A. S. Masoum, "Charging Infrastructure for Commercial Electric Vehicles: Challenges and Future Works," *IEEE Access*, vol. 9, pp. 121476–121492, 2021, doi: <https://doi.org/10.1109/access.2021.3108817>.
- [155] M. S. Mastoi *et al.*, "A study of charging-dispatch strategies and vehicle-to-grid technologies for electric vehicles in distribution networks," *Energy Reports*, vol. 9, pp. 1777–1806, Dec. 2023, doi: <https://doi.org/10.1016/j.egy.2022.12.139>.
- [156] M. Featherman, S. (Jasper) Jia, C. B. Califf, and N. Hajli, "The impact of new technologies on consumers beliefs: Reducing the perceived risks of electric vehicle adoption," *Technological Forecasting and Social Change*, vol. 169, p. 120847, Aug. 2021, doi: <https://doi.org/10.1016/j.techfore.2021.120847>.
- [157] A. Poullikkas, "Sustainable options for electric vehicle technologies," *Renewable and Sustainable Energy Reviews*, vol. 41, pp. 1277–1287, Jan. 2015, doi: <https://doi.org/10.1016/j.rser.2014.09.016>.
- [158] C.Hung Tran. "Améliorations d'une chaîne de conversion de l'énergie solaire en électricité autonome en vue d'application dans les pays en voie de développement," PhD dissertation. Université de Reims Champagne-Ardenne, 2019
- [159] S.Heroual, B.Belabbas,T.Allaoui "Pi Controller Based On Photovoltaic System With Hybrid Battery –Supercapacitor Energy Storage" 4th international black sear modern scientific reaserch congres , rize,-6 june, 2023 .
- [160] S. Koohi-Fayegh, M.A. Rosen. "A review of energy storage types, applications and recent

developments", *Journal of Energy Storage*, vol. 27, pp. 101047, 2020.

[161] L.Abdelouadoud. Contribution au Développement de Techniques de Recherche de la Topologie Optimale d'un Générateur Photovoltaïque. PhD dissertation. University of Biskra, 2022.

[162] S.Heroual, B.Belabbas , T.Allaoui , M.Meraouah, H.Chibani , and A.Slimani , "Application of MPPT Algorithm Based on Lyapunov Stability for Photovoltaic Systems". *Algerian Journal of Renewable Energy and Sustainable Development*, vol 6 pp 02, 15 Dec 2024.

[163] I. E. Atawi, A. Abuelrub, A. Q. Al-Shetwi, and O. H. Albalawi, "Design of a wind-PV system integrated with a hybrid energy storage system considering economic and reliability assessment," *Journal of Energy Storage*, vol. 81, pp. 110405–110405, Mar. 2024, doi: <https://doi.org/10.1016/j.est.2023.110405>.

[164] S. Heroual, B.Belabbas,T.Allaoui , "Management of Hybrid Pv/Battery System Under Variable Load Conditions",Bilsel International World Science And Research Congress ,24-25 June, 2023,Istanbul.

[165] K .Kaced,"Étude des techniques MPPT pour systèmes photovoltaïques dans des conditions partiellement ombragées" ,Ph.D. thesis. École Nationale Polytechnique ENP,2018.

[166] W. Qiu et al., "Modeling, testing, and mitigation of electromagnetic pulse on PV systems," *Solar Energy*, vol. 264, pp. 112010–112010, Nov. 2023, doi:<https://doi.org/10.1016/j.solener.2023.112010>.

[167] S.Heroual ,B.Belabbas ,Y.Diab , A.Ma'arif , M.Metwally Mahmoud, T. Allaoui, and N. Benabdalla, "Enhancement of Transient Stability and Power Quality in Grid-Connected PV Systems Using SMES," *International Journal of Robotics and Control Systems*,2025, Vol. 5, No. 2, 2025, pp. 990-1005 doi: <http://dx.doi.org/10.31763/ijrcs.v5i2.1760>

[168] R. T. Moyo, P. Y. Tabakov, and S. Moyo, "Design and Modeling of the ANFIS-Based MPPT Controller for a Solar Photovoltaic System," *Journal of Solar Energy Engineering*, vol. 143, no. 4, Nov. 2020, doi: <https://doi.org/10.1115/1.4048882>.

[169] D. Khodair et al., "Modeling and Simulation of Modified MPPT Techniques under Varying Operating Climatic Conditions," *Energies*, vol. 16, no. 1, p. 549, Jan. 2023, doi: <https://doi.org/10.3390/en16010549>.

[170] A. N. Abdalla et al., "Integration of energy storage system and renewable energy sources based on artificial intelligence: An overview," *Journal of Energy Storage*, vol. 40, p. 102811, Aug. 2021, doi: <https://doi.org/10.1016/j.est.2021.102811>.

[171] S.Heroual,B.Belabbas and Y.Diab , "Optimizing Power Flow in Photovoltaic-Hybrid Energy Storage Systems: A PSO and DPSO Approach for PI Controller Tuning." *International Transactions on Electrical Energy Systems*, vol. 2025, no. 1, Jan. 2025, <https://doi.org/10.1155/etep/9958218>

[172] S. Choudhury, "Review of energy storage system technologies integration to microgrid: Types, control strategies, issues, and prospects," *Journal of Energy Storage*, vol. 48, p. 103966, Apr. 2022, doi: <https://doi.org/10.1016/j.est.2022.103966>.

[173] W. Wang, B. Yuan, Q. Sun, and R. Wennersten, "Application of energy storage in integrated

energy systems — A solution to fluctuation and uncertainty of renewable energy,” *Journal of Energy Storage*, vol. 52, p. 104812, Aug. 2022, doi: <https://doi.org/10.1016/j.est.2022.104812>.

[174] S.Nyamathulla, C. Dhanamjayulu, “A review of battery energy storage systems and advanced battery management system for different applications: Challenges and recommendations,” *Journal of Energy Storage*, vol. 86, pp. 111179–111179, May 2024, doi: <https://doi.org/10.1016/j.est.2024.111179>.

[175] G. Sadeghi, “Energy storage on demand: Thermal energy storage development, materials, design, and integration challenges,” *Energy Storage Materials*, vol. 46, pp. 192–222, Apr. 2022, doi: <https://doi.org/10.1016/j.ensm.2022.01.017>.

[176] G. K. Joshi, B. Rongali, and M. Biswal, “A Review on Mechanical Energy Storage Technology,” *IEEE Xplore*, Jul. 01, 2022. <https://ieeexplore.ieee.org/abstract/document/9862382/>.

[177] M.Kanwal Khan, M. Raza, M. Shahbaz, U. Farooq, and Muhammad Usman Akram, “Recent advancement in energy storage technologies and their applications,” *Journal of energy storage*, vol. 92, pp. 112112–112112, Jul. 2024, doi: <https://doi.org/10.1016/j.est.2024.112112>.

[178] A. Rahman, J. Kim, and S. Hossain, “Recent advances of energy storage technologies for grid: A comprehensive review,” *Energy Storage*, vol. 108, Jan. 2022, doi: <https://doi.org/10.1002/est2.322>.

[179] B. Deng et al., “Design high-performance biomass-derived renewable carbon material for electric energy storage system,” *Journal of Cleaner Production*, vol. 309, p. 127391, Aug. 2021, doi: <https://doi.org/10.1016/j.jclepro.2021.127391>.

[180] V. Vahidinasab and M. Habibi, “Electric energy storage systems integration in energy markets and balancing services,” *Energy Storage in Energy Markets*, vol. 9, pp. 287–316, 2021, doi: <https://doi.org/10.1016/b978-0-12-820095-7.00019-4>.

[181] R. Sharma et al., “Progress and challenges in electrochemical energy storage devices: Fabrication, electrode material, and economic aspects,” *Chemical Engineering Journal*, vol. 468, pp. 143706–143706, Jul. 2023, doi: <https://doi.org/10.1016/j.cej.2023.143706>.

[182] O. Gerard, A. Numan, S. Krishnan, M. Khalid, R. Subramaniam, and R. Kasi, “A review on the recent advances in binder-free electrodes for electrochemical energy storage application,” *Journal of Energy Storage*, vol. 50, p. 104283, Jun. 2022, doi: <https://doi.org/10.1016/j.est.2022.104283>.

[183] F. Naseri, C. Barbu, and T. Sarikurt, “Optimal sizing of hybrid high-energy/high-power battery energy storage systems to improve battery cycle life and charging power in electric vehicle applications,” *Journal of Energy Storage*, vol. 55, p. 105768, Nov. 2022, doi: <https://doi.org/10.1016/j.est.2022.105768>.

[184] A. A. Kebede et al., “Techno-economic analysis of lithium-ion and lead-acid batteries in stationary energy storage application,” *Journal of Energy Storage*, vol. 40, p. 102748, Aug. 2021, doi: <https://doi.org/10.1016/j.est.2021.102748>.

[185] R. Yudhistira, D. Khatiwada, and F. Sanchez, “A comparative life cycle assessment of lithium-ion and lead-acid batteries for grid energy storage,” *Journal of Cleaner Production*, vol. 358, p. 131999,

Apr. 2022, doi: <https://doi.org/10.1016/j.jclepro.2022.131999>.

[186] N. E. Galushkin, N. N. Yazvinskaya, and D. N. Galushkin, “Nickel-cadmium batteries with pocket electrodes as hydrogen energy storage units of high-capacity,” *Journal of Energy Storage*, vol. 39, p. 102597, Jul. 2021, doi: <https://doi.org/10.1016/j.est.2021.102597>.

[187] M. N. Razali, M. S. Mahmud, S. S. Mohd Tarmizi, and M. K. N. Mohd Zuhan, “Synergistic Effect of Electrolyte and Electrode in Nickel Cadmium Aging Battery Performances,” *Springer Proceedings in Materials*, vol. 104, pp. 339–349, 2024, doi: https://doi.org/10.1007/978-981-99-9848-7_31.

[188] X. Yi, C. Kirk, and N. Robertson, “Nickel hydroxide-based energy storage devices: nickel-metal hydride batteries vs. nickel hydroxide hybrid supercapacitors,” *Carbon Neutrality*, vol. 3, no. 1, Dec. 2024, doi: <https://doi.org/10.1007/s43979-024-00114-7>.

[189] Z. Huang et al., “High-Energy Room-Temperature Sodium–Sulfur and Sodium–Selenium Batteries for Sustainable Energy Storage,” *Electrochemical energy reviews*, vol. 6, no. 1, Jun. 2023, doi: <https://doi.org/10.1007/s41918-023-00182-w>.

[190] G. Kear, A. A. Shah, and F. C. Walsh, “Development of the all-vanadium redox flow battery for energy storage: a review of technological, financial and policy aspects,” *International Journal of Energy Research*, vol. 36, no. 11, pp. 1105–1120, May 2011, doi: <https://doi.org/10.1002/er.1863>.

[191] A. G. Olabi, Q. Abbas, A. Al Makky, and M. A. Abdelkareem, “Supercapacitors as next generation energy storage devices: Properties and applications,” *Energy*, vol. 248, p. 123617, Jun. 2022, doi: <https://doi.org/10.1016/j.energy.2022.123617>.

[192] J. Jaguemont, “Gestion thermique d’un pack de batteries lithium-ion en conditions hivernales incluant le vieillissement. Phd thesis Trois-Rivières, Université du Québec à Trois-Rivières, 194 p.,” 2015.

[193] T. Mesbahi, “Influence des stratégies de gestion d’une source hybride de véhicule électrique sur son dimensionnement et sa durée de vie par intégration d’un modèle multi physique,” Phd thesis 2016.

[194] B. Hredzak, V. G. Agelidis, and G. D. Demetriades, “A Low Complexity Control System for a Hybrid DC Power Source Based on Ultracapacitor–Lead–Acid Battery Configuration,” *IEEE Trans. Power Electron.*, vol. 29, no. 6, pp. 2882–2891, Jun. 2014.

[195] R. Carter, A. Cruden, and P. J. Hall, “Optimizing for Efficiency or Battery Life in a Battery/Supercapacitor Electric Vehicle,” *IEEE Trans. Veh. Technol.*, vol. 61, no. 4, pp. 1526–1533, May 2012

[196] M. E. Choi, S. W. Kim, and S. W. Seo, “Energy Management Optimization in a Battery/Supercapacitor Hybrid Energy Storage System,” *IEEE Trans. Smart Grid*, vol. 3, no. 1, pp. 463–472, Mar. 2012

[197] R. S. Sankarkumar and R. Natarajan, “Energy management techniques and topologies suitable for hybrid energy storage system powered electric vehicles: An overview,” *International Transactions on Electrical Energy Systems*, vol. 123, Mar. 2021, doi: <https://doi.org/10.1002/2050-7038.12819>.

- [198] T. Sutikno and W. Arsadiando, “A Review of Recent Advances on Hybrid Energy Storage System for Solar Photovoltaics Power Generation,” *IEEE Access*, vol. 10, pp. 42346–42364, Jan. 2022, doi: <https://doi.org/10.1109/access.2022.3165798>.
- [200] Z. Cabrane, J. Kim, K. Yoo, and M. Ouassaid, “HES-based photovoltaic/batteries/supercapacitors: Energy management strategy and DC bus voltage stabilization,” *Solar Energy*, vol. 216, pp. 551–563, Mar. 2021, doi: <https://doi.org/10.1016/j.solener.2021.01.048>.
- [201] Z. Cabrane, M. Ouassaid, and M. Maaroufi, “Analysis and evaluation of battery-supercapacitor hybrid energy storage system for photovoltaic installation,” *International Journal of Hydrogen Energy*, vol. 41, no. 45, pp. 20897–20907, Dec. 2016, doi: <https://doi.org/10.1016/j.ijhydene.2016.06.141>.
- [202] W. F. Faris, S. I. Ihsan, and M. Ahmadian, “A comparative ride performance and dynamic analysis of passive and semi-active suspension systems based on different vehicle models,” *International Journal of Vehicle Noise and Vibration*, vol. 5, no. 1/2, p. 116, 2009, doi: <https://doi.org/10.1504/ijvnv.2009.029195>.
- [203] I. Shchur, I. Bilyakovskyy, and V. Turkovskiy, “Improvement of switched structure semi-active battery/supercapacitor hybrid energy storage system for electric vehicles,” *IET Electrical Systems in Transportation*, Mar. 2021, doi: <https://doi.org/10.1049/els2.12017>.
- [204] S. Heroual, B. Belabbas, T. Allaoui, “Fuzzy Logic Control Of Pi Regulator For The Buck-Boost Converter Side Battery Energy Storage“, First national conference on engineering, 05 Et 06 Dec 2023, Tiaret.
- [205] E. A. Narvaez Cubillos, C. A. Cortés Guerrero, and C. L. Trujillo Rodríguez, “Topologies for Battery and Supercapacitor Interconnection in Residential Microgrids with Intermittent Generation,” *Ingeniería*, vol. 25, no. 1, pp. 6–19, Mar. 2020, doi: <https://doi.org/10.14483/23448393.15668>.
- [206] W. Jing, C. Hung Lai, S. H. W. Wong, and M. L. D. Wong, “Battery-supercapacitor hybrid energy storage system in standalone DC microgrids: a review,” *IET Renewable Power Generation*, vol. 11, no. 4, pp. 461–469, Mar. 2017, doi: <https://doi.org/10.1049/iet-rpg.2016.0500>.
- [207] V. Mali, B. Tripathi, K. Kumar, S. Dwivedi, and Ranjan Behera, “Exploring various Topology using DC-DC Converter in Hybrid Energy Storage System for Electric Vehicles,” *IECON 2020 The 46th Annual Conference of the IEEE Industrial Electronics Society*, pp. 1–6, Oct. 2022, doi: <https://doi.org/10.1109/iecon49645.2022.9968407>.
- [208] R. R. Thakkar, Y. Srinivasa. Rao, and R. R. Sawant, “Performance Analysis of Electrical Equivalent Circuit Models of Lithium-ion Battery,” *2020 IEEE Pune Section International Conference (PuneCon)*, vol. 123, Dec. 2020, doi: <https://doi.org/10.1109/punecon50868.2020.9362386>.
- [209] H. He, R. Xiong, and J. Fan, “Evaluation of Lithium-Ion Battery Equivalent Circuit Models for State of Charge Estimation by an Experimental Approach,” *Energies*, vol. 4, no. 4, pp. 582–598, Mar. 2011, doi: <https://doi.org/10.3390/en4040582>.
- [210] M. Tomasov, M. Kajanova, P. Bracinik, and D. Motyka, “Overview of Battery Models for Sustainable Power and Transport Applications,” *Transportation Research Procedia*, vol. 40, pp. 548–

555, 2019, doi: <https://doi.org/10.1016/j.trpro.2019.07.079>.

[211] K. E. Thomas, J. Newman, and R. M. Darling, “Mathematical Modeling of Lithium Batteries,” *Advances in Lithium-Ion Batteries*, pp. 345–392, 2002, doi: https://doi.org/10.1007/0-306-47508-1_13.

[212] Paul, B. Suthar, Venkatasailanathan Ramadesigan, Shriram Santhanagopalan, R. D. Braatz, and V. R. Subramanian, “Efficient Simulation and Reformulation of Lithium-Ion Battery Models for Enabling Electric Transportation,” *Journal of The Electrochemical Society*, vol. 161, no. 8, pp. E3149–E3157, Jan. 2014, doi: <https://doi.org/10.1149/2.018408jes>.

[213] Q. Dai, J. C. Kelly, L. Gaines, and M. Wang, “Life Cycle Analysis of Lithium-Ion Batteries for Automotive Applications,” *Batteries*, vol. 5, no. 2, p. 48, Jun. 2019, doi: <https://doi.org/10.3390/batteries5020048>.

[214] S. Marín-Coca, E. Roibás-Millán, and S. Pindado, “Analytical modelling and sizing of supercapacitors for spacecraft hybrid energy storage systems,” *Acta astronautica*, vol. 211, pp. 382–392, Oct. 2023, doi: <https://doi.org/10.1016/j.actaastro.2023.06.041>.

[215] Z. Cabrane and S. H. Lee, “Electrical and Mathematical Modeling of Supercapacitors: Comparison,” *Energies*, vol. 15, no. 3, p. 693, Jan. 2022, doi: <https://doi.org/10.3390/en15030693>.

[216] G. Feng, R. Qiao, and P. T. Cummings, “Modeling of Supercapacitors,” *Springer eBooks*, pp. 2282–2289, Jan. 2015, doi: https://doi.org/10.1007/978-1-4614-5491-5_1758.

[217] W. C. I *et al.*, “A Bidirectional DC/DC Converter for Renewable Energy Source-Fed EV Charging Stations with Enhanced DC Link Voltage and Ripple Frequency Management,” *Results in Engineering*, pp. 103469–103469, Nov. 2024, doi: <https://doi.org/10.1016/j.rineng.2024.103469>.

[218] Z. Cabrane, M. Ouassaid, and M. Maaroufi, “Management and control of the integration of supercapacitor in photovoltaic energy storage,” *2017 International Conference on Green Energy Conversion Systems (GECS)*, pp. 1–6, Mar. 2017, doi: <https://doi.org/10.1109/gecs.2017.8066128>.

[219] M. Z. Daud, A. Mohamed, and M. A. Hannan, “An Optimal State of Charge Feedback Control Strategy for Battery Energy Storage in Hourly Dispatch of PV Sources,” *Procedia Technology*, vol. 11, pp. 24–31, 2013, doi: <https://doi.org/10.1016/j.protcy.2013.12.158>.

[220] E. H. Houssein, M. A. Mahdy, Doaa Shebl, and W. M. Mohamed, “A Survey of Metaheuristic Algorithms for Solving Optimization Problems,” *Studies in computational intelligence*, pp. 515–543, Jan. 2021, doi: https://doi.org/10.1007/978-3-030-70542-8_21.

[221] D. J. Mankowitz *et al.*, “Faster sorting algorithms discovered using deep reinforcement learning,” *Nature*, vol. 618, no. 7964, pp. 257–263, Jun. 2023, doi: <https://doi.org/10.1038/s41586-023-06004-9>.

[222] S. Almufti, “The novel Social Spider Optimization Algorithm: Overview, Modifications, and Applications,” *ICONTECH INTERNATIONAL JOURNAL*, vol. 5, no. 2, pp. 32–51, Jun. 2021, doi: <https://doi.org/10.46291/icontechvol5iss2pp32-51>.

[223] Xueqin Lü *et al.*, “Overview of improved dynamic programming algorithm for optimizing energy distribution of hybrid electric vehicles,” *Electric power systems research*, vol. 232, pp. 110372–

110372, Jul. 2024, doi: <https://doi.org/10.1016/j.eprs.2024.110372>.

[224] B. A. Attea *et al.*, “A review of heuristics and metaheuristics for community detection in complex networks: Current usage, emerging development and future directions,” *Swarm and Evolutionary Computation*, vol. 63, p. 100885, Jun. 2021, doi: <https://doi.org/10.1016/j.swevo.2021.100885>.

[225] A. Khare and S. Agrawal, “Effective heuristics and metaheuristics to minimise total tardiness for the distributed permutation flowshop scheduling problem,” *International Journal of Production Research*, pp. 1–17, Nov. 2020, doi: <https://doi.org/10.1080/00207543.2020.1837982>.

[226] X.-S. Yang, “Metaheuristic Optimization: Algorithm Analysis and Open Problems,” *Lecture notes in computer science*, pp. 21–32, Jan. 2011, doi: https://doi.org/10.1007/978-3-642-20662-7_2.

[227] K. Rajwar, K. Deep, and S. Das, “An exhaustive review of the metaheuristic algorithms for search and optimization: taxonomy, applications, and open challenges,” *Artificial Intelligence Review*, Apr. 2023, doi: <https://doi.org/10.1007/s10462-023-10470-y>.

[228] F. Firdouse, M. Surender Reddy, "A hybrid energy storage system using GA and PSO for an islanded microgrid applications". *Energy Storage*, 2023, vol. 5, no. 7, p. e460, <https://doi.org/10.1002/est2.460>.

[229] A. Raghavan, P. Maan, A. K. Shenoy, "Optimization of day-ahead energy storage system scheduling in microgrid using genetic algorithm and particle swarm optimization". *IEEE Access*, 2020, vol. 8, pp. 173068-173078, <https://doi.org/10.1109/ACCESS.2020.3025673>

[230] S. Heroual, B. Belabbas, T. Allaoui, and M. Denai, “Performance enhancement of a hybrid energy storage systems using meta-heuristic optimization algorithms: Genetic algorithms, ant colony optimization, and grey wolf optimization,” *Journal of Energy Storage*, vol. 103, pp. 114451–114451, Nov. 2024, doi: <https://doi.org/10.1016/j.est.2024.114451>.

[231] A. Hashemi and M. B. Dowlatshahi, “Exploring Ant Colony Optimization for Feature Selection: A Comprehensive Review,” *Springer Tracts in Nature-Inspired Computing*, pp. 45–60, 2024, doi: https://doi.org/10.1007/978-981-99-7227-2_3.

[232] Y. Poudel and P. Bhandari, “Control of the BLDC Motor Using Ant Colony Optimization Algorithm for Tuning PID Parameters,” *Archives of Advanced Engineering Science*, Jan. 2023, doi: <https://doi.org/10.47852/bonviewaaes32021184>.

[233] R. Gao, Q. Xiao, W. Zhang, and Z. Feng, “Parameter Solution of Fractional Order PID Controller for Home Ventilator Based on Genetic-Ant Colony Algorithm,” *Journal of Electrical Engineering and Technology*, Sep. 2024, doi: <https://doi.org/10.1007/s42835-024-02039-8>.

[234] M. Megrini, A. Gaga, and Y. Mehdaoui, “Enhancement of Field Oriented Control for Permanent Magnetic Synchronous Motor using Ant Colony Optimization,” *WSEAS TRANSACTIONS ON POWER SYSTEMS*, vol. 19, pp. 18–25, Mar. 2024, doi: <https://doi.org/10.37394/232016.2024.19.3>.

[235] R. Wongsathan, “Integrated neural network-based MPPT and ant colony optimization-tuned PI bidirectional charger-controller for PV-powered motor-pump system,” *Engineering and Applied*

Science Research, vol. 51, no. 5, pp. 605–617, 2024, Accessed: Oct. 23, 2024.: doi:<https://ph01.tci-thaijo.org/index.php/easr/article/view/257427>

[236] M. A. Awadallah et al., “Multi-objective Ant Colony Optimization: Review,” *Archives of Computational Methods in Engineering*, Sep. 2024, doi: <https://doi.org/10.1007/s11831-024-10178-4>.

[237] Águila-León, C. Vargas-Salgado, D. Díaz-Bello, C. Montagud-Montalvá, "Optimizing photovoltaic systems: A meta-optimization approach with GWO-Enhanced PSO algorithm for improving MPPT controllers" *Renewable Energy*, 2024, vol. 230, p. 120892, <https://doi.org/10.1016/j.renene.2024.120892>

[238] H. Ulutas, R. B. Günay, M. E. Sahin, "Detecting diabetes in an ensemble model using a unique PSO-GWO hybrid approach to hyperparameter optimization". *Neural Computing and Applications*, 2024, vol. 36, no. 29, pp. 18313–18341, <https://doi.org/10.1007/s00521-024-10160-y>.

[239] Y. Liu, A. As’arry, M. K. Hassan, A. A. Hairuddin, H. Mohamad, "Review of the grey wolf optimization algorithm: variants and applications". *Neural Computing and Applications*, 2024, vol. 36, no. 6, pp. 2713-2735, <https://doi.org/10.1007/s00521-023-09202-8>

[240] A. B. Kancherla, N. B. Prasad, D. R. Kishore, "PV-Based Grid Integrated EV with GWO Optimized PI Controller for Boost Integrated Luo Converter ". *Journal of The Institution of Engineers (India): Series B*, 2024, vol. 105, no. 2, pp. 309-321, <https://doi.org/10.1007/s40031-023-00968>

[241] E. dada and S. joseph, , “application of grey wolf optimization algorithm: recent trends, issues, and possible horizons,” *gazi university journal of science*, May 2021, doi: <https://doi.org/10.35378/gujs.820885>

[242] Y. Liu, Azizan As’arry, Mohd Khair Hassan, Abdul Aziz Hairuddin, and H. Mohamad, “Review of the grey wolf optimization algorithm: variants and applications,” *Neural Computing and Applications*, Nov. 2023, doi: <https://doi.org/10.1007/s00521-023-09202-8>.

[243] S. KILIÇARSLAN, “PSO + GWO: a hybrid particle swarm optimization and Grey Wolf optimization based Algorithm for fine-tuning hyper-parameters of convolutional neural networks for Cardiovascular Disease Detection,” *Journal of Ambient Intelligence and Humanized Computing*, Oct. 2022, doi: <https://doi.org/10.1007/s12652-022-04433-4>.

[244] Y. Liu, Azizan As’arry, Mohd Khair Hassan, Abdul Aziz Hairuddin, and H. Mohamad, “Review of the grey wolf optimization algorithm: variants and applications,” *Neural Computing and Applications*, Nov. 2023, doi: <https://doi.org/10.1007/s00521-023-09202-8>.

[245] K. Mostafaei, M. Yousefi, O. Kreuzer, and M. N. Kianpour, “Simulation-based mineral prospectivity modeling and Gray Wolf optimization algorithm for delimiting exploration targets,” *Ore Geology Reviews*, vol. 177, p. 106458, Feb. 2025, doi: <https://doi.org/10.1016/j.oregeorev.2025.106458>.

[246] K. Khan, I. Samuilik, and A. Ali, “A Mathematical Model for Dynamic Electric Vehicles: Analysis and Optimization,” *Mathematics*, vol. 12, no. 2, p. 224, Jan. 2024, doi: <https://doi.org/10.3390/math12020224>.

[247] F. Adegbohun, A. von Jouanne, B. Phillips, E. Agamloh, and A. Yokochi, “High Performance

- Electric Vehicle Powertrain Modeling, Simulation and Validation,” *Energies*, vol. 14, no. 5, p. 1493, Mar. 2021, doi: <https://doi.org/10.3390/en14051493>.
- [248] A. O. Kıyıklı and H. Solmaz, “Modeling of an Electric Vehicle with MATLAB/Simulink,” *International Journal of Automotive Science and Technology*, pp. 9–15, Jan. 2019, doi: <https://doi.org/10.30939/ijastech..475477>.
- [249] D. R. Sahoo, “Design and Analysis of Electric Vehicle with Battery System,” *Revista Gestão Inovação e Tecnologias*, vol. 11, no. 3, pp. 136–145, Jun. 2021, doi: <https://doi.org/10.47059/revistageintec.v11i3.1922>.
- [250] Z.-J. M. Shen, B. Feng, C. Mao, and L. Ran, “Optimization models for electric vehicle service operations: A literature review,” *Transportation Research Part B: Methodological*, vol. 128, pp. 462–477, Oct. 2019, doi: <https://doi.org/10.1016/j.trb.2019.08.006>.
- [251] T. A. T. Mohd, M. K. Hassan, and W. A. Aziz, “Mathematical modeling and simulation of an electric vehicle,” *Journal of Mechanical Engineering and Sciences*, vol. 8, pp. 1312–1321, 2015.
- [252] L. Qi, X. Wu, X. Zeng, et al., “An electro-mechanical braking energy recovery system based on coil springs for energy saving applications in electric vehicles,” *Energy*, vol. 200, p. 117472, 2020
- [253] K. Chaudhari, N. K. Kandasamy, A. Krishnan, A. Ukil, and H. B. Gooi, “Agent-Based Aggregated Behavior Modeling for Electric Vehicle Charging Load,” *IEEE Transactions on Industrial Informatics*, vol. 15, no. 2, pp. 856–868, Feb. 2019, doi: <https://doi.org/10.1109/tii.2018.2823321>.
- [254] E. Çelik *et al.*, “Improving speed control characteristics of PMDC motor drives using nonlinear PI control,” *Neural Computing and Applications*, vol. 36, no. 16, pp. 9113–9124, Feb. 2024, doi: <https://doi.org/10.1007/s00521-024-09568-3>.
- [255] V. S. R. Kosuru and A. Kavasseri Venkitaraman, “Trends and Challenges in Electric Vehicle Motor Drivelines - A Review,” *International journal of electrical and computer engineering systems*, vol. 14, no. 4, pp. 485–495, Apr. 2023, doi: <https://doi.org/10.32985/ijeces.14.4.12>.
- [256] X. Hua, A. Thomas, and K. Shultis, “Recent progress in battery electric vehicle noise, vibration, and harshness,” *Science Progress*, vol. 104, no. 1, p. 003685042110052, Jan. 2021, doi: <https://doi.org/10.1177/00368504211005224>.
- [257] R. Kawamoto *et al.*, “Estimation of CO2 Emissions of Internal Combustion Engine Vehicle and Battery Electric Vehicle Using LCA,” *Sustainability*, vol. 11, no. 9, p. 2690, May 2019, doi: <https://doi.org/10.3390/su11092690>.
- [258] K. Y. Yap, H. H. Chin, and J. J. Klemeš, “Solar Energy-Powered Battery Electric Vehicle charging stations: Current development and future prospect review,” *Renewable and Sustainable Energy Reviews*, vol. 169, p. 112862, Nov. 2022.
- [259] P;Saini, R. Kumar, and P.K. Juneja. 'Design of the PI Controller for the Consistency of Stock in the Paper Machine Headbox using Particle Swarm Optimisation (PSO)'. International Conference on Innovative Sustainable Computational Technologies (CISCT). 2019
- [260] Zhenyu, C. Xiaoqing, 'Optimization of the energy management strategy for the hybrid energy

storage system of trams based on competitive particle swarm algorithms'. *Journal of Energy Storage*, 2024, vol. 75, p. 109698.

[261] C.Haipeng, "Optimal energy management strategy for an islanded microgrid with hybrid energy storage." *Journal of Electrical Engineering & Technology* 2024,16,1313-1325.

[262] B. Labdai, L.Hemici,. Nezli, N. Bounar, A. Boulkroune , L. Chrifi-Alaoui, "Control of a DFIG Based WECS with Optimized PI controllers via a duplicate PSO algorithm," 2019 International Conference on Control, Automation and Diagnosis (ICCAD), Grenoble, France, 2019,pp. 1-6,

[263] A. G. Gad, "Particle Swarm Optimization Algorithm and Its Applications: A Systematic Review," *Archives of Computational Methods in Engineering*, vol. 29, no. 5, pp. 2531–2561, Apr. 2022, doi: <https://doi.org/10.1007/s11831-021-09694-4>.

[264] S.Tijjani,and M.Mohd, "An enhanced particle swarm optimization with position update for optimal feature selection," *Expert systems with applications*, vol. 247, pp. 123337–123337, Aug. 2024, doi: <https://doi.org/10.1016/j.eswa.2024.123337>.